AUBURN

SAMUEL GINN
COLLEGE OF ENGINEERING

Research Report

EXPERIMENTAL VALIDATION OF ANALYSIS METHODS AND DESIGN PROCEDURES FOR STEEL PILE BRIDGE BENTS

Submitted to

The Alabama Department of Transportation

Prepared by

Justin D. Marshall, Ph.D., P.E.
J. Brian Anderson, Ph.D., P.E.
Jonathon Campbell
Zachary Skinner
Stephen T. Hammett, P.E., S.E.C.B.

JUNE 2017

Highway Research Center

Harbert Engineering Center
Auburn, Alabama 36849

www.eng.auburn.edu/research/centers/hrc.html

1. Report No. ALDOT 930-859	2. Government Accession No.	3. Recipient Catalog No.
4 Title and Subtitle EXPERIMENTAL VALIDATION OF ANALYSIS METHODS AND DESIGN PROCEDURES FOR STEEL PILE BRIDGE BENTS		**5 Report Date** June 2017
		6 Performing Organization Code
7. Author(s) Justin D. Marshall, J. Brian Anderson, Jonathon Campbell, Zachary Skinner, Stephen T. Hammett		**8 Performing** ALDOT 930-859
9 Performing Organization Name and Address Highway Research Center Department of Civil Engineering 238 Harbert Engineering Center Auburn, AL 36849		**10 Work Unit No. (TRAIS)**
		11 Contract or Grant No.
12 Sponsoring Agency Name and Address Alabama Department of Transportation 1409 Coliseum Boulevard Montgomery, Alabama 36130-3050		**13 Type of Report and Period Covered** Technical Report
		14 Sponsoring Agency Code

15 Supplementary Notes

16 Abstract

Structural analysis of steel pile bent bridges without sway bracing may result in significantly higher forces in the piles than expected by ALDOT bridge engineers. The reason for the higher than expected pile loads was undetermined, but a preliminary study highlighted the fact that the assumptions used in the analysis could have a significant impact on the numerical results. The higher than expected forces resulted from load cases with lateral loads. This research project has investigated this type of bridge bent through three different full-scale load tests to determine the behavior of this type of bridge under lateral forces. In addition to the load tests, analysis models were calibrated with the load tests to determine the best way to model the pile bents. Based on the load tests and analysis model results, a design procedure was developed.

17 Key Words Full-scale testing, soil-structure interaction, steel pile foundation	**18 Distribution Statement** No restrictions. This document is available to the public through the National Technical Information Service, Springfield, Virginia 22161		
19 Security Classification (of this report) Unclassified	**20 Security Classification (of this page)** Unclassified	**21 No. of pages** 304	**22 Price**

FORM DOT F 1700.7 (8-72)

Research Report

ALDOT Research Project #930-859

EXPERIMENTAL VALIDATION OF ANALYSIS METHODS AND DESIGN PROCEDURES FOR STEEL PILE BRIDGE BENTS

Submitted to

The Alabama Department of Transportation

Prepared by

Justin D. Marshall
J. Brian Anderson
Jonathon Campbell
Zachary Skinner
Stephen T. Hammett

Highway Research Center

and

Department of Civil Engineering

at Auburn University

JUNE 2017

DISCLAIMERS

The contents of this report reflect the views of the authors, who are responsible for the facts and the accuracy of the data presented herein. The contents do not necessarily reflect the official views or policies of Auburn University or the Federal Highway Administration. This report does not constitute a standard, specification, or regulation.

NOT INTENDED FOR CONSTRUCTION, BIDDING, OR PERMIT PURPOSES

Justin D. Marshall, Ph.D., P.E.
J. Brian Anderson, Ph.D., P.E.
Research Supervisors

ACKNOWLEDGEMENTS

Abstract

Recent experience with structural analysis of steel pile bent bridges with battered piles and no sway bracing resulted in significantly higher forces in the piles than what was expected by ALDOT bridge engineers. A preliminary study was unable to determine the precise reason for the higher than expected pile loads, but did discover that the assumptions used in the analysis could have a significant impact on the numerical results. It was also clear that the higher than expected forces resulted from load cases with lateral loads.

This research project has investigated steel pile bridge bents through three different full-scale load tests to determine the behavior of this type of bridge under lateral forces. One load test occurred on a bridge under construction in both the bare bent condition as well as with the deck in place with live load. The second test was an existing bridge in-service bridge. The final tests were bent only tests which were loaded laterally to failure.

In addition to the load tests, analysis models were calibrated with the load tests to determine the best way to model the pile bents. The models were used to determine how accurate assumed modeling practices replicate the behavior seen in full-scale tests. Based on the load tests and analysis model results, a design procedure was developed which includes recommendations for the bridge geometry as well as how the pile elements should be modeled and designed.

Table of Contents

List of Tables

Chapter 1   Introduction

1.1   Overview

One of the most common bridge types in Alabama is the multi-span bridge with simply supported precast/prestressed concrete girders and pile bents consisting of a cast-in-place, reinforced concrete bent cap and driven steel HP piles. Typically, the exterior piles are battered at a 1.5:12 slope. When the bent is located within the flow channel, the steel piles are encased in concrete three feet above the mudline. The pile encasements are typically extended at least five feet below the projected ground elevation. These concrete encasements serve as protection to prevent section loss of the steel piles. If the clear height of the piles is greater than 14 feet, welded sway bracing is used in order to provide sufficient lateral stiffness and strength. The welded sway bracing can be configured as one-story as shown in Figure 1-1 or two-story. This bridge type is very common for the Alabama Department of Transportation (ALDOT); therefore, effective analysis and design procedures for these bridges are a necessity to provide efficient bridge designs.

Driven steel pile bridge bents are efficient structures, but are difficult to model accurately. The steel piles play a part in the resistance of both gravity and lateral loads. Due to the combination of flexural and axial effects on the piles, the overall structure is highly indeterminate. Changes in stiffness in the elements can therefore cause significant changes in the element forces. The stiffness of the piles is dependent on a number of assumptions including but not limited to the degree of composite behavior between the steel pile and concrete encasement, the rigidity of the connection between the steel pile and the cast-in-place bent cap, and the

1

interaction between the steel pile and the surrounding soil. The pile flexural stiffness, end fixity, and unbraced length have a significant impact on the overall bent lateral stiffness; therefore these critical assumptions play a key part in performing the analysis accurately.
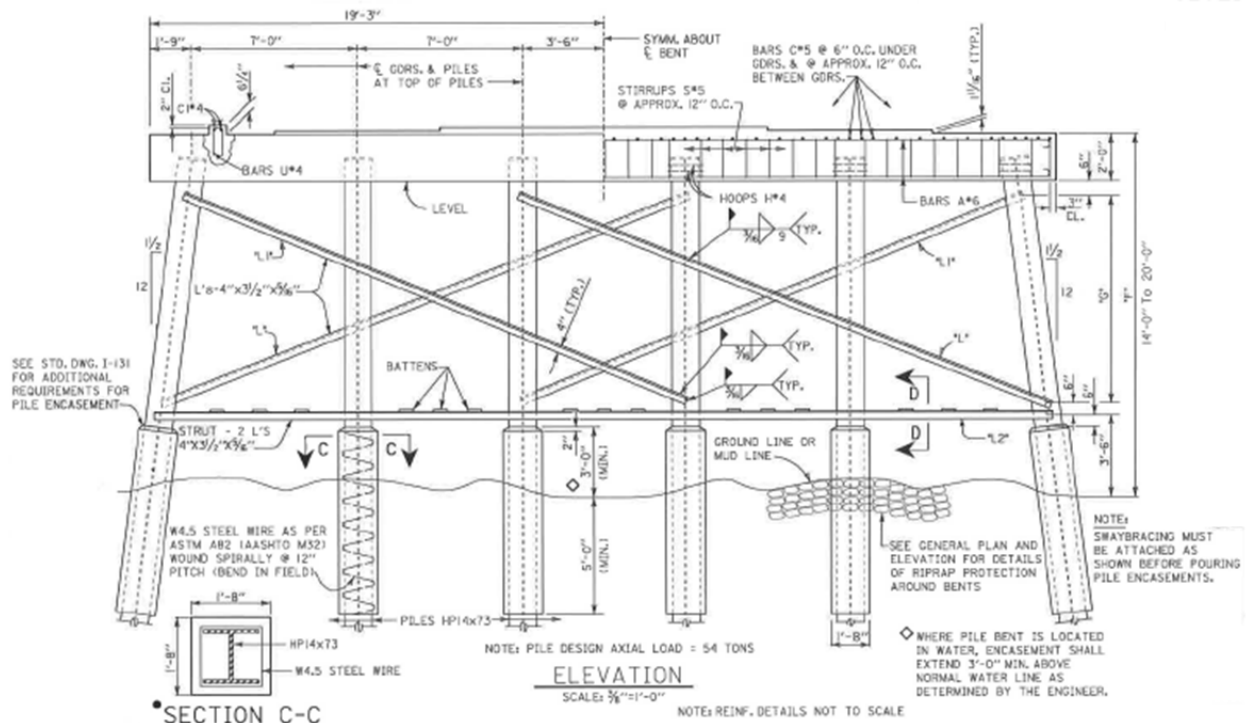
Figure 1-1 Typical Pile Bent Substructure with One-Story Sway Bracing

A better understanding of how these pile bents perform under gravity and lateral load is necessary to validate analysis methods and design procedures and model the pile bents correctly. In order to better gain this understanding, a series of load tests was performed on newly constructed and existing bridges. The tested pile bents were instrumented during testing to determine forces and moments in the piles and bent cap and also the degree of composite behavior of the concrete encasement. The results from these tests were then used to calibrate numerical models which can be used to analyze existing pile bent designs and develop recommendations for assumptions to be made in analysis and design procedures for Load and Resistance Factor Design (LRFD) of pile bent bridge substructures.

1.2 Problem Statement

Recent correspondence with the ALDOT Bridge Bureau indicated an issue with the analysis and design of a steel pile bridge bent without sway bracing. An independent consultant submitted a design package for a pile bent that included significantly higher pile design forces than were anticipated by ALDOT designers. An additional analysis was performed by a different consultant who was unable to determine the reason for the discrepancy in the pile forces. He did indicate, however, that assumptions made in the analysis could significantly affect the pile forces and that the design forces came from load combinations including lateral loads. The research detailed in this thesis examines the behavior of steel pile bents under gravity and lateral loading and calibrates analytical models to include proper assumptions listed in the previous section.

1.3 Research Objectives

The research objectives for this report include:

- Identify the dead, live and lateral load transfer mechanism (load path) within the steel pile bent including the cast-in-place cap beam, steel HP piles and concrete encasement.

- Use the load testing data to develop accurate modeling assumptions for including soil-pile-interaction for the driven piles using FB-Multipier (BSI 2010).

- Develop calibrated analytical models which will be used to determine appropriate boundary conditions, including soil-pile-interaction, composite sections, and connection springs for steel pile bent bridge models.

- Evaluate the effect of the 1.5:12 batter of the exterior steel piles.

- Develop recommended analysis procedures for modeling of steel pile bents that provides a balance between accuracy, required effort and design economy.

- Develop LRFD design procedures for steel pile bent bridges which are coupled with the analysis recommendations.

1.4   Research Scope

The research for this project was broken up into two phases: analytical modeling and full-scale testing. Three test sites were selected for full scale load testing with detailed modeling conducted prior to the execution of the lateral load tests. Modeling was conducted to predict cap deflections and pile forces during lateral testing. The models were used to select the maximum force for the lateral load tests so in service bents would not suffer permanent damage. The first site was a bridge under construction located in Shorter, Alabama on Macon County Road 9. The selected bent was subjected to two lateral load tests, one prior to the casting of the deck, and one after the deck was cast. The bent featured four HP 14x89 piles with battered exterior piles and 30in diameter concrete encasements. The second bent tested was an existing bridge on U.S. Highway 331 in southern Montgomery County. The bent tested was constructed with six HP 10x42 piles with 16in square concrete encasements. The final test site featured two bents constructed for research only. Both bents were constructed with four HP 12x42 piles. The first bent was designed based on the standard ALDOT detail featuring battered exterior piles and 12 inches of embedment in the pile cap. The second bent was an experimental bent featuring all vertical piles embedded 18 inches into the pile cap. These two pile bents were tested to failure. After all field tests were complete, the resulting data was reduced to produce moment diagrams and deflection profiles. The field test results were compared to the initial model results. The models were then calibrated to more closely match the observed behavior of the piles. The final portion of the research was the development of design and analysis recommendations for these types of bridge superstructures. The recommended procedures were based on the results of the tests and models and provide a guideline for bridge engineers to be able to accurately model and understand the complex behavior as part of the design process.

4

1.5   Organization of Report

This report is divided into 11 chapters. Chapter 1 is an introductory chapter providing the motivation for the research project, objectives and a summary of the research performed. Chapter 2 provides a background on steel pile bridge bents and an overview of theoretical behavior of deep foundations under lateral loads and analysis methods. Chapter 3 details the preliminary modeling of the bridges to be tested in preparation for the full-scale tests. Chapters 4 and 5 detail the testing, analysis and results of a new construction pile bent bridge constructed in Macon County Alabama. Chapter 6 describes the testing, analysis and results of an in service pile bent bridge in South Montgomery, Alabama located on US Highway 331 South. Chapter 7 reports on the calibrated analytical models for the two previously tested bridges and what was learned from those models. Chapter 8 describes the testing to failure of two stand-alone bents at the Auburn University National Geotechnical Experimentation Site. The analytical models calibrated to those tests and the findings from those models are presented in Chapter 9. Chapter 10 outlines the design and analysis procedures that were developed based on the results of the testing and analysis program. The summary, conclusions and recommendations are provided in Chapter 11.

Chapter 2   Background and Literature Review

2.1   Background and Description of Pile Bent Substructures

The multi-span bridge with simply supported precast-prestressed concrete girders and intermediate bents consisting of driven steel piles and a reinforced concrete bent cap is widely used in the state of Alabama. This section provides a detailed description of pile bent substructures and the typical construction process for pile bents with driven steel HP piles.

Pile bents are a part of the substructure of the bridge system. The elements of a bridge system can be divided into two separate groups: superstructure and substructure. The superstructure of a bridge is made up of all components above the bridge's supports including the bridge deck, girders, and intermediate diaphragms. The substructure of a bridge is comprised of all the bridge elements required to support the bridge superstructure (Tonias & Zhao, 2007). Substructure elements can include piers, abutments, bearings, pedestals and backwalls. Pile Bents fall into the category of piers. Piers act as intermediate supports for the bridge superstructure located at discrete points along the length of bridge. The most common types of piers are column bents and pile bents. A typical pile bent can bee seen in Figure 2-1.

Figure 2-1 Typical Pile Bent with Galvanized Steel HP Piles and Reinforced Concrete Cap

2.1.1 Pile Bent Description

Typical intermediate pile bents consist of either precast or steel piles driven into the ground by means of a hydraulic, diesel or air hammer. The exterior piles in these bents are typically battered at a 1.5:12 slope. Steel HP piles are one of the most common pile sections used in pile bent substructures. The flanges and webs of these sections are of equal thickness, and they are proportioned this way to reduce the hard driving stresses which they are subjected to (Bowles 1996). These steel HP piles are typically encased in non-structural concrete to prevent section loss. The cross section of these encasements can be either circular or square. Alternatively, galvanized piles have been used by ALDOT for corrosion protection. The bent shown in Figure 2-1 consists of galvanized steel HP piles. The other primary element of a typical pile bent is a

cast-in-place reinforced concrete bent cap, which is cast following pile driving. The top of the piles are typically embedded a minimum of 12 inches into the bottom of the bent cap. In cases where encasements are used, a two-inch embedment of the encasement into the cap is used which eliminates the need for chairs for the reinforcement cage of the cap. This w focuses on pile bents where steel HP piles encased in non-structural concrete were utilized. The bent focused on is shown in Figure 2-2.

Figure 2-2 Driven Steel Pile Bridge Bent with Concrete Encasements

2.2   Lateral Load Testing Background

This section details lateral load testing procedures commonly performed on single piles and pile groups. It also details the requirements for lateral load tests on pile foundations per ASTM D3966 including design of the testing apparatus, testing configurations and instrumentation recommendations.

Lateral load testing of piles and pile groups is commonly performed on new construction projects where pile foundations are being implemented. Field tests provide the most reliable relationship between the applied load and the foundation's lateral movement (ASTM 2007). The

reference standard these load tests must follow is ASTM D3966 "Standard Test Methods for Deep Foundations Under Lateral Loads". This specification provides guidelines and recommended procedures for lateral load tests performed on deep foundations.

2.3 Theoretical Behavior of Deep Foundations Under Lateral Loads

Piles, like other structural elements are designed for strength and serviceability limit states. They are designed so that they have adequate strength under ultimate loads, but also so that excessive deflections do not occur under service level loads. In a majority of cases, the maximum tolerable deflection will control the design of piles (Poulos and Davis 1980). Lateral loading of a pile is a soil-structure interaction problem in which the deflection of the pile and the lateral resistance of the soil are interdependent (Reese and Wang 2006). A knowledge of the relationships between pile deflection, slope, shear and bending moment is important in the design of pile foundations. Piles are checked for adequate strength against the maximum bending moments from ultimate loads and are checked to ensure the maximum deflection is less than the allowable under service loads. A figure of the relationship of the deflection, slope, bending moment, shear force and soil reaction as a function of pile depth can be seen in Figure 2-3.
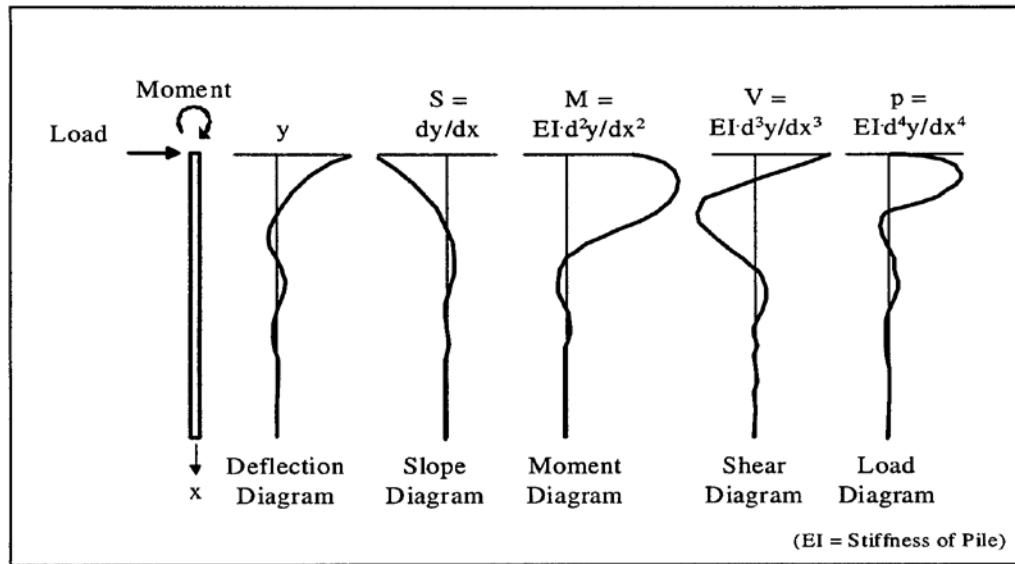
Figure 2-3 Solutions to Pile Deflections and Forces as a Function of Depth (Reese and Wang 2006)

2.4 Pile to Cap Modeling

Pile groups which consist of a pile cap are typically modeled as a fixed-head condition, meaning the rotation of the top of the pile which is embedded into the cap is fully restrained. Lateral load tests by Gerber and Rollins (2009) showed that the piles groups that are capped do not behave as fully fixed in terms of load and deflection, but somewhere between unrestrained and fully restrained. A nine-pile group was constructed and loaded without a cap, then following the first test, the group was capped and reloaded. It was found that the deflections of the piles decreased by 40% in the test where the piles had been capped and the lateral resistance of the pile group increased by 51%. Analyses were performed using a fixed-head and free-head condition and then compared to the results from the load tests. According to theoretical results, the deflection of the pile group with the cap should have been approximately 25% of the measured deflection of the pile group without the cap; however, the actual deflection of the group with the cap was 60% of the deflection of the group without the cap. The cap appeared to

10

provide some rotational restraint of the pile heads, but not full restraint. Modeling the piles as fully restrained will result in pile deflections which are less than actual results, but will result in bending moments in the cap that are overly conservative.

Mokwa and Duncan (2003) developed a practical approach for approximating the level of moment restraint provided by the pile cap at the top of a pile group. A fully fixed-head condition is rarely achieved in the field; therefore assuming a fully restrained pile-head can lead to under estimations of lateral deflections of the pile and overly conservative values of bending moments in the cap. Suggested methods for calculating a rotational restraint coefficient, $K_{M\theta}$, are presented by Mokwa and Duncan to improve the estimates of deflections of pile groups under lateral load. The coefficient to modify rotational restraint was completely dependent on the axial stiffness of the piles.

2.5   Soil Structure Interaction

Geotechnical structures interact axially and laterally with the soil surrounding them. Geotechnical design focuses on understanding, quantifying, and predicting these behaviors. The following sections detail the general methods used to calculate axial capacity and predict lateral behavior of driven piles in cohesive and cohesionless soil.

2.5.1   Axial Capacity

Pile axial capacity is developed through both end bearing and side friction. Figure 2- shows a graphical representation of the components of pile capacity.
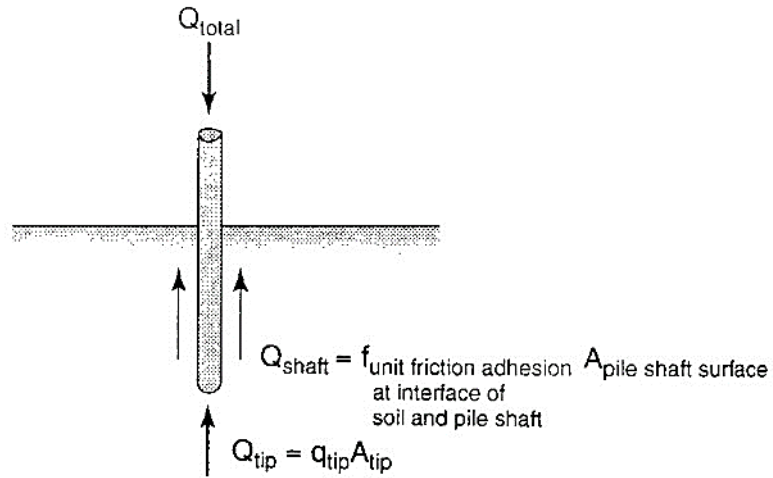
Figure 2-4 – Pile Capacity Theory (McCarthy, 2007)

The end bearing capacity for piles is a function of the pile end area and the strength of the soil itself. **Equation 2-1** shows the equation used for the calculation of end bearing pressure adapted from the calculation of bearing capacity for shallow foundations (McCarthy, 2007).

$$q_{tip} = cN_c + 0.4\gamma BN_\gamma + \sigma'_v N_q \qquad \text{Equation 2-1 (McCarthy, 2007)}$$

Where

$q_{tip} = End\ bearing\ pressure\ at\ pile\ tip$

$c = Cohesion\ shear\ strength\ of\ soil$

$N_c = N_\gamma = N_q = Bearing\ capacity\ factors\ for\ deep\ foundations$

$B = Pile\ tip\ diameter$

$\gamma = Unit\ weight\ of\ soil$

$\sigma'_v = Effective\ vertical\ Stress$

12

Equation 2-2 shows how the bearing capacity of the soil is used to determine the contribution of end bearing capacity to the overall capacity of the pile.

$$Q_{tip} = q_{tip} A_{tip}$$ **Equation 2-2 (McCarthy, 2007)**

Where

$Q_{tip} = Pile\ end\ bearing\ capacity$

$A_{tip} = Area\ of\ pile\ tip$

The second portion of pile capacity is developed through friction between the pile and the soil. The friction force is developed as the pile is driven through soil. Figure 2- shows graphically the theory behind the calculation of side friction. The side friction is derived from a pile sliding against soil particles. The amount of friction is dependent on the type of pile and the horizontal stress condition of the soil.
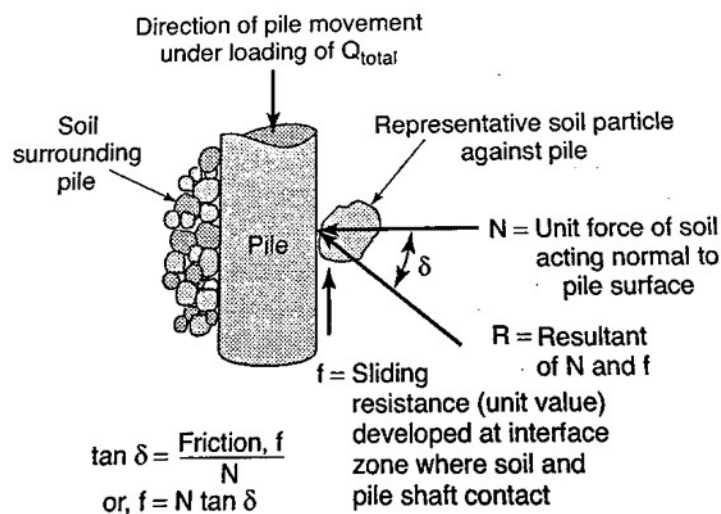
Figure 2-5 – Side Friction Theory (McCarthy, 2007)

The Beta method is used to calculate the unit friction adhesion between the surface of the pile and the soil and the friction contribution to the overall pile capacity. **Equation 2-3** shows the calculation of the unit side friction created by the pile being driven into soil.

13

$$f_{soil} = \beta\sigma'_v \qquad\qquad \textbf{Equation 2-3} \text{ (McCarthy, 2007)}$$

Where

$f_{soil} = Unit\ friction\ adhesion\ between\ the\ surface\ of\ the\ pile\ and\ soil$

$\beta = Beta\ coefficient$

The Beta coefficient takes into account the horizontal strength of the soil and the type of pile analyzed. The calculation of the coefficient is shown in **Error! Reference source not found.**.

$$\boldsymbol{\beta = Ktan(\delta)} \qquad\qquad \textbf{Equation 2-4 (McCarthy, 2007)}$$

Where

$K\ =\ Lateral\ earth\ pressure\ coefficient$

$tan(\delta) = Interface\ coefficient$

Once the unit skin friction has been calculated, it is used with the embedded area of the pile to calculate the side friction capacity. The calculation is shown in **Error! Reference source not found.**.

$$\boldsymbol{Q_{shaft} = f_{soil}A_{shaft}} \qquad\qquad \textbf{Equation 2-5 (McCarthy, 2007)}$$

Where

$Q_{shaft} =\ Side\ friction\ capacity\ of\ the\ pile$

$A_{shaft} = Effective\ surface\ area\ of\ pile\ embedded\ in\ soil$

The total capacity of the pile is determined using **Error! Reference source not found.**.

$$Q_{Total} =\ Q_{tip} +\ Q_{shaft} \qquad\qquad \textbf{Equation 2-6} \text{ (McCarthy, 2007)}$$

Where

$Q_{Total} = Total\ pile\ capacity$

2.5.2 Lateral Capacity

P-y curves are used to characterize the lateral behavior of soil. The soil is modeled as a series of nonlinear springs acting at various locations along the depth of the pile. Figure 2- shows a series of theoretical nonlinear springs acting on a driven pile. As the pile deflects, the soil resistance increases as the theoretical springs compress. As lateral load increases the soil will push back until the shear strength of the soil is overcome or the structural element fails. Figure 2-7 shows a p-y curve developed to illustrate the typical lateral behavior of soils.
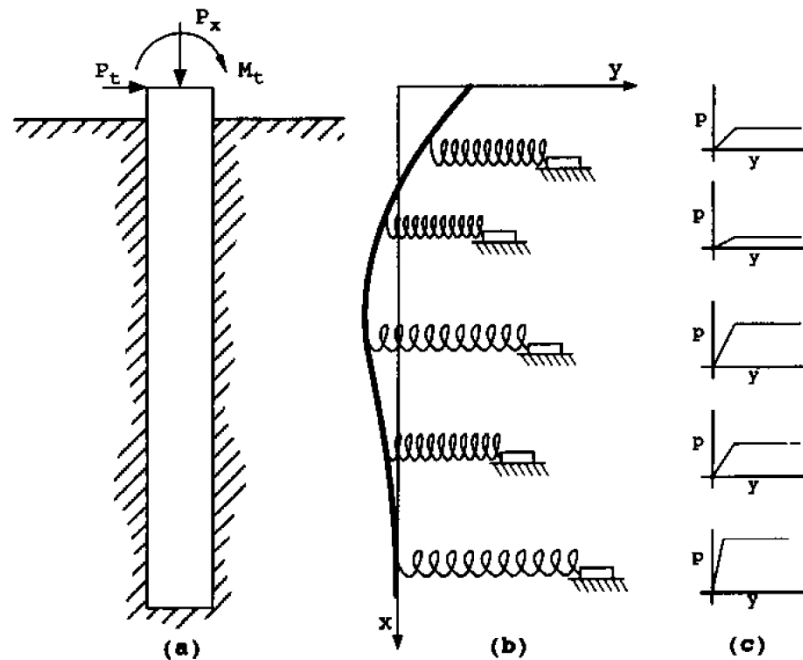
Figure 2-6 –Nonlinear Springs Acting on a Driven Pile (Reese & Wang, 2006)

15
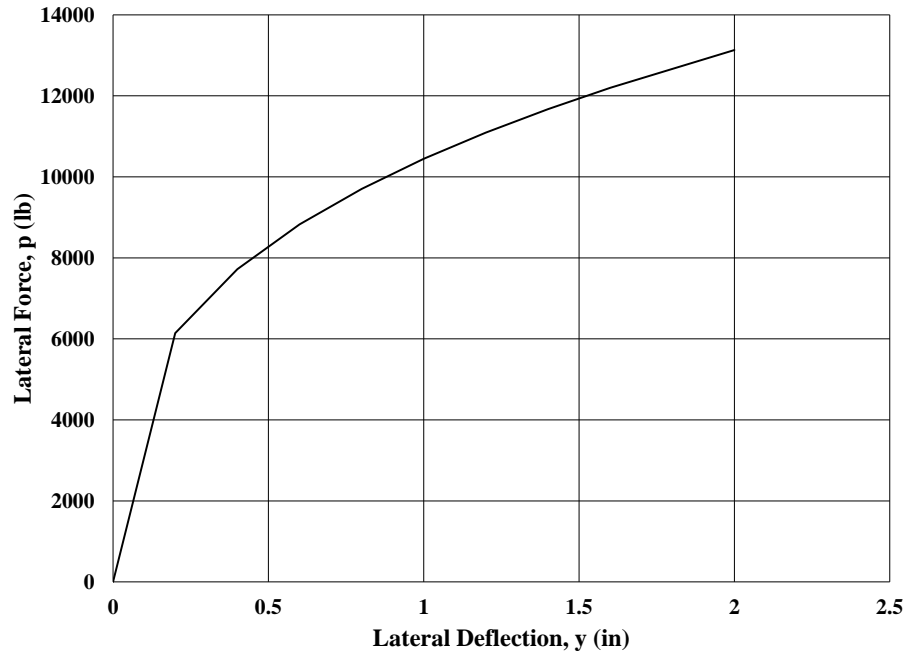
Figure 2-7 – Sample p-y Curve

2.6   Software Implementation

In order to validate findings from experimental testing, computer software programs were used in this research study to create structure models which simulated the geometry and loading conditions from the field tests. Two software programs were used to create models to analyze the tested bridge bents. Preliminary models were built in FB-Multipier (BSI 2004) to determine the lateral loads to apply to the bents to ensure that strength limit states would not be reached and that excessive deflections would not occur. Following load testing, structural models were created in SAP 2000 to validate the results of the field tests. The models would represent the as-built geometry of the bents at the time of testing as well as material properties determined from laboratory testing. The models would also include pile-to-cap connections which would simulate the behavior of the bents during the load testing. Soil-pile interaction would be included in the model by linear springs located along the length of the pile. The loads applied to the these bents simulate the actual loading conditions during each of the load tests including the effects of lateral

16

loads applied and wheel loads from the load trucks used during the tests. Final calibrated models of the bents tested to failure were also created in FB Multipier to investigate the impact of different bent configurations to enable the developed design and analysis recommendations to be vetted.

2.6.1 FB Multipier

FB Multipier is modeling software used to analyze various types of geotechnical structures. The software requires the input of soil profiles and properties, structural geometries, and pertinent structural properties.

2.6.1.1 Soil Properties

Soil properties of the in place soil are required to produce accurate FB Multipier models. Each soil type modeled requires the input of different soil properties from unit weight to axial and lateral strength parameters. Strength parameters for cohesive soils included the undrained shear strength and principal strain values under lateral loads. Strength parameters for cohesionless soils include the friction angle and the subgrade modulus, K_0.

2.6.1.2 Modeled Soil Behavior

FB Multipier models break down soil behavior into lateral, axial, torsional, and tip categories. These categories have built in models derived from spring behavior. Lateral behavior is defined by a series of p-y curves that define the lateral deflection a pile experiences under a certain amount of load.

The axial behavior is defined by the type of structural element analyzed. T-z curves that define the amount of axial force required to move the structural element in a downward direction model the soil behavior during the installation process of the structural element.

The torsional behavior is described by T-Theta curves that are defined as the force required to rotate a structural element about the long axis of the pile.

The tip model reflects the type of structural element analyzed. The built in Q-z models are used to simulate the installation process of the selected structural element.

2.6.1.3 Structural Behavior

The structural elements in FB Multipier can be analyzed by considering either gross section properties or full cross section properties. The software analyzes the structural elements as linear elastic elements until yielding is determined. Yielding is considered as failure when the software analyzes the bent model. The concrete elements modeled in the software include the bent caps and encasements. Concrete elements require the following data for analysis: unit weight, compressive strength (fc'), and young's modulus. The software also generates the reinforcement layout in the bent cap to accurately model the bent cap behavior. The steel elements modeled include the steel reinforcement and driven piles. The steel properties required for analysis include: unit weight, yield stress, and elastic modulus. The piles modeled also require the input of section properties such as depth, web thickness, width, and flange thickness.

2.6.1.4 Pushover Analysis

FB Multipier contains built in programming to test a bent to failure. The program requires two load cases. The first load case is used to specify the initial conditions. The second load case specifies what condition increases. The amount of load on the bent increases in each load case by the amount of load specified in the second load case. The number of load cases allowed to run is specified prior to running the analysis. FB Multipier will then run the analysis for each specified load case until the bent experiences failure.

2.6.2 SAP 2000

The structural analysis software used to determine the correlation between results from the field tests and theoretical values was SAP 2000. The program was chosen based on its

availability and user prior knowledge of the software interface. SAP is a useful product for performing simple static, linear elastic analyses to complex dynamic, non-linear inelastic analyses (CSI 2011). Object based models are created in the program and converted to element based models in order to perform the finite element analysis. For each of the models created and reported on in this thesis, static linear-elastic and nonlinear displacement based analyses were performed. Two-dimensional frame models were developed using SAP's predefined 2D frame templates. The frame section designer and element springs tools were used in creating these models to simulate the actual cross-sections of the piles in each of the test bents.

Chapter 3   Preliminary Modeling and Behavior Prediction

3.1 Purpose

Comprehensive modeling using FB Multipier was conducted prior to full-scale field lateral load testing. Models simulated the existing soil conditions and the pile properties to predict the bent behavior during load testing. The models were used to predict the axial forces, shear forces, flexural moment, and lateral deflection caused by the application of lateral load. The model simulations were used to determine the maximum loads to be applied during the field load tests. The models were also used to determine the size and stroke length of the jacks needed to test the bents. Model predictions for axial load and moment in the piles were compiled for each pile and were then compared to the data gathered from the field load tests. After load testing, the models were refined and calibrated to the results of the field load tests.

3.2 Overview

FB Multipier models were created for each bridge bent and reaction bent studied in this project. Soil properties from site specific soil exploration reports were used to determine the soil properties for each layer of soil in the FB Multipier soil profile. The geometries and properties of the structural elements of the bents were acquired from design documents provided by ALDOT. Where available, field data such as concrete compressive strength was used in the models to make more accurate predictions of bent behavior.

Initial models were run to assess the magnitude of deflection expected to occur under lateral load testing. A target load was determined and simulated on each bent cap. In the case of the in service bridges, the resulting prediction was used to determine if the target load created a

20

sufficient, but not excessive, amount of force to be accurately measured in the field load testing operations. The AUNGES bents were designed to be tested to failure so the initial models were run to predict the amount of force required to fail the bents. The target values were used to create a loading schedule to be used in the field load tests. The target values were analyzed in FB Multipier to produce detailed profiles of behavior prediction for each pile during each load test. The results of these simulated load tests are presented in this chapter. The profiles were compared to the values determined from the data reduction of the load test data.

3.3 Alabama County Road 9 Bridge

The Macon County Road 9 bridge was under construction in the summer of 2014. The model bent featured four 31.5 feet long HP 14x89 piles with 5 feet of clear height above ground. The exterior piles were battered at 1.5/12 slope. All piles were encased with 30 inch diameter concrete encasements from the bottom of the pile cap to 5 feet below the expected ground surface. The piles were oriented for weak axis bending in the direction of lateral loading. The cap was modeled as a 31.75 inch by 31.75 inch square cap to approximate trapezoidal cap shown in the construction documents. Figure 3-1 shows FB Multipier rendering of the County Road 9 bridge bent.
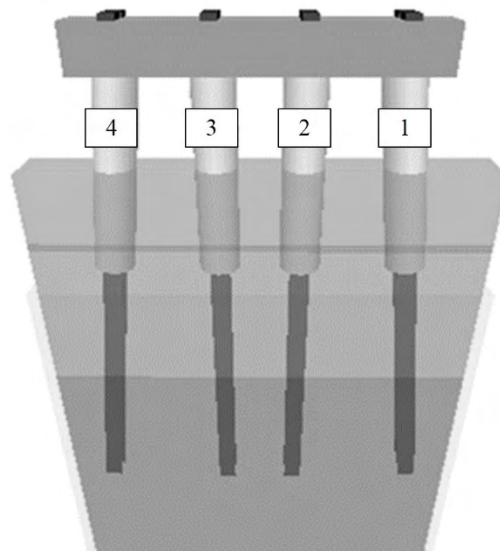
Figure 3-1 – FB Multipier Rendering of Macon County Road 9 Bridge Bent

The preliminary model was created using the bridge design plans and the boring logs provided by ALDOT. The pile properties were entered into FB Multipier from the AISC Manual of Steel Construction. An initial estimate of 5,000 psi was used for the compressive strength of the concrete encasements. The steel piles were assumed to have an elastic modulus of 29,000 ksi and a yield stress of 60 ksi. The p-y, q-z, and t-z curves for each soil layer were constructed from default FB Multipier options. The simulated load test featured ten load increments. The increments were as follows: 10 kips, 20 kips, 30 kips, 40 kips, 50 kips, 55 kips, 60 kips, 65 kips, 70 kips, and 75 kips. The axial load and bending moment predictions were compiled at node locations along the length of each pile for the distinct loading increments. The centerline deflection of the pile cap was also recorded at each loading increment. The first model created simulated the initial construction condition of the bent without the bridge deck in place. The second model simulated the bent with the added stiffness of a bridge deck, but without any additional axial load. The third model included the weight distribution of an LC-5 ALDOT load truck centered over the roadway and bent. The fourth model included the load truck with the

22

outer wheel centered over the exterior girder on the opposite the applied lateral load. A fifth model was created to simulate the reaction bent needed to field test the bent. The reaction model was subjected to the expected maximum magnitude of loading to ensure the design had sufficient strength and did not experience excessive deflection. Piles were named Pile 1, Pile 2, Pile 3, and Pile 4. Pile 4 was the leading pile, furthest away from the applied load and was battered. Pile 1, also battered, was the trailing pile closest to the load application point. Piles 2 and 3 were both vertical interior piles. This naming convention was used in every model simulation for the Macon County Road 9 bent. The piles were spaced at 8 feet center to center spacing which was greater than five times the diameter of the pile. Therefore, p-multipliers to reduce the lateral capacities of the piles were not needed and were not included in any model simulations.

3.3.1   Soil Properties

Boring logs were provided in the design drawings provided by ALDOT. SPT N-counts were used to construct a soil profile representative of the soil the piles were driven into. The soil was modeled in four discrete layers. Correlations of N-count values to soil properties such as friction angle and undrained shear strength were used. Figure 3-2 shows the pertinent soil parameters developed from the provided boring logs.
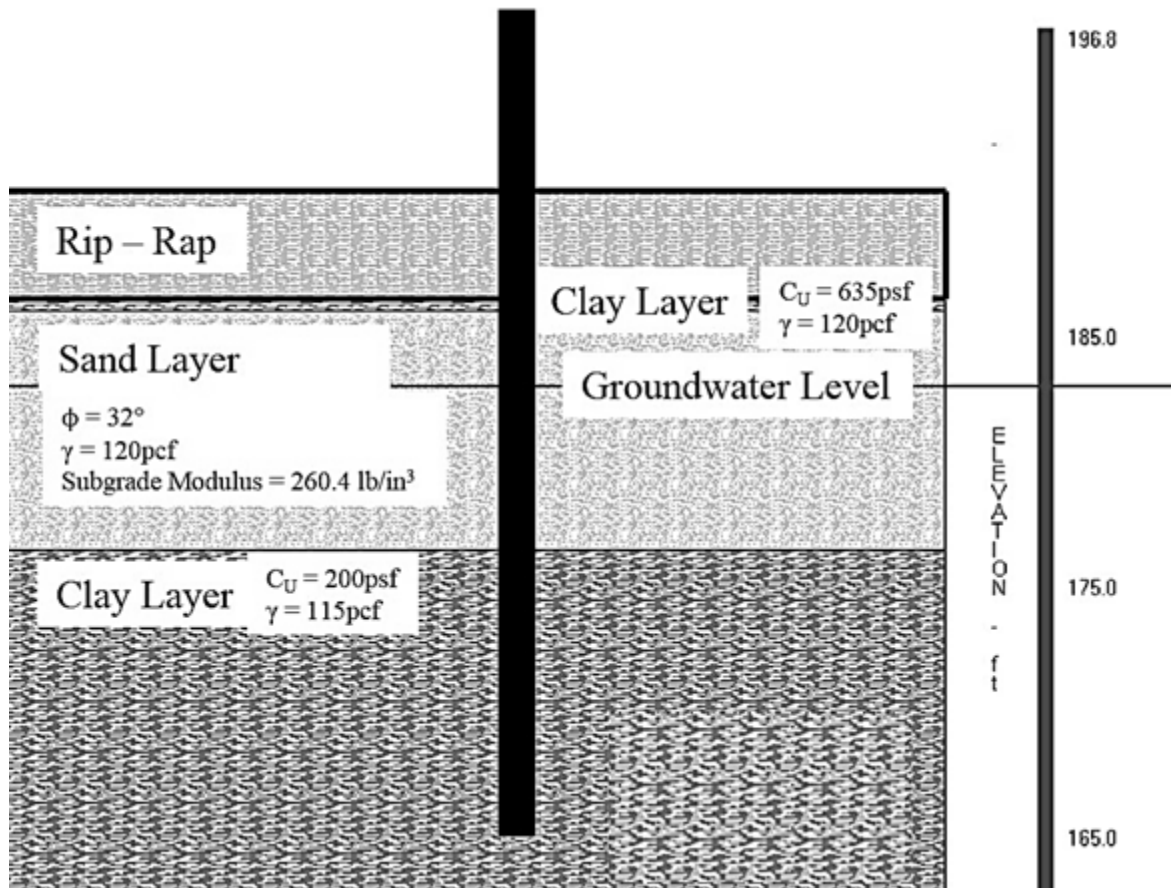
Figure 3-2 – Macon County Road 9 Bridge Soil and Pile Profile (Adapted from FB Multipier)

The top layer of clay was removed and replaced with rip-rap for scour resistance. The remaining soil was a small clay layer, a sand layer, and a bearing layer of clay. The rip-rap was neglected during the model simulation due to the uncertainty in determining the pertinent properties for simulation. The soil profile and properties discussed above were used for each load test simulation including the reaction bent analysis model.

3.3.2 Pre-Deck Bent Model and Behavior Prediction

The initial model was designed to simulate the first load test, which would occur prior to the casting of the bridge deck. The bent was modeled as a single, stand-alone bent. Figure 3-3 shows the predicted load versus deflection behavior of the bent without added deck stiffness.
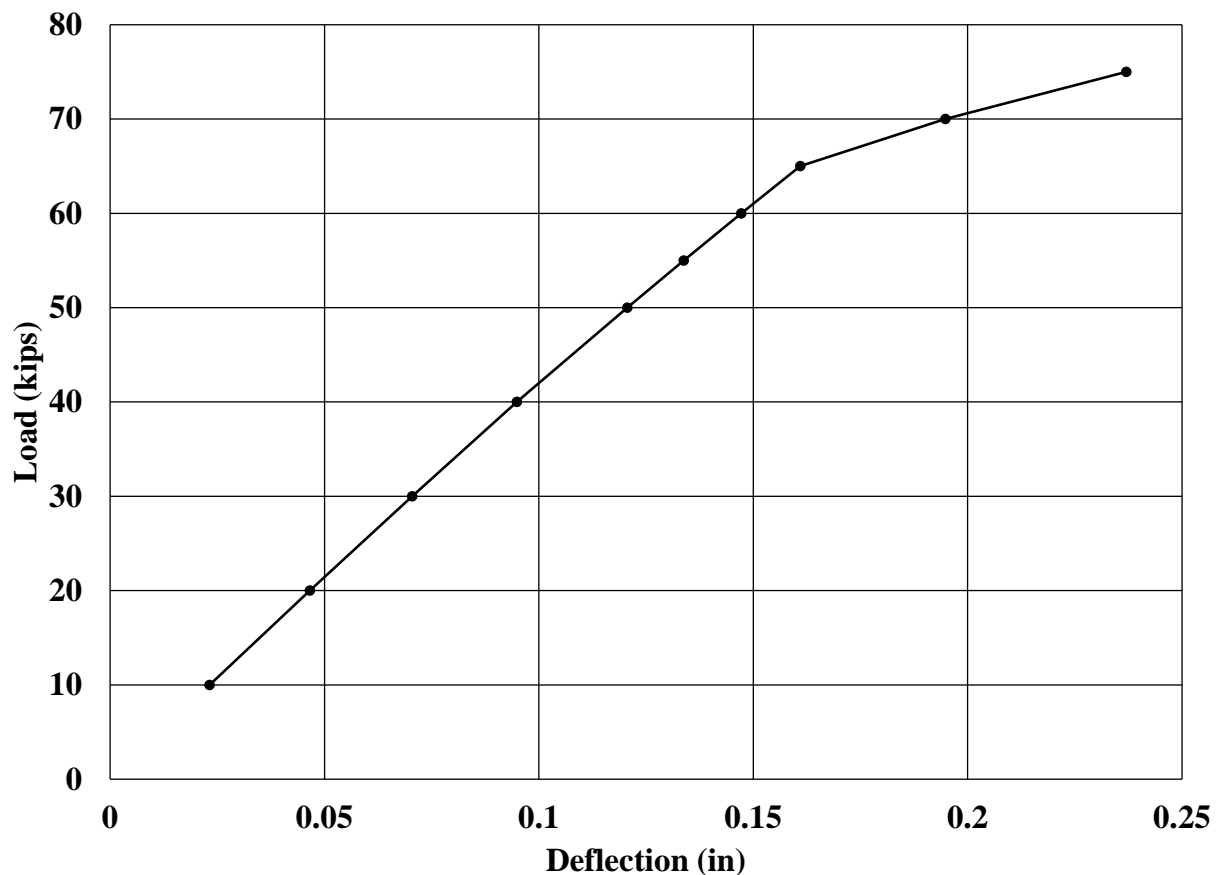
Figure 3-3 – Load versus Deflection Chart without Deck

The following figures, Figure 3-4, Figure 3-5, Figure 3-6, and Figure 3-7, show the pertinent results from model simulations. The figures show the theoretical distribution of axial load and bending moment with depth for each individual pile. Axial load profiles were used to analyze the effect of lateral load on the distribution of axial loads in the piles, and bending moment profiles were used to verify the accuracy of model predictions.
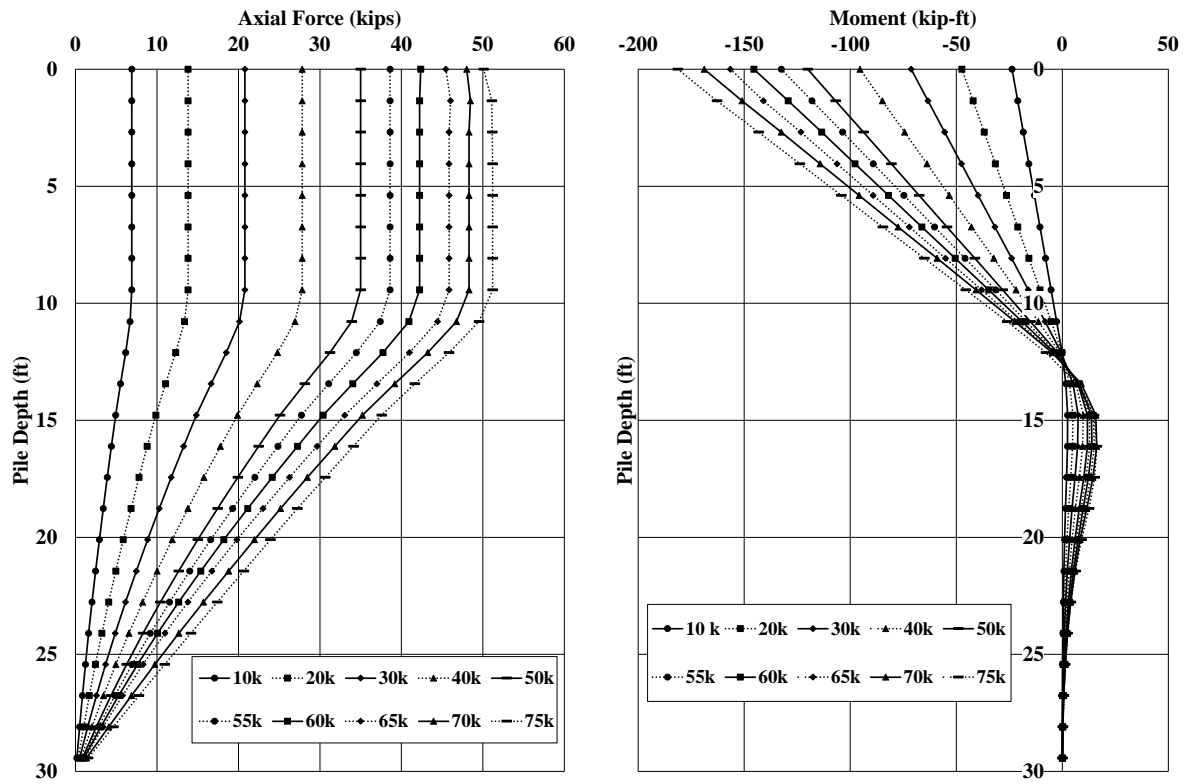
Figure 3-4 – Axial Load and Moment Profiles for Pile 1 without Deck
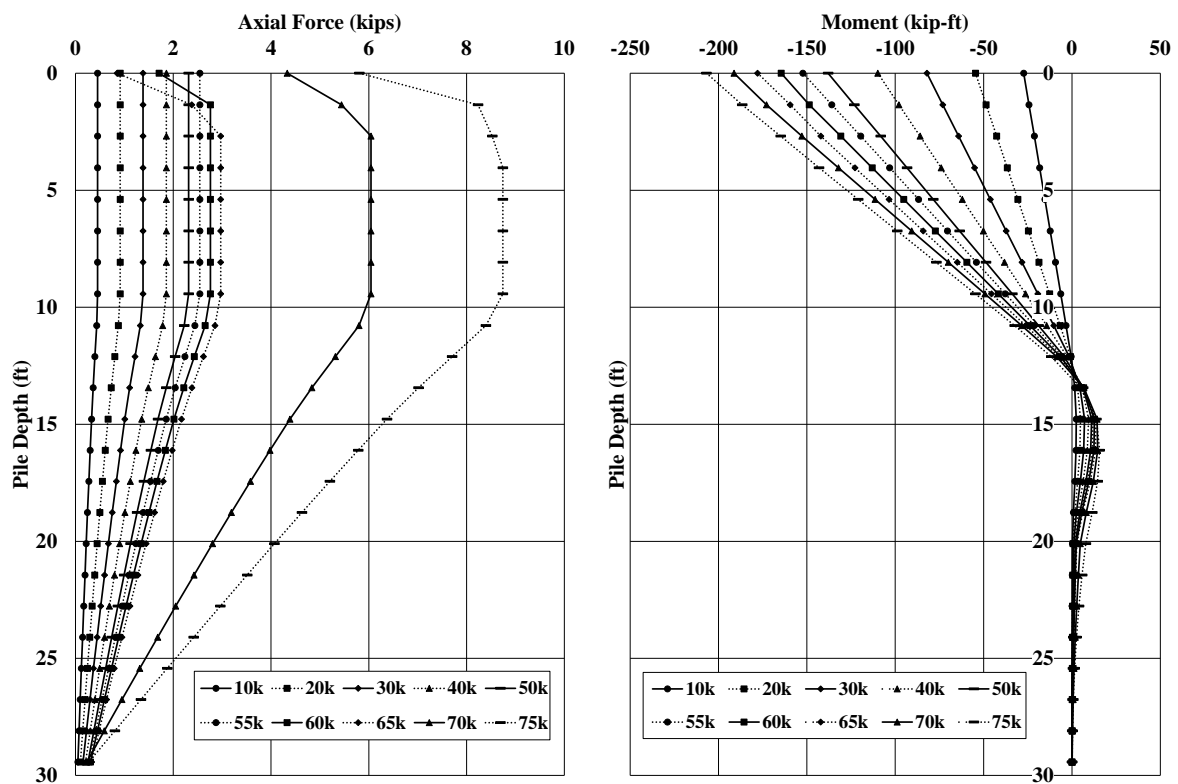
Figure 3-5 – Axial Load and Moment Profiles for Pile 2 without Deck

27
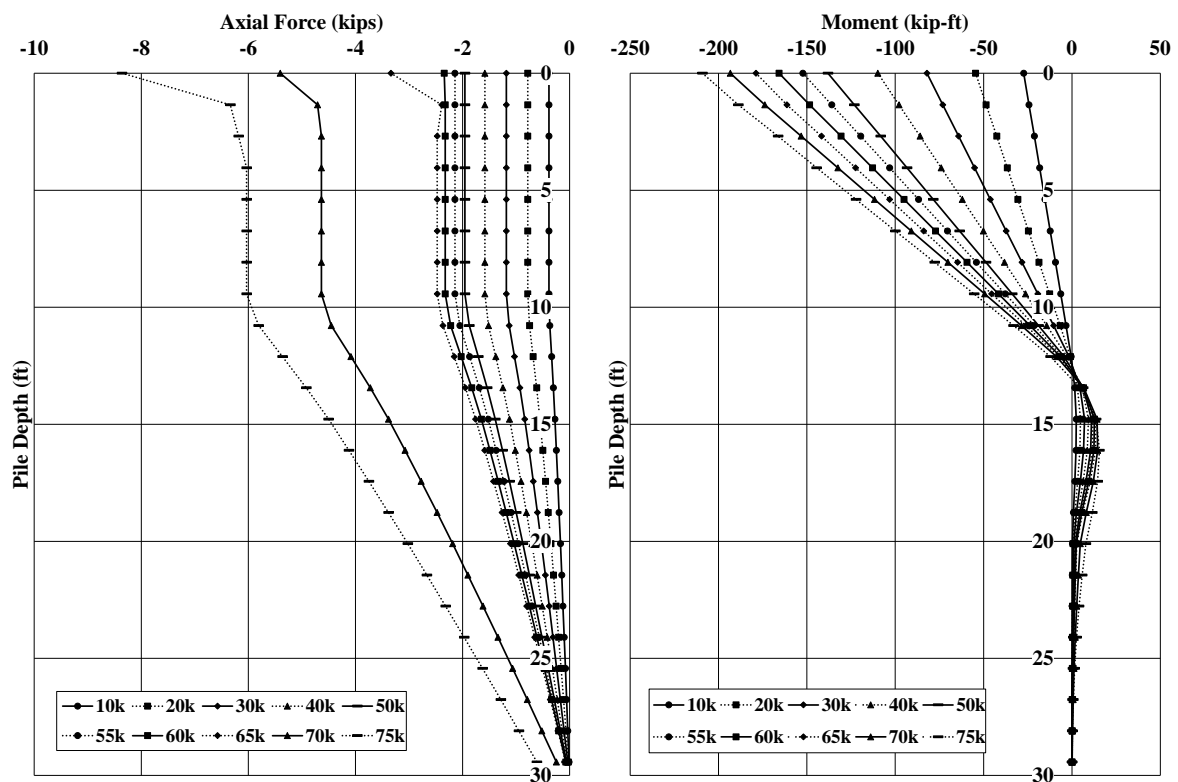
Figure 3-6 – Axial Load and Moment Profiles for Pile 3 without Deck

28
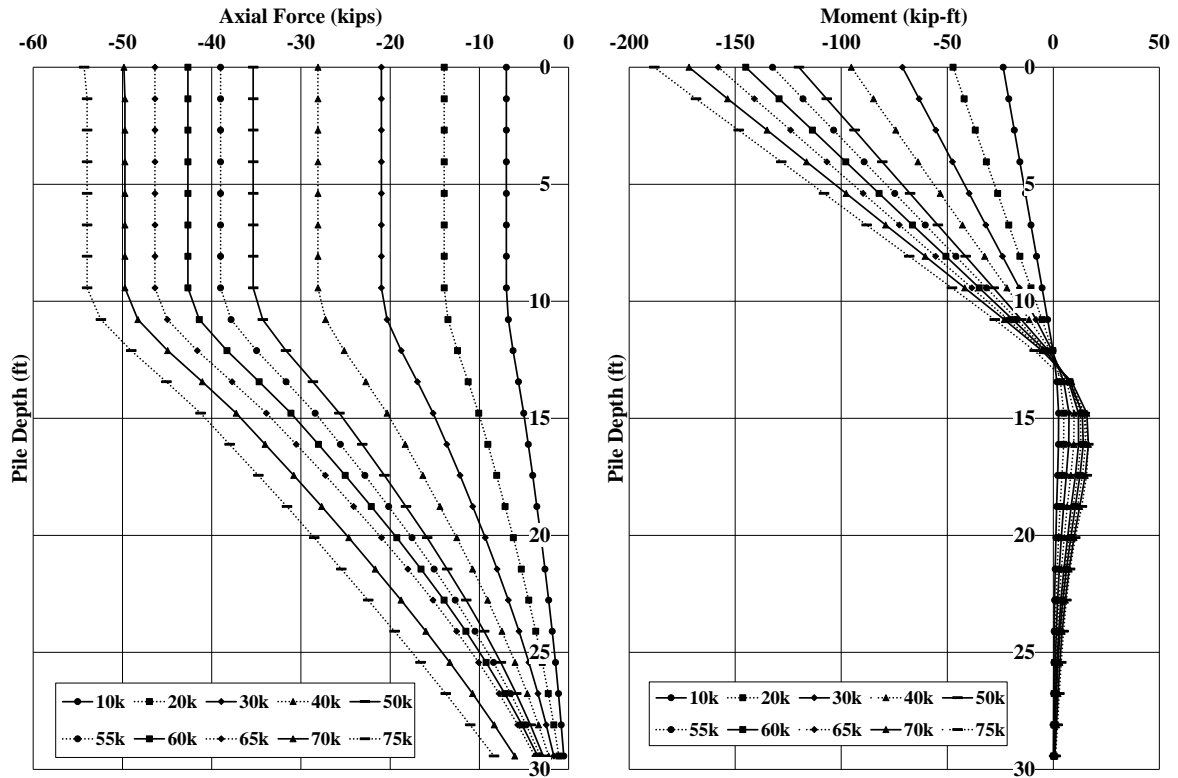
Figure 3-7 – Axial Load and Moment Profiles for Pile 4 without Deck

3.3.3 Post-Deck Bent Model and Behavior Prediction

The three models were created to simulate the load tests that would occur after the casting of

the bridge deck. The models were subjected to the same loading schedule as the model for the

bent without a deck. The first model simulated the load test of the bent with only the added

stiffness of the deck. Initial models assumed a spring value that was applied at the centerline of

the cap opposite the point of load application. After load testing, a more refined value for this

spring constant was determined by comparing the observed load versus deflection charts with

and with the bridge deck to determine the theoretical amount of added stiffness provided by the

bridge deck. This spring value was used in all subsequent models as a baseline for added deck

stiffness. All soil properties and structural parameters were the same as the model without the

added bridge deck stiffness. Figure 3-8 shows the load versus deflection behavior prediction for the bent with the addition of the bridge deck.
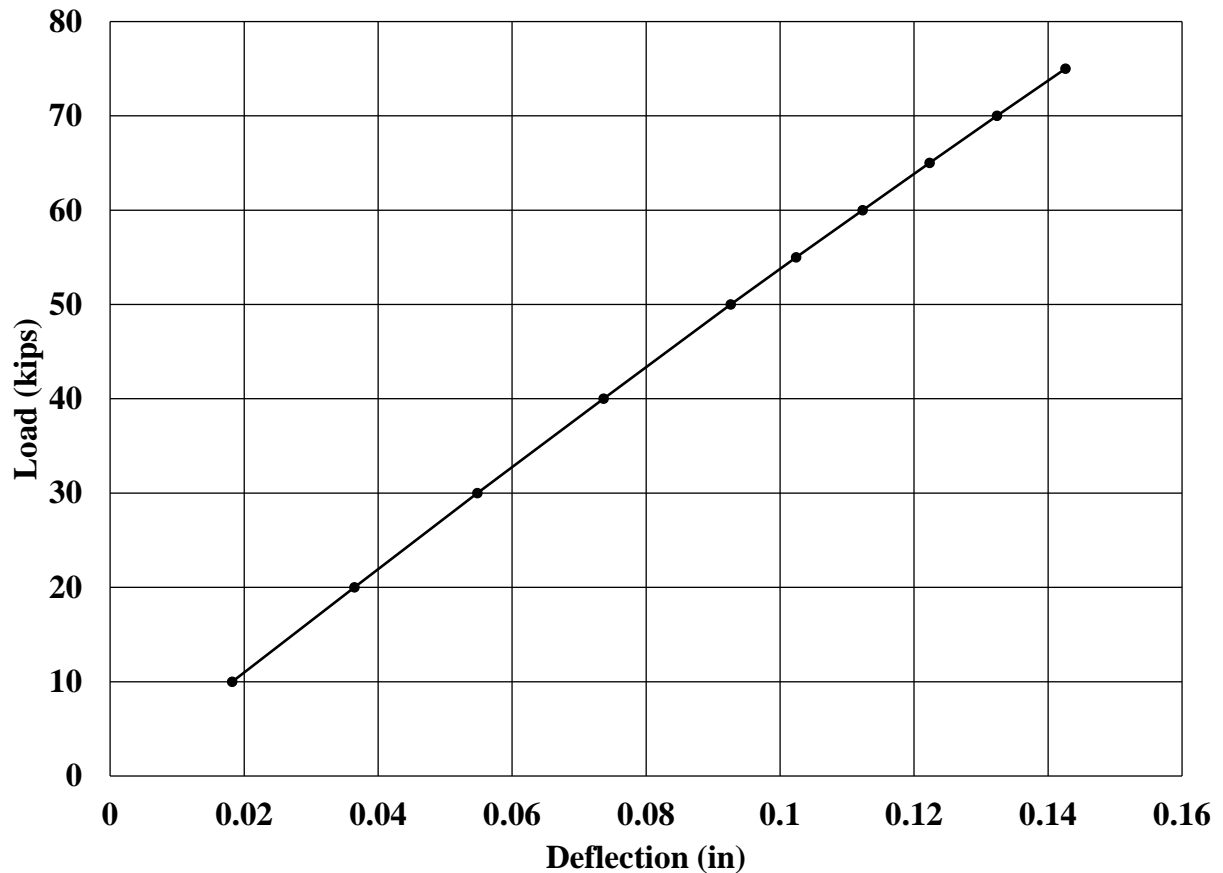
Figure 3-8 – Load versus Deflection Chart with Deck and no Load Truck

Figure 3-9, Figure 3-10, Figure 3-11, and Figure 3-12, show the pertinent results from model simulations. The figures show the theoretical distribution of axial load and bending moment with depth for each individual pile. Axial load profiles were used to analyze the effect of lateral load on the distribution of axial loads in the piles, and bending moment profiles were used to verify the accuracy of model predictions.

Figure 3-9 – Axial Load and Moment Profiles for Pile 1 with Deck and no Load Truck

Figure 3-10 – Axial Load and Moment Profiles for Pile 2 with Deck and no Load Truck

Figure 3-11 – Axial Load and Moment Profiles for Pile 3 with Deck and no Load Truck

32

Figure 3-12 – Axial Load and Moment Profiles for Pile 4 with Deck and no Load Truck

The third and fourth models of the Macon County Road 9 bent included the addition of axial load from an LC-5 Load truck. Figure 3-13 shows the layout wheel load magnitudes of the load truck.
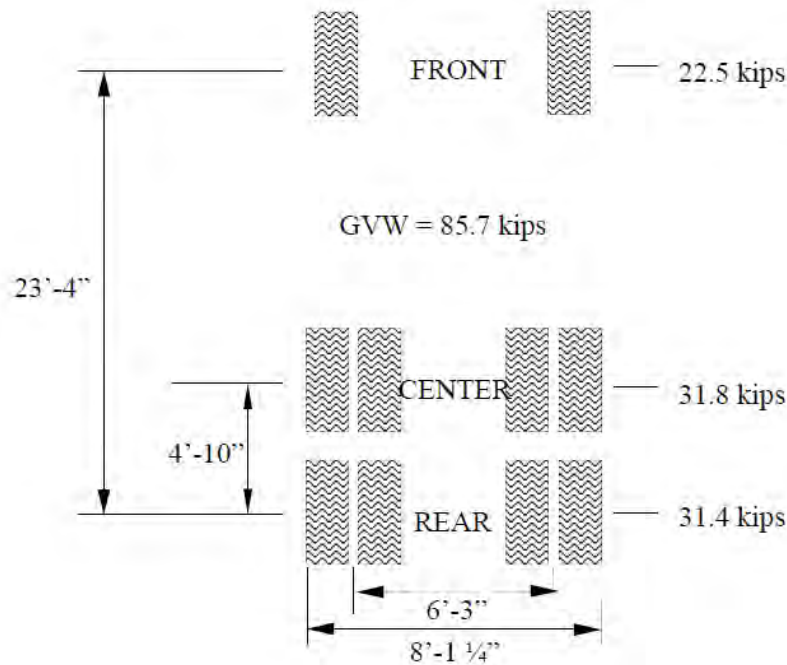
Figure 3-13 – Layout of LC-5 Load Truck (Miller 2013)

The third model simulated the placement of the center of the center axle over the center of the roadway and bent. All axial loads were assumed to be applied at bearing locations above the tops of the piles. For the placement over the center of the roadway and bent, it was assumed that the bearings for the two center piles each carried half of the load truck weight. This equated to axial loads of 42.85 kips applied at the central bearing locations. The simulated load test was then conducted at the same ten loading increments as the simulations mentioned above. Figure 3-14 shows the load versus deflection behavior prediction of the bent with the bridge deck attached and the load truck centered over the roadway and bent.
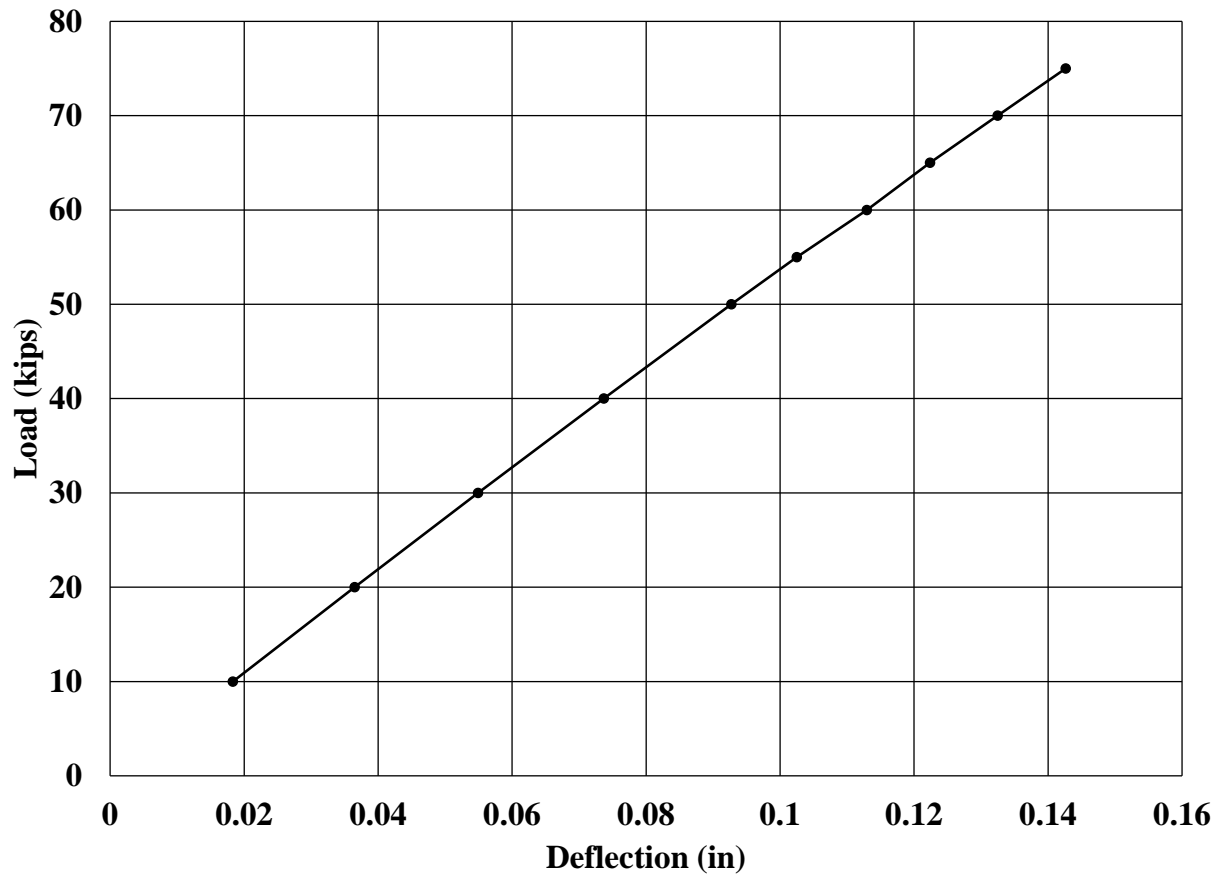
Figure 3-14 – Load versus Deflection Chart with Deck and Load Truck Centered over the Roadway

Figure 3-15, Figure 3-16, Figure 3-17, and Figure 3-18, show the pertinent results from model simulations. The figures show the theoretical distribution of axial load and bending moment with depth for each individual pile. Axial load profiles were used to analyze the effect of lateral load on the distribution of axial loads in the piles, and bending moment profiles were used to verify the accuracy of model predictions.
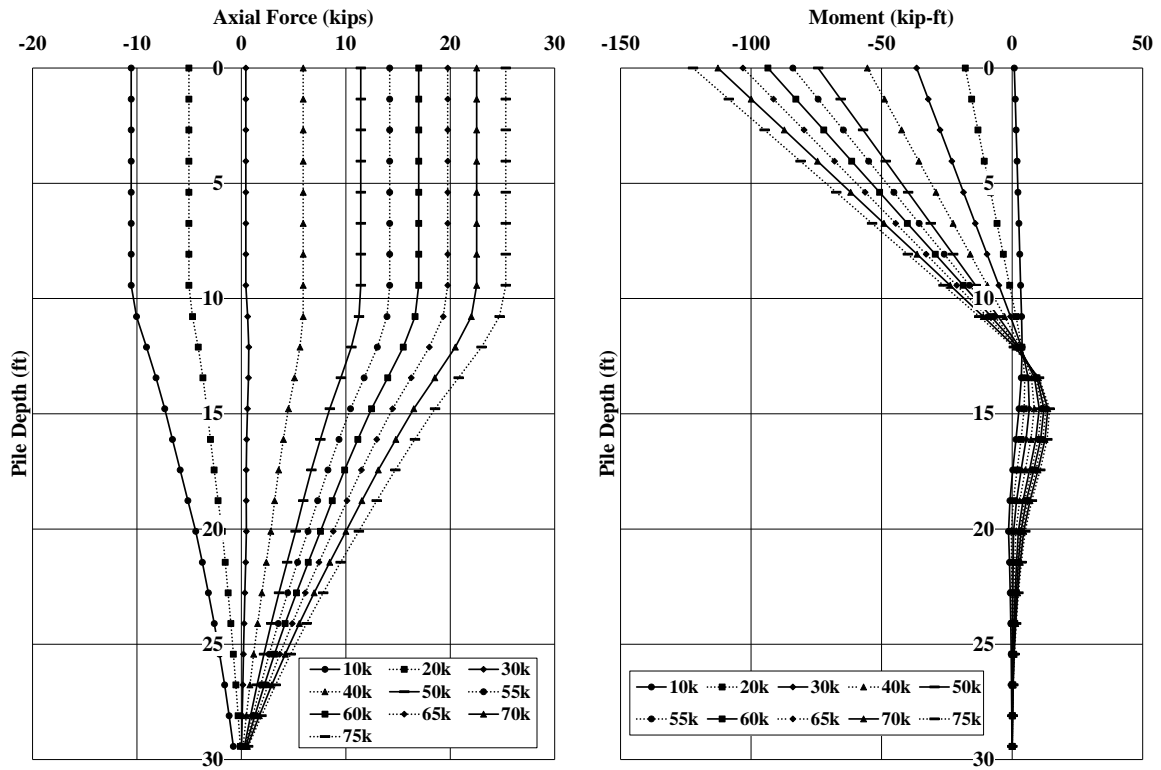
Figure 3-15 – Axial Load and Moment Profiles for Pile 1 and Load Truck Centered over the Roadway
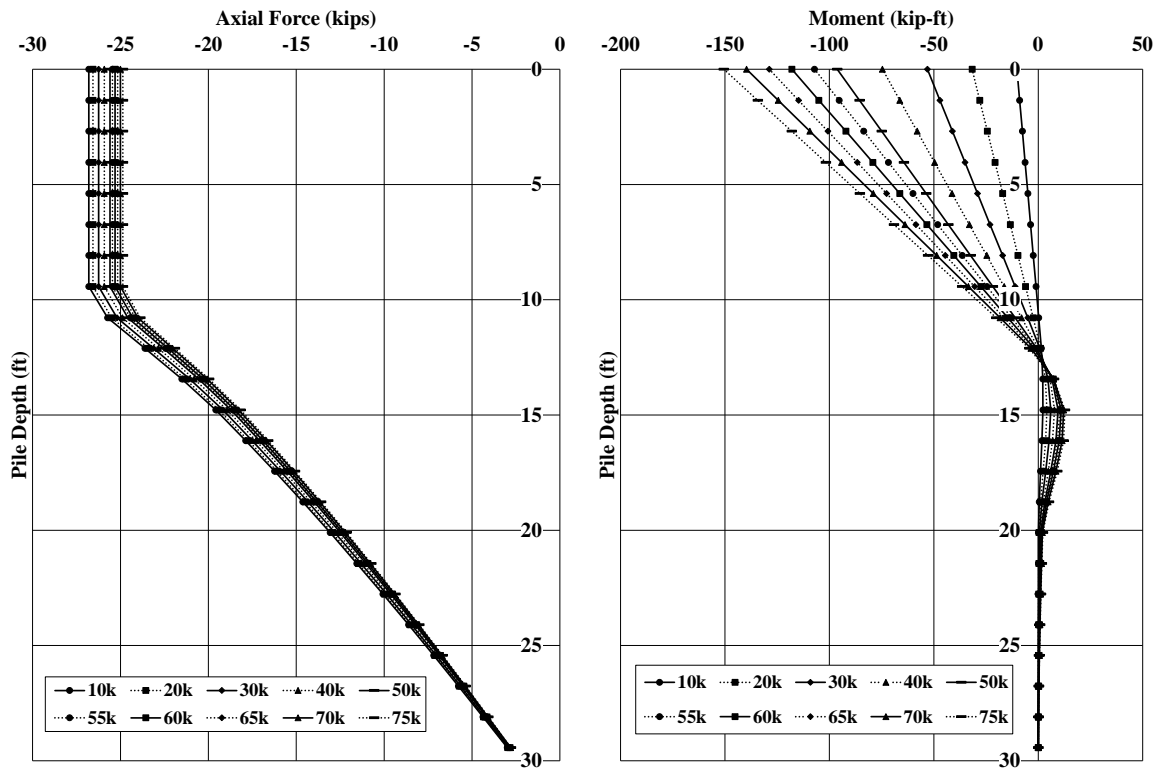
Figure 3-16 – Axial Load and Moment Profiles for Pile 2 with Load Truck Centered over the Roadway

36
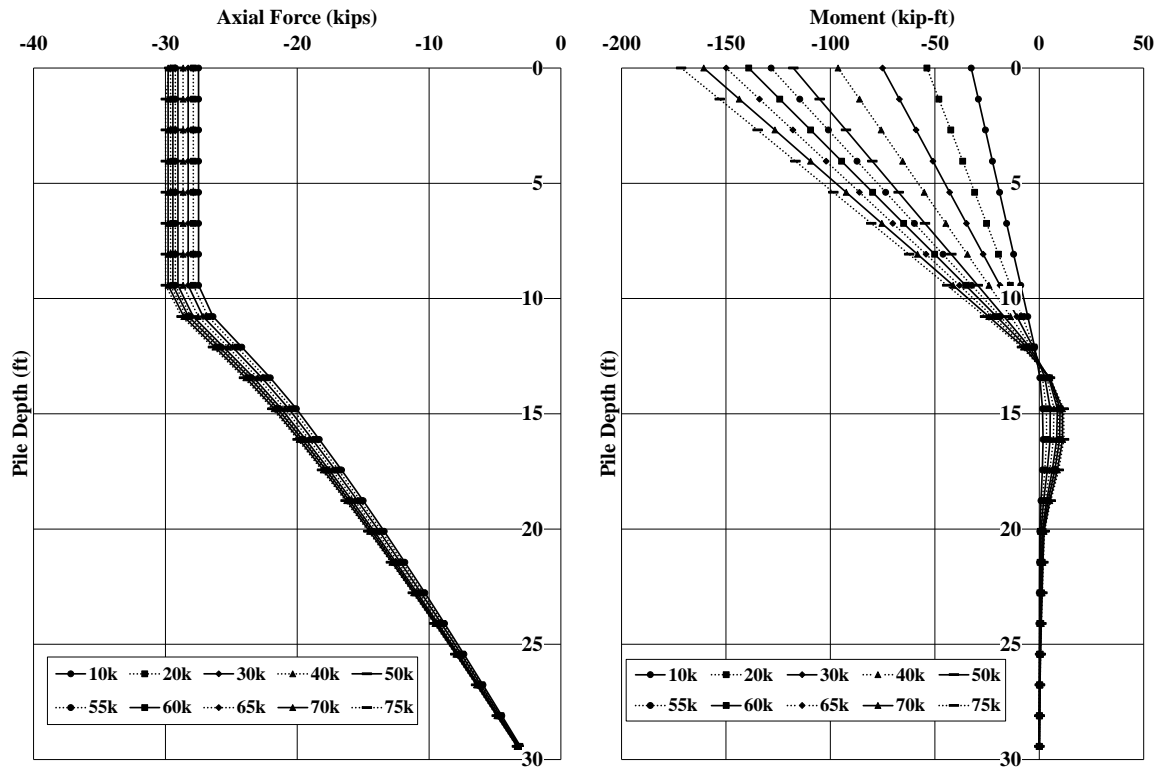
Figure 3-17 – Axial Load and Moment Profiles for Pile 3 with Load Truck Centered over the Roadway
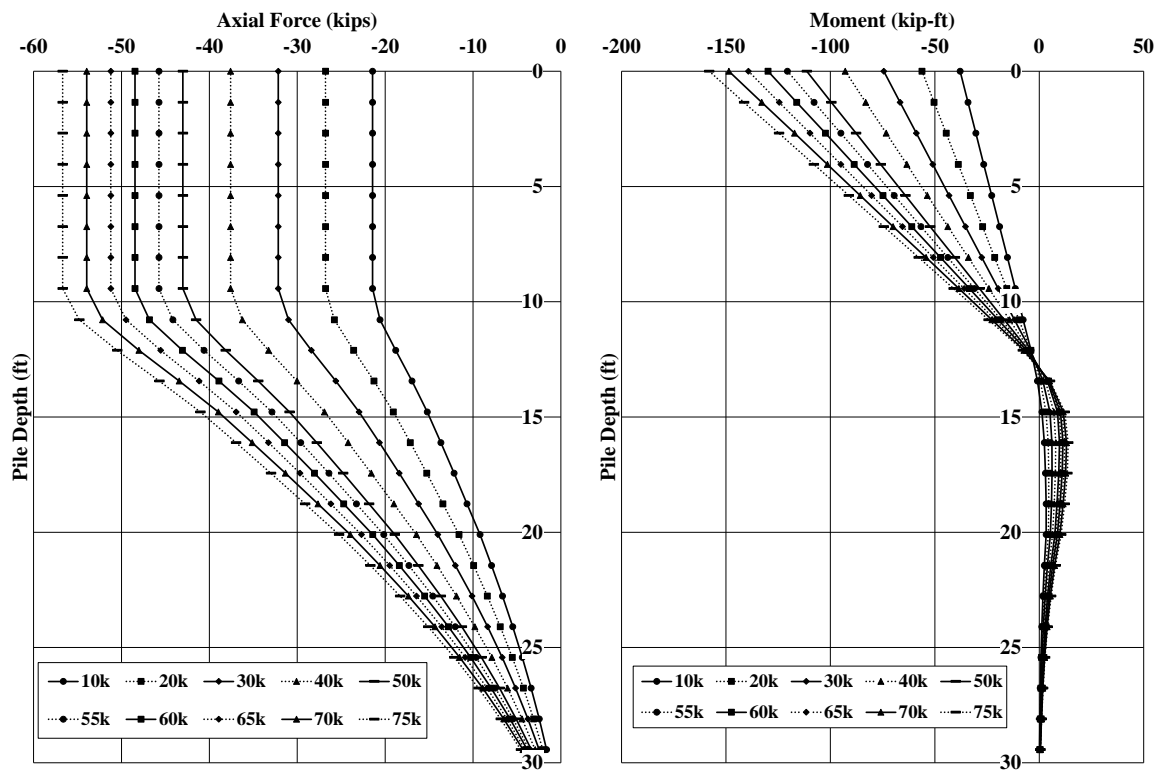
Figure 3-18 – Axial Load and Moment Profiles for Pile 4 with Load Truck Centered over the Roadway

37

The fourth model simulated the placement of the load truck's exterior tire at the edge of the exterior girder on the opposite side of the applied load. It was assumed that the majority of the load was transferred to the exterior girder and into the bent through the bearing location below it. A small portion was assumed to have been transferred into the bearing location below Pile 3. The axial load at the Pile 4 bearing location was 52.22 kips and the load at the Pile 3 bearing location was 33.48 kips. Figure 3-19 shows the prediction for the load versus deflection behavior of the bent with the load truck placed over the exterior girder.
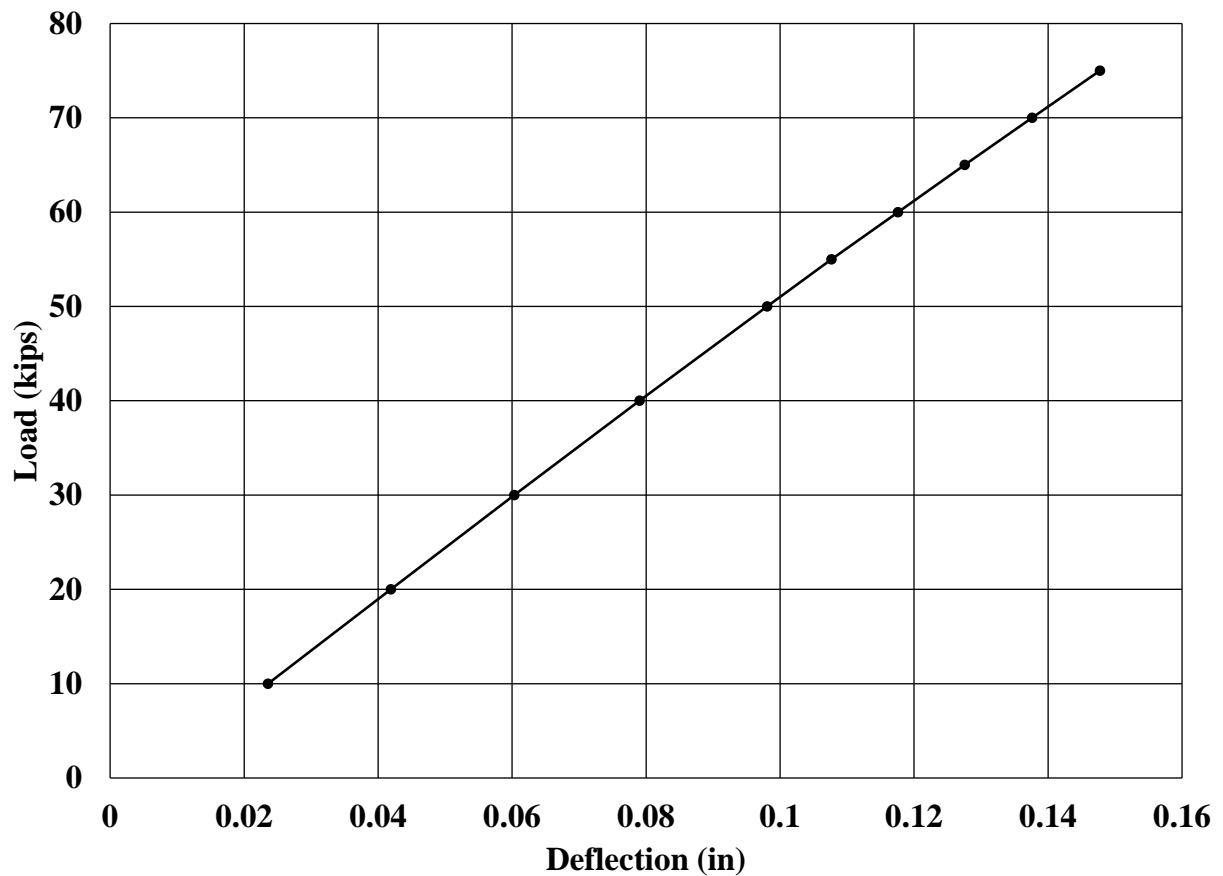
Figure 3-19 – Load versus Deflection Chart with Deck and Truck over the Exterior Girder

Figure 3-20, Figure 3-21, Figure 3-22, and Figure 3-23, show the pertinent results from model simulations. The figures show the theoretical distribution of axial load and bending moment with depth for each individual pile. Axial load profiles were used to analyze the effect

38

of lateral load on the distribution of axial loads in the piles, and bending moment profiles were used to verify the accuracy of model predictions.
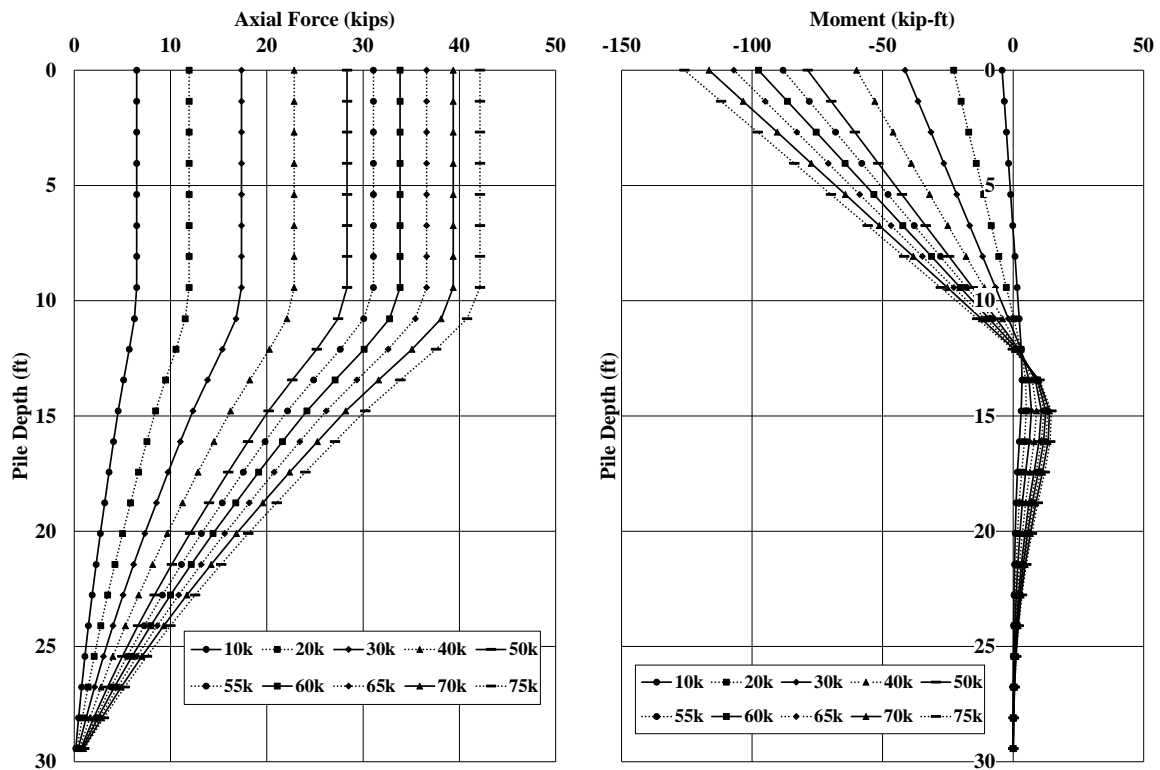
Figure 3-20 – Axial Load and Moment Profiles for Pile 1 with Load Truck over the Exterior Girder
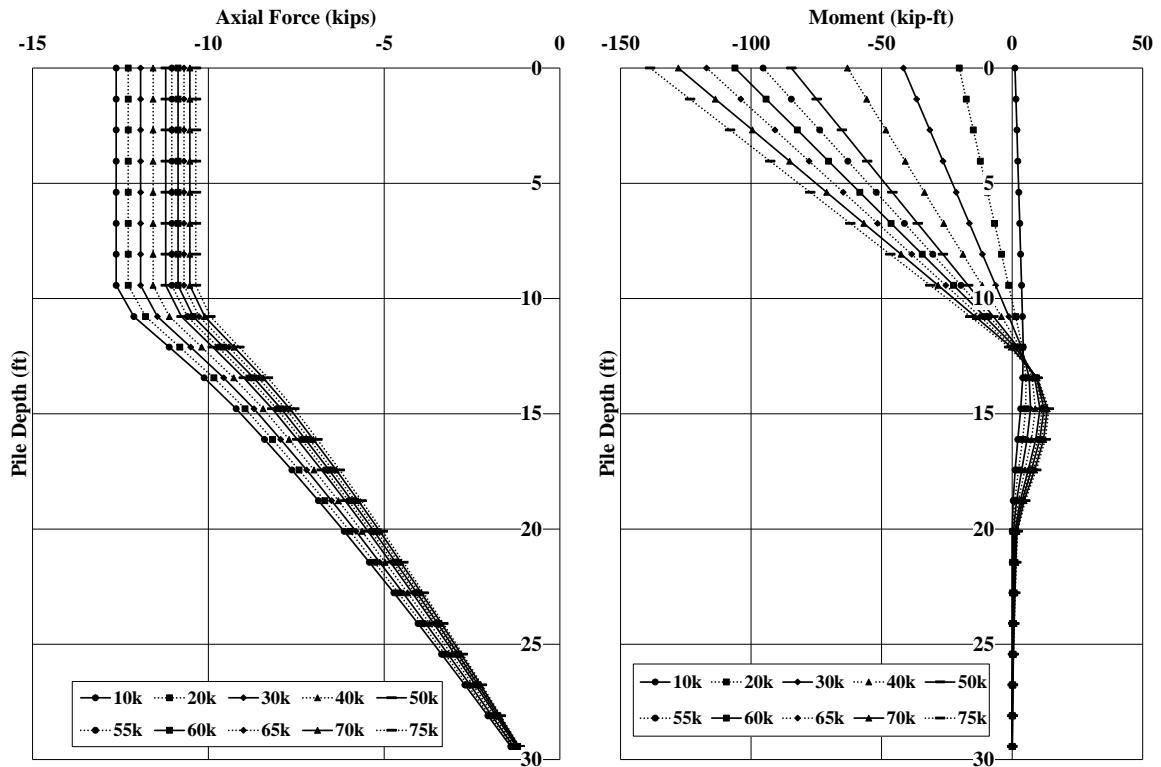
Figure 3-21 – Axial Load and Moment Profiles for Pile 2 with Load Truck over the Exterior Girder
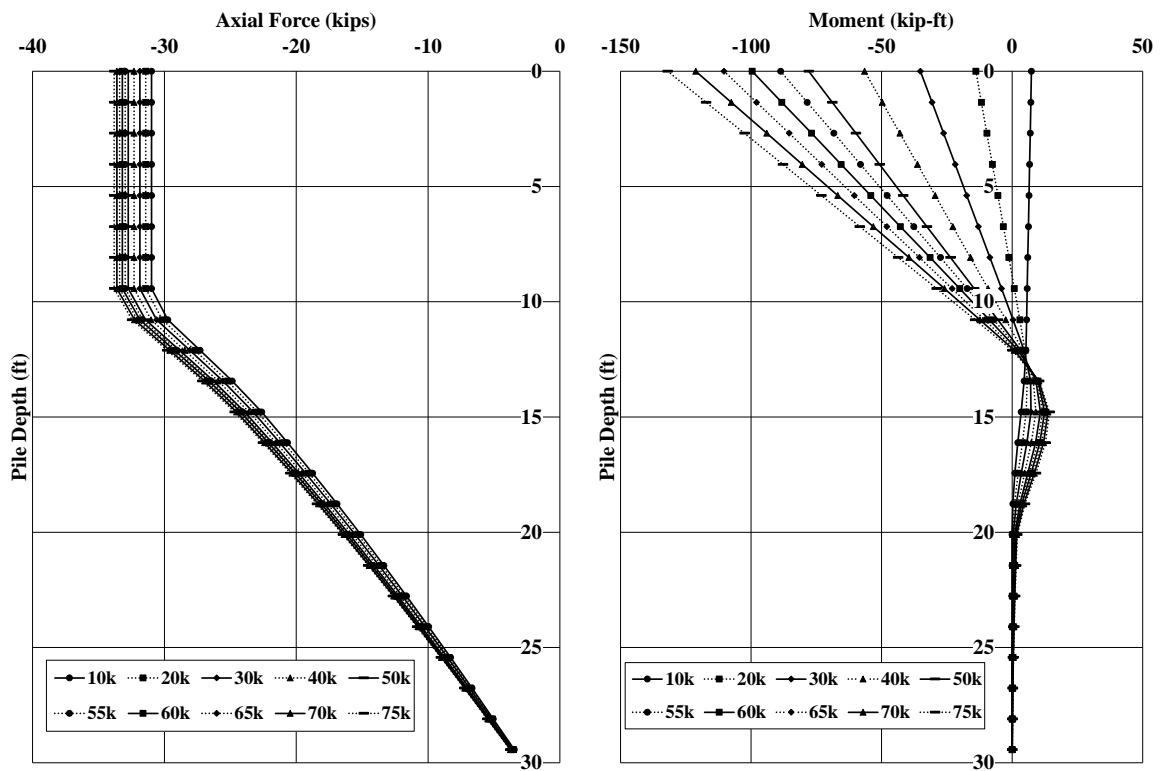
Figure 3-22 – Axial Load and Moment Profiles for Pile 3 with Load Truck over the Exterior Girder
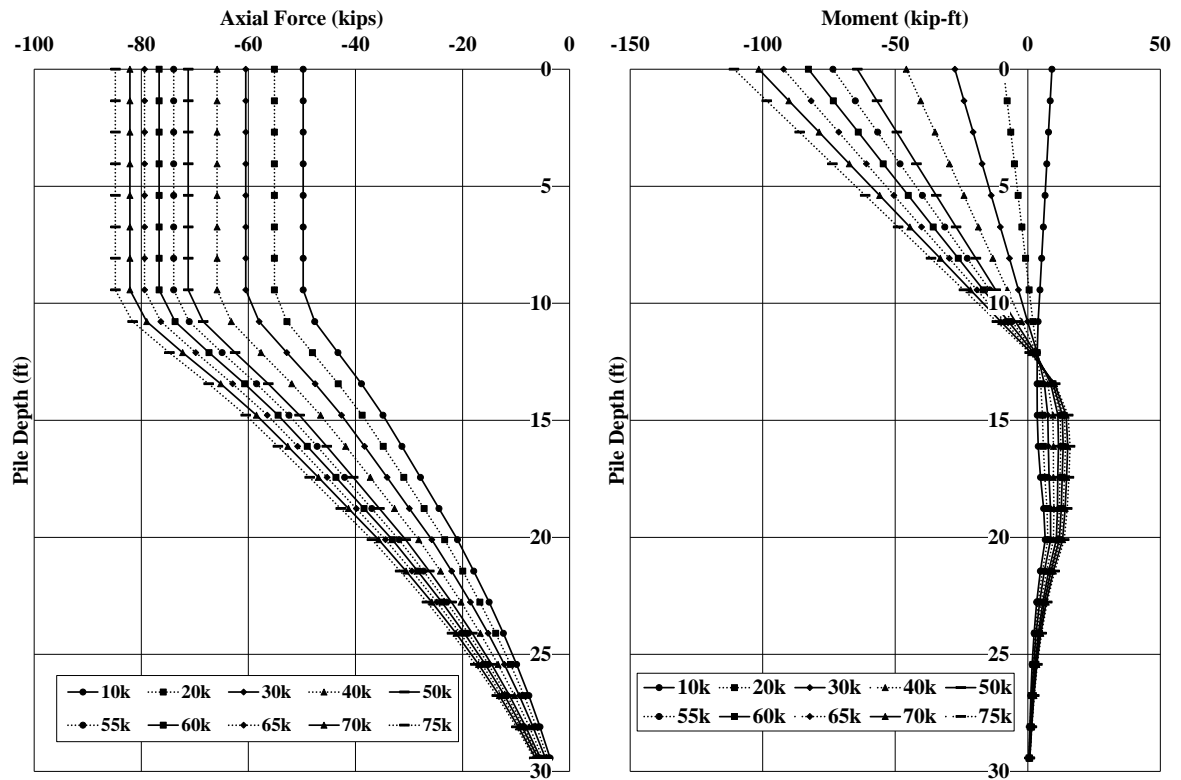
Figure 3-23 – Axial Load and Moment Profiles for Pile 4 with Load Truck over the Exterior Girder

The load versus deflection predictions for each of the simulated load tests were graphed together to compare the predicted behavior. Figure 3-24 shows the comparison of the predicted model load versus deflection curves.

41
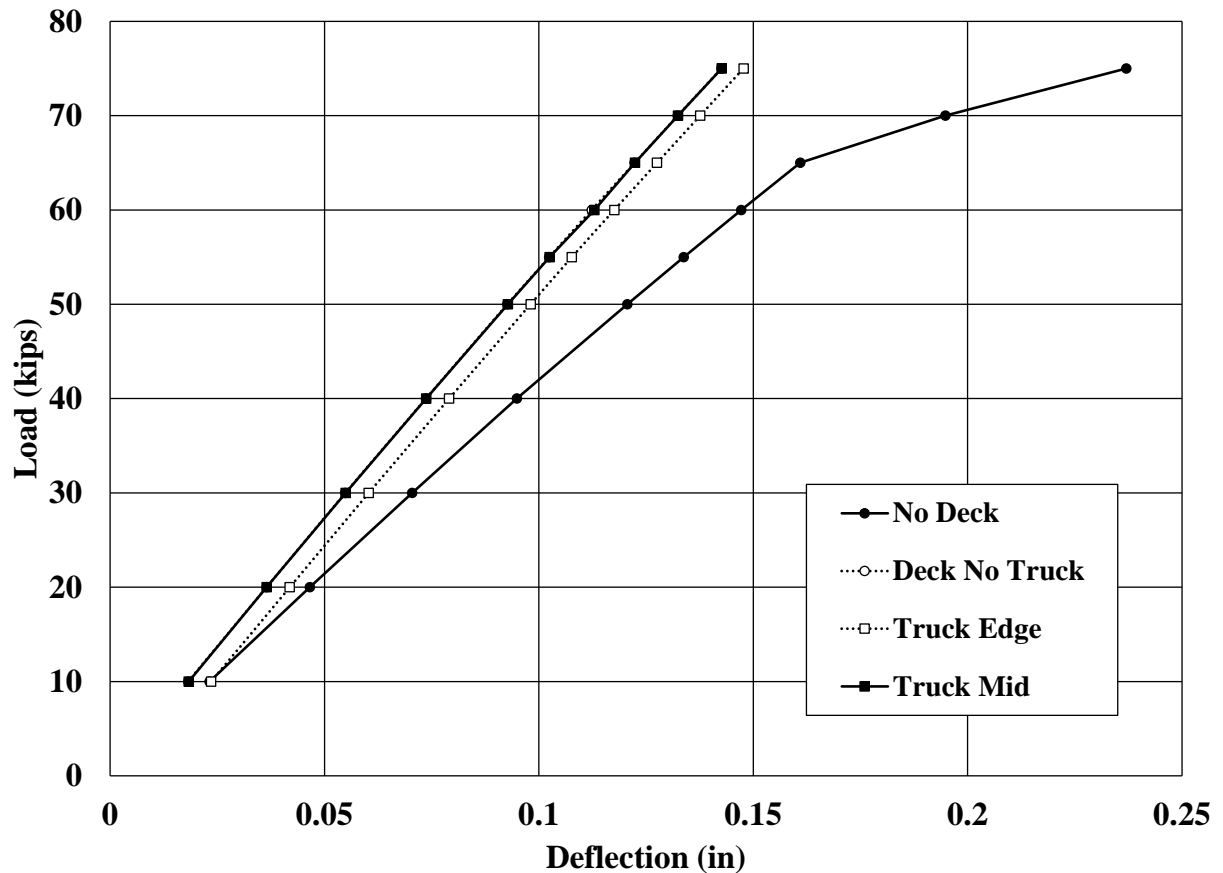
Figure 3-24 – Comparison of Load versus Deflection Curves from Model Simulations

The models predicted that the bent prior to the casting of the deck would experience the greatest deflection. Without the added stiffness of the bridge deck, the bent deflects more and seems to suggest a slight amount of yielding of the soil will occur as no structural elements reached stresses near yielding or failure according to the FB Multipier analysis. The models without the truck load and with the truck centered over the roadway and bent was expected to experience the least amount of lateral deflection and experience nearly identical deflections. The curve with the truck over the exterior girder was predicted to deflect at the same rate as the other two models with the bridge deck, but the addition of the load at the edge of the deck seems to have induced an initial deflection due to the unsymmetrical nature of the loading. The curves will

be compared to observed load versus deflection curves to determine the accuracy of modeling predictions and as a method of calibrating the models to produce realistic predictions.

3.3.4   Reaction Bent

The Macon County Road 9 bent required a reaction bent to react against to produce the lateral loads in the bent during field load testing. The soil profile used in the bent models was used to analyze the behavior of the proposed reaction bent except the top clay layer was not replaced with rip-rap as in the bent models. The reaction bent featured two 35 feet long HP14x89 piles. The piles were oriented for weak axis bending in the direction of lateral loading. The two piles were driven in line with a 4 feet center to center spacing. The pile closest to the test bent was battered towards the second reaction pile with a 1.5/12 slope. A piece of pile cutoff was to serve as a brace between the two reaction piles. Figure 3-25 shows the rendering of the FB Multipier model of the reaction bent.

Figure 3-25 – FB Multipier rendering of the Macon County Road 9 Bridge Reaction Bent

The reaction bent model was only analyzed at the maximum expected loading increment. The analysis was used to determine if the reaction bent had sufficient strength for the field lateral load tests, and to assure that the expected deflection did not exceed the stroke length of the jacks that were to be used to load the test bent.

3.4 U.S. Highway 331 Bridge

The second bridge bent modeled was a bridge on U.S. Highway 331 in southern Montgomery County, Alabama. The bridge featured 6 HP10x42 piles 28 feet long with 10 feet of clear height above ground. The piles were encased in 16 inch square concrete encasements. The exterior piles were battered at a 1.5/12 slope. The piles were oriented for weak axis bending in the direction of the lateral load. The piles and girders were spaced at 5 feet center to center. The pile cap was

modeled as a 21 inch by 21 inch square cap to approximate the existing trapezoidal cap. Figure 3-26 shows a rendering of the FB Multipier model of the Highway 331 bent.
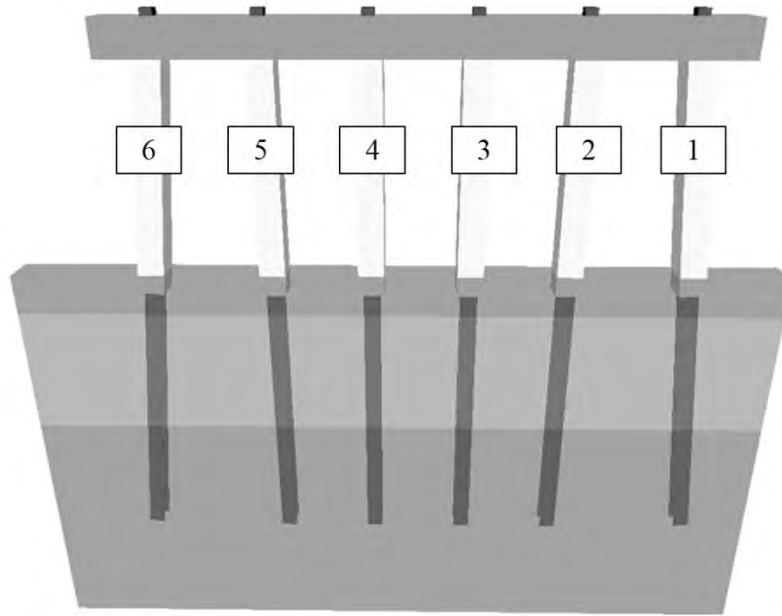
Figure 3-26 – FB Multipier Rendering of Highway 331 Bridge Bent

The model was created using construction documents provided by ALDOT. The pile properties were entered into FB Multipier from the AISC Manual of Steel Construction. An initial estimate of 4,000 psi was used for the compressive strength of the concrete encasements. The steel piles were assumed to have an elastic modulus of 29,000 ksi and a yield stress of 50 ksi. The p-y, q-z, and t-z curves for each soil layer were constructed from default FB Multipier options. The simulated load test featured ten load increments. The increments were as follows: 10 kips, 20 kips, 30 kips, 40 kips, 50 kips, 55 kips, 60 kips, 65 kips, 70 kips, and 75 kips. The axial load and bending moment predictions were compiled at node locations along the length of each pile for the distinct loading increments. The centerline deflection of the pile cap was also recorded at each loading increment. Two load tests were simulated. The first test was a test of the bent alone. The second test included the weight of an LC-5 load truck place over the exterior

girder opposite the application of the load. Piles were named Pile 1, Pile 2, Pile 3, Pile 4, Pile 5, and Pile 6. Pile 6 was the leading pile, furthest away from the applied load and was battered. Pile 1, also battered, was the trailing pile closest to the load application point. Piles 2, 3, 4, and 5 were all vertical interior piles. This naming convention was used in every model simulation for the Highway 331 bent. The piles were spaced at 8 feet center to center spacing which was greater than five times the diameter of the pile. Therefore, p-multipliers to reduce the lateral capacities of the piles were not needed and were not included in any model simulations.

3.4.1   Soil Properties

The soil profile was compiled using SPT boring logs included in the construction documents. Three distinct soil layers were modeled. The pertinent soil properties used for the model analysis were determined using the SPT N-counts included with the boring logs. Figure 3-27 shows the soil profile used for model analysis and the pertinent soil properties for each soil layer. The water table was not identified in the provided boring logs, so it was not included in the soil profile.
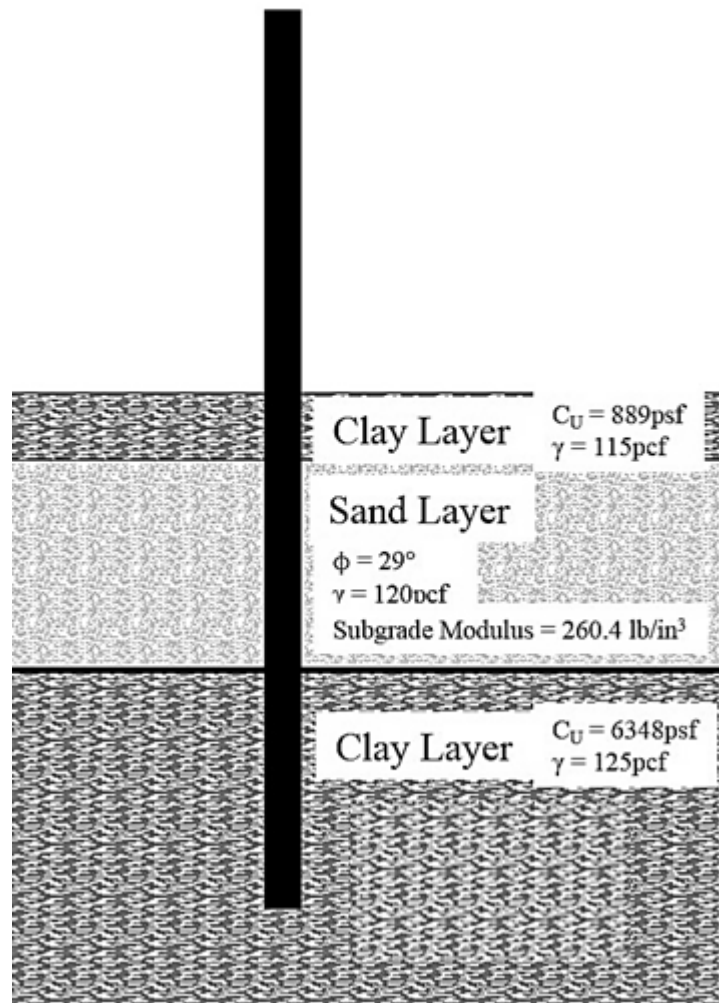
Figure 3-27 – Highway 331 Bridge Soil and Pile Profile (Adapted from FB Multipier)

Clay Layer $C_U = 889psf$ $\gamma = 115pcf$

Sand Layer $\phi = 29°$ $\gamma = 120pcf$ Subgrade Modulus = 260.4 lb/in³

Clay Layer $C_U = 6348psf$ $\gamma = 125pcf$

3.4.2   Bent Model and Behavior Prediction

The initial model simulated the test bent with no additional load truck loading applied. The stiffness of the attached bridge deck was modeled as a spring attached to the center of the cap opposite the applied load. The spring stiffness used was the same as the spring stiffness used in the Alabama County Road 9 bent models. The stiffness value was calculated from observed differences in the load versus deflection behavior of the Alabama County Road 9 bent field tests.

Figure 3-28 shows the predicted load versus deflection behavior for the Highway 331 bridge bent without additional load truck axial load.
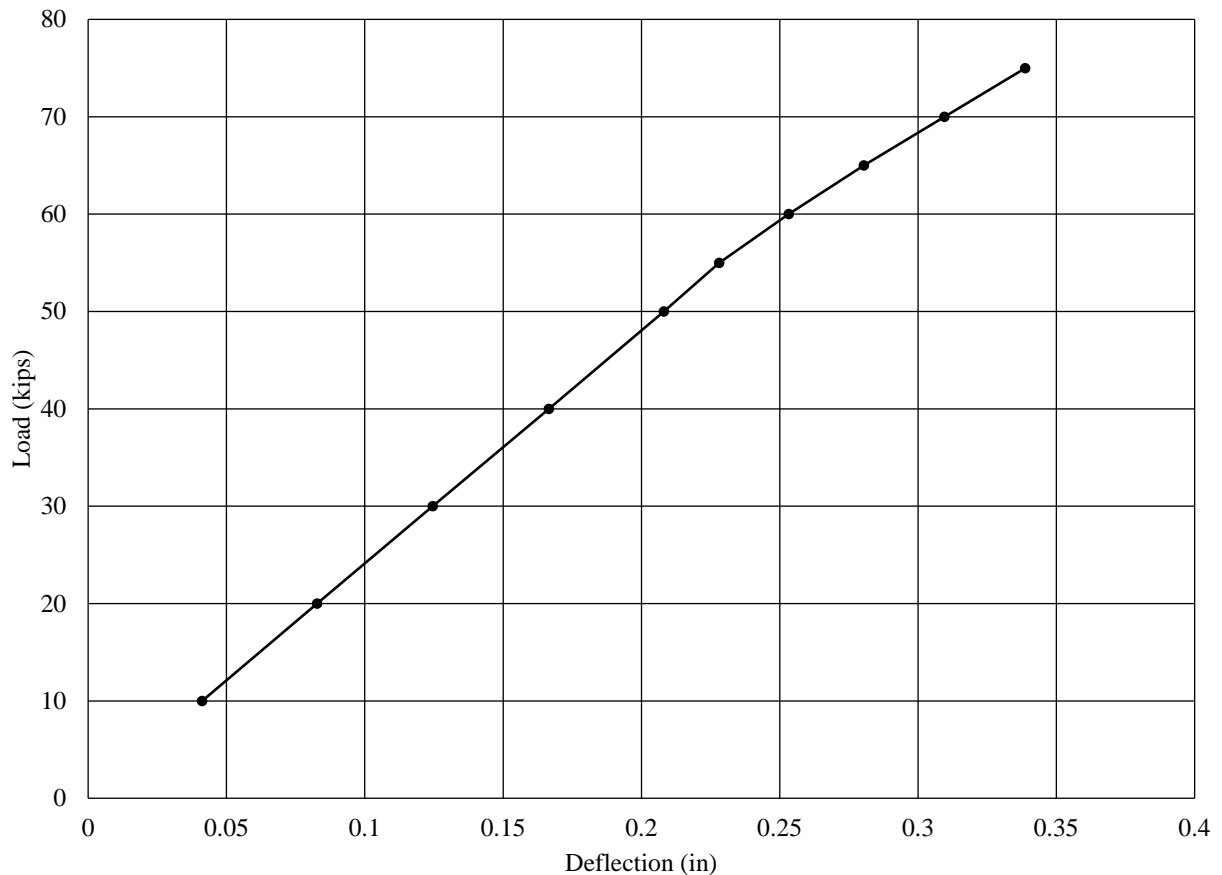
Figure 3-28 – Load versus Deflection Chart with no Load Truck

Figure 3-29, Figure 3-30, Figure 3-31, Figure 3-32, Figure 3-33, and Figure 3-34, show the pertinent results from model simulations. The figures show the theoretical distribution of axial load and bending moment with depth for each individual pile. Axial load profiles were used to analyze the effect of lateral load on the distribution of axial loads in the piles, and bending moment profiles were used to verify the accuracy of model predictions.

48
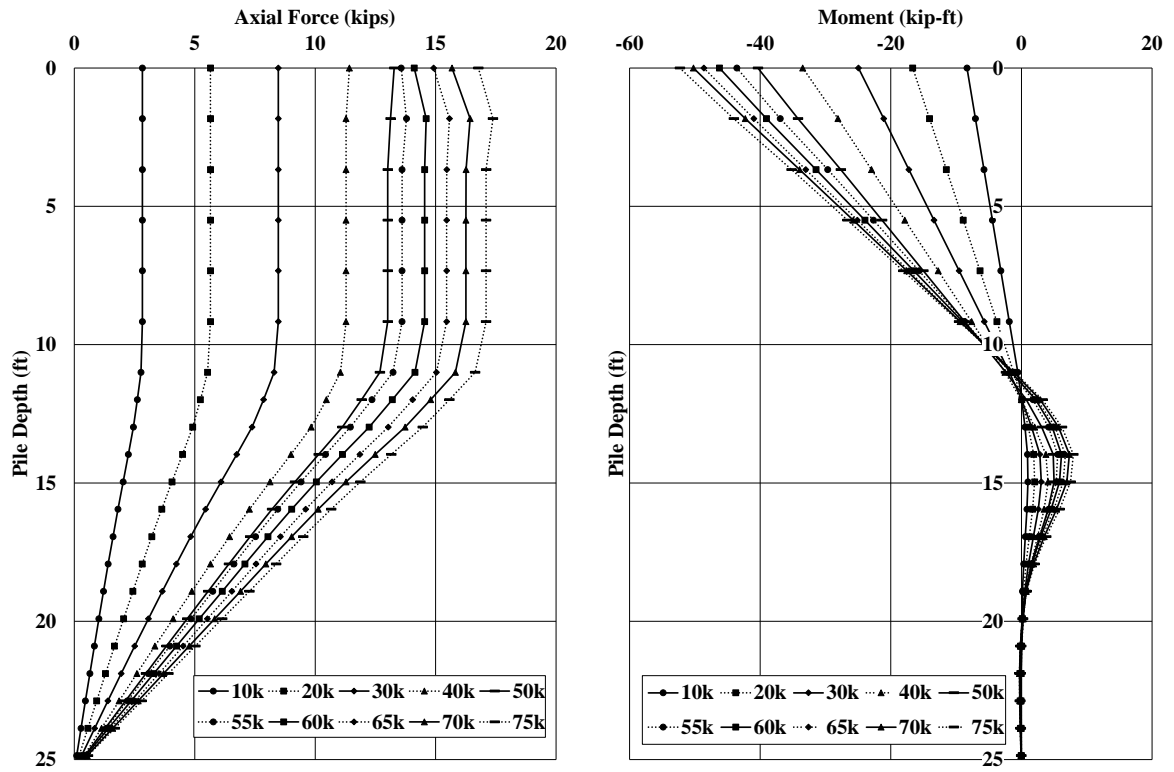
Figure 3-29 – Axial Load and Moment Profiles for Pile 1 with no Load Truck
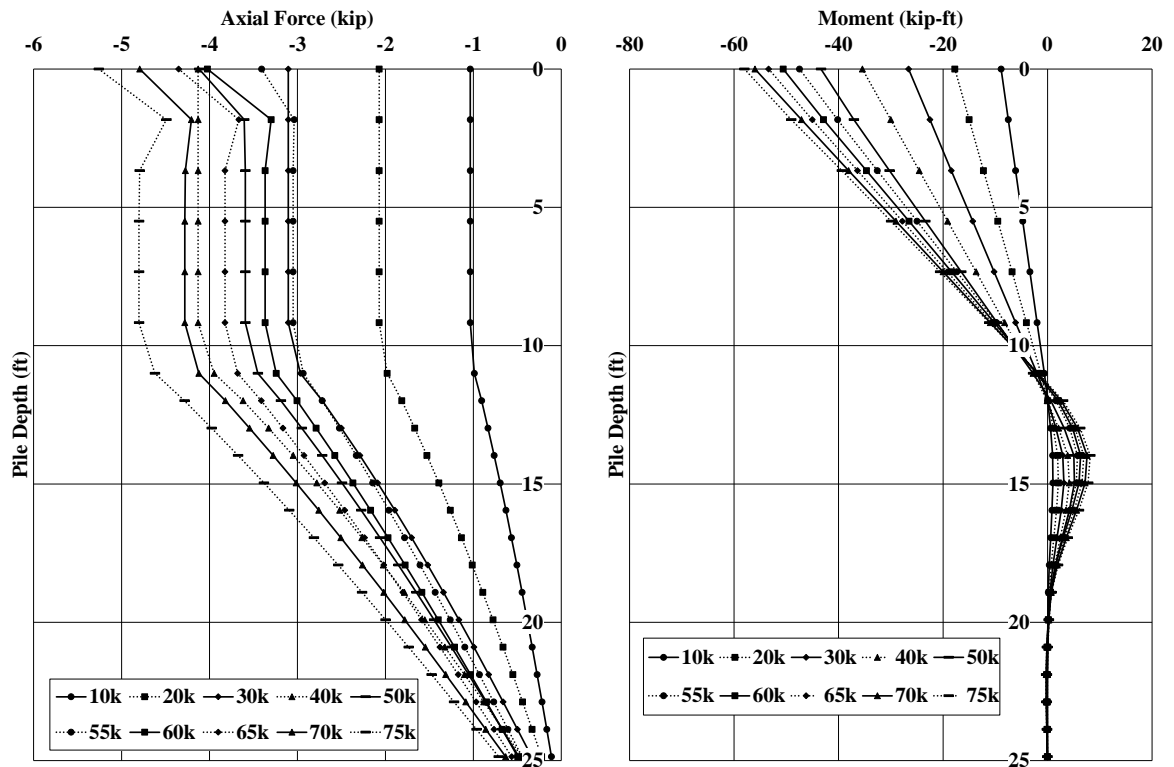
Figure 3-30 – Axial Load and Moment Profiles for Pile 2 with no Load Truck
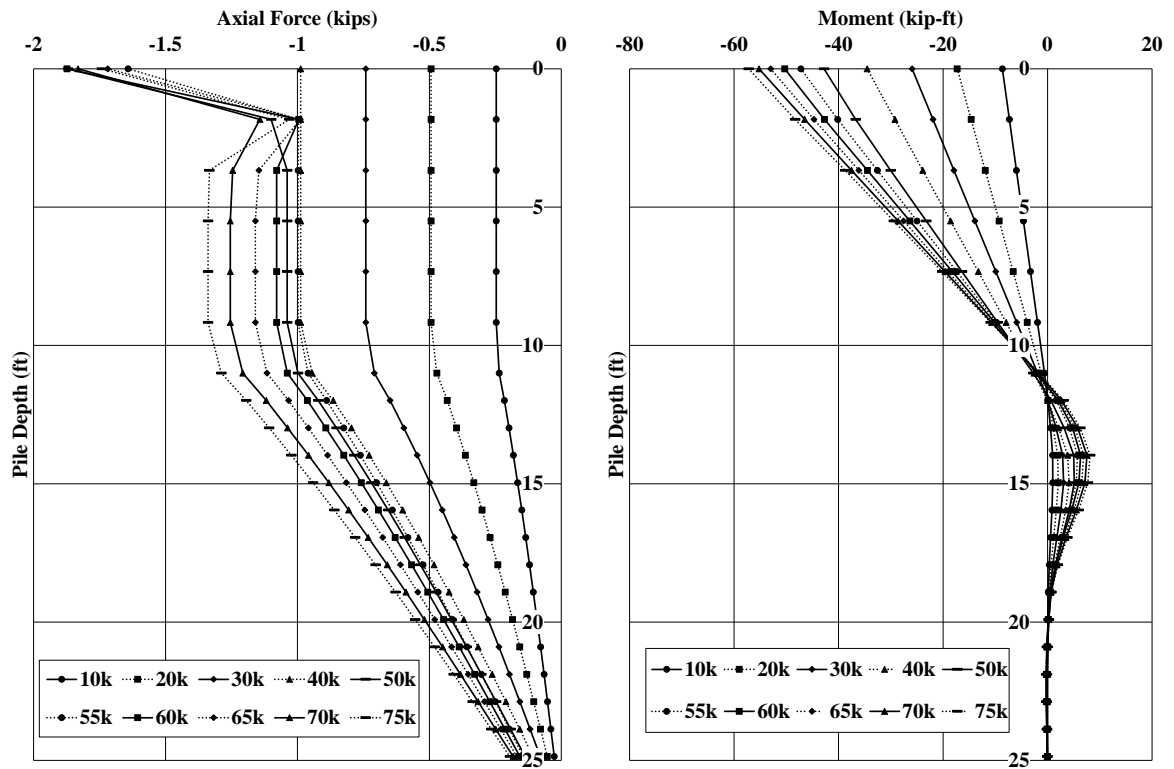
Figure 3-31 – Axial Load and Moment Profiles for Pile 3 with no Load Truck
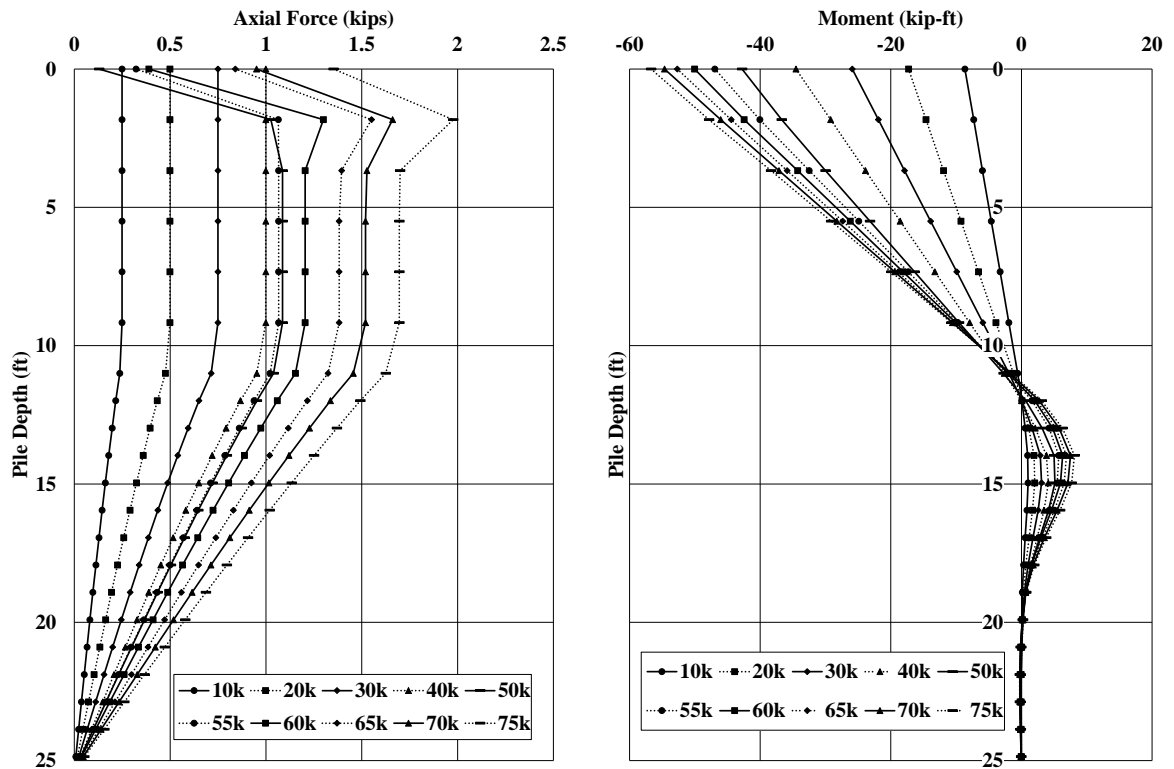
Figure 3-32 – Axial Load and Moment Profiles for Pile 4 with no Load Truck
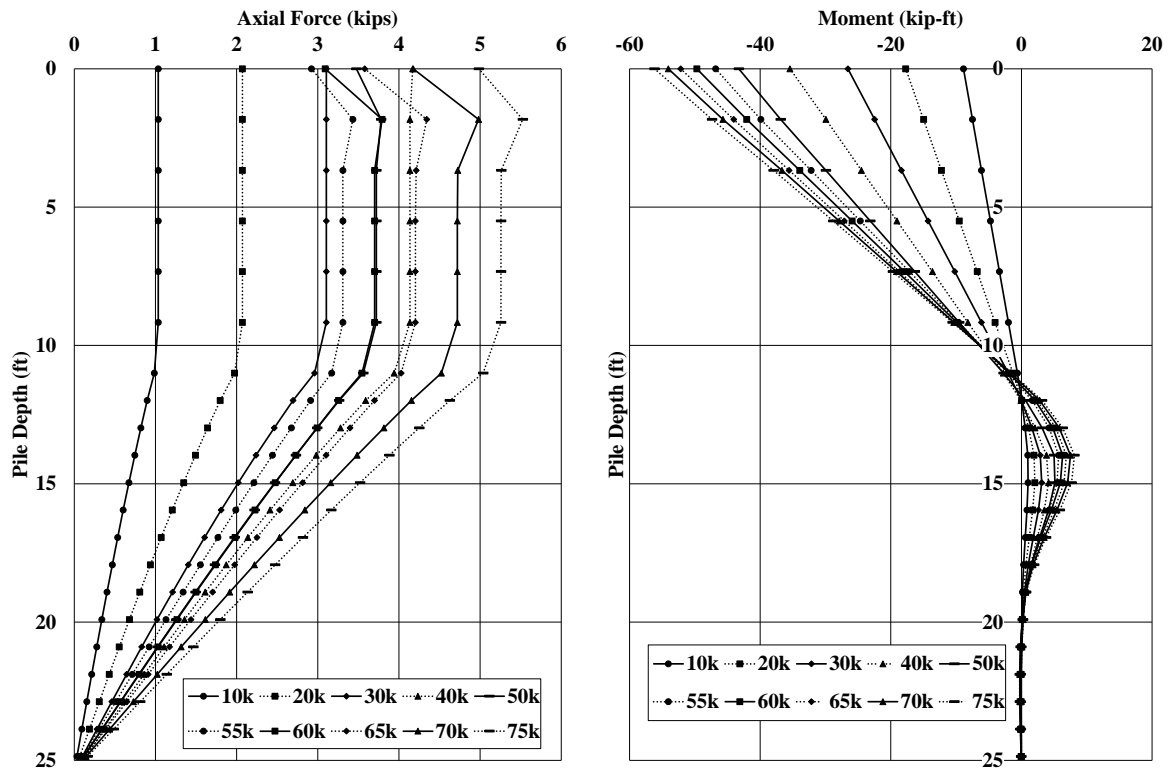
Figure 3-33 – Axial Load and Moment Profiles for Pile 5 with no Load Truck
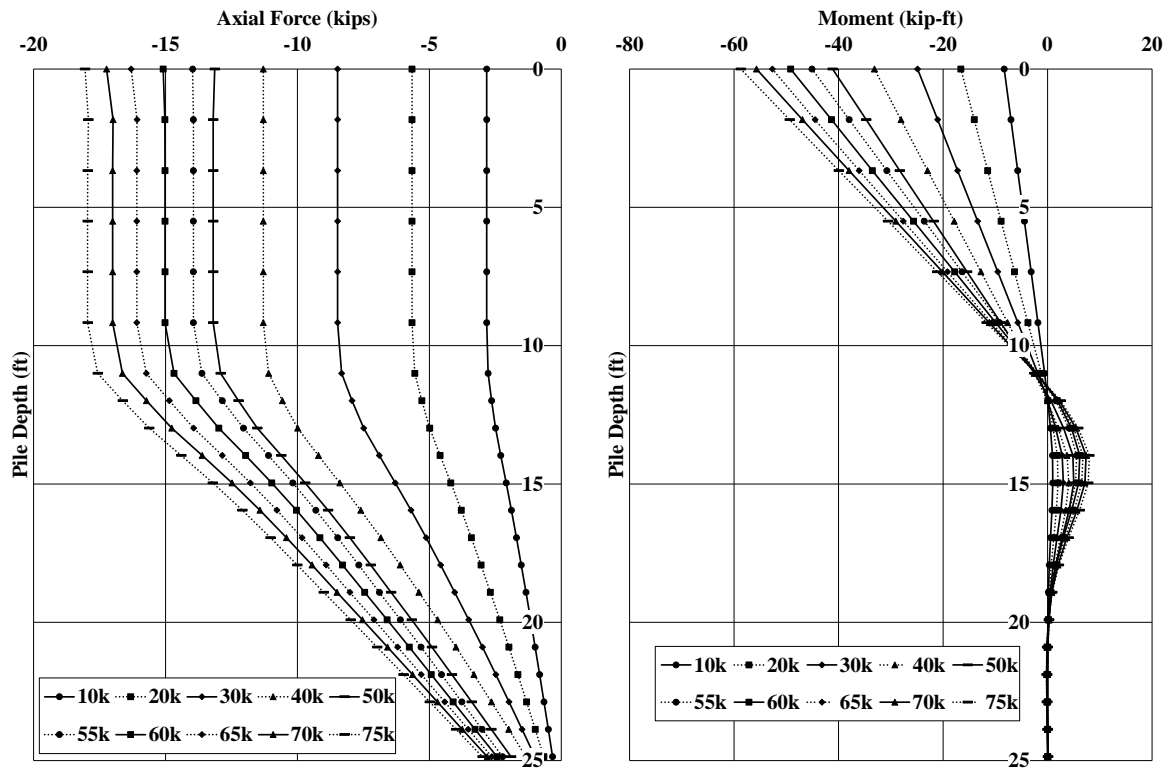
Figure 3-34 – Axial Load and Moment Profiles for Pile 6 with no Load Truck

51

The second model simulation for the Highway 331 bridge simulated the placement of an LC-5 load truck's exterior tire at the edge of the exterior girder opposite the load application point. It was assumed that the load from the load truck was carried only in the bearing locations beneath girders 5 and 6 (above piles 5 and 6). The weight of the truck was split evenly between these two locations at a magnitude of 42.85 kips at each bearing location. Figure 3-35 shows the predicted load versus deflection behavior of the bent with the addition of the load truck.
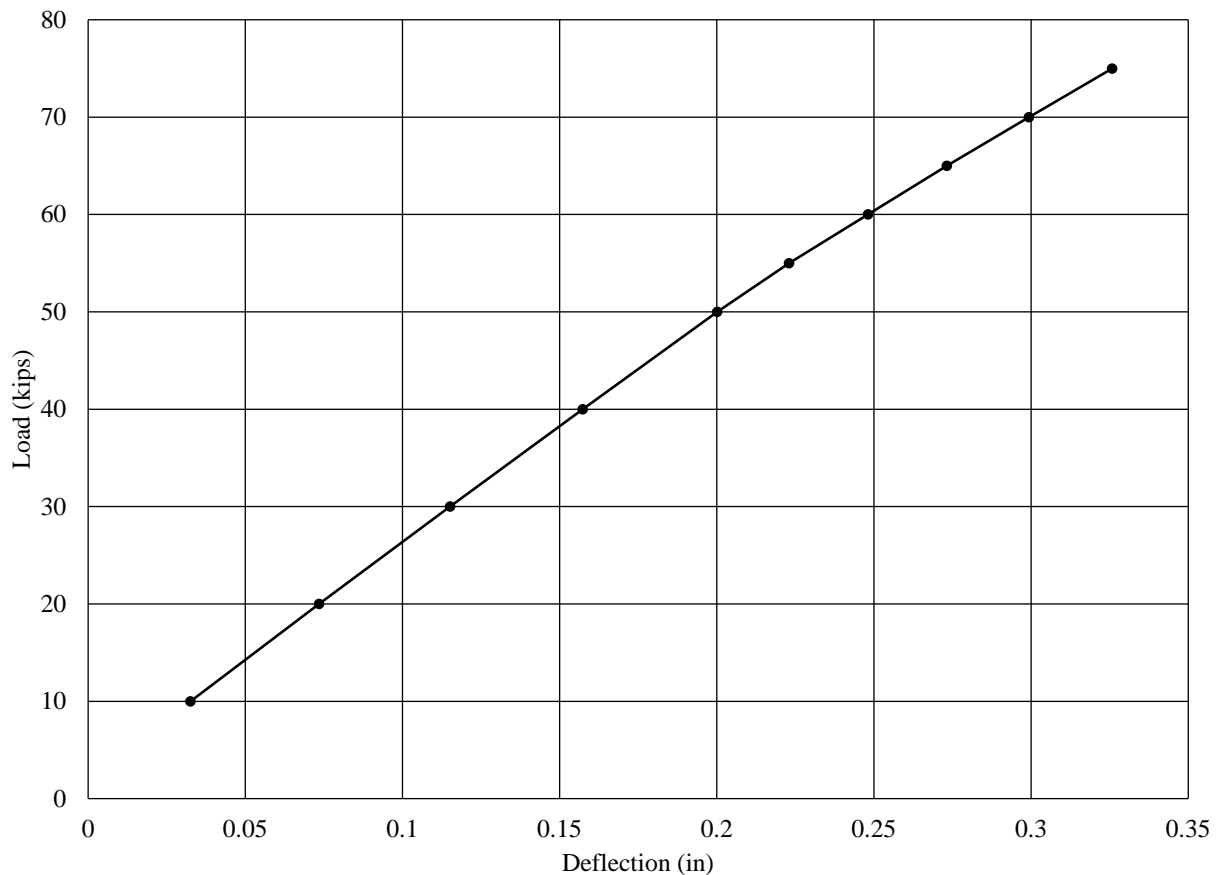
Figure 3-35 – Load versus Deflection Chart with Deck and Truck over the Exterior Girder

Figure 3-36, Figure 3-37, Figure 3-38, Figure 3-39, Figure 3-40, and Figure 3-41, show the pertinent results from model simulations. The figures show the theoretical distribution of axial load and bending moment with depth for each individual pile. Axial load profiles were used to

analyze the effect of lateral load on the distribution of axial loads in the piles, and bending moment profiles were used to verify the accuracy of model predictions.
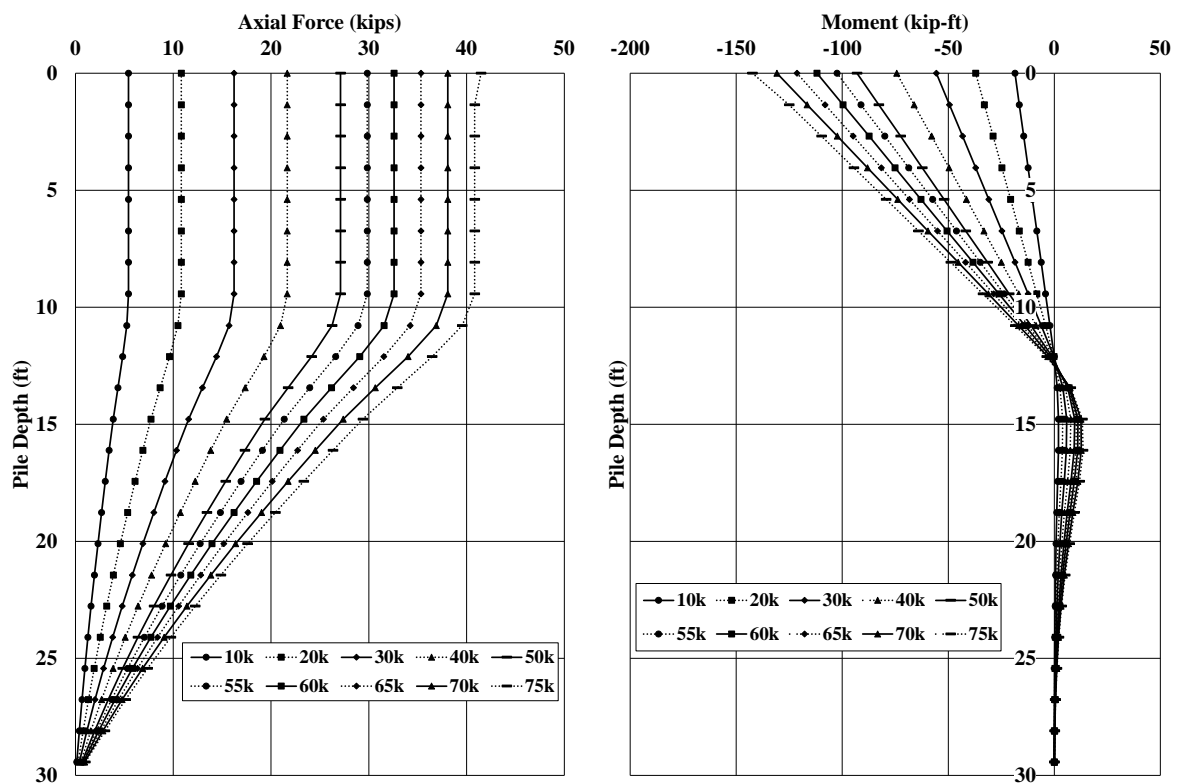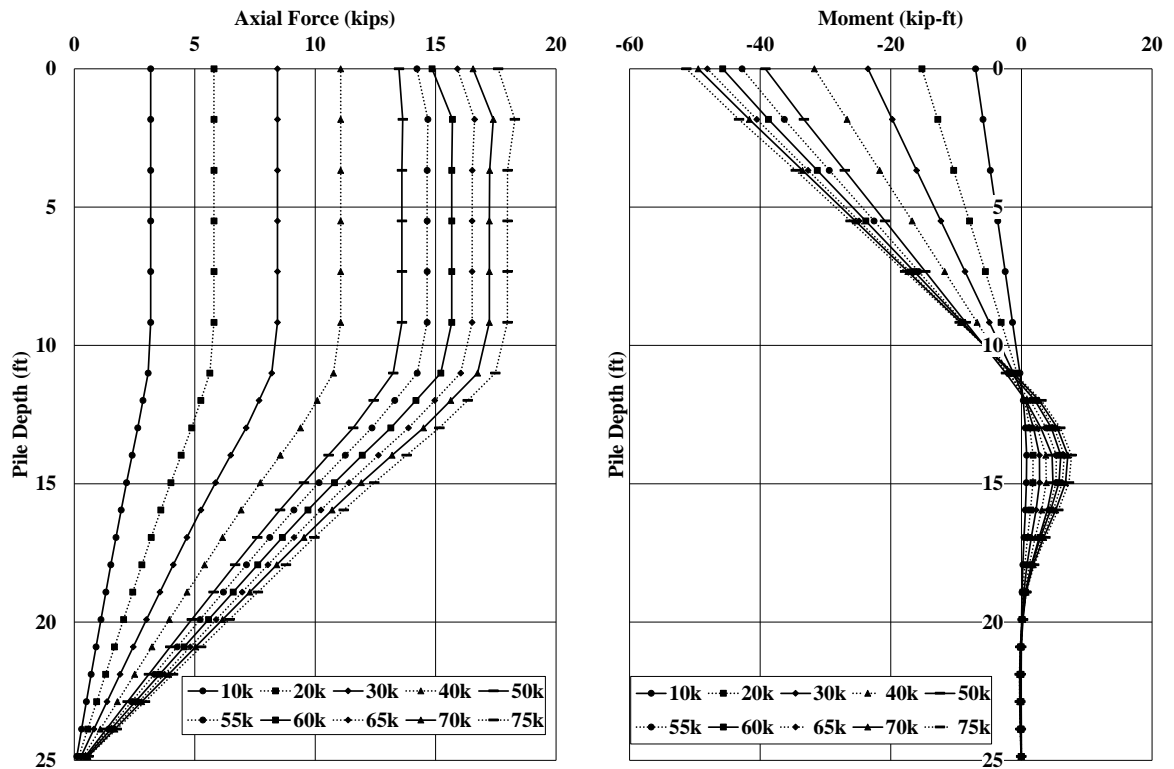

Figure 3-36 – Axial Load and Moment Profiles for Pile 1 with Load Truck over the Exterior Girder
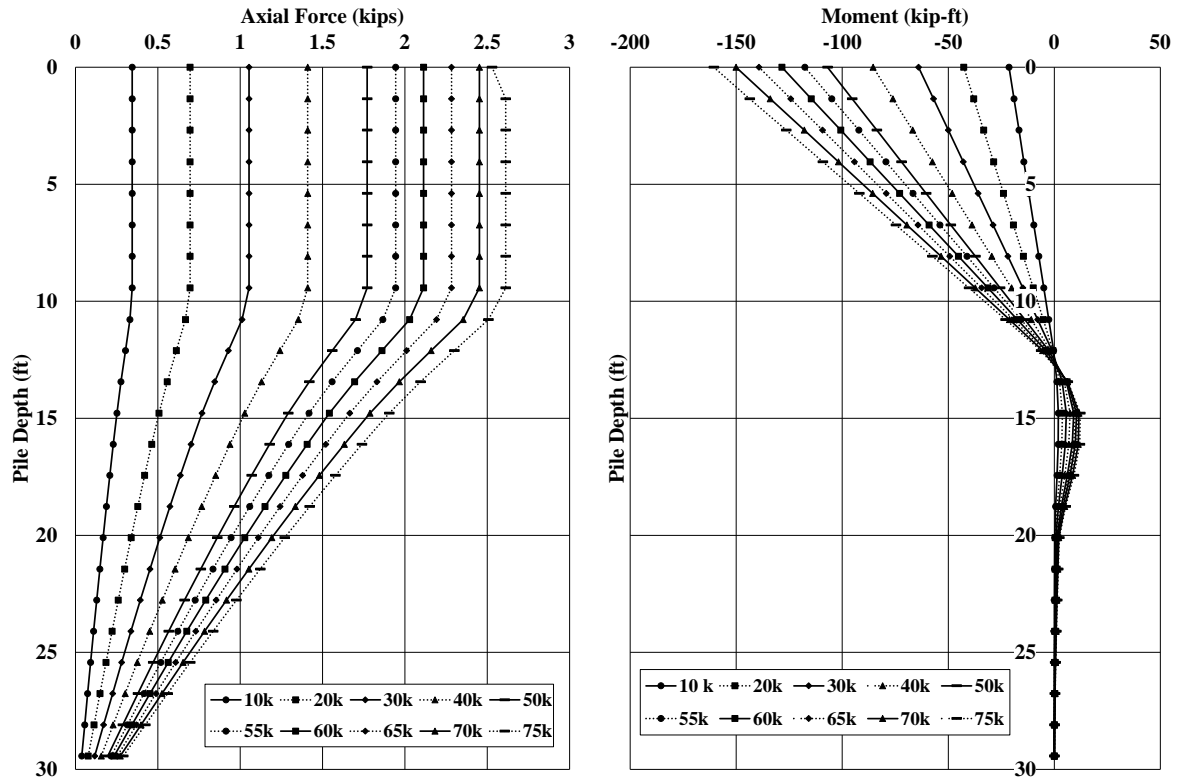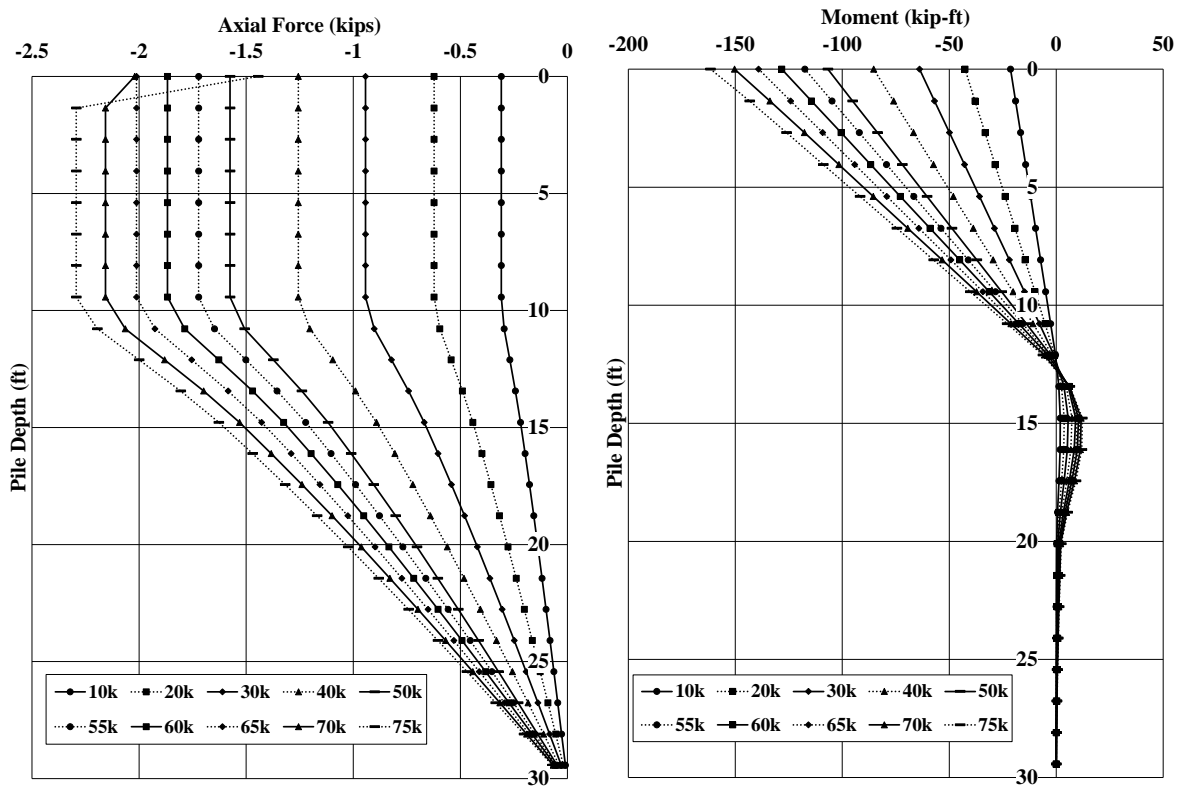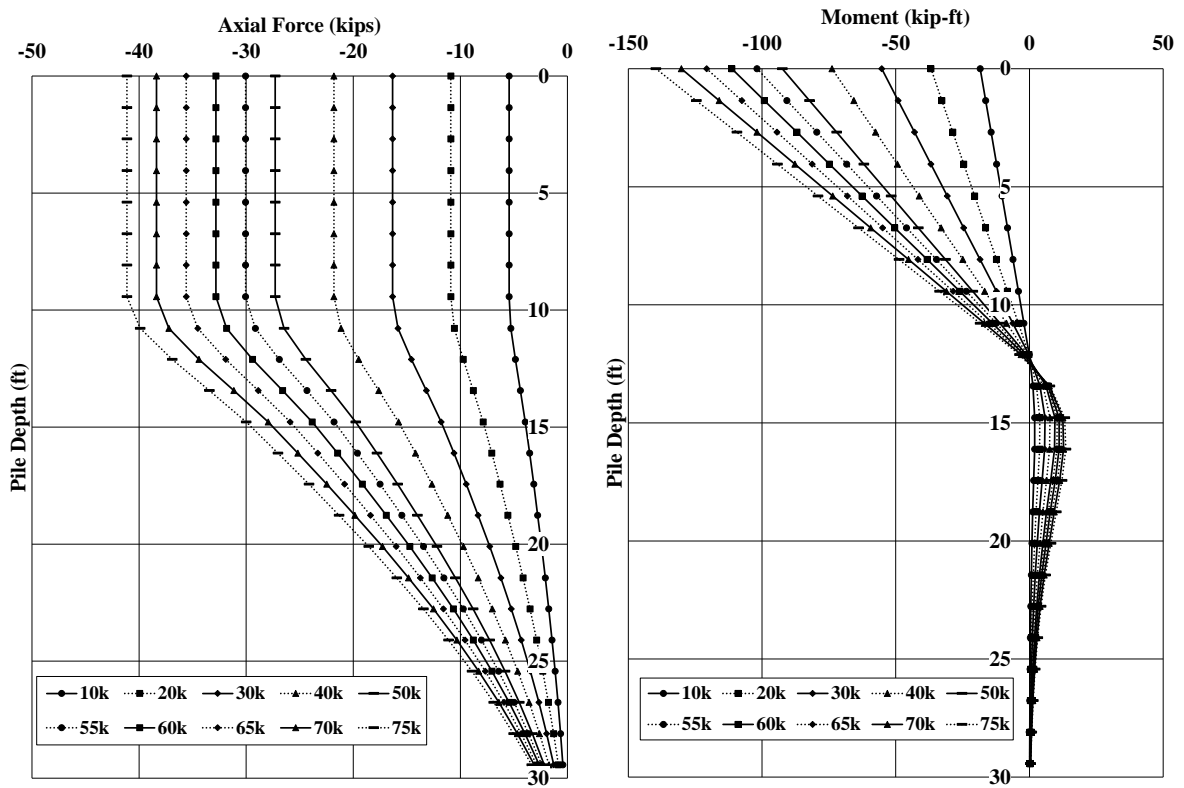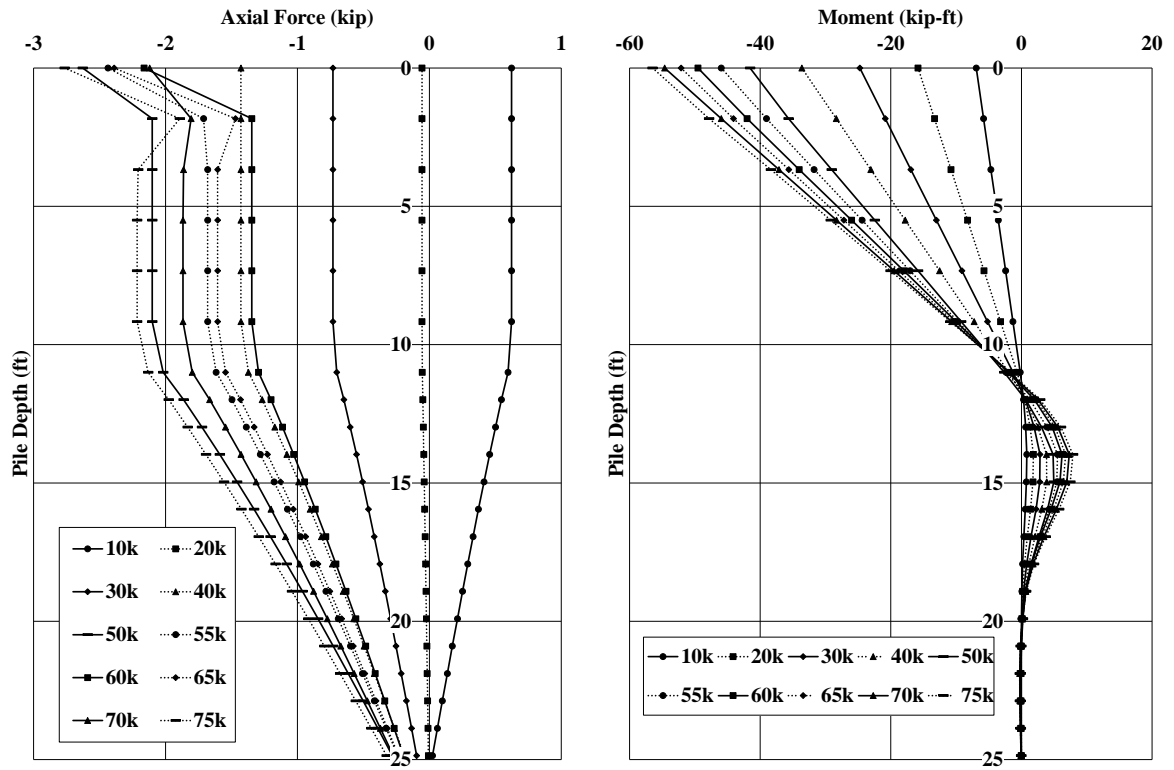
Figure 3-37 – Axial Load and Moment Profiles for Pile 2 with Load Truck over the Exterior Girder
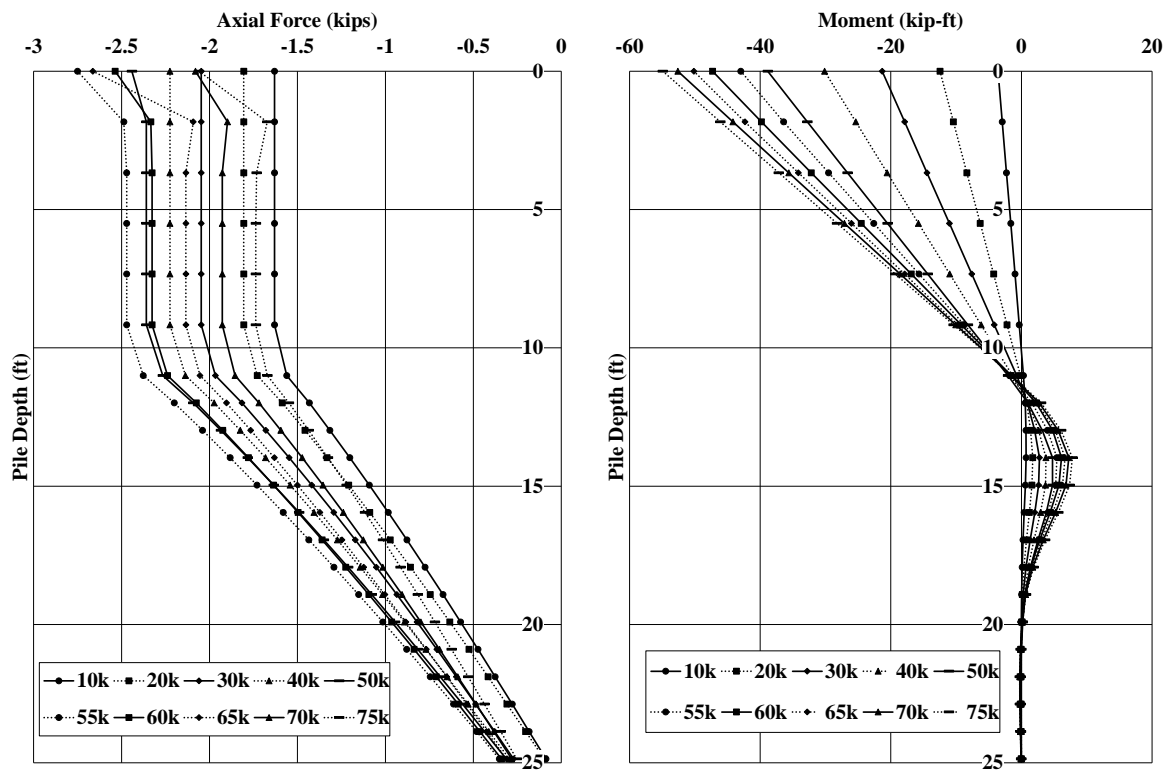
Figure 3-38 – Axial Load and Moment Profiles for Pile 3 with Load Truck over the Exterior Girder
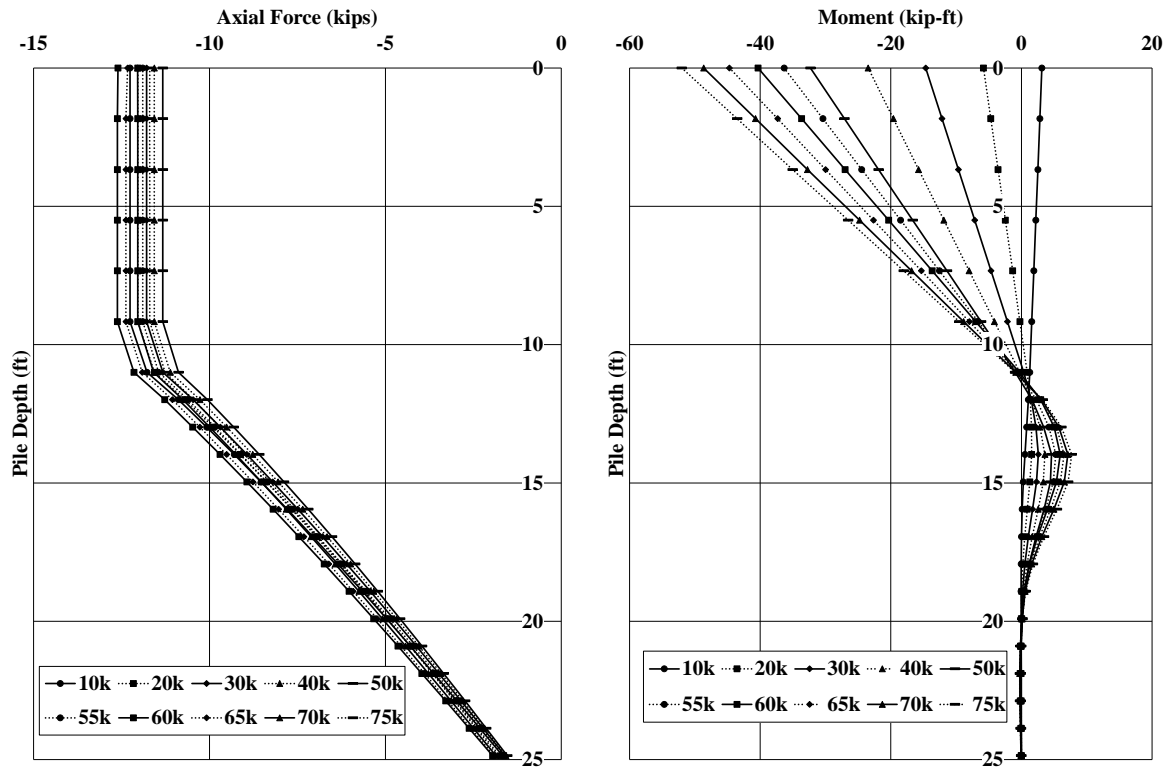
Figure 3-39 – Axial Load and Moment Profiles for Pile 4 with Load Truck over the Exterior Girder
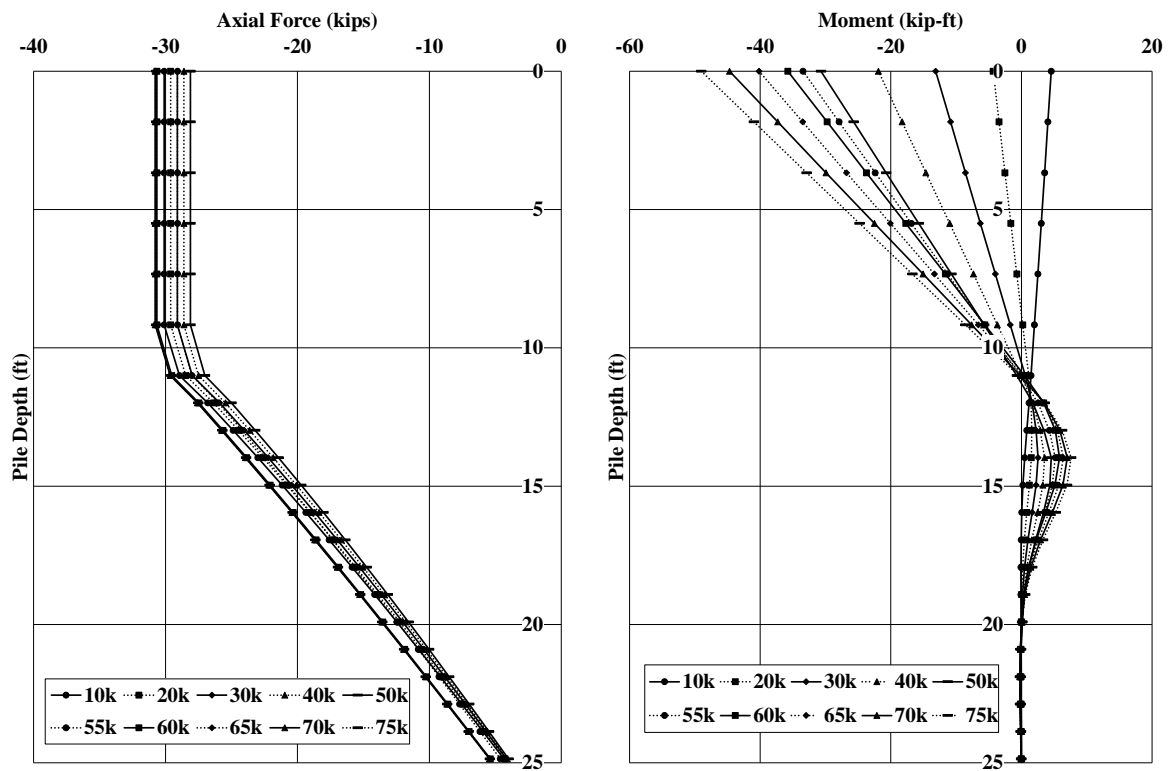
Figure 3-40 – Axial Load and Moment Profiles for Pile 5 with Load Truck over the Exterior Girder
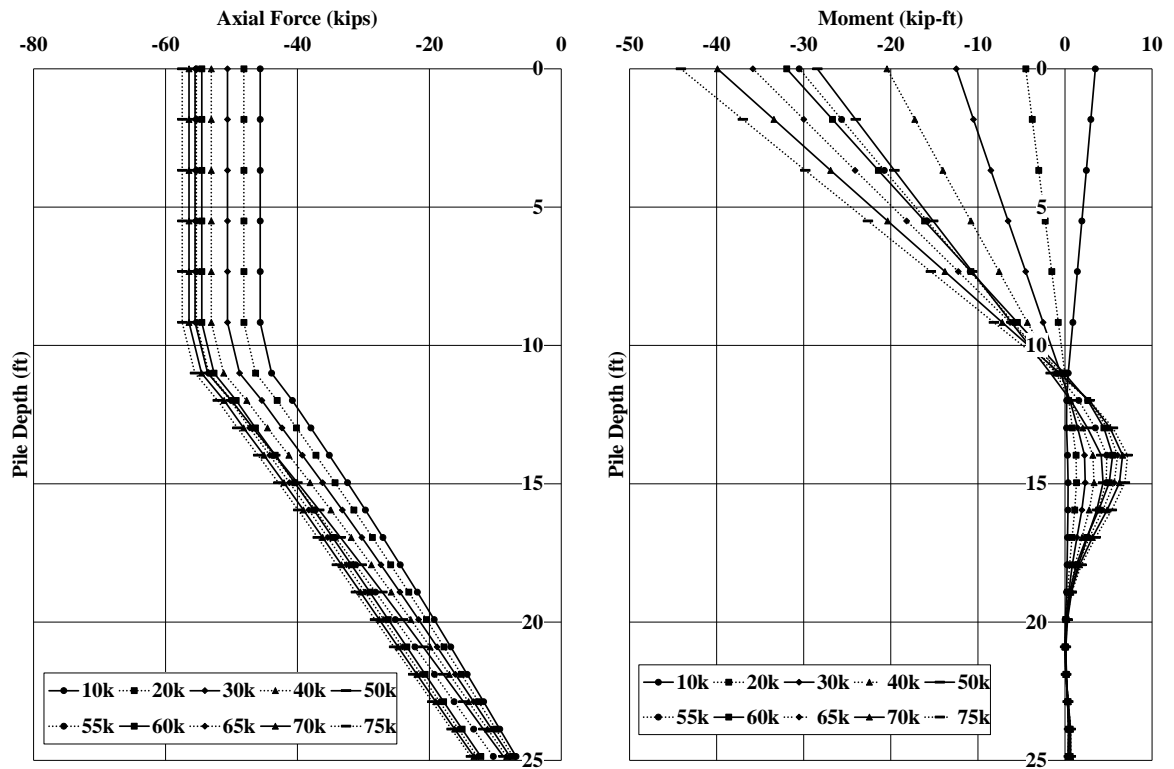
Figure 3-41 – Axial Load and Moment Profiles for Pile 6 with Load Truck over the Exterior Girder

The load versus deflection predictions for each of the simulated load tests were graphed together to compare the predicted behavior. Figure 3-42 shows the comparison of the predicted model load versus deflection curves.

56
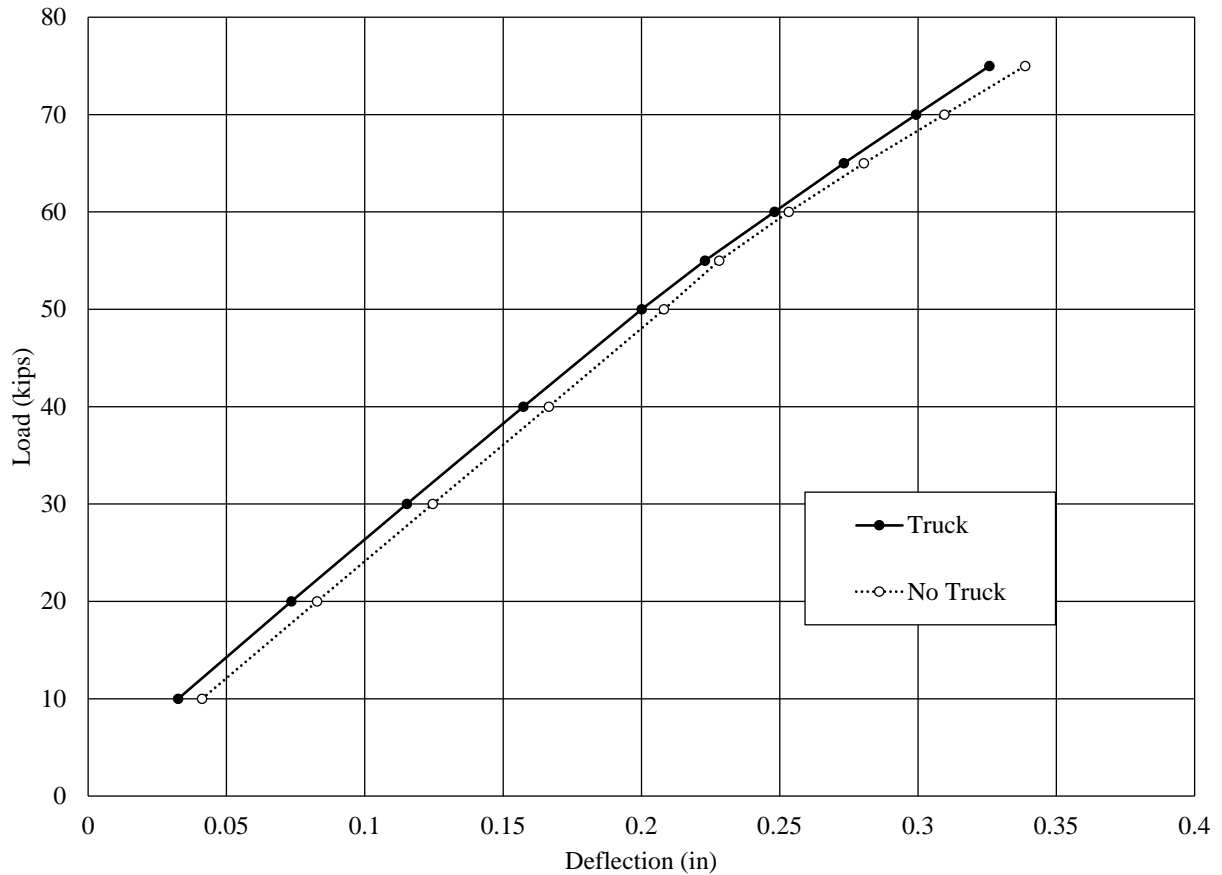
Figure 3-42 – Comparison of Load versus Deflection Curves from Model Simulations

The simulations predicted the bent with no truck would deflect more than the bent with additional load due to the load truck.

3.5 AUNGES Test Bents

The final phase of modeling simulated the bents constructed at the AUNGES located at the NCAT test track facility in Opelika, Alabama. The models simulated four load tests on two separate stand-alone bents. Initial models were developed to design the two test bents. Parametric model analysis of the two proposed bent types was conducted to aid in the selection of pile length and to assure the proposed bent designs were able to feasibly be tested to failure with the available hydraulic jacks. The first modeled bent featured four 35 feet long HP12x53 piles with 9 feet of clear height between the ground surface and the bottom of the pile cap. The

exterior piles were battered with a 1.5/12 slope and the two interior pile were vertical. The piles were oriented for weak axis bending in the direction of lateral load. The piles were spaced 8 feet center to center. The second bent was identical to the first bent except that no piles were battered. The pile cap for the battered pile bent model was modeled as 54 inches wide and 24 inches tall to model the 12 inch embedment of the actual piles. The pile cap for the vertical pile bent was modeled as a 36 inch by 36 inch square cap. Figure 3-43 and Figure 3-44 show the FB Multipier rendering of the two piles at AUNGES.
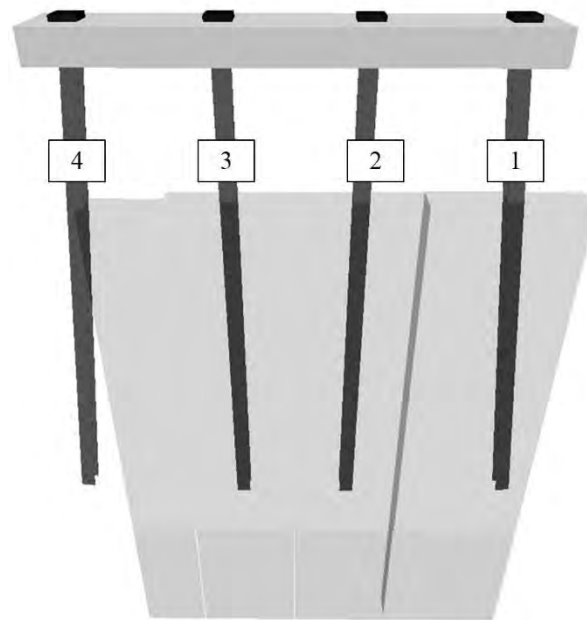
Figure 3-43 – FB Multipier Rendering of the Battered Pile Test Bent
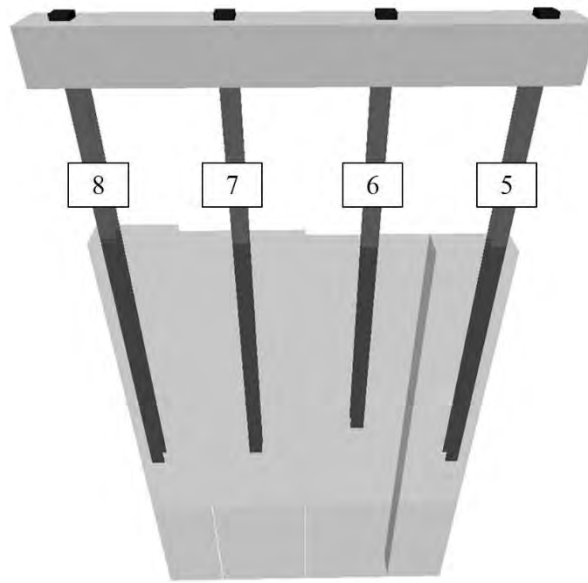
Figure 3-44 – FB Multipier Rendering of the Vertical Pile Test Bent

The models were created to resemble standard ALDOT bridge configurations. The pile properties were entered into FB Multipier from the AISC Manual of Steel Construction. An initial estimate of 5,000 psi was used for the compressive strength of the concrete cap. The steel piles were modeled with an elastic modulus of 29,000 ksi and 58 ksi according to coupon tests conducted on the piles. The q-z and t-z curves for each soil layer were constructed from default FB Multipier options. The p-y curves were developed from dilatometer testing conducted on site. The initial simulations (bent dead load only) for each model simulated a load test with twelve loading increments. The increments were as follows: 10 kips, 20 kips, 30 kips, 40 kips, 50 kips, 60 kips, 70 kips, 80 kips, 90 kips, 100 kips, 110 kips, and 120 kips. The two bent models were also analyzed using a pushover analysis to determine the force required to fail the bents. This analysis was used to develop a loading schedule for the full-scale load tests. The axial load and bending moment predictions were compiled at node locations along the length of each pile for the distinct loading increments. The centerline deflection of the pile cap was also recorded at each loading increment. Another model was created to simulate the reaction bent needed to field

test the bent. The reaction model was subjected to the expected maximum magnitude of loading to ensure the design had sufficient strength and did not experience excessive deflection. Piles were named Pile 1, Pile 2, Pile 3, and Pile 4 on the battered pile bent and Pile 5, Pile 6, Pile 7, and Pile 8 on the vertical pile bent. Pile 1 and Pile 5 were the leading piles, furthest away from the applied load. The piles were spaced at 8 feet center to center spacing which was greater than five times the diameter of the pile. Therefore, p-multipliers to reduce the lateral capacities of the piles were not needed and were not included in any model simulations.

3.5.1   Soil Properties

The soil profile used in the AUNGES bent models was created from dilatometer and SPT data collected on May 28, 2015. The drill rig used to push the dilatometer was operated by an ALDOT drilling team. The dilatometer was operated by Dr. Anderson. Readings were taken every 20 centimeters until the drill rig could no longer push the dilatometer. The SPT was conducted by the same ALDOT drilling crew. The SPT was terminated at a depth of 50 feet with N-counts recorded every 5 feet. The SPT data was used to determine the soil type, and the dilatometer data was used to calculate unit weight, undrained shear strength, and to determine the p-y curves to be used in the analysis of the test bents. Figure 3-45 shows the soil profile for the AUNGES test bents.
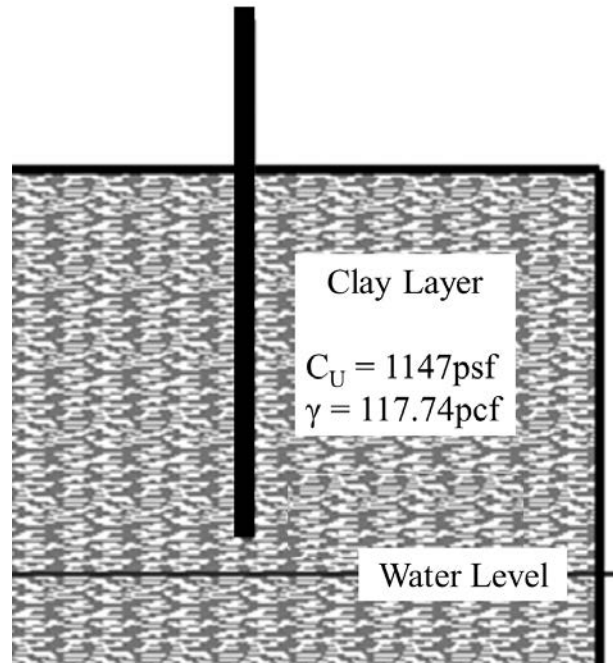
Figure 3-45 – AUNGES Soil and Pile Profile (Adapted from FB Multipier)

Table 3.1 – p-y Values Determined from Dilatometer Data

y (in)	p (lb)
0	0
0.2	6141
0.4	7719
0.6	8825
0.8	9703
1	10445
1.2	11093
1.4	11672
1.6	12197
2	13129
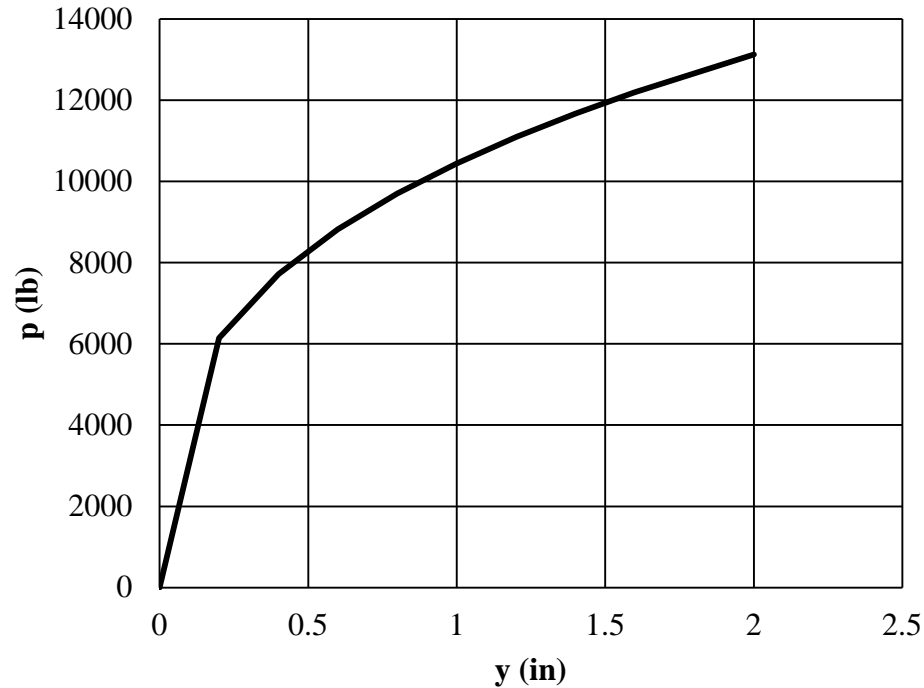
Figure 3-46 – p-y curve Developed from Dilatometer Test

3.5.2 Battered Pile Test Bent Model and Behavior Prediction

The initial model on the battered pile bent was a full pushover analysis. The result was a target load to fail the bent as well as a schedule target when field testing the actual bent. The pushover analysis began at 70 kips and increased in 5 kip increments until an element experienced failure and the model analysis failed to converge on a single solution. The target failure load for the Battered pile bent was 140 kips.

The second model was subjected to the bent dead loads and increasing amounts of lateral load at the same schedule created from the pushover analysis starting at 10 kips and increasing in 10 kip increments until reaching the predicted failure load. The following figures, Figure 3-47, Figure 3-48, Figure 3-49, Figure 3-50, Figure 3-51, Figure 3-52, and Figure 3-53 show the pertinent results from model simulations. The figures show the theoretical distribution of bending moment with depth for each individual pile. Bending moment profiles were used to

verify the accuracy of model predictions. The models also predicted the load versus deflection behavior to be compared with the wire pot data, and produced deflected shapes at the loads where inclinometer tests were scheduled to be conducted on piles 2 and 3. These predictions were used to assess the accuracy of the model predictions, and to verify calibrated models accurately predicted the observed behavior.
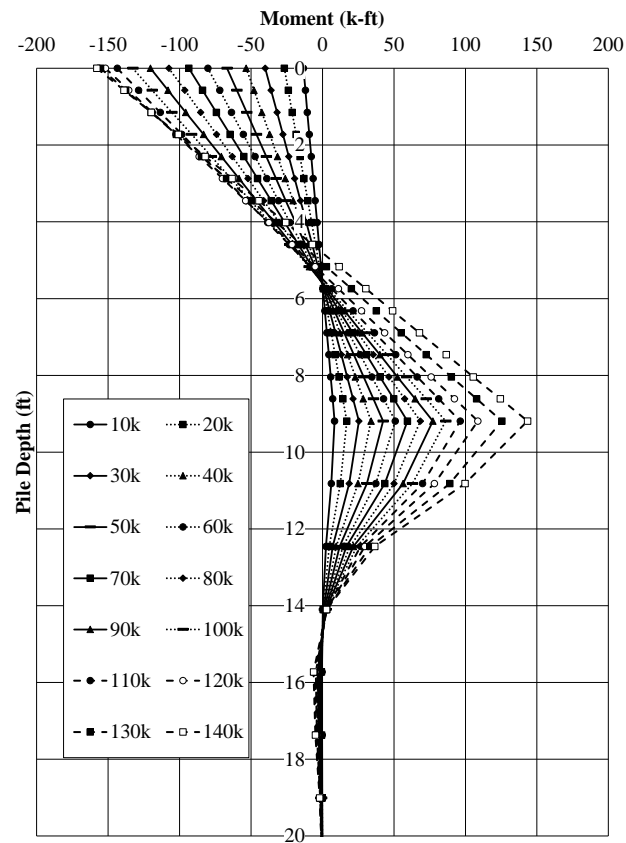
Figure 3-47 – Pile 1 Moment Profile for Battered Pile Bent
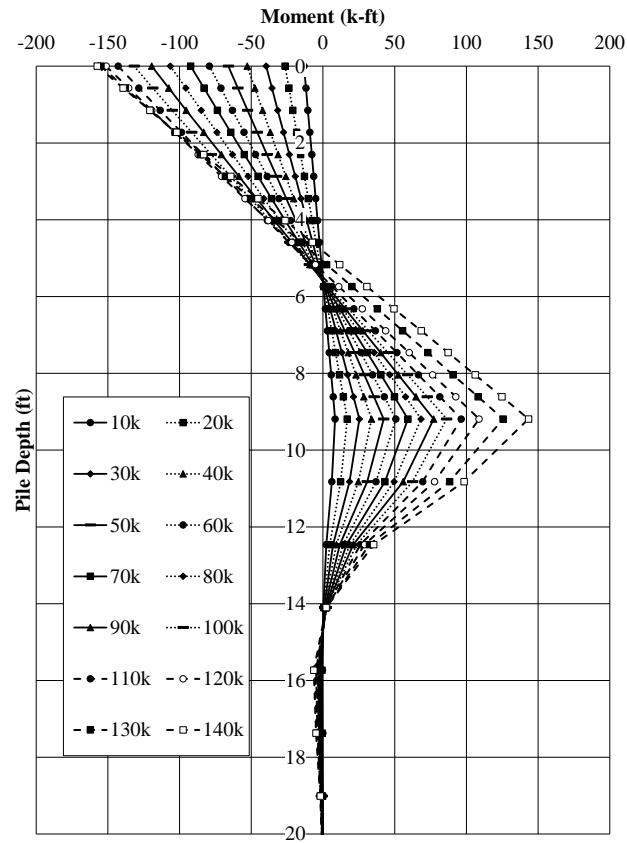
Figure 3-48 – Pile 2 Moment Profile for Battered Pile Bent
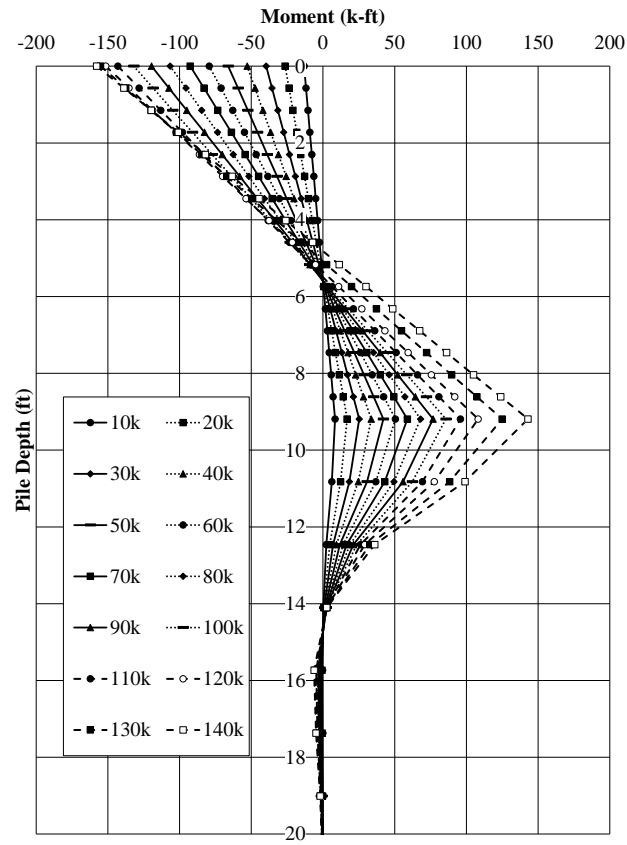
Figure 3-49 – Pile 3 Moment Profile for Battered Pile Bent
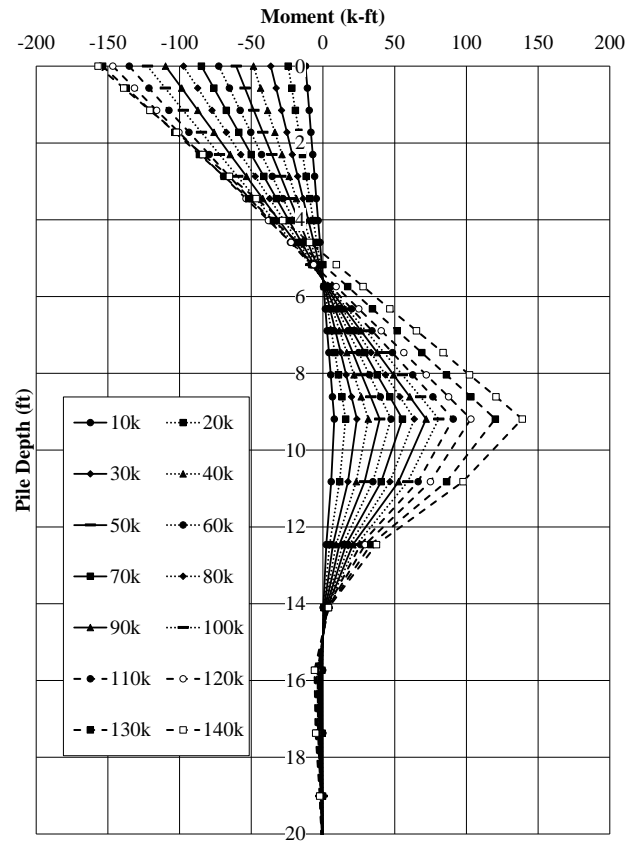
Figure 3-50 – Pile 4 Moment Profile for Battered Pile Bent
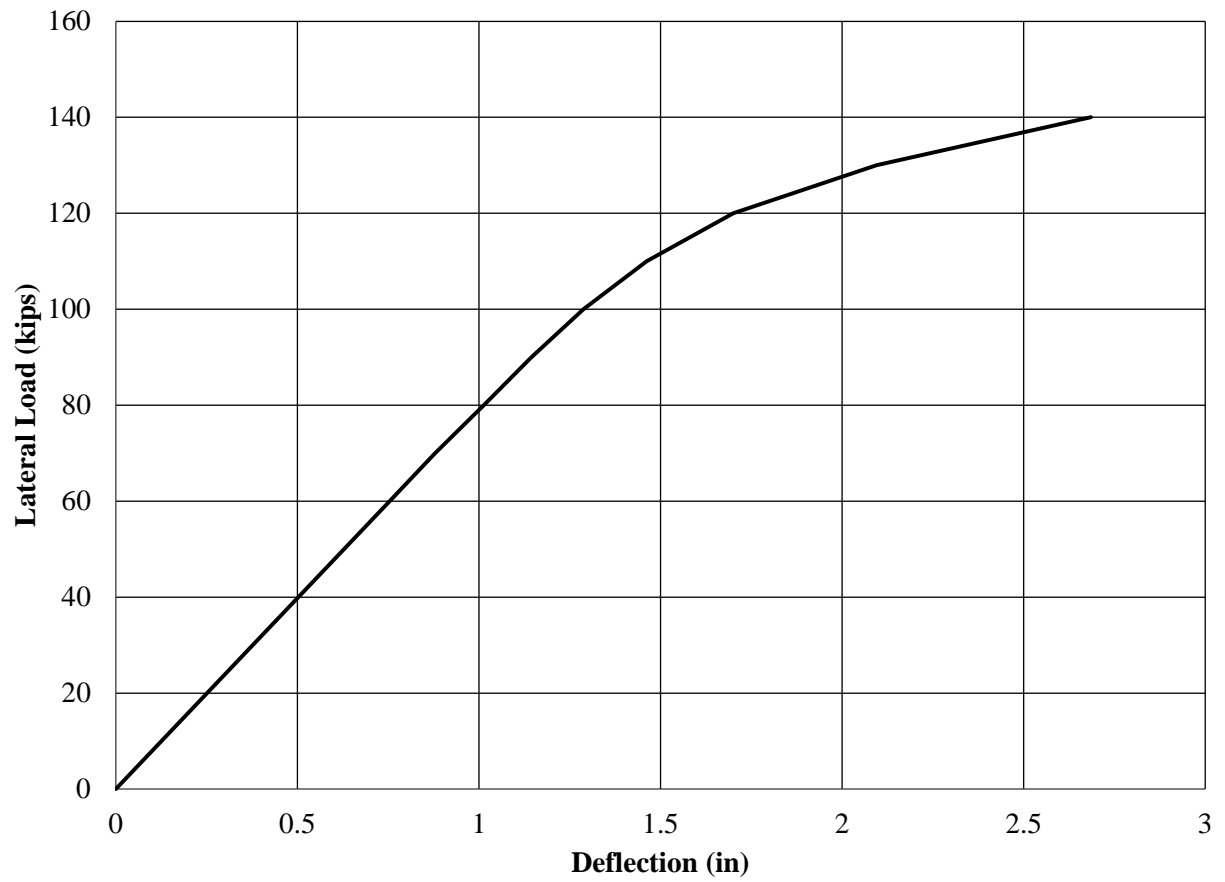
Figure 3-51 – Load versus Deflection Behavior for Battered Pile Bent
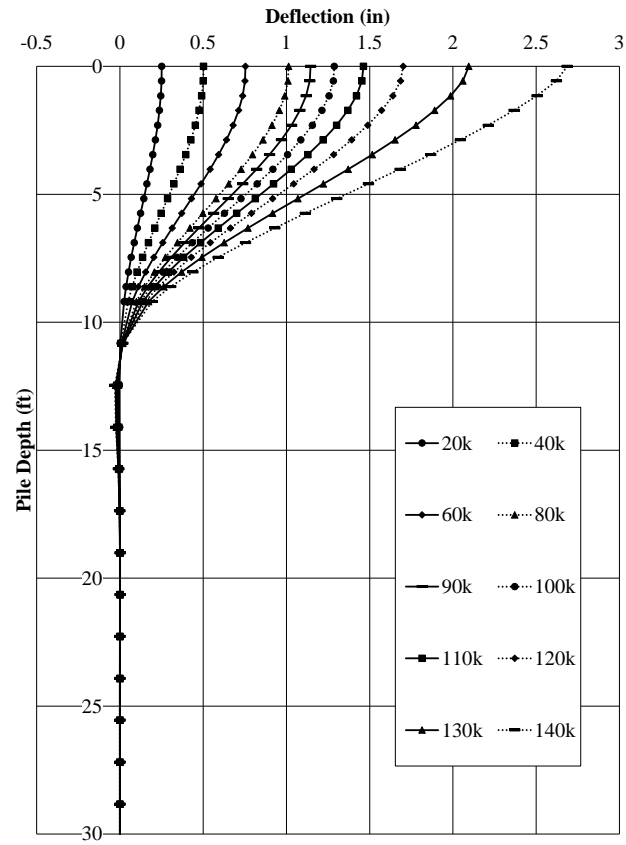
Figure 3-52 – Pile 2 Model Deflected Shape
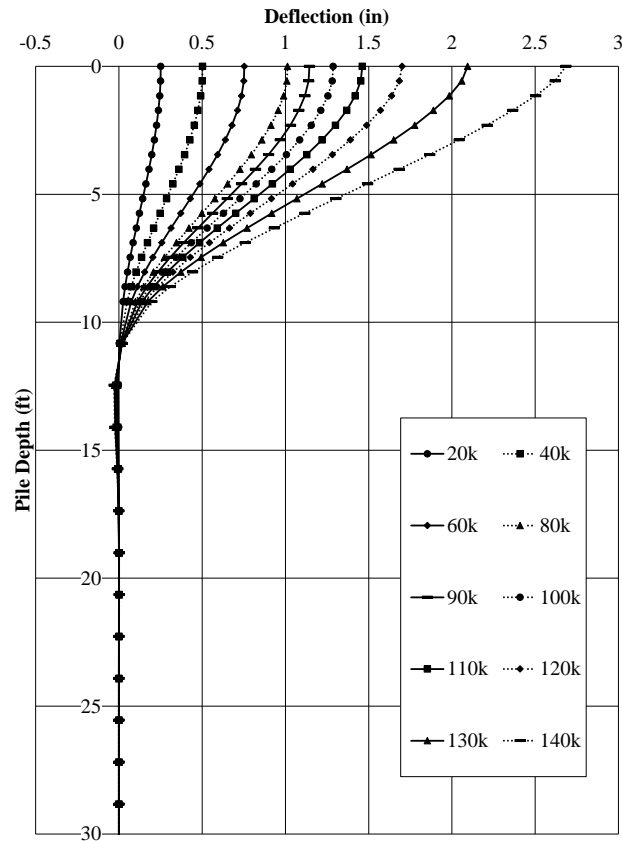
Figure 3-53 – Pile 3 Model Deflected Shape

3.5.3   Vertical Pile Test Bent Model and Behavior Prediction

The initial model on the battered pile bent was a full pushover analysis. The result was a target load to fail the bent as well as a schedule target when field testing the actual bent. The pushover analysis began at 70 kips and increased in 5 kip increments until an element experienced failure and the model analysis failed to converge on a single solution. The target failure load for the Vertical pile bent was 120 kips.

The second model was subjected to the bent dead loads and increasing amounts of lateral load at the same schedule created from the pushover analysis starting at 10 kips and increasing in 10 kip increments until reaching the predicted failure load. The following figures, Figure 3-54,

69

Figure 3-55, Figure 3-56, Figure 3-57, Figure 3-58, Figure 3-59, and Figure 3-60 show the pertinent results from model simulations. The figures show the theoretical distribution of bending moment with depth for each individual pile. Bending moment profiles were used to verify the accuracy of model predictions. The models also predicted the load versus deflection behavior to be compared with the wire pot data, and produced deflected shapes at the loads where inclinometer tests were scheduled to be conducted on piles 5 and 7. These predictions were used to assess the accuracy of the model predictions, and to verify calibrated models accurately predicted the observed behavior.
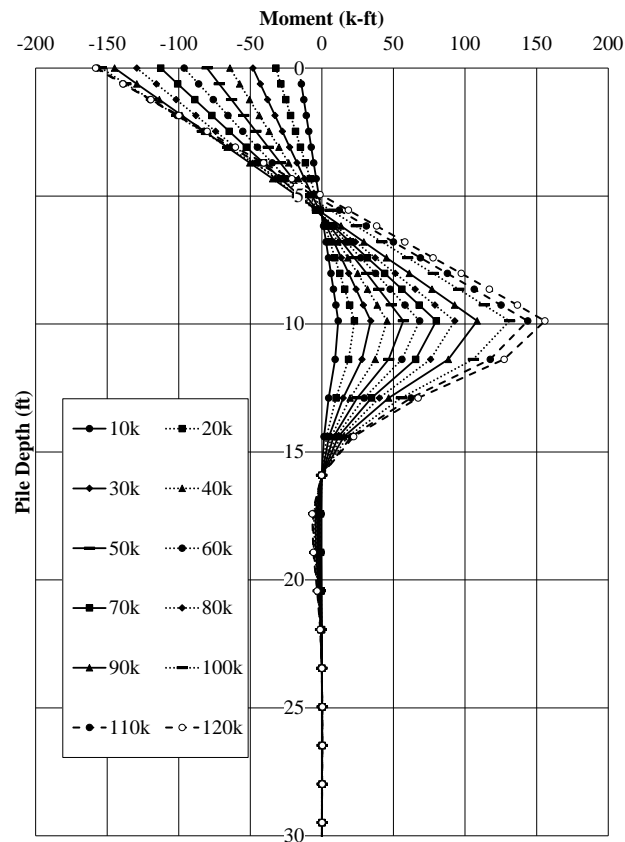
Figure 3-54 – Pile 5 Moment Profile for Vertical Pile Bent
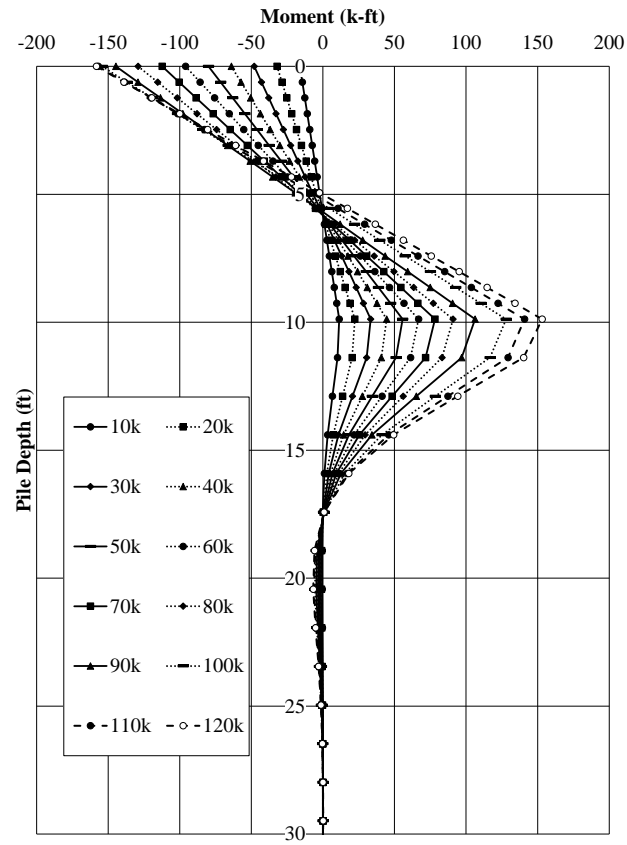
Figure 3-55 – Pile 6 Moment Profile for Vertical Pile Bent

71
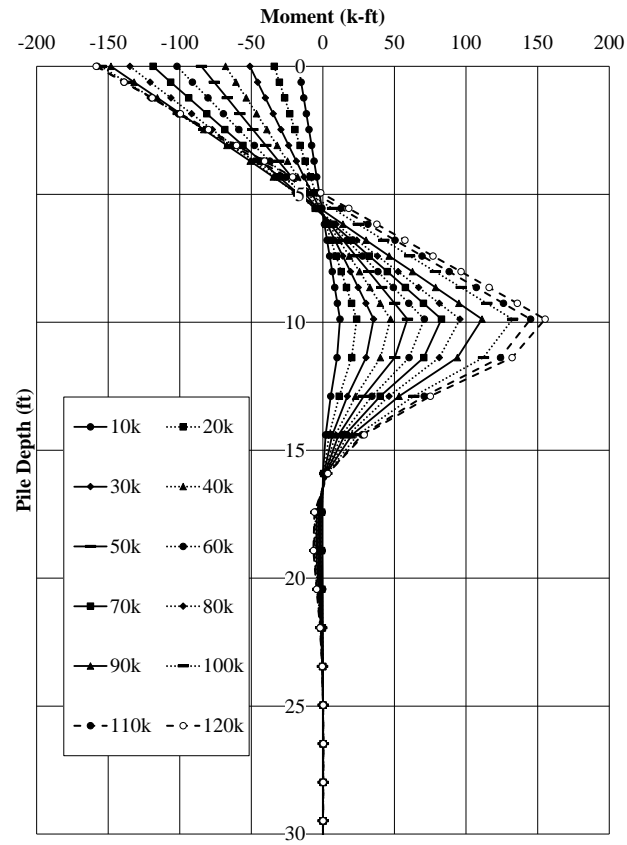
Figure 3-56 – Pile 7 Moment Profile for Vertical Pile Bent

72
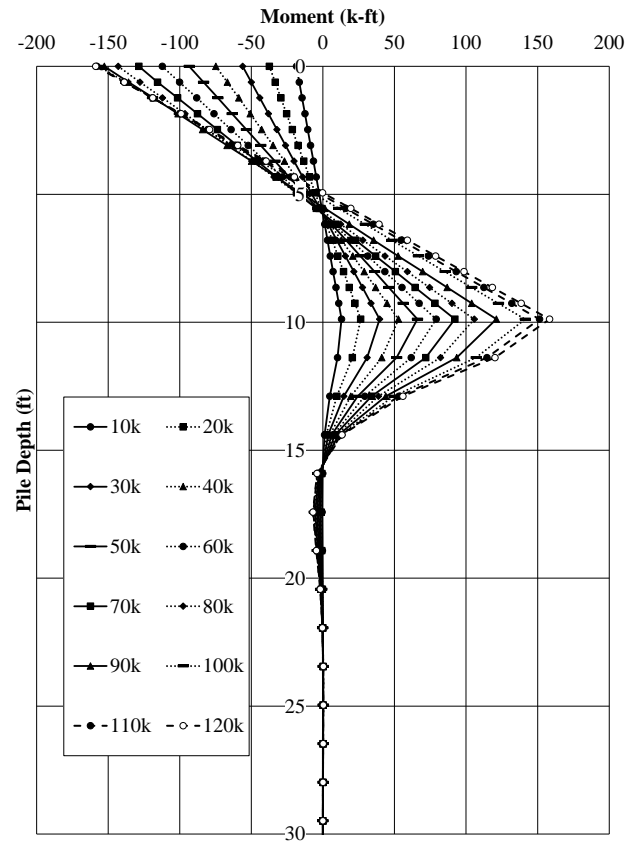
Figure 3-57 – Pile 8 Moment Profile for Vertical Pile Bent

73
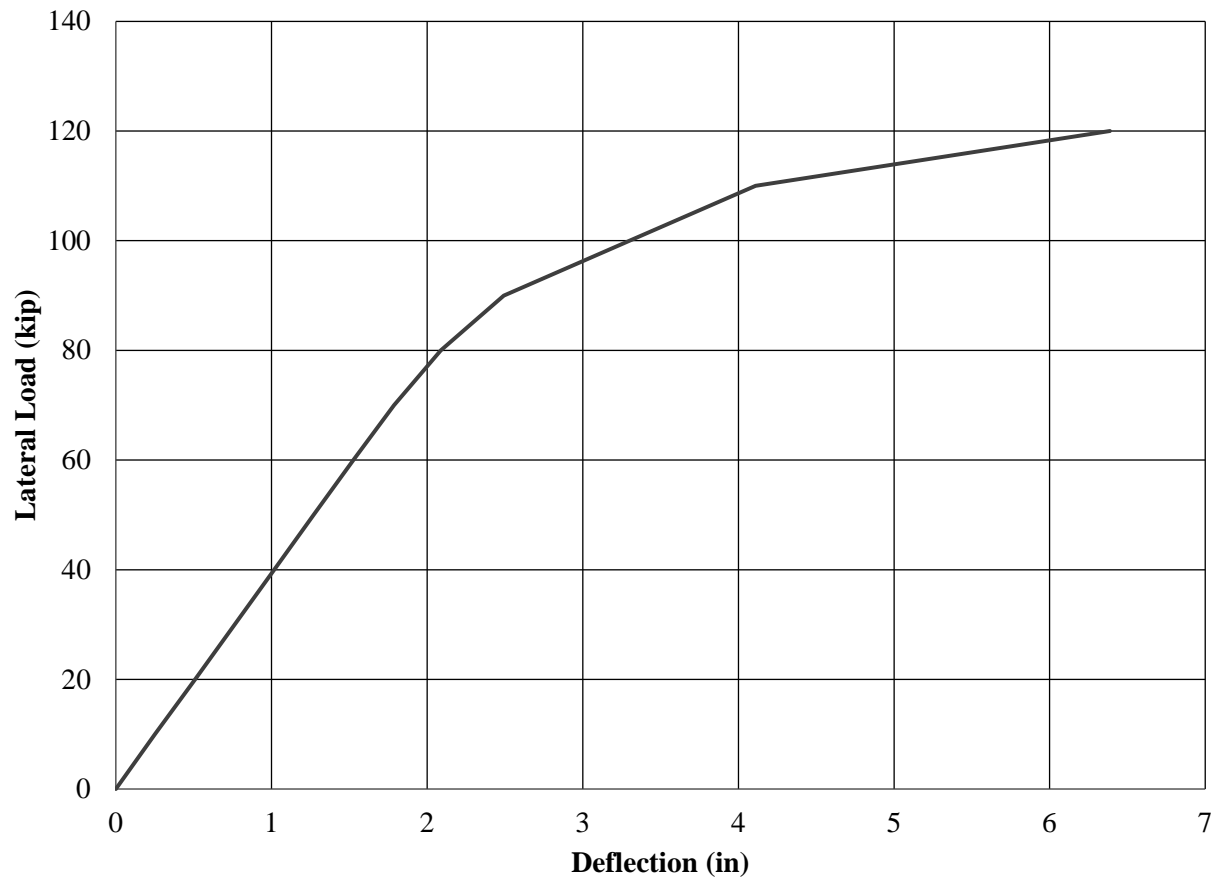
Figure 3-58 – Load versus Deflection Behavior for Vertical Pile Bent

74
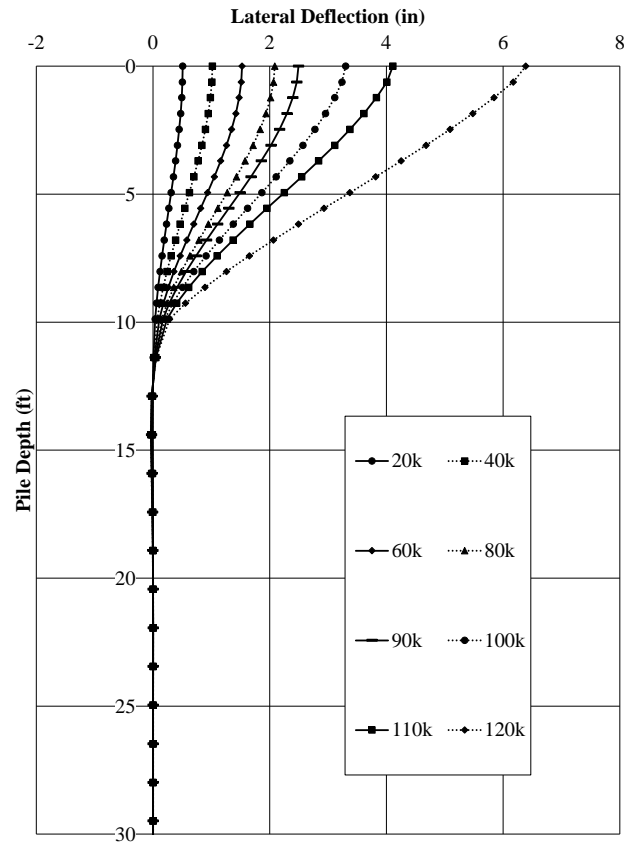
Figure 3-59 – Pile 5 Model Deflected Shape
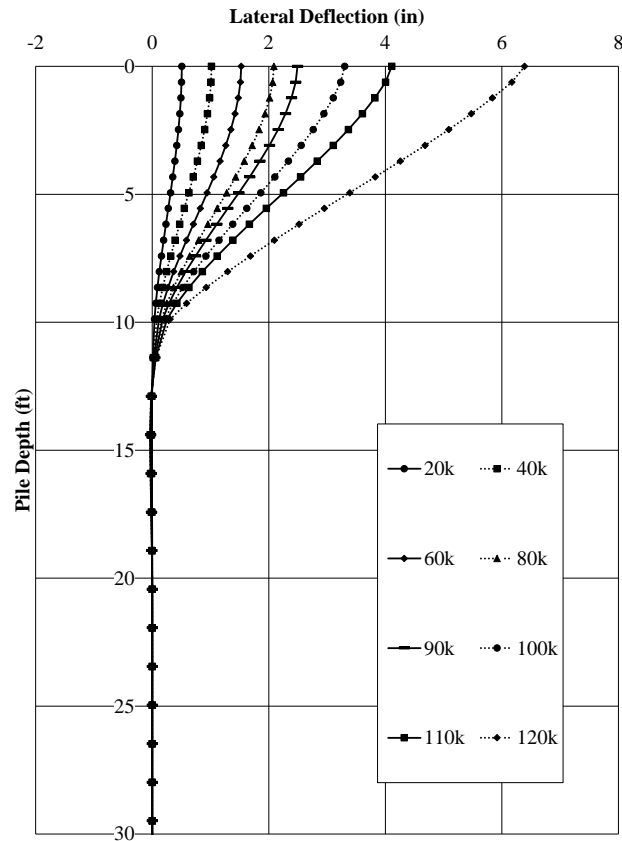
Figure 3-60 – Pile 7 Model Deflected Shape

3.5.4 Pipe Pile Reaction Bent

The reaction bent for the AUNGES bents was a 9 pile bent cap consisting of a 3x3 grid of steel pipe piles. The pipe piles were 41 feet long with an outer diameter of 10.75 inches. The piles were assumed to have an elastic modulus of 29,000 ksi and a yield stress of 43 ksi. The pile cap was 10 feet by 10 feet wide and 33 inches deep. The concrete of the pile cap was assumed to have a compressive strength of 5,000 psi. The soil profile used for the reaction model was the same soil profile used in the test bent models. The model was run to determine if the pile group would be able to provide the required reaction to sufficiently load the test bents without experiencing excessive deflections. The pipe piles extended out of the concrete cap. The loading

plan for the field load tests involved loading the pile cap by the using two steel reaction beams to bear against these pile extensions. FB Multipier was used to analyze the free lengths of the piles to ensure they were structurally sound for the intended application. All models verified that the pile group was sufficient to provide the required reaction forces for the field load tests without causing failures in the free length of the piles.

4. Field Test 1-Macon County Bridge

4.1 Introduction

A multi-span bridge under construction in Macon County, Alabama was used for the first field test for this research project. The bridge was a replacement bridge spanning over Old Town Creek on Macon County Road 9 in Shorter, AL. The bridge consists of six 40 ft spans with four AASHTO Type I girders spaced at 8 ft on center. A plan view of the bridge can be seen in Figure 4-1. The intermediate bents consisted of a reinforced concrete cap beam with 4 driven HP14x89 steel piles spaced at eight feet on center. The two exterior piles in the bent were battered at a 1.5:12 slope. The piles in bents 3 and 4 were galvanized while bents 2, 5, and 6 were encased in non-structural concrete. The pile encasements in bents 2, 5 and 6 were circular with a diameter of 30 in. Bent 5 was used as the test bent for the first lateral load test. A figure of the bent geometry with dimensions taken from the design drawings can be seen in Figure 4-2.
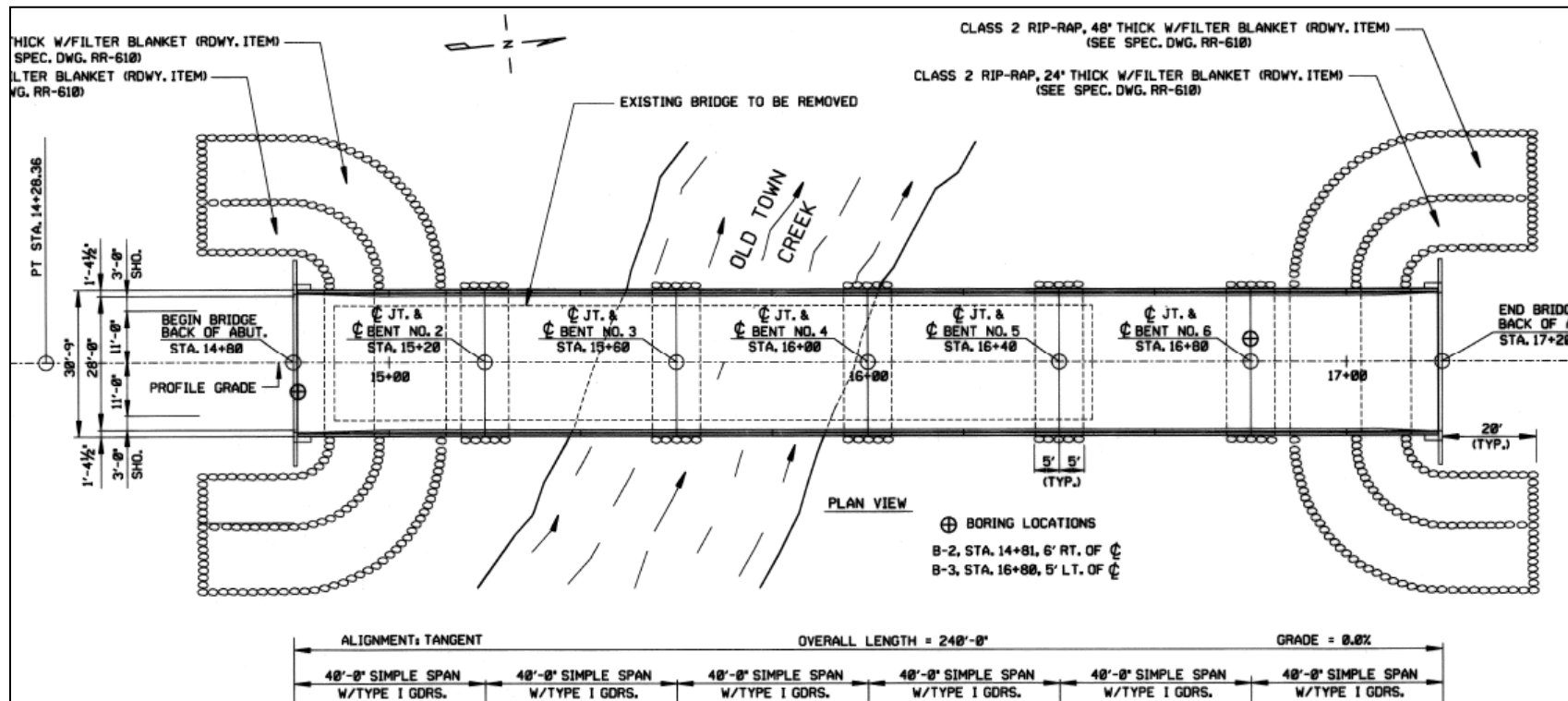
Figure 4-1 Macon County Bridge Overall Plan (Weatherford & Associates 2013)

79

LEVEL

PILE CAP PLATE (SEE STD. DWG. I-131 FOR DETAILS.)

SYMM. ABOUT ₵ BENT

BARS C•5 @ 12" o.c.

4 BARS A•8 — EL.197.781

EL.197.781

STIRR. S•5

EL.195.781

2 BARS B•8 — HOOPS H•4

8 EQ. SP.

EL.195.781

3" CL.

USE ROUND PILE ENCASEMENTS 2'-6" DIA.

CLASS 2 RIP-RAP, 24" THICK W/FILTER BLANKET(RDWY. ITEM).

HP14x89 PILES

5' MIN.

W4.5 STEEL WIRE AS PER ASTM A82 (AASHTO M32) WOUND SPIRALLY @ 12" PITCH (BEND IN FIELD)

ELEVATION
SCALE: ¼"=1'-0"

APPROX. GROUND LINE EL. 188.00 (BENT NO. 4)
APPROX. GROUND LINE EL. 190.00 (BENT NO.5 & 6)

(NI) EXTEND ENCASEMENTS A MINIMUM OF 3'-0" BELOW BOTTOM OF RIPRAP.

Figure 4-2 Elevation View of Bent 5 (Weatherford & Associates 2013)

This chapter details how the driven pile bent bridge in Macon County was tested as well as the analysis and results from that test. It contains sections on instrumentation, testing configurations, and the procedure used for testing. It also contains the results and analysis from the test as well as a discussion of the results.

4.2 Instrumentation

This section details how the test bent was instrumented. It contains the instrumentation layout for the bent, the different types of instrumentation used, and how each of the different types of instrumentation was installed.

4.2.1 Instrumentation Layout

In order to measure axial forces and bending moments in the driven piles, electrical resistance strain gages were installed on the inside of flanges on both sides of the web. A pair of gages was installed at each instrumented location in order to measure weak axis bending, which was the direction in which the piles were displaced. To obtain a moment versus depth profile for each of the piles, four total sections along the length of the piles were instrumented. An image

80

showing the instrumentation configuration at a single section can be seen in Figure 4-3. The instrumentation configuration shown in Figure 3-3 is representative of the instrumented sections above grade. The sections below grade were instrumented similarly, but a gage for measuring strong axis bending (green gage) was not installed and the gages were installed on the inside of the pile flanges so that they were protected during driving of the piles. The instrumentation layout for the gages installed along the length of the steel piles can be seen in Figure 4-4. The cables connected to each of the gages were color coded so that they could be easily identified during the tests. The gages above grade were connected using red wires while the gages below grade were connected with blue wires. The highest instrumented section above grade was labeled as black and the lower section was labeled as red. This labeling convention was used for the above and below grade conditions. The piles in the bent were labeled Piles 1, 2, 3 and 4 with Pile 1 being the far right pile facing Old Town Creek and Pile 4 being the far left pile facing Old Town Creek. This numbering convention will be used henceforth in this chapter.
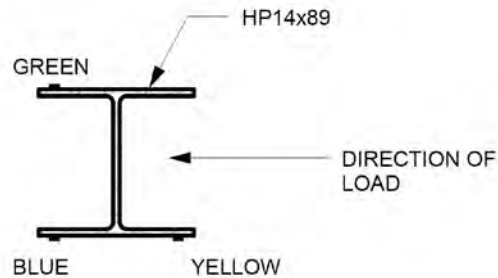
Figure 4-3 Strain Gage Layout at Typical Instrumented Section

81
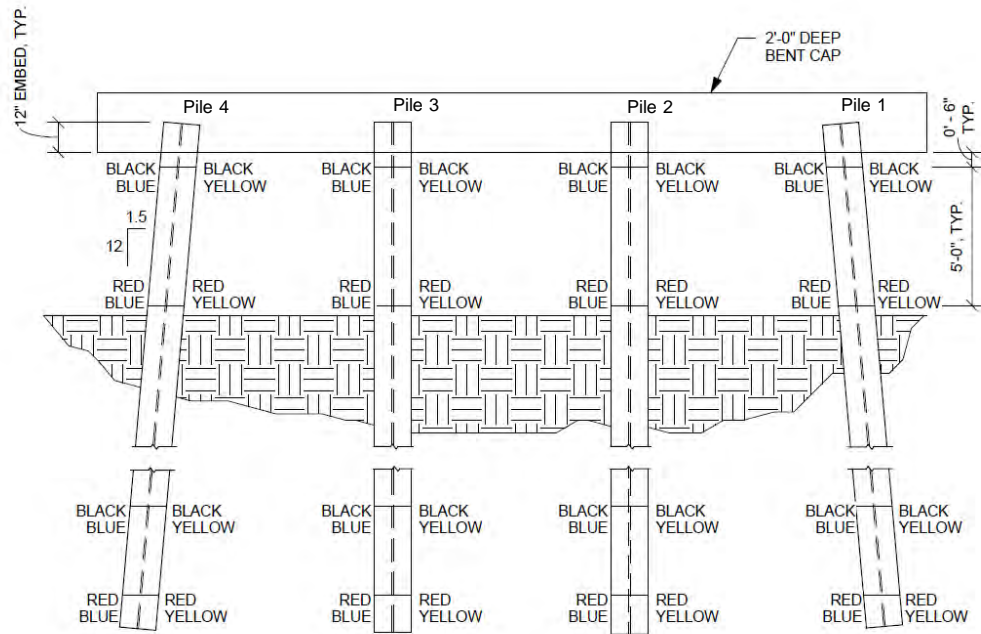
Figure 4-4 Steel Pile Instrumentation Layout Facing Old Town Creek

Figure 4-4 only shows the gages used for moment calculations about the axis in which they were loaded. A single gage (shown as the green gage in Figure 3-3) was installed at each section on the opposite flange for strong axis moment calculations. The instrumentation layout for the single gages installed to monitor strong axis bending can be seen in Figure 4-5.
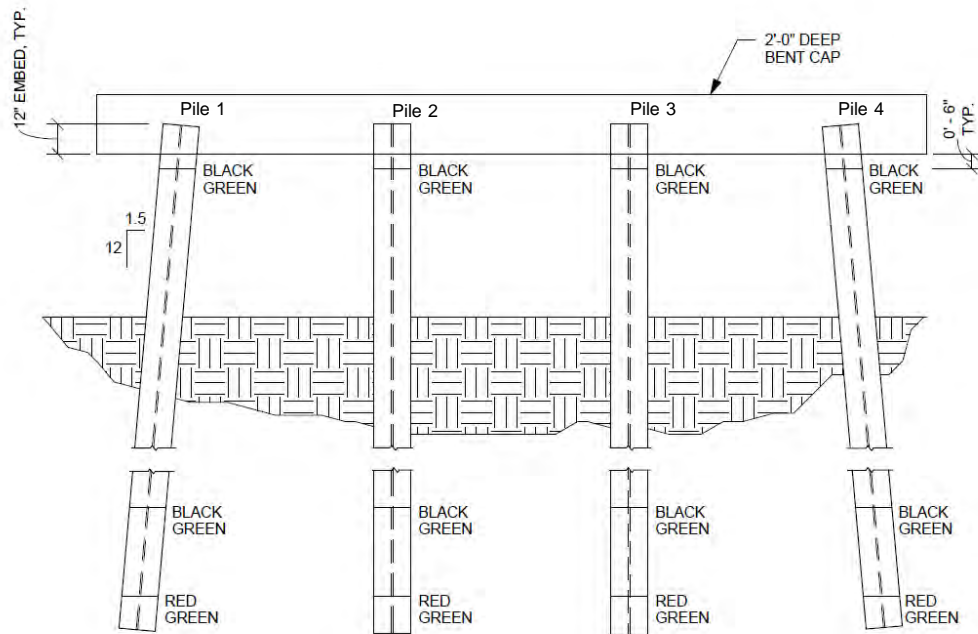
Figure 4-5 Steel Pile Instrumentation Layout Facing Away from Old Town Creek

As seen in the instrumentation layouts above, two sections below grade were instrumented and two sections above grade were instrumented. The gages below grade were installed prior to driving on the inside of the flanges to decrease the frictional resistance between the soil and the pile during the driving process. Two five-foot lengths of L2x2x3/8 were welded to the inside of the flanges over the strain gages were installed to provide additional protection during the driving process. The ends of the angles were cut at an angle and a plate was welded at the ends to act as a driving tip.

After concrete encasements were cast around the driven piles and rip rap was placed, a pair of electrical resistance strain gages were installed on the concrete surface at the same sections as the previously installed steel gages. These gages were installed so that a strain profile over the entire composite cross section could be obtained. A total of 12 concrete surface strain gages were installed: four on Piles 1 and 2 and two on Piles 3 and 4. The instrumentation layout for the concrete surface strain gages can be seen in Figure 4-6.

83
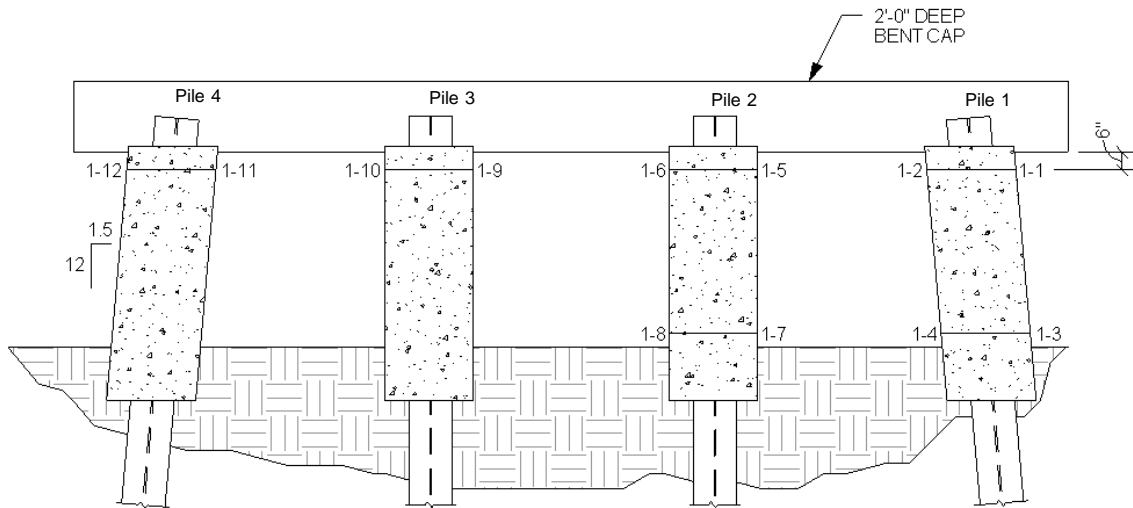
Figure 4-6 Concrete Encasement Instrumentation Layout Facing Old Town Creek

In addition to strain monitoring, WDS P-60 series draw wire sensors from Micro-Epsilon with a 1000 mm (39") range were installed on the bent cap to measure the total lateral deflection of the cap during the load test. These draw wire sensors will be referred to as wirepots for the remainder of this report. Four wirepots were installed at each corner of the bent cap cross section. An image of the wirepot configuration on the cap can be seen in Figure 4-.
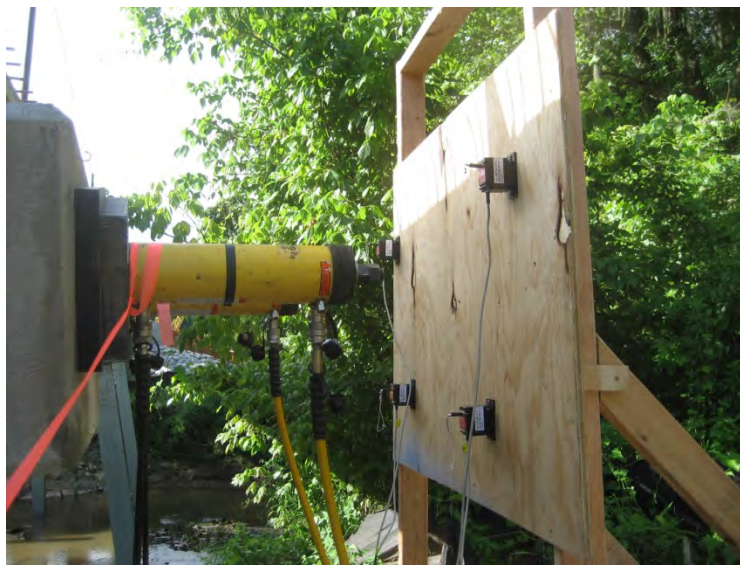
Figure 4-7 Wirepot Configuration

4.3 Testing Equipment and Setup

A frame consisting of two driven HP14x89 piles was used to react against the bridge bent during the lateral load test. The load was applied by pulling the bent and the reaction frame together using high-strength steel threaded rods and center-hole hydraulic jacks. A cut-off section of pile was used as a diagonal brace to achieve frame action in the system. This cut-off section was welded to the two vertical piles in the reaction frame. Two pile cut-offs were welded to the top of the vertical members of the frame. These horizontal members were used to anchor the threaded rods to the reaction frame. The reaction frame configuration used for this load test can be seen in Figure 4-8.

Figure 4-8 Reaction Frame Configuration

Twelve foot sections of 1 1/8 in. diameter threaded rod with a yield strength of 105 ksi were connected using high strength steel coupling nuts to span the entire length of the bent cap. The threaded rods were anchored to the reaction frame using pieces of HSS6x6x1/2. These pieces of HSS6x6x1/2 spanned between the flanges of the horizontal members of the frame as seen in Figure 4-9. The rods were anchored using a nut and washer combination, and were hand tightened prior to lateral load application to ensure adequate bearing of the tube to the flanges of the horizontal members of the reaction frame. These twelve foot segments were joined using high-strength steel hex coupling nuts. The rods were threaded to the coupling nuts from both ends and hand tightened to ensure the full strength of the rods could be adequately developed.

86

Figure 4-9 Threaded Rod End Anchorage at Reaction Frame

The threaded rods were fed through two center-hole hydraulic cylinders that were connected to the end face of the bent cap. Two Enerpac #RRH-3010 long stroke hydraulic cylinders were used for the test. Each cylinder had a capacity of 30 tons (60 kips). The cylinders were connected to an Enerpac ZU4 Class ZU4408JB pump fitted with valves to provide equal pressure on both of the cylinders.

Two 1 ¾"x12"x1-0" A36 steel anchor plates were used as bearing plates on the jack end of the bent cap. A 1" elastomeric bearing pad was placed between the bent cap and the anchor plate to promote an even load distribution over the end face of the concrete bent cap. The anchor plates were designed using a maximum jack load of 120 kips and an allowable concrete stress of

0.85f'$_c$. A conservative concrete compressive strength of 3 ksi was used for the allowable concrete stress at the face of the bent cap. The jack end anchorage can be seen in Figure 4-10.

Figure 4-10 Steel Anchor Plate with Bearing Pad at Jack End

Two threaded rod sections were instrumented with electrical resistance gages in order to monitor the lateral load being applied to the bent during testing. The gages were installed using procedures previously mentioned in 3.2.2. Prior to testing, the rods were calibrated using the to measure axial force and the P3 strain indicator to read axial strain in the rods. The load and strain measurements were used to create stress vs. strain curves for each of the rods from which calibration factors were created for accurate load monitoring during the load test.

For measurement of lateral displacement of the bent cap during testing, displacement wirepots were utilized. A reference beam was necessary to anchor the wirepots. A wooden frame was constructed to anchor the wirepots and serve as a reference. The wooden reference frame can be seen in Figure 4-11 .

Figure 4-11 Wooden Reference Frame for Wirepot Installation

A Campbell Scientific datalogger was used to record data from the electrical resistance gages on the steel piles, concrete pile encasements, sister bars, and threaded rods. The datalogger was also used to record data from the displacement string pots. During the lateral load test, data was recorded once every 15 seconds for the entirety of the test.

Four multiplexers were used to wire in the strain gages and displacement pots. The first three multiplexers were programmed for 120 ohm resistance gages. The strain gages installed on the steel piles were wired into these first three multiplexers. The fourth multiplexer was programmed for 350 ohm resistance gages. The remainder of the strain gages installed on the concrete pile

encasements and the threaded rods were wired into this multiplexer. The wire pots were wired directly into the datalogger.

4.4 Testing Procedure

This section consists of the procedures used during testing. One set of data was recorded for this test. The data set included strain, load, and displacement measurements. The datalogger was programmed so that the output received from the electrical resistance strain gages installed on the threaded rods was in pounds. A laptop connected to the datalogger was used to graphically display the outputs from each of the gaged threaded rods so that the load in the system could be monitored throughout the duration of the load test. Each gaged threaded rod consisted of two strain gages located on opposite sides of the rod. The relative strains in each of the gages were averaged and converted to stresses then force based on their elastic modulus and cross sectional area. A calibration factor was also built into the program within the Campbell Scientific datalogger. A display of the force in both rods was monitored to ensure that each of the jacks was exerting a relatively equal load to prevent major eccentric loading of the bent cap.

4.4.1 Static Lateral Load Test

On June 27, 2014 a static lateral load test was performed on the test bent. At the time of testing, the girders on both the forward and back spans had been set. The strategy for the load test was to load the bent in 10 kip increments up to 60 kips, holding each load increment for five to ten minutes, and then unloading the bent in two to three unloading increments and holding each unloading increment for three to five minutes. An image of the entire test setup can be seen in Figure 4-12.

Figure 4-12 Field Test Setup

Both load and displacement were monitored throughout the entirety of the test to ensure that excessive displacements did not occur and that the load in one jack was not significantly higher than the other. During the loading phases, the pressure in the jacks was increased using a hand-held remote which extended and retracted the pistons.

The bent was loaded in 10 kips increments up to 60 kips, holding at each increment for ten minutes. The bent was then unloaded to 35 kips in three increments, holding at each increment for five minutes. After observation of small displacements at the 60 kip load increment, it was decided to reload the bent in five kip increments up to a total lateral load of 75 kips. The load was held for five minutes at each load increment for this reloading phase. Once the 75 kip load increment was completed, the bent was unloaded in four increments.

4.5 Analysis, Results, and Discussion of Load Test

This section contains measured data as well as results from the full lateral load test. The methods and assumptions made for calculating axial forces and bending moments is also outlined in this section.

4.5.1 Strains

At sections above ground, strain data was captured on both the concrete encasement surfaces as well as the steel piles embedded within the encasements. The strain distribution across the composite section was of major interest, seeing that it had an effect on the method of calculating axial forces and bending moments at the section. For all strain data, compressive strains are considered positive and tensile strains are considered negative. An average of the strains at each loading increment was used in developing the strain profiles since data was recorded for five to ten minutes at each load.

Upon observation, it was clear that the sections above ground in which concrete and steel surfaces were instrumented, were not behaving fully composite. The strain profile across the entire cross section was not linear. Notably, the steel section was straining significantly more than the concrete. Strain profiles at each of the above ground sections in which concrete and steel surfaces were instrumented for graphical representation of the non-composite behavior. Strain profiles at each cross section can be seen in Figure 4-13 through Figure 4-22. The instrumented sections on the concrete surface occur at +/- 15 in. on each of the plots. The strain profiles for each pile are divided into two separate plots ranging from 10-40 kips and 50-75 kips in order to better determine behavior between load increments.

Upon observation, none of the concrete surface gages installed on the upper section of pile 1 were functioning correctly; therefore, this section was not considered in the calculations of axial forces and moments. As stated previously, the upper instrumented sections were located six

92

inches from the bottom of the bent cap and the lower instrumented sections were located five feet below the upper instrumented sections. Concrete encasements were only instrumented at the upper locations on piles 3 and 4, therefore strain profiles at the lower sections for these piles are not included in the figures below.
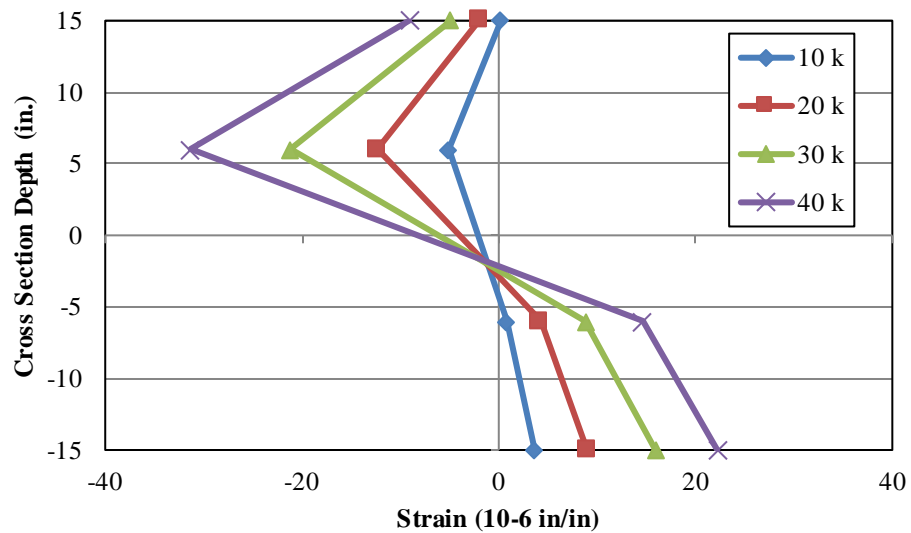
Figure 4-13 Pile 1 Lower Section Strain Profile
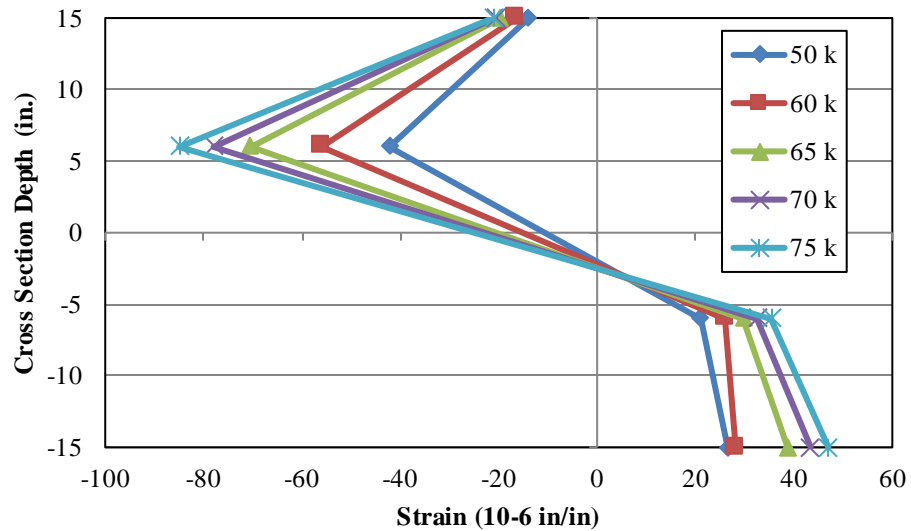
Figure 4-14 Pile 1 Lower Section Strain Profile
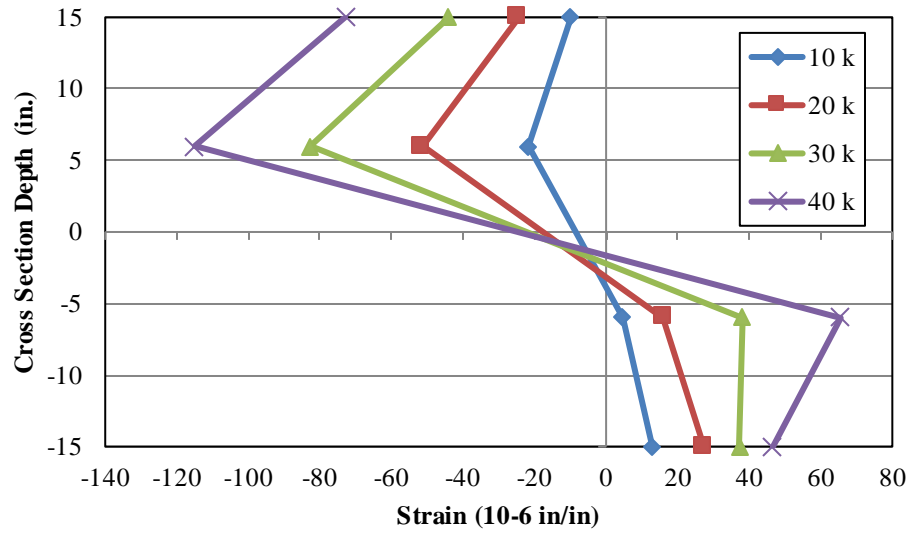
Figure 4-15 Pile 2 Upper Section Strain Profile
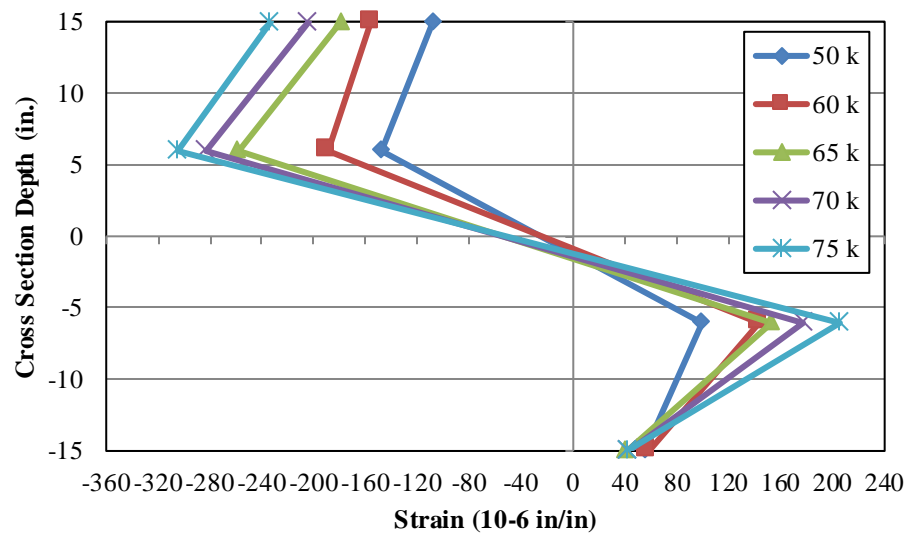
Figure 4-16 Pile 2 Upper Section Strain Profile

94
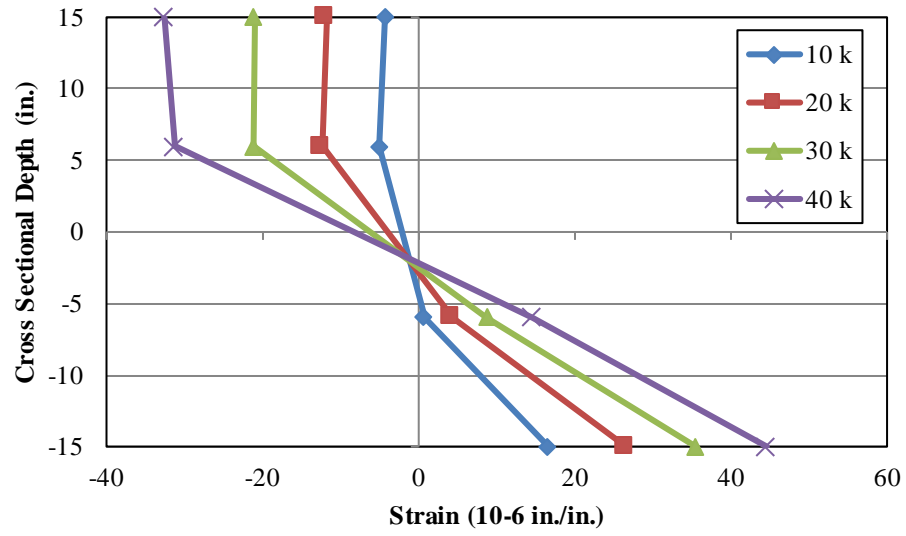
Figure 4-17 Pile 2 Lower Section Strain Profile
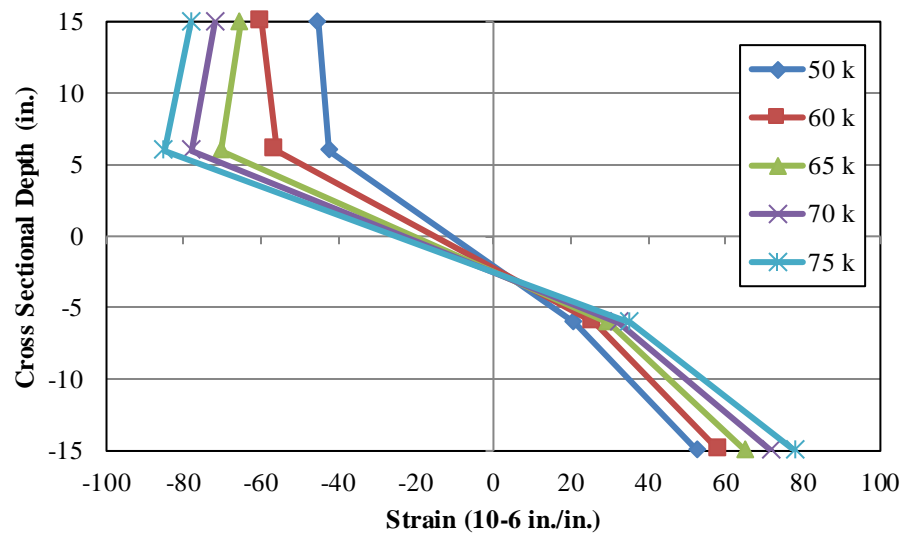
Figure 4-18 Pile 2 Lower Section Strain Profile

95
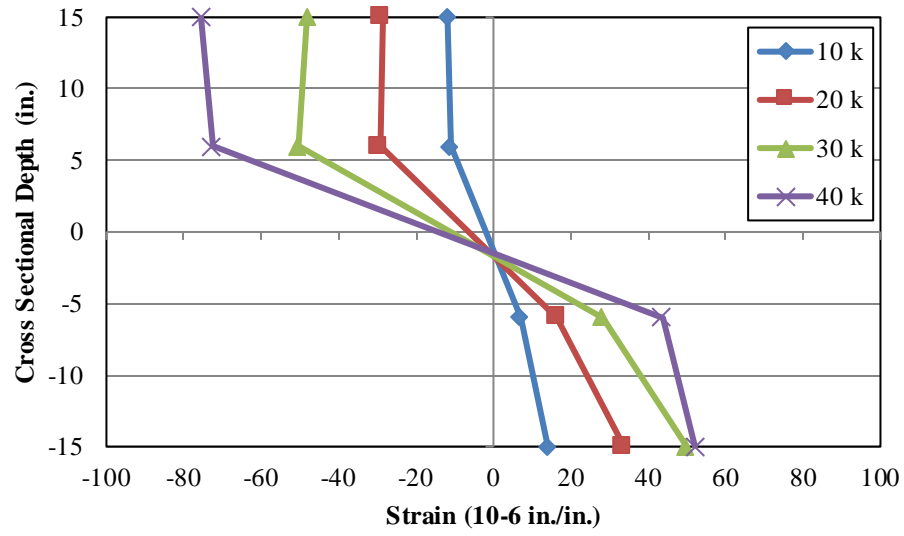
Figure 4-19 Pile 3 Upper Section Strain Profile
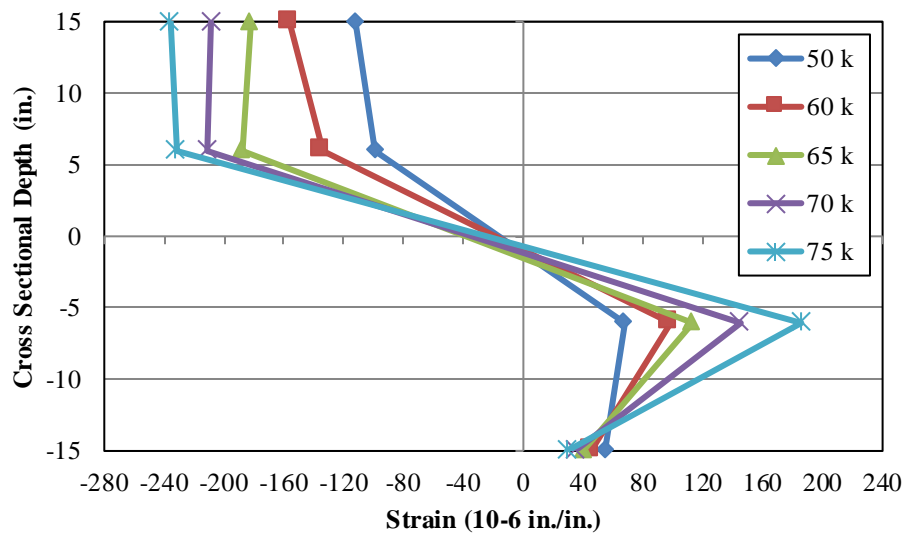
Figure 4-20 Pile 3 Upper Section Strain Profile

96
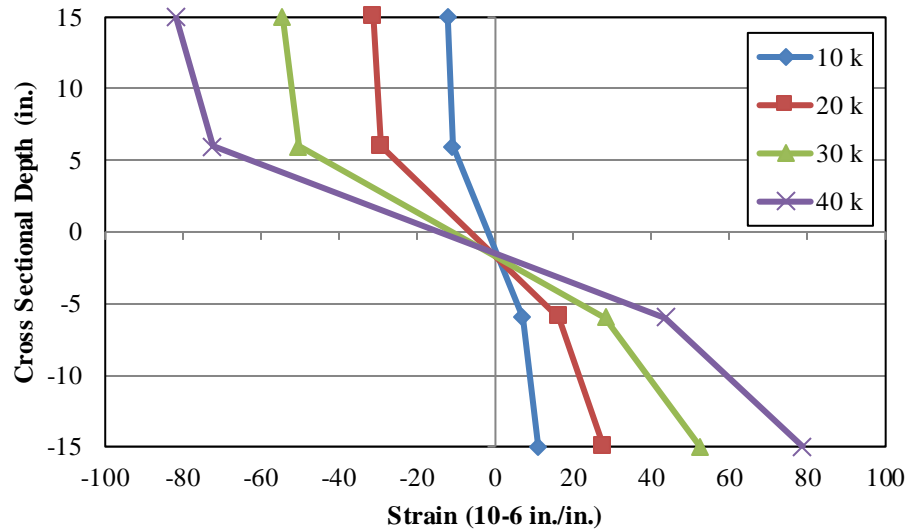
Figure 4-21 Pile 4 Upper Section Strain Profile
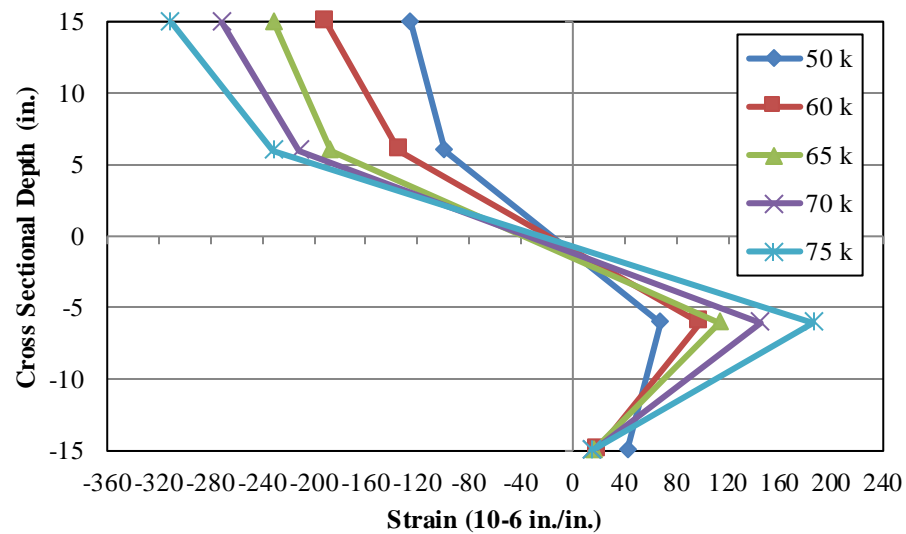
Figure 4-22 Pile 4 Upper Section Strain Profile

A number of different factors can be attributed to the piles not behaving perfectly composite. It is likely that the cracks had formed in the concrete due to the concrete being restrained by the steel pile. These restrain cracks would have formed prior to the piles being displaced during the tests. The locations of these cracks are very difficult to determine; therefore, the gages installed on the tension faces of the encasements have extremely variable results as the applied load

97

increases. Once the concrete cracks, bond stresses between the concrete and the steel are developed which can cause slipping.

The level of composite behavior, however, is of little concern to bridge designers seeing that they do not account for the stiffness or strength of the concrete encasements in their pile design. The encasements are in place primarily to prevent section loss of the steel piles in cases where the bent is located within the flow channel.

4.5.2 Axial Force and Bending Moment Calculations from Strain Data

For axial force and bending moment calculations at instrumented pile sections, two different approaches were used. As previously mentioned, the instrumented sections where both steel and concrete surfaces were instrumented did not behave perfectly composite. The method for computing axial forces and bending moments at this location became more involved due to the non-linear strain profile over the cross section. This section details how axial forces and bending moments were calculated at sections with and without concrete encasements.

The axial stress at cross sections where the piles were not encased in concrete was computed by taking the average of the compressive and tensile strains on the cross section and multiplying it by the modulus of elasticity of the steel pile. The force was then computed by multiplying the axial stress by the gross cross-sectional area of the steel pile. The method used for computing the axial force in the steel pile can be seen in Equation 4-1.

$$P = \left(\frac{\varepsilon_c + \varepsilon_t}{2}\right) E A_g \qquad \text{(Equation 4-1)}$$

Where:

P = axial load in pile (kips)

ε_c=compressive strain (in./in.)

ε_t=tensile strain (in./in.)

98

E = modulus of elasticity (ksi)

A_g = gross cross-sectional area (in.^{2})

For these computations, the modulus of elasticity used for the steel piles was assumed to be 29,000 ksi and the gross cross-sectional area used for HP14x89 was 26.1 in.^{2}.

At sections where the steel piles were not encased in concrete, bending moment calculations are performed assuming a linear strain distribution over the pile cross section. Using the two measured strains on the tension and compression sides of the pile flange, the curvature of the cross section can be computed using Equation 4-2.

$$\varphi = \frac{\varepsilon_c - \varepsilon_t}{h} \qquad \text{(Equation 4-2)}$$

Where:

φ=curvature (in.$^{-1}$)

ε_c=compressive strain (in./in.)

ε_t=tensile strain (in./in.)

h=distance between measured strains (in.)

The curvature was then used to calculate bending moments at the cross section using Equation 4-3.

$$M_b = \varphi E I \qquad \text{(Equation 4-3)}$$

Where:

M_b = bending moment (kip-in)

E = modulus of elasticity (ksi)

I = moment of inertia (in.^{4})

The piles were being loaded in the weak axis direction, therefore I_y of the HP14x89 was used as the moment of inertia used for calculation of bending moment, which was 326 in^4.

A different approach was necessary for computing axial forces and bending moments at the instrumented sections where both steel and concrete strains were measured. Had the sections behaved in a truly composite manner, i.e. the strain profile over the cross section was linear, then a transformed section analysis could have been used to compute the bending moments on the cross section.

A basic integration approach was considered for axial force and bending moment calculations. The cross section was divided into six areas, and the strains at the centroid of these areas were linearly interpolated based on the measured strains. Figure shows the cross section divided into these six areas. The trapezoidal rule for integration was used to calculate these areas. For concrete stress calculations where steel areas were also present, the areas of the steel were subtracted from the concrete area.
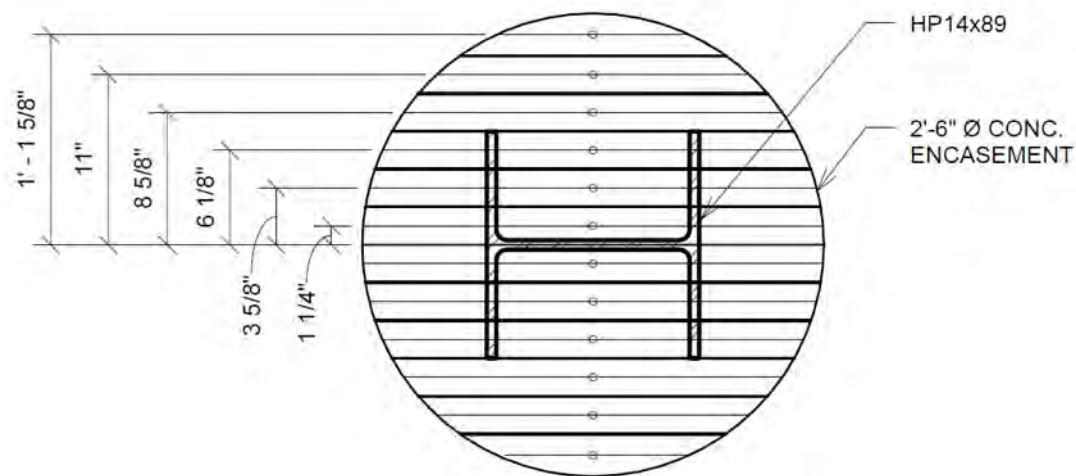
Figure 4-23 Composite Cross-Section Geometry

Axial Stresses at each of these locations were computed using Hooke's Law. This assumption was made assuming the section remained uncracked during the load tests. Equation 4-4 was used to calculate the axial force on the cross section.

$$P = \int_A \sigma dA \qquad \text{(Equation 4-4)}$$

100

The strains and cross sectional areas of both the concrete and steel were used for this calculation. Implementing Hooke's Law and separating the steel and concrete terms, equation 4-5 can be shown as:

$$P = \sum(\varepsilon_{i,c} E_c A_{i,c}) + \sum(\varepsilon_{i,s} E_s A_{i,s)} \qquad \text{(Equation 4-5)}$$

Where:

P = axial force on cross section (kips)

$\varepsilon_{i,c}$ = strain in concrete (in./in.)

E_c = modulus of elasticity of concrete (ksi)

$A_{i,c}$ = incremental area of concrete (in^2)

$\varepsilon_{i,s}$ = strain in steel (in./in.)

E_s = modulus of elasticity of steel (ksi)

Moment equilibrium was used in order to calculate the bending moment on the cross section. Moments were summed about the center of the composite cross section using the forces calculated using equation 4-5. Equation 4-6 was used to calculate bending moments at each instrumented cross section where steel and concrete surfaces were instrumented.

$$M_b = \int_A \sigma y dA \qquad \text{(Equation 4-6)}$$

Similar to axial forces computation, the cross section was divided into incremental areas. The strain at the centroid of each of these areas was determined using linear interpolation, and the incremental area was calculated using the trapezoidal rule. The moment arm, y, for this calculation was the distance from the centroid of the incremental area to the centroid of the composite cross section. The relationship in equation 4-6 simplifies to equation 4-7. This equation was used to compute bending moments on the composite cross section where d_i is the distance from the centroid of the incremental area to the centroid of the composite cross section.

101

$$M_b = \sum \varepsilon_{i,c} E_c * d_i * A_{i,c} + \sum \varepsilon_{i,s} E_s * d_i * A_{i,s} \qquad \text{(Equation 4-7)}$$

The modulus of elasticity used for the concrete encasements was based on cylinder tests performed by the contractor. The approximated concrete modulus of elasticity was calculated using Equation 4-8. This equation was simplified from the equation for approximate modulus of elasticity in ACI 318-11 (ACI 2011), assuming normal weight concrete with a unit weight of 150 pcf. For this computation, the measured compressive strength from cylinder breaks at 28 days was used and the lightweight concrete factor was taken as 1.0.

$$E_c = 57{,}000\lambda\sqrt{f'_c} \qquad \text{(Equation 4-8)}$$

Where:

E_c = concrete modulus of elasticity (psi)

λ=lightweight concrete factor

f'_c = specified 28-day concrete compressive strength (psi)

Cylinder breaks were made at 8 and 28 days. The 28-day tests were performed on June 16, nine days before the load test was performed. For all calculations from this load test, the measured compressive strengths from the 28-day cylinder tests were used. An average of the two cylinder strengths was used in computing the modulus of elasticity of the concrete encasements. Table 4-1 shows the cylinder test results for the concrete encasements used in bent 5 at the Old Town Creek Bridge.

Table 4-1 Concrete Properties

Test Date	Age (days)	Specified Compr. Strength (psi)	Actual Compr.Strength (psi)
05/2714	8	3000	3590
06/16/14	28	3000	4720
06/16/14	28	3000	4780

The specified 28 day compressive strength for these pile encasements was 3000 psi. These encasements are typically used to prevent pile section loss in terms of corrosion, and are not used in structural calculations for the piles. The actual measured compressive strengths from these cylinder tests at 28 days indicated that the concrete used for the encasements exceeded their specified compressive strength considerably. The value of E_c used from the average of the measured compressive strengths was 3928 ksi.

4.5.3 Axial Forces

The axial forces calculated were found to be well beyond theoretical values. Due to the large cross sectional area of the concrete encasements, minor changes in strain result in a large change in axial forces. The forces that were calculated were not feasible considering equilibrium therefore they were deemed too inaccurate to report.

4.5.4 Bending Moments

Bending moment profiles for each pile can be seen in Figure 4-24 through Figure 4-31. The pile depth is measured from the top of the pile head, which is embedded one foot into the cast-in-place bent cap. The first instrumented section occurred six inches below the bottom of the cap, therefore the first point on each of the bending moment profile occurs at -1.5 feet. The top of the rip-rap varied slightly at each pile location, but occurred at an average of -7.0 feet. The ground elevation below the rip-rap layer occurs at approximately -10.0 feet. Negative moments at below ground cross sections indicates curvature reversal meaning the pile flanges that were in tension or compression at sections instrumented above ground were now opposite. The stiffness of the concrete section was much larger relative to the steel pile section, therefore the bending moments carried by the concrete section are transferred into the ground at the level in which the encasements terminate. A small amount of bending moment is shed into the pile itself at the

103

location which the encasements stop. Therefore, the bending moments carried by the steel section below ground are very small in comparison to the above ground composite moments.
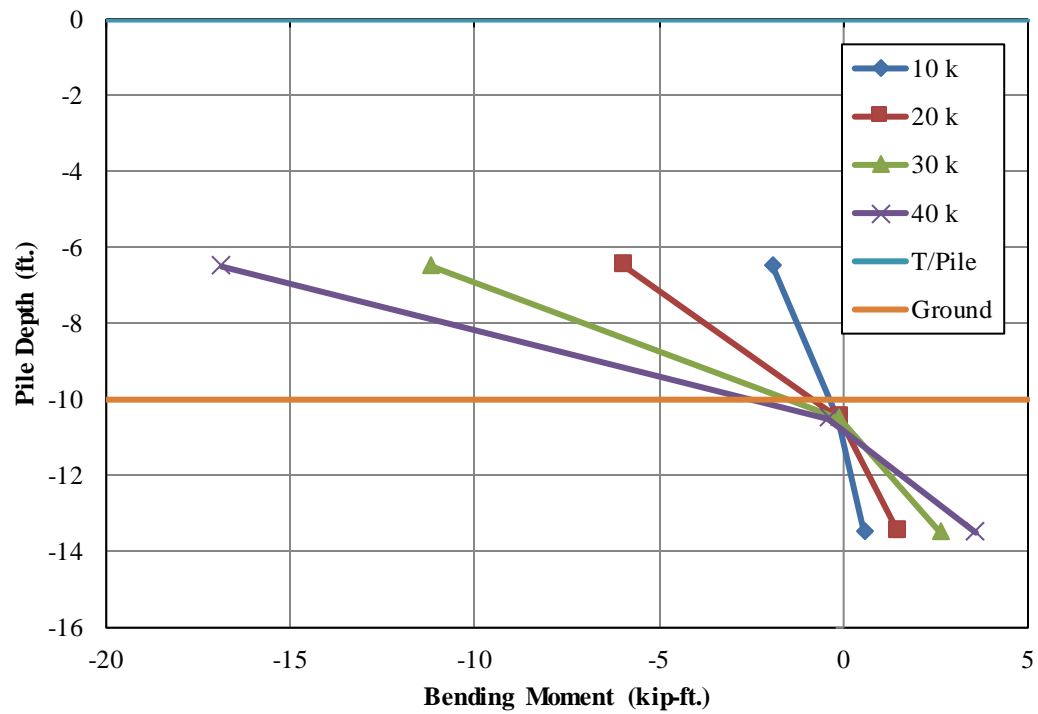
Figure 4-24 Pile 1 Bending Moment Profile
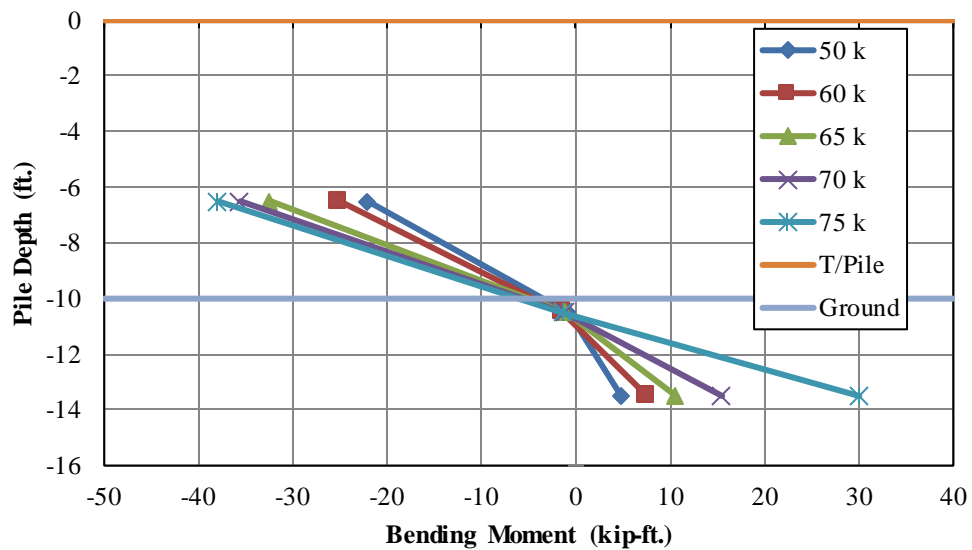
Figure 4-25 Pile 1 Bending Moment Profile
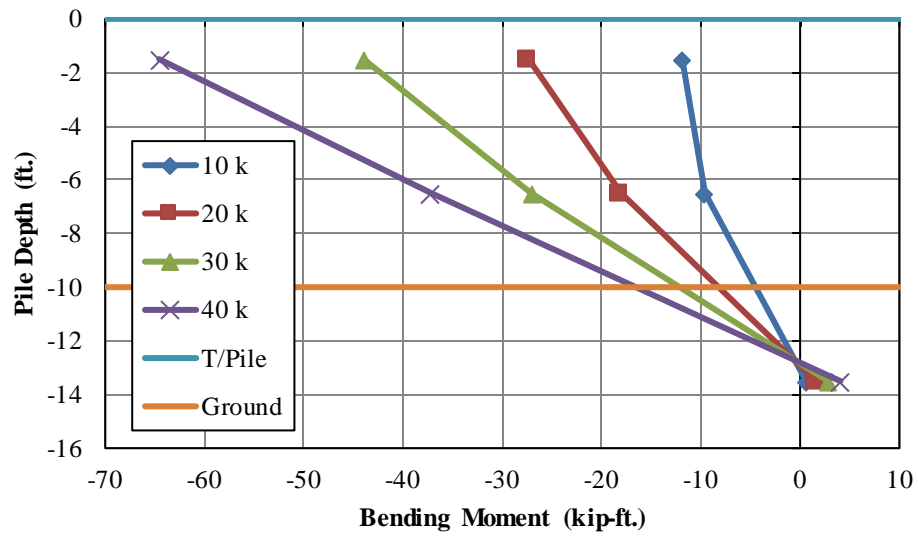
Figure 4-26 Pile 2 Bending Moment Profile
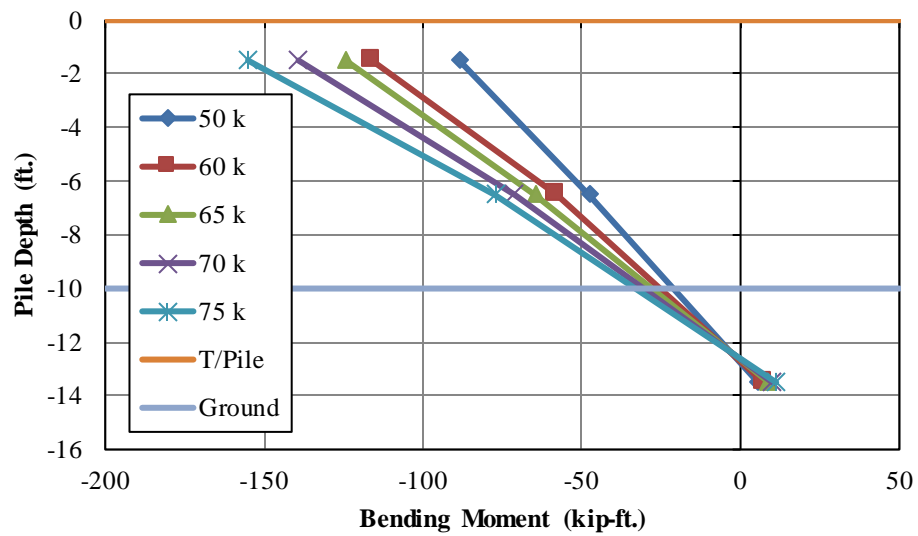
Figure 4-27 Pile 2 Bending Moment Profile
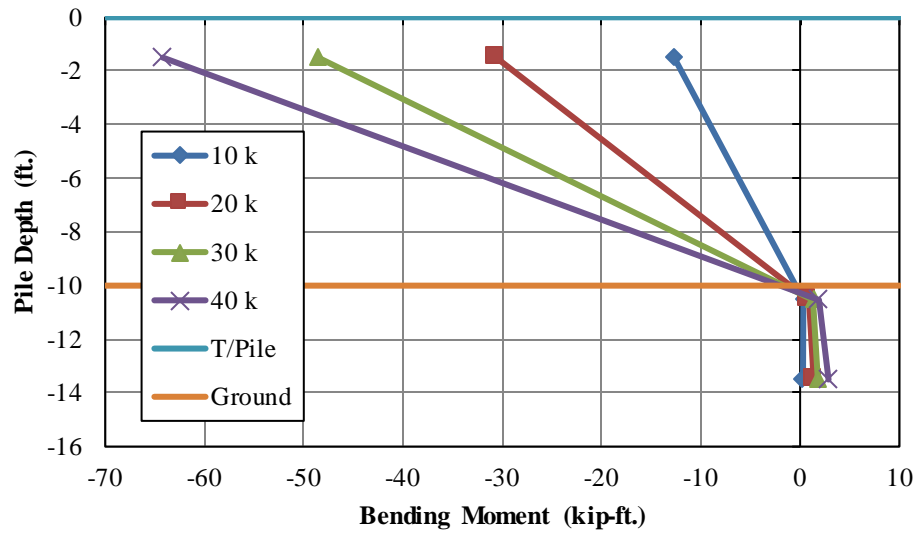
Figure 4-28 Pile 3 Bending Moment Profile
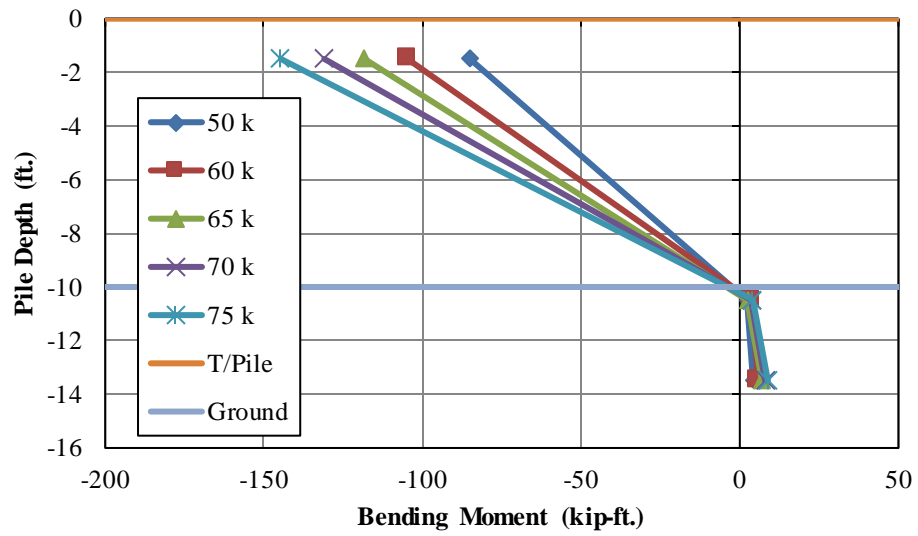
Figure 4-29 Pile 3 Bending Moment Profile

106
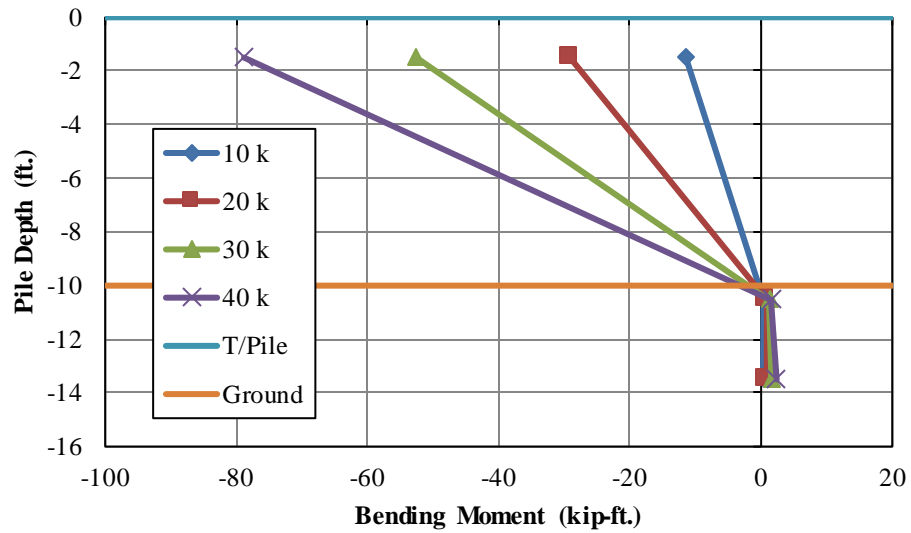
Figure 4-30 Pile 4 Bending Moment Profile
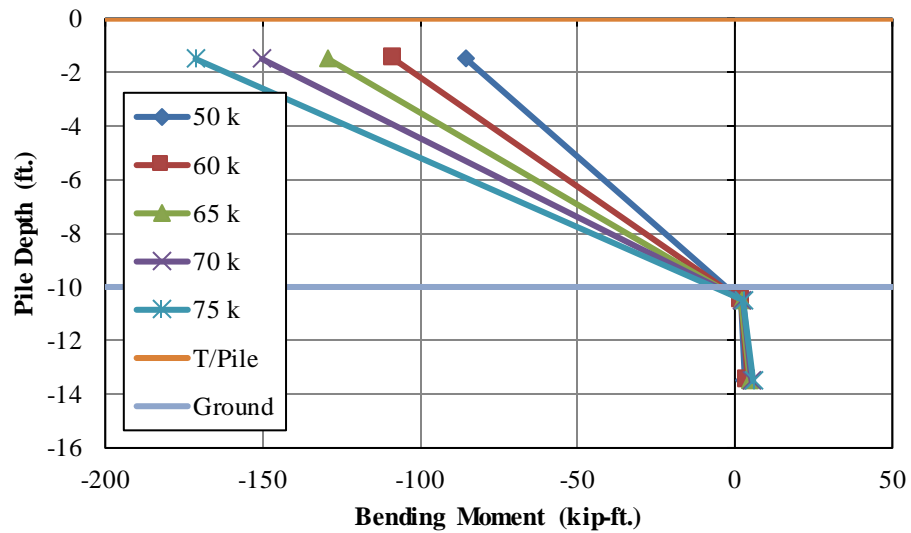
Figure 4-31 Pile 4 Bending Moment Profile

4.5.5 Displacement Wire Potentiometers

Lateral displacement data was recorded during the load test using displacement wirepots. Wirepots were installed in each corner of the bent cap to obtain a load versus average lateral deflection relationship for the pile bent substructure. Four wirepots were also used to ensure that no significant twisting of the cap was present due to eccentric loading. The load versus deflection

plot for the load test can be seen in Figure 4-32. The recorded displacement for each of the four wirepots as well as the average deflection can be seen in the figure.
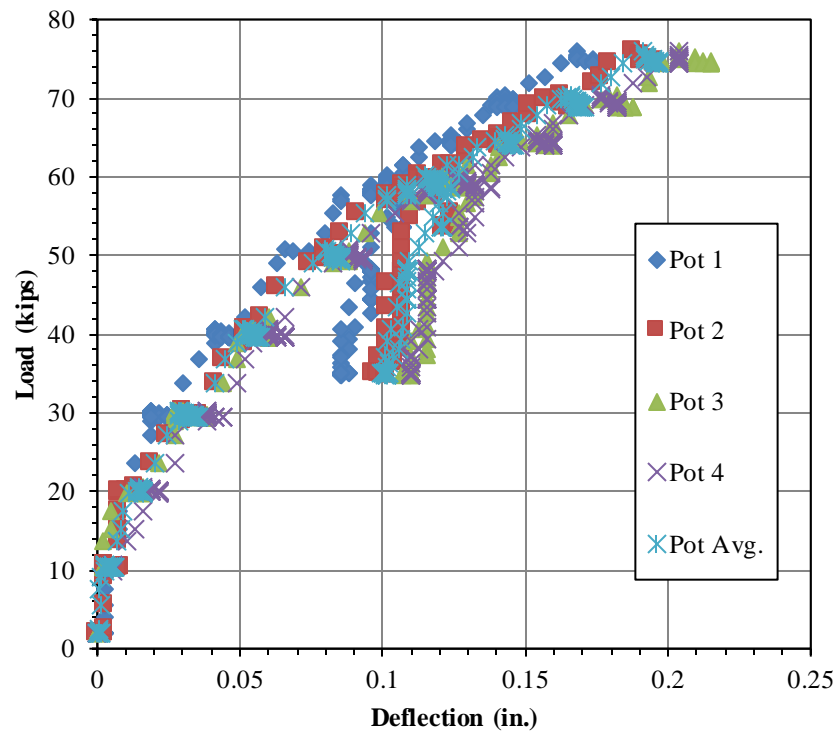
Figure 4-32 Load-Deflection Plot – Macon County Test 1

The recorded deflection for each of the four plots is very similar for the entire duration of the load test. This similarity in deflections is important in that there was little effect due to eccentric loading, meaning that the load in each of the hydraulic jacks remained virtually the same throughout the duration of the test. This similarity in each of the wirepots also proved that there was little very little twisting of the cap.

The bent deflected an average of 0.2 in. at a maximum lateral load of 75 kips. The large overall stiffness of the bent can be attributed to a number of reasons. The lateral stiffness of the pile bent structure is heavily dependent on the stiffness of the vertical elements which in this case are the piles. The flexural stiffness of a single pile with respect to a concentrated load is a function of the unbraced length cubed. The test bent for the Macon County Bridge had pile clear

heights of around 5 feet, making the bridge extremely stiff. The stiffness is also a function of the modulus of elasticity of the elements and their moment of inertia. For the encased steel piles, the moment of inertia of the concrete section alone is 487 times greater than the moment of inertia of the steel piles in the direction in which they were loaded in the test. This additional stiffness increases the overall stiffness of the bent significantly.

4.5.6 Bridge Bent Behavior

The Macon County Bridge bent was very stiff during the lateral load test. The high stiffness of the bent can be attributed to the small free height of the piles and the additional stiffness of the circular concrete encasements. The shape of the bending moment profile in each of the four piles during the load test was similar to the theoretical shape of the bending moment profile with the piles behaving in a fixed head condition with the maximum bending moment at the top of the pile. Although a complete profile was not captured with the instrumentation used, the curvature reversal of the piles below finished grade could clearly be seen. The bending moment dissipated quickly as the pile depth increased. This dissipation can be partially attributed to the load carried by the concrete encasement being transferred to the soil and the steel pile where it is terminated. Due to the large amount of load carried by the encasement relative to the steel pile, the remanding load transferred through the pile is small. The maximum bending moment that was calculated from measured strains was much smaller than the maximum bending moment at the bottom of the bent cap. This dissipation in moment can be attributed in part to the lateral load transfer from the pile to the soil at these depths. The lateral resistance of the soil results in shear forces in the pile, causing curvature reversal. From measured strains on the concrete encasements and the steel piles, it was observed that the piles were not acting perfectly composite. This level of composite behavior can likely be attributed to the presence of small shrinkage cracks

developed due to the steel pile restraining the concrete. However, a cracked section analysis was not used.

4.6 Chapter Summary

The bent performed very well and was exceptionally stiff under lateral loads easily exceeding service level lateral loads. Bending moment values were relatively high for each of the four piles. The maximum moment value occurred at the top of the pile indicating that the connection between the bent and the pile cap had significant moment capacity. The measured strains gave inconclusive results with regards to the axial forces in each of the piles under lateral loading. The pile section encased in concrete did not appear to act perfectly composite, but this level of composite behavior is of little interest to designers since they do not take into consideration the stiffness or strength of the concrete encasements in the design of the piles. The addition of these encasements only increases the performance and stiffness of the pile bents.

5. Field Test 2 – Macon County Bridge

5.1 Introduction

The Macon County Route 9 replacement bridge under construction was also used for the second field test. The second test was completed following casting of the concrete roadway. The barrier rails had not yet been cast at the time of testing. The roadway consisted of a 7 in. concrete deck with a width of 30'-9", a typical width for standard 12 ft. lanes. A typical roadway cross section can be seen in Figure 5-1. Three tests were performed in this test: a purely lateral load test and two combined gravity and lateral tests. ALDOT load trucks were used for application of gravity load. For the first combined gravity and lateral load test, the load truck was positioned in the center of the roadway with the back-center wheel axle centered over the bent. For the second combined lateral and gravity load test, the load truck was positioned on the edge of the roadway over the piles that were expected to be in axial compression due to overturning from lateral load. The instrumentation used in the first load test was also used for this second load test. Load transfer through the bridge deck was not within the scope of this research; therefore, the bridge deck was not instrumented prior to load testing.
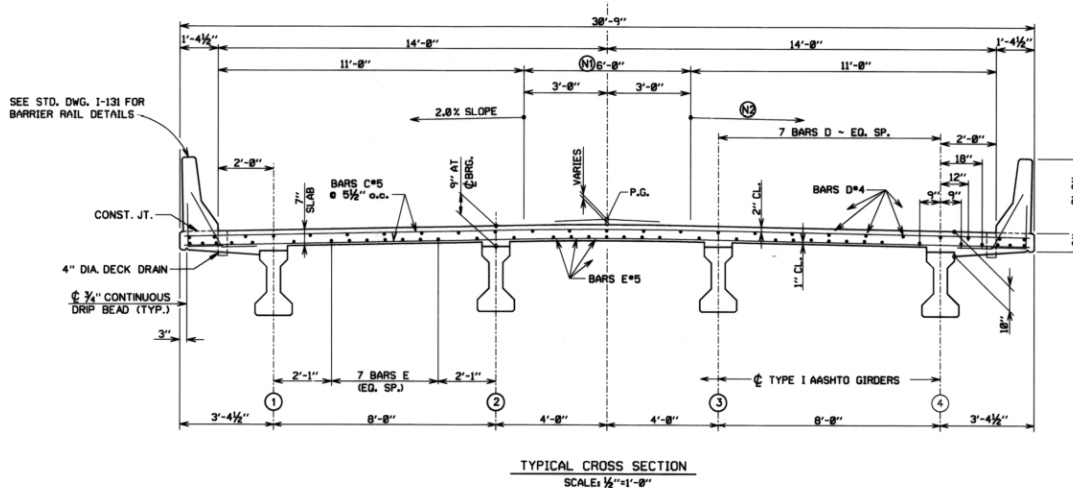
Figure 5-1 Typical Roadway Cross Section (Weatherford & Associates 2013)

This chapter details the instrumentation, testing methods, and equipment used for the second load test at the Macon County replacement bridge. This section also details the analysis, results and discussion of the data collected during the load tests.

5.2 Instrumentation, Test Equipment and Setup

The instrumentation used for the first load test on the Macon County Bridge was also used for the second load test. The instrumentation installed on the steel piles, concrete encasements, and sister bars were used to calculate axial forces and bending moments during the tests. For instrumentation layouts, instrumentation used, and installation procedures, see Section 4.2. The same reaction piles were used but had been repaired following a weld rupture which had occurred in the previous test.

5.2.1 Truck Live Load

For the combined lateral and gravity load tests, an ALDOT load truck was used for gravity load application. The load truck configuration used for this load test was LC-5. The load truck with this configuration weighed a total of 85,700 lbs. A figure of the LC-5 configuration can be seen in Figure 5-2 . The geometry and axle loads for the load truck in the LC-5 configuration can

112

be seen in Figure 5-3. In this figure, the GVW shown in the total truck weight. The loads shown represent the total load for each of the three axles.
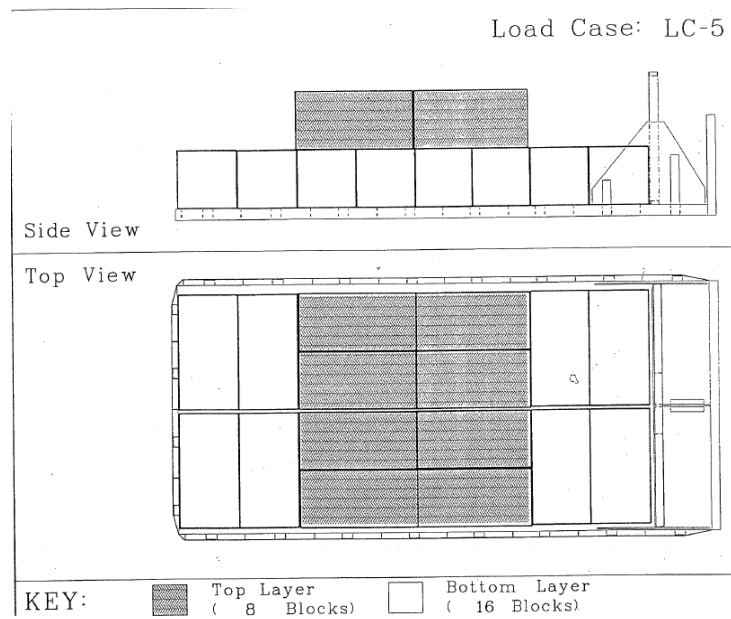
Figure 5-2 ALDOT Load Truck LC-5 Configuration (ALDOT)
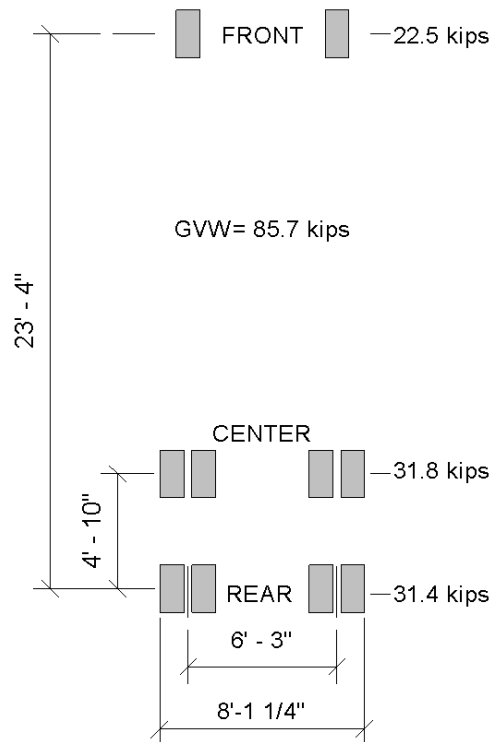
Figure 5-3 LC-5 Geometry and Axle Loads

During the test, the truck was positioned so that the center axle of the truck seen in Figure 5-3 was centered over the bent centerline. Two different tests were completed, with the transverse position of the load truck varying. In each of these tests the longitudinal positioning of the load truck remained the same.

5.3 Testing Procedure

This section details the procedure for each of the tests performed on the Macon County replacement bridge and how the loads and deflections were monitored during the testing of the bridge. Three separate load tests were performed. The first test performed was a purely lateral load test with the only axial load being the self-weight of the structure. The second and third tests were combined lateral and axial tests. An ALDOT Load Truck in configuration LC-5 was used for axial load application. The load truck's center of gravity was positioned directly over the bent for each test. The load truck was positioned in the center of the roadway for the first test and positioned so that the outside wheels were over the exterior girder for the second test.

5.3.1   Static Lateral Load Test

The first test performed on September 18, 2014 was a purely lateral load test with no ALDOT load truck. This test was executed similarly to the load test on the bent in Chapter 4. The bent was loaded in ten kip increments up to a total lateral load of 60 kips. The load was held for five minutes at each loading increment to obtain a sufficient amount of data for each load. Once the total load was reached, the bent was unloaded in four unloading increments. A specified load was not used in each of the unloading increments. However, the load at each unloading increment was recorded and held for three minutes to obtain a sufficient amount of data. The bent was unloaded in this manner until the load in the threaded rods was due to initial tension.

5.3.2 Combined Lateral and Gravity Load Test – Truck Centered in Roadway

The second test performed was a combined lateral and gravity test using an ALDOT load truck with the LC-5 configuration. The truck was centered over the roadway for the first test to theoretically distribute the truck load evenly to each of the four piles in the test bent. The back middle wheel axle was centered over the test bent to ensure that the truck load's center of gravity was directly over the bent. Data was recorded as the truck entered the bridge roadway and continued to be recorded for five minutes after it reached its intended position. The position of the load truck during the first combined lateral and gravity test can be seen in Figure 5-4.

Figure 5-4 ALDOT Load Truck Centered in Roadway
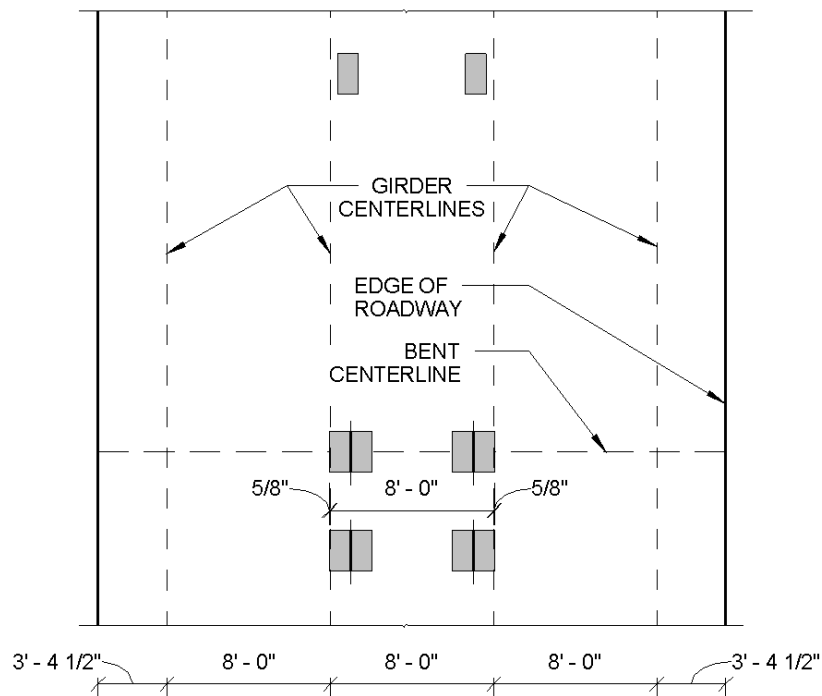
Figure 5-5 Position of Load Truck Centered Over Roadway

Once the truck was positioned correctly and sufficient data was recorded, the bridge was loaded laterally. The bent was loaded in 10 kip increments up to a total lateral load of 60 kips. Each load increment was held for five minutes to obtain a sufficient amount of data. Once the 60 kip load increment was reached, the bent was then loaded in 5 kips increments up to a total lateral load of 75 kips. Each load increment from 65 kips to 75 kips was also held for five minutes. Once the total load was reached, the bent was then unloaded in four unloading increments. Each unloading increment was held for three minutes to obtain sufficient data. The bent was unloaded until the load in the threaded rods reached the initial load.

5.3.3   Combined Lateral and Gravity Load Test – Truck Positioned at Edge of Roadway

The third test performed was a combined lateral and gravity load test as well. For this test, the ALDOT load truck was positioned at the edge of the roadway with its outside wheel centered

116

over the exterior girder. Similarly to the second test, the load truck's back center axle was centered over the test bent.

The truck was positioned over the side of the bent in which the piles were expected to be in axial compression due to overturning. The goal was to apply the gravity load to induce maximum compression in the exterior battered pile. The truck's positioning for the third test can be seen in Figure 5-6 and Figure 5-7.

Figure 5-6 ALDOT Load Truck Positioned at Edge of Roadway
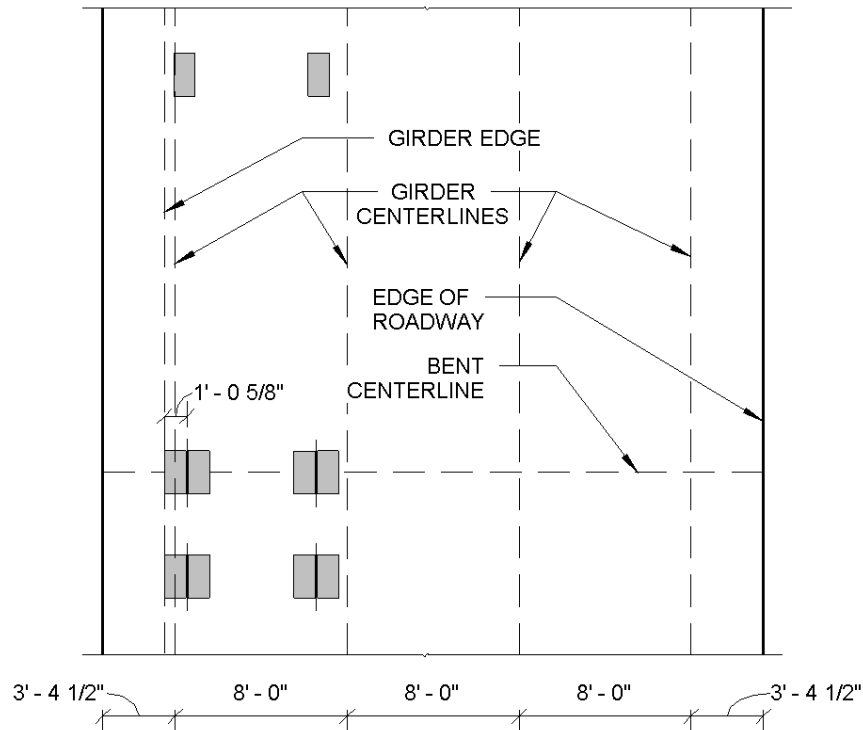
Figure 5-7 Position of Load Truck Over Exterior Girder

The truck was positioned appropriately and data was recorded for five minutes to obtain axial force information in the piles. The bent was then loaded laterally in 10 kip increments up to a total lateral load of 60 kips. The load was held for five minutes at each loading increment to obtain sufficient strain data. After the last loading increment was completed, the bent was then unloaded in a series of four increments. Each unloading increment was held for three minutes before proceeding to the next increment. The bent was unloaded until the force in the threaded rods reached its initial load.

5.4 Analysis, Results and Discussion of Load Test

This section contains measured data as well as results from the three load tests performed. The methods and assumptions made for calculating axial forces and bending moments is also outlined in this section.

118

5.4.1 Strains

Measured strains from gages instrumented on the concrete surface and the steel piles were observed in order to determine the functionality of the gages. At sections in which the concrete surface and the steel pile were both instrumented, the strain distribution across the composite cross section was inspected to determine whether or not the cross section was acting compositely. Similarly to the measured strains in the first load test outlined in Chapter 4, the encased sections did not appear to behave fully compositely. The strain distributions over the composite cross sections were not linear. This nonlinear strain distribution was accounted for when calculating axial forces and bending moments at the cross sections in which strains were measured on the concrete and the steel pile.

Upon observation, neither of the concrete surface gages on the upper instrumented section on Pile 1 appeared to be functioning correctly therefore they are not included in the bending moment profiles.

5.4.2 Axial Force and Bending Moment Calculations from Strain Data

Two different approaches for calculating bending moments and axial forces were implemented. The first approach was used for sections in which strains were measured on the concrete surfaces and the steel piles. This approach consisted of linearly interpolating the strains at discrete points along the cross section and integrating over the area. The second approach was used for calculating bending moments at instrumented cross sections not including concrete encasements. This approach used the curvature of the cross section based on measured strains and the bending moment was calculated by multiplying the curvature by their moment of inertia and their modulus of elasticity. The moment of inertia of the axis about which the piles were loaded was used in these calculations. The concrete strengths used in the load test outlined in Chapter 4 were used again for axial force and bending moment calculations for the load tests in

119

this chapter as well. These concrete strengths were based on compressive tests performed at 28 days after placement of the encasements. A modulus test was not performed on cylinder samples from the concrete placed in the bent cap or the encasements; therefore the modulus of elasticity for the concrete encasements was approximated using the empirical equation given in chapter 3. For further details regarding the calculation of bending moments and axial forces, refer to Section 4.5.2.

5.4.3 Axial Forces

The axial forces calculated were found to be well beyond theoretical values. Due to the large cross sectional area of the concrete encasements, minor changes in strain result in a large change in axial forces. The forces that were calculated were not feasible considering equilibrium therefore they were deemed too inaccurate to report.

5.4.4 Bending Moments

The bending moment profiles for each of the piles for each load test are provided in this section. For calculation of bending moments for each of the piles, the strain at each gage location was averaged during each load increment to account for relaxation during loading. Both concrete surface gages on pile 1 located 6 inches from the bottom of the cap were found to be faulty during the test. The lower gages at the lowest instrumented section of pile 1 were also faulty leaving two functioning instrumented sections for pile 1. The bending moment profile for pile 1 is not included in the sections below due to a lack of sufficient data points. The instrumented sections on piles 3 and 4 located five feet from the bottom of the cap are not included in the bending moment profiles due to the lack of concrete surface gages at these locations. For all bending moment profiles shown in this section, zero elevation occurs at the top of the pile which occurs at the centerline of the bent cap. The first data point occurs at elevation -1.5 ft. which is

120

located 6" below the bottom of the cap. The top of the rip-rap layer occurs at approximately -7.0 ft. and the ground elevation below the rip rap layer occurs at approximately -10.0 feet.

5.4.4.1 Lateral Only

The bending moment profiles for piles 2, 3 and 4 for the lateral load test with no additional gravity load can be seen in Figure 5-9 through Figure 5-11. The maximum bending moments occurred at the instrumented location six inches from the bottom of the cap indicating a fixed head condition of the pile to the bent cap which was to be expected. The maximum bending moments ranged from 92 kip-ft to 137 kip-ft. The inflection point for each of the piles seemed to occur near the ground surface or slightly below ground surface. This observation is more apparent in piles 3 and 4 where gages at both instrumented sections below ground were functioning correctly. In pile 2 the lowest below ground instrumented section was the only section used in determining the bending moment profile; therefore the approximate inflection point observed from the bending moment profile is lower than expected. Theoretically the inflection point should occur near ground level, however the addition of the rip rap creates a difficult condition to effectively predict where the inflection point will occur. The slope of the moment diagram for pile three seems to change at the 30 kip load increment with the values of bending moment increasing significantly from the instrumented section above. Upon further inspection of the bending moments at this section plotted against applied load, it is clear that no apparent increase in bending moment begins to occur until the 30 kip load increment. This trend was especially apparent in the loading conditions in which the load truck was on the bridge, which can be seen in Figure 5-8.
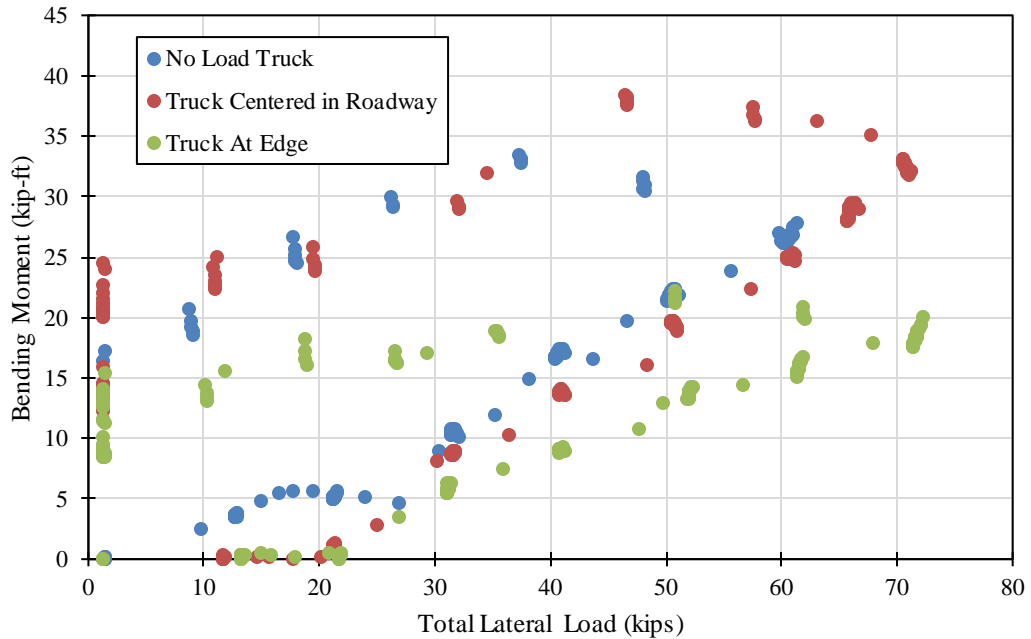
Figure 5-8 Pile 3 Bending Moment versus Total Lateral Load Comparison

The figure above carries out the bending moments through the unloading phases as well and clearly shows that the values of bending moment do not appear to return to zero. While this was the case with the majority of the instrumented sections, only this section on pile 3 did not return to within 10 kip-ft. The magnitude of the bending moment, however is very small at this section relative to the moments calculated at the section above ground. Only the lower instrumented section on Pile 3 (non-encased section) seemed to exhibit this behavior. In each of the other piles with the exception of Pile 1, the magnitude of the bending moment at the lowest instrumented section ranged from 2 to 10 kip-ft during the duration of the tests.
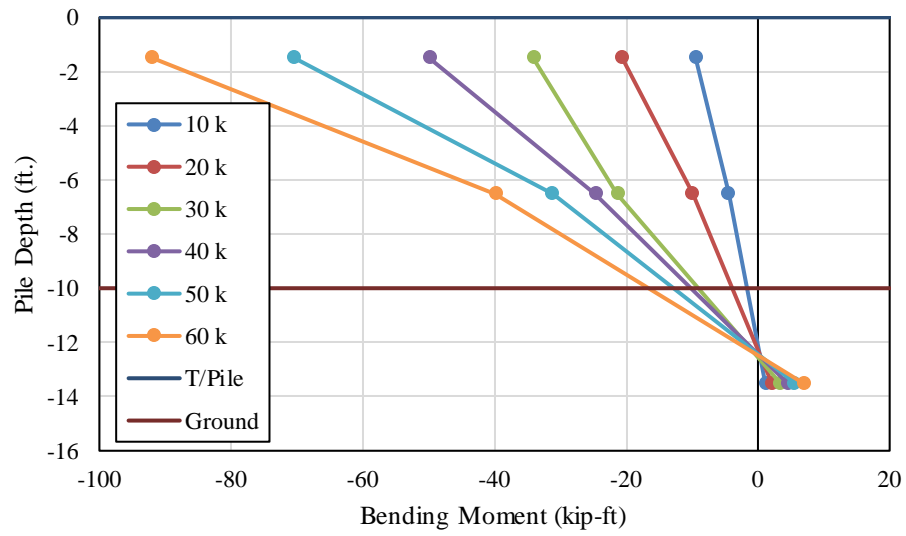
Figure 5-9 Pile 2 Bending Moment Profile
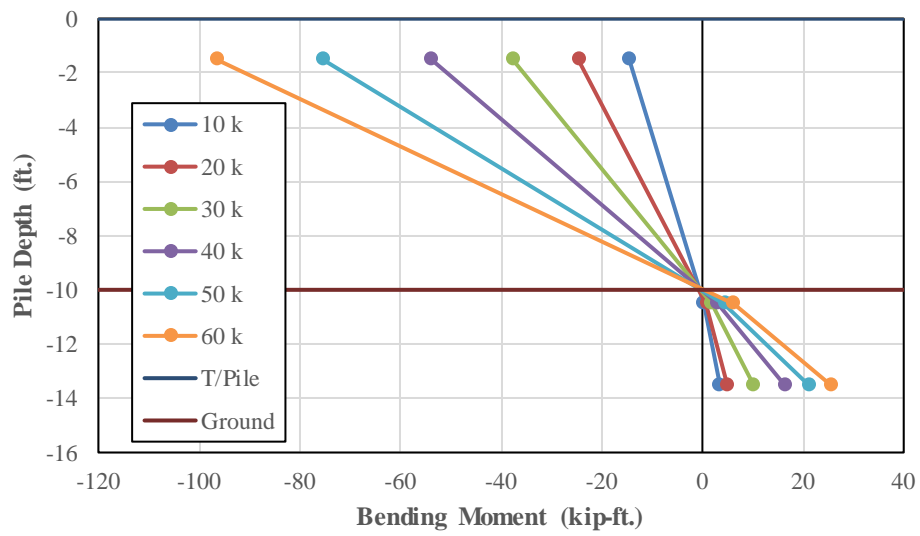
Figure 5-10 Pile 3 Bending Moment Profile

123
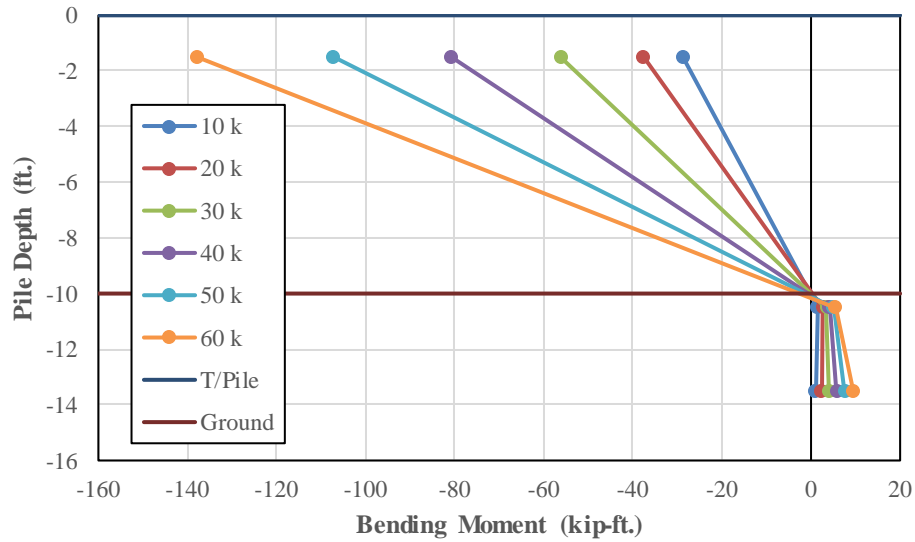
Figure 5-11 Pile 4 Bending Moment Profile

5.4.4.2 Combined Lateral and Gravity with Truck Centered on Roadway

The bending moment profiles for piles 2, 3 and 4 for the combined lateral and gravity load test in which the load truck was centered over the roadway can be seen in Figure 5-12 through Figure 5-17. The maximum bending moments, located at the instrumented section six inches below the bottom of the cap, ranged from 120 kip-ft. to 167 kip-ft. These bending moment values were relatively higher than the bending moments from the lateral load test in which no additional gravity load was applied.
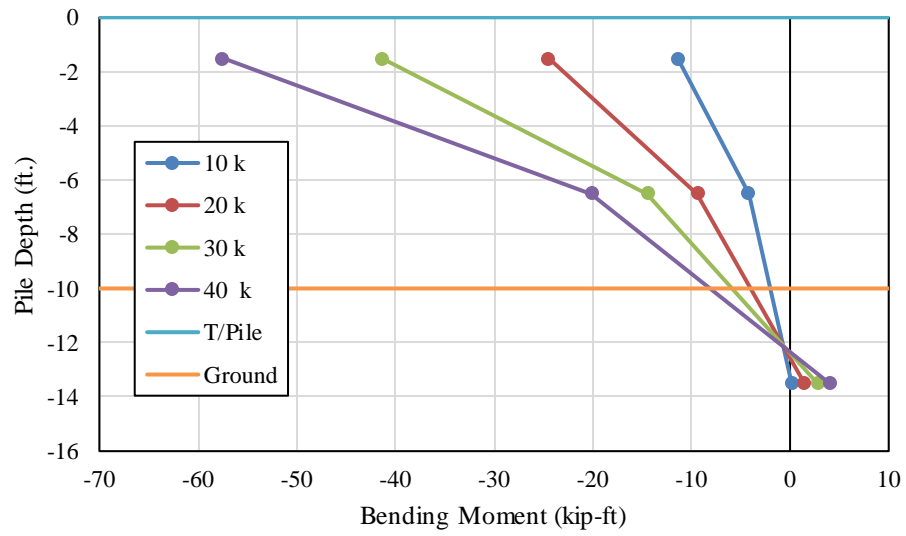
Figure 5-12 Pile 2 Bending Moment Profile
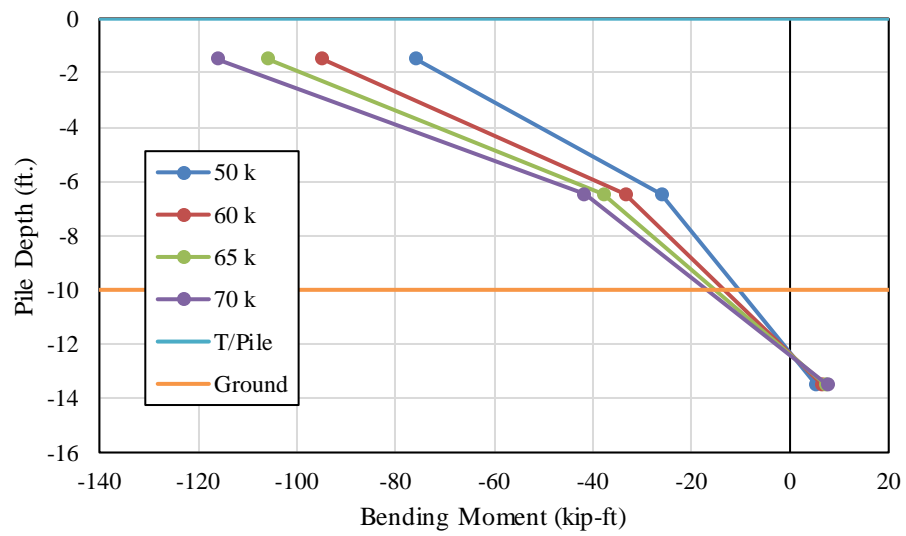
Figure 5-13 Pile 2 Bending Moment Profile

125
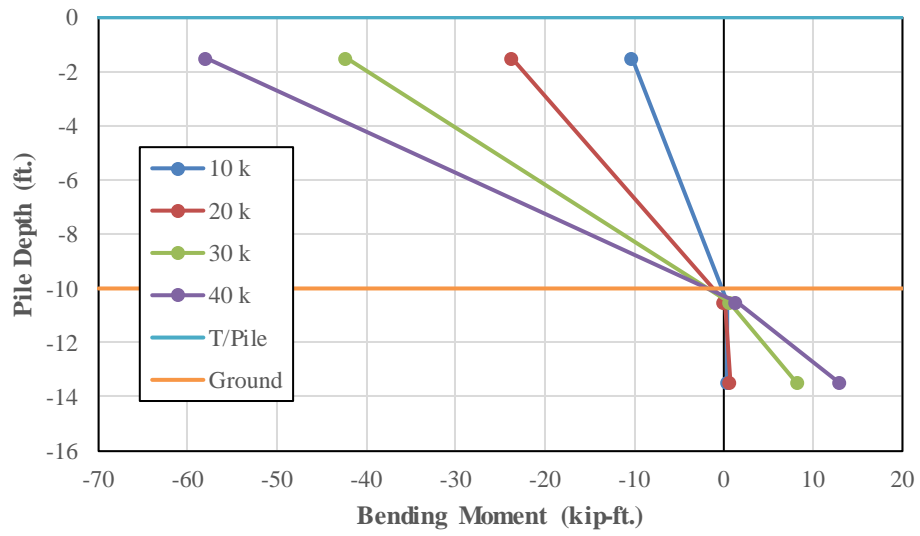
Figure 5-14 Pile 3 Bending Moment Profile
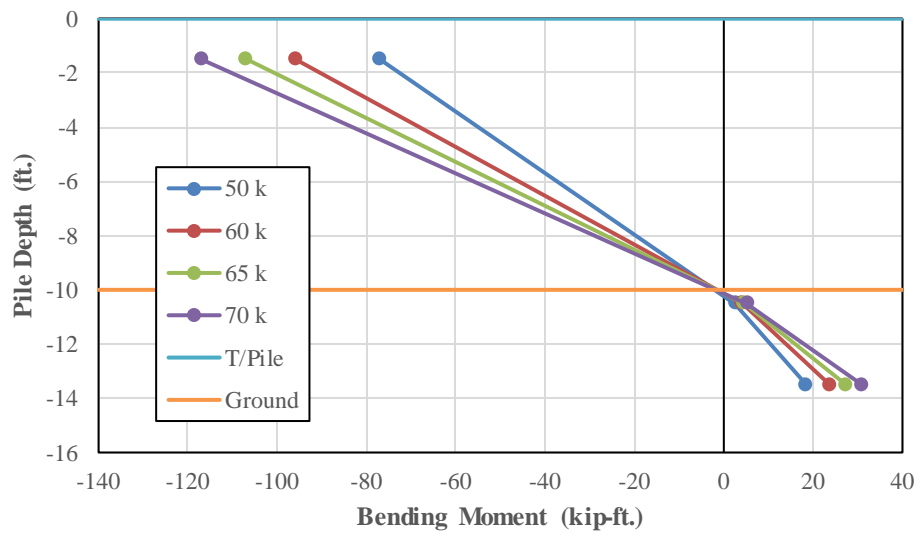
Figure 5-15 Pile 3 Bending Moment Profile

126
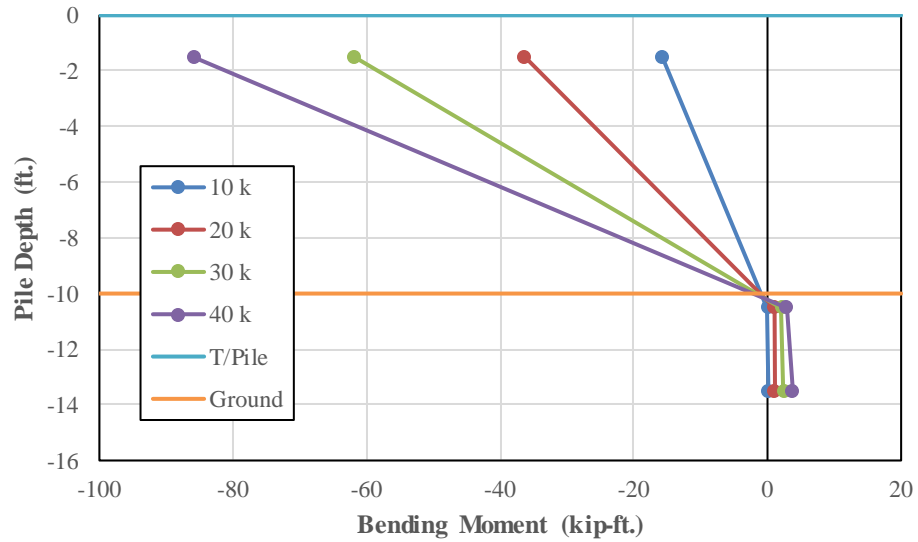
Figure 5-16 Pile 4 Bending Moment Profile
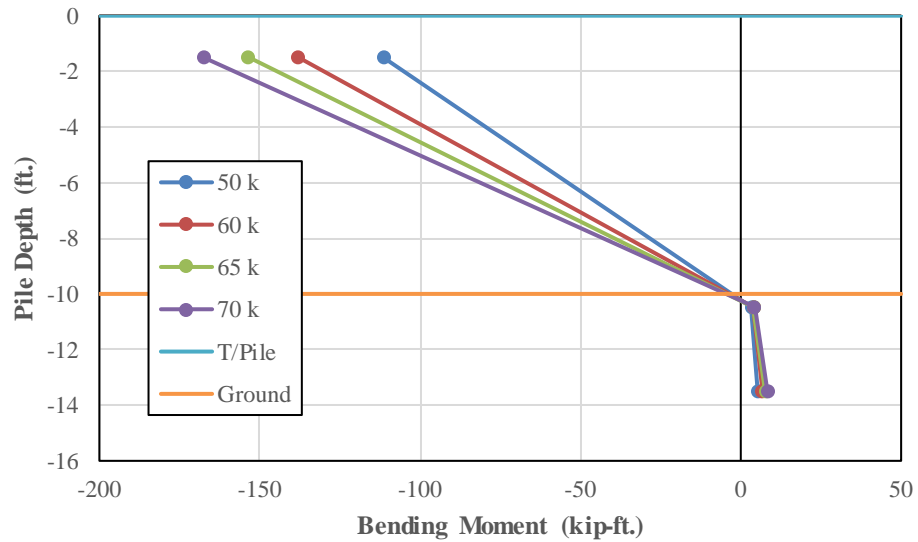
Figure 5-17 Pile 4 Bending Moment Profile

5.4.4.3 Combined Lateral and Gravity with Truck at Edge of Roadway

The bending moment profiles for piles 2, 3 and 4 for the combined lateral and gravity load test in which the load truck was positioned at the edge of the roadway can be seen in Figure 5-18 through Figure 5-23. The maximum bending moment values, located at the instrumented section

127

six inches from the bottom of the cap ranged from 107 kip-ft. to 142 kip-ft. These bending moment values fell in between the values from the lateral load test with no additional gravity load and the combined lateral and gravity load test in which the load truck was centered over the roadway. Notably, the maximum bending moments occurred in Pile 4 which is the leading pile in the load test meaning that his pile is expected to be in axial compression due to overturning.
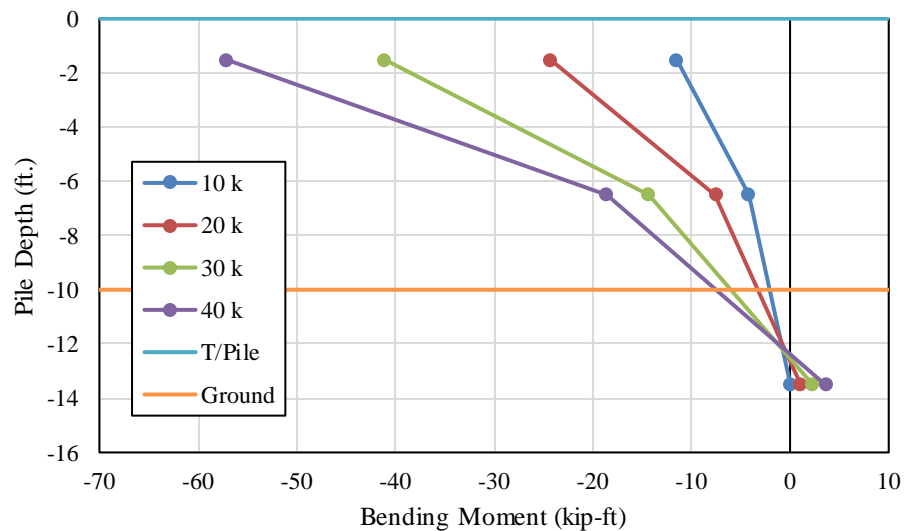
Figure 5-18 Pile 2 Bending Moment Profile
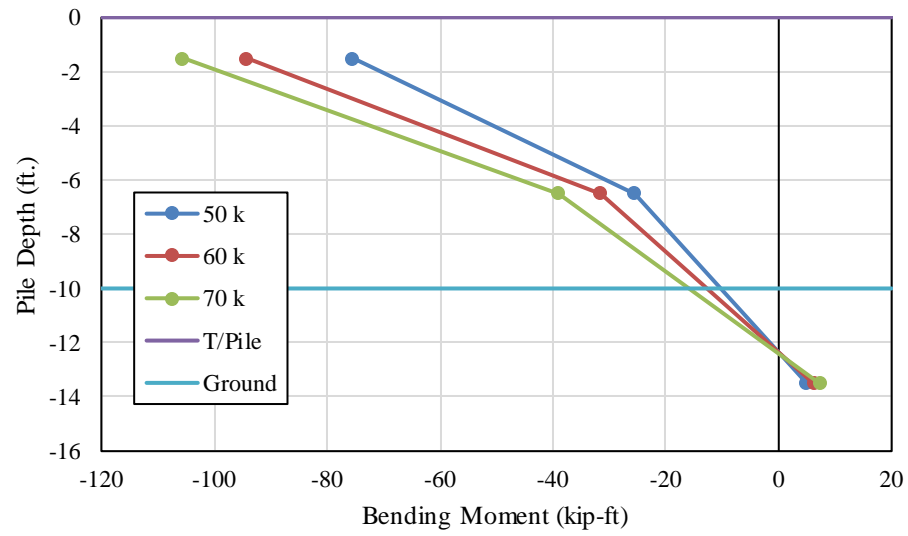
Figure 5-19 Pile 2 Bending Moment Profile
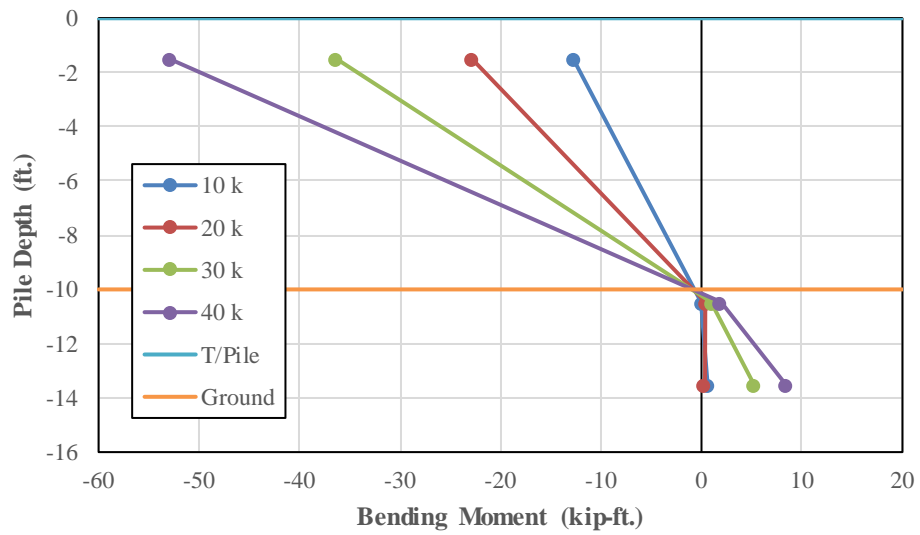
Figure 5-20 Pile 3 Bending Moment Profile

129
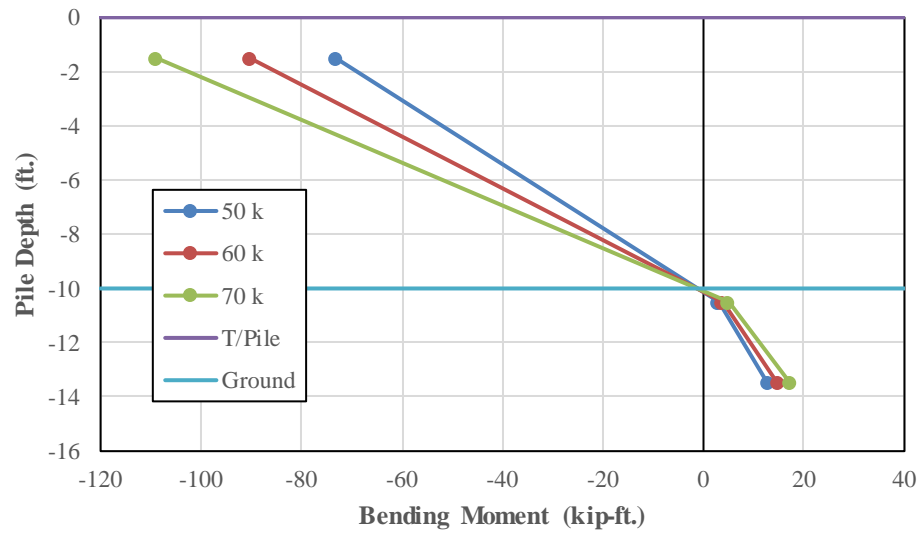
Figure 5-21 Pile 3 Bending Moment Profile
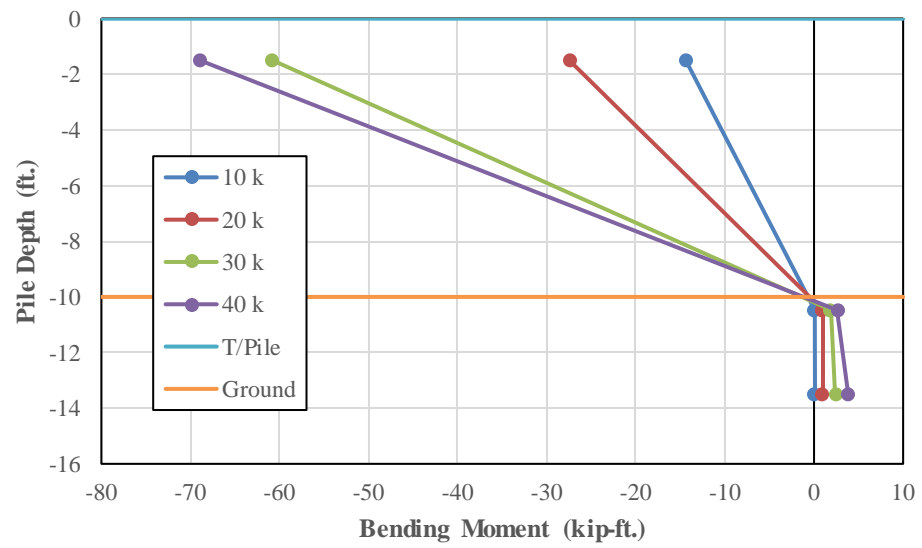
Figure 5-22 Pile 4 Bending Moment Profile

130
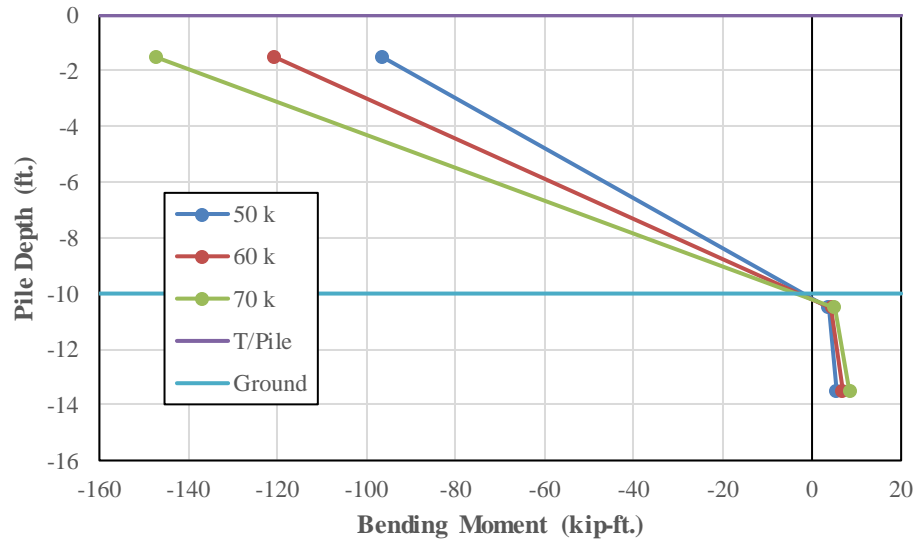
Figure 5-23 Pile 4 Bending Moment Profile

5.4.5 Displacement String Pots

Load versus displacement figures for each of the three load tests can be seen in Figure 5-24 through Figure 5-26. A comparison of the load versus average wirepot displacement for each of the three load tests can be seen in Figure 5-27. The bent appeared to be extremely stiff under each of the three loading conditions, deflecting around an average of 0.1" in each of the three tests. The bent appeared to exhibit increased stiffness with the addition of gravity load. Notably, the bent was loaded to a total lateral load of 60 kips in the first load test as opposed to 70 kips in the second and third tests. Figure 5-27 contains the load-displacement data up to a total lateral load of 60 kips; the data from the 70 kips load increment is not included in this plot.

131
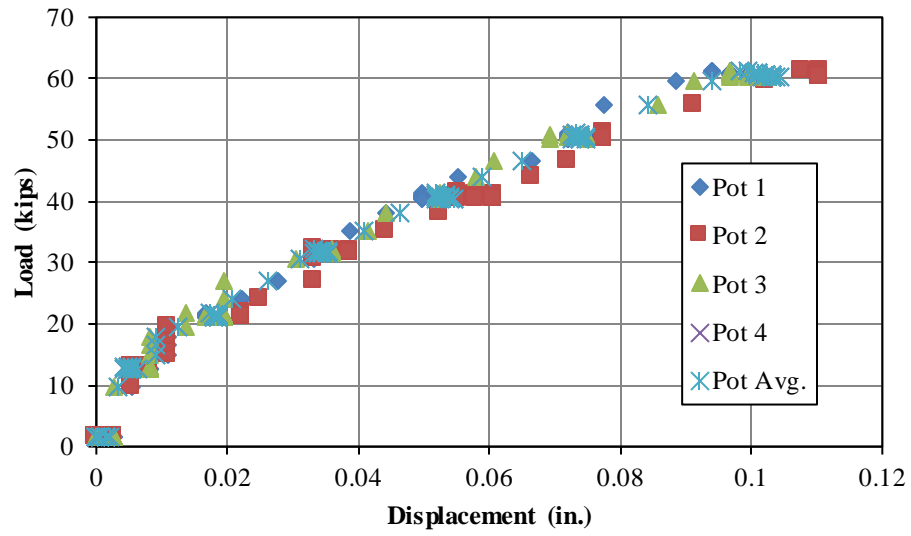
Figure 5-24 Load-Displacement with No Load Truck
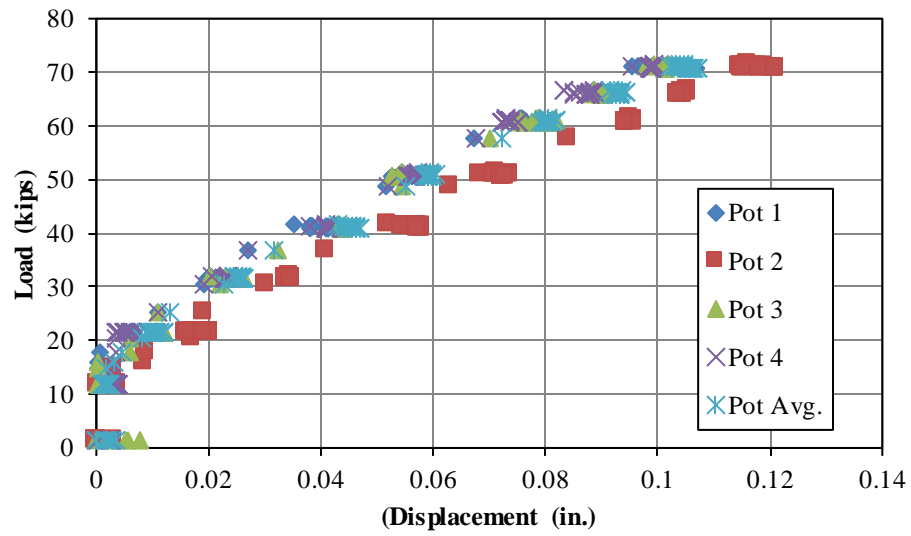
Figure 5-25 Load-Displacement with Truck Centered on Roadway
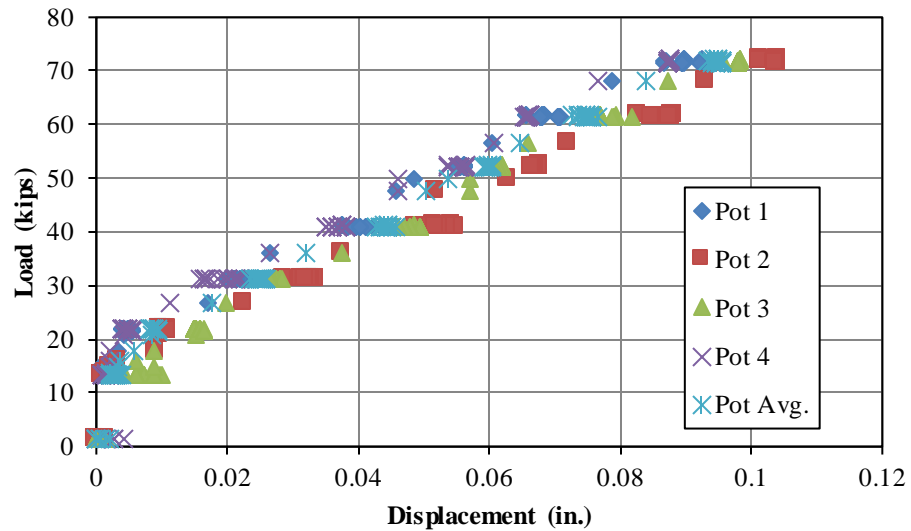
Figure 5-26 Load-Displacement with Truck at Edge of Roadway
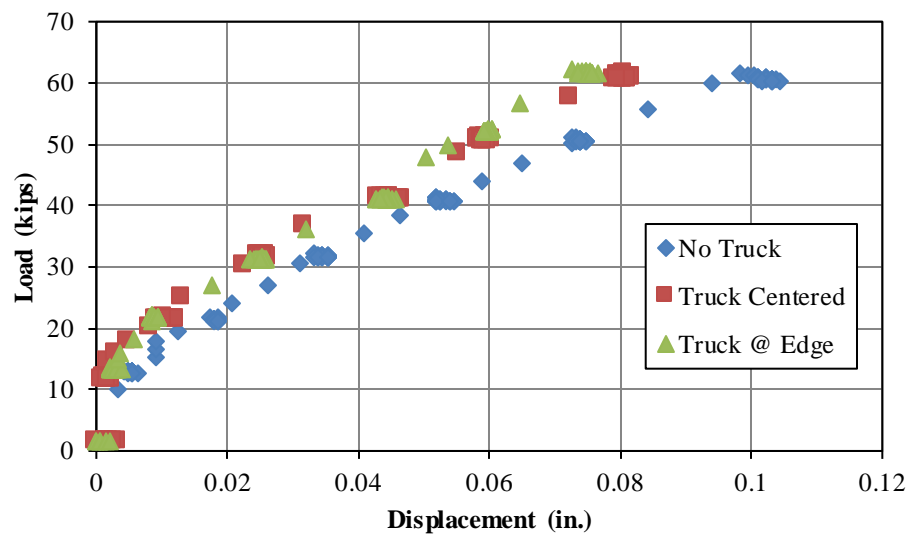
Figure 5-27 Load-Displacement Comparison of Three Tests

The bent behaved extremely stiff in each of the three load tests, however it is clear that the bent's stiffness increased slightly with the addition of gravity load. The total bent cap deflection with no truck was higher than the deflections in each of the combined lateral and gravity load tests; however these deflections were extremely small. There was likely lateral displacement caused by the truck loads in the opposite direction of the displacement caused by the lateral load.

133

The increased compressive force in the piles results in smaller lateral displacements. The cracks that were likely present in the encasements are not as effected when the compressive force in the piles is larger. The moment of inertia of the encased pile section is closer to the uncracked moment of inertia which results in a larger flexural stiffness.

5.4.6   Bridge Bent Behavior

The bridge bent appeared to behave extremely stiff under each of the three loading conditions described in this chapter. The bent deflected around 0.1" in each of the tests, and behaved slightly stiffer in each of the tests in which gravity load was also applied. The displacements during the lateral load test without gravity load were smaller than the displacements during the tests with the load truck. Due to the small changes in displacements it is determined that the addition of gravity load has very little effect on the lateral stiffness of the bridge bent. The total bent deflection was roughly half of the total deflection measured in the load test conducted before the bridge deck was placed, indicating that the addition of the bridge deck provides a significant amount of addition stiffness.

The bending moment profiles for each of the piles indicate a fixed head condition between the top of the pile and the bent cap which is to be expected. The maximum bending moments were relatively high in magnitude, ranging from 92 kip-ft. to 160 kip-ft. These large bending moments can be attributed to the large stiffness of the pile sections with concrete encasements. The inflection point of each of the piles appeared to occur at or below ground surface which is to be expected.

5.5 Chapter Summary

The bridge bent performed very well under each of the three loading conditions, behaving extremely stiff in each case. It can be determined that the addition of gravity load has little effect

on the lateral stiffness of the bridge bent. The addition of the bridge deck clearly increased the stiffness of the bent when comparing the displacements in each of the three tests conducted to the displacements from the test conducted before the bridge deck had been placed. The addition of gravity load, did however have an effect on the magnitude of the bending moments at the instrumented locations six inches from the bottom of the cap. The maximum bending moments were higher in each of the loading conditions with additional gravity load compared to the lateral load test without additional gravity load which is to be expected due to the increased flexural stiffness of the piles due to the larger compressive force.

6. Field Test 3 – US 331 Bridge

6.1 Introduction

An existing multi-span bridge with driven steel pile bents was used for the third load test of the project. The bridge, located on US 331 in South Montgomery, Alabama, consisted of pile bents with 6 driven HP10x42 piles with 16 in. square concrete encasements. The two exterior piles in the bents were battered at a 1.5:12 slope. The bents consisted of a reinforced concrete bent cap, with a trapezoidal cross section of the same geometry as the cap used in the Macon County load test.

For this load test, both the north and south bound bridges were utilized. A bent on the southbound bridge was used as the test bent while the northbound bridge was used to react against. A loading mechanism similar to the Macon County test was used for the US 331 test, using threaded rods as tension members and hydraulic cylinders to essentially pull the two bridges together.

This chapter details how the driven pile bent bridge was tested as well as the analysis and results from that test. It contains sections on instrumentation, testing configurations, and the procedure used for testing. It also contains the results and analysis from the test as well as a discussion of the results.

6.2 Instrumentation

This section details how the test bent and reaction bent were instrumented. It contains the instrumentation layout for the two bents and the types of instrumentation used

6.2.1 Instrumentation Layout

In order to determine axial forces and bending moments during the different load tests, electrical resistance strain gages were installed on piles in the test bent and the reaction bent. To effectively capture the approximate bending moment profile in each of the piles, three sections were instrumented on the test bent. At each of these sections, a pair of strain gages was installed: one gage on each face of the piles. Strain gages were installed on the concrete encasements due to the inability to access the steel piles.

The piles were numbered with the far right pile being Pile 1 and the far left pile being Pile 6. This numbering scheme is looking South down the bridge. The instrumentation layout for the test bent can be seen in Figure 6-1. The reaction bent was also instrumented so that its behavior during the load tests could be monitored as well. This bent was not instrumented as heavily as the test bent. Three piles in the bent were instrumented with only two sections being instrumented. An image of the reaction bent instrumentation layout with the numbering scheme included can be seen in Figure 6-2. Note that this figure is also shown facing south which would be against traffic for this bridge.
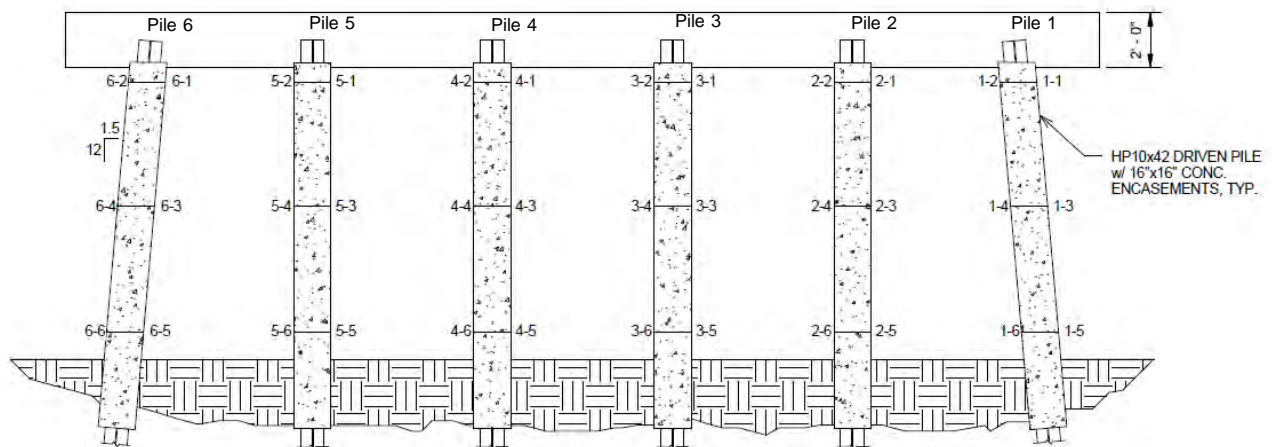
Figure 6-1 Test Bent Instrumentation Layout

137
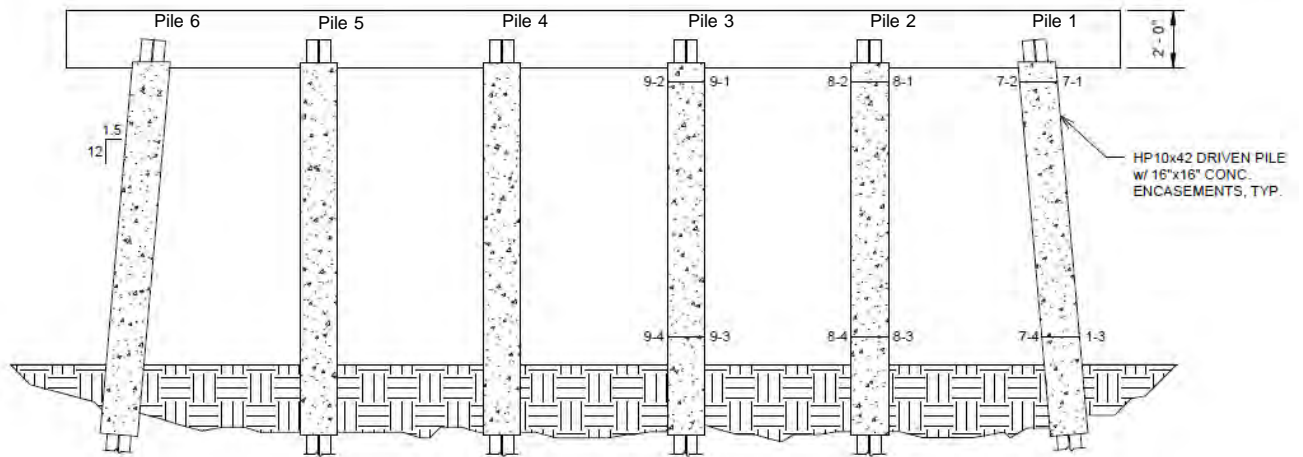
Figure 6-2 Reaction Bent Instrumentation Layout

Displacement wirepots were used in order to measure lateral deflection during the load tests. Two wirepots were installed on the outside face of the test bent and were installed on the same end as the hydraulic cylinders. One wirepot was installed on the top right corner of the bent cap face and the other was installed on the bottom left corner of the cap face. These locations were chosen to be able to obtain an average displacement of the bent cap and to determine whether or not the cap was twisting at all during the test. The wirepot layout on the bent cap can be seen in Figure 6-3.
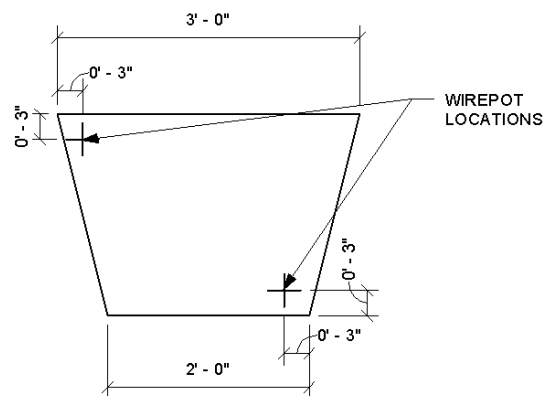
Figure 6-3 Wirepot Layout on Bent Cap Face

138

6.2.2 Electrical Resistance Gages on Concrete Surfaces

One day prior to load testing, concrete surface strain gages were installed at each of the locations shown in Figure 6-1 and Figure 6-2. PL-60-11-3LT strain gages from Texas Measurements were used for strain measurements at each of the instrumented sections. The selected gages were 60 mm in length, providing adequate length for averaging over the concrete surface. The gages came with pre-attached cables which allowed for an easier soldered connection to be made to cables which were connected to the data acquisition system.

6.2.3 Displacement Wirepots

Displacement wirepots were used to measure the lateral deflection of the test bent during the load tests. Two WDS P-60 wirepots with a 1 meter range from Micro-Epsilon were used in this test. The wirepots were attached to the bent by predrilling holes into the outside face of the bent cap using a concrete drill bit. Once the holes were drilled, a small metal hook was placed inside and the hole was filled with a five-minute epoxy to ensure that hook was properly anchored to the face of the cap. Prior to the test, the wirepots were mounted onto a sheet of plywood attached to a wooden reference frame. Two wirepots were installed for used during the load tests: one at the top right corner of the bent cap face and another on the bottom left corner. The installed wirepots can be seen in Figure 6-4.

Figure 6-4 Field-Installed Wirepots

6.3 Testing Equipment and Setup

This section includes details on the testing configuration used for this load test. It also details the reaction bent configuration, the hydraulic jacks and threaded rods used to apply the lateral load, the reference beam used to mount the wirepots, and the data acquisition system.

6.3.1 Reaction Against Adjacent Bent

The bent adjacent to the test bent on the northbound bridge was used as a reaction bent for the load tests. Similar to the Macon County tests, high strength steel threaded rods were used as tension members. In these tests, the rods were anchored at the end of the test bent where the hydraulic jacks were located and at end of the reaction bent. The rods spanned on each side of the bent cap and were held in place by 135 degree hooks made of steel reinforcing bars. The rods were anchored at the far end of the reaction bent by a piece of HSS6x6x1/2 with pre-drilled holes. The rods continued through the HSS section and were anchored at each end using a nut

and washer combinations. Center-hole hydraulic cylinders were used on the far end of the test bent to apply the lateral load through the tension members.

6.3.2 Hydraulic Jacks

Center-hole hydraulic jacks were used to apply the lateral load in the load tests. The threaded rods were fed through these hydraulic jacks and were anchored on the end using a double nut and washer combination. Two Enerpac #RRH-3010 long stroke hydraulic cylinders were used for the test. Each cylinder had a capacity of 30 tons or 60 kips. The cylinders were connected to an Enerpac ZU4 Class ZU4408JB pump fitted with valves to provide equal pressure on both of the cylinders. An image of the two hydraulic cylinders and the pump shown from the bridge deck above can be seen in Figure 6-5.

Figure 6-5 Hydraulic Cylinders and Pump Seen From Bridge Deck

6.3.3 Truck Live Load

For the combined lateral and gravity load test, an ALDOT load truck was used for gravity load application. The load truck in configuration LC-5 was used for this test. The truck had a total weight of 87,500 pounds. During the test, the truck was positioned so that its center of gravity was directly over the test bent. The truck was placed in the left lane of the bridge so that the truck would be induce axial load in the piles that would be expected to be in axial compression due to the effect of lateral load. An image of the ALDOT load truck configured in LC-5 can be seen in Figure 6-6.

Figure 6-6 ALDOT Load Truck in Configuration LC-5

6.3.4 Threaded Rods/Anchorage

High strength steel threaded rods were used as tension members to apply the lateral load in these load tests. The threaded rods used were 1 1/8" in diameter and had a yield strength of 105 ksi. For the majority of the length that the rods spanned, 12 foot long sections were used and

were coupled using steel hex coupling nuts. Shorter sections of threaded rod were used toward the hydraulic jack end and the anchored end of the reaction bent to avoid having to thread the nuts over a long portion of the rods a the anchored locations. Two instrumented sections of threaded rod, three feet in length, were coupled near the hydraulic cylinder end of the bridge bent. These instrumented rods were used to monitor the lateral load during each of the tests. They were placed near the hydraulic cylinders so that the cables from the instrumentation could be connected into the data acquisition system.

On the hydraulic cylinder end of the test bent, the rods were anchored by a section of HSS6x6x1/2 with pre-drilled holes. The rods continued through the tube section and were fed through the center-hole hydraulic cylinders. The two cylinders would bear directly on the tube sections and a ½" thick elastomeric bearing pad was placed between the tube and the bent cap in order to ensure an even load distribution over to bent cap face. The rods were anchored using a double nut and washer combination. Theses nuts were tightened so that they were flush with the piston of the cylinders. An image of the end anchorage at the hydraulic cylinder end of the test bent can be seen in Figure 6-7.

Figure 6-7 Threaded Rods Anchored on Jack End

The threaded rods spanned the entire length of the test bent and the reaction bent plus an additional 25 feet in between the bents. On the far end of the reaction bent, the threaded rods were anchored in a similar fashion as the hydraulic jack end. A piece of HSS6x6x1/2 with pre-drilled holes spanned between the two rods with the rods continuing through the tube. A piece of ½" thick elastomeric bearing material was placed in between the tube and the face of the bent cap to ensure an even load distribution over the bearing area. The two rods were anchored using a nut and washer combination and were hand tightened until the nut was flush with the face of the tube section.

The threaded rods had to be suspended from the bent cap before they were tensioned in place; therefore intermediate supports for the rods located at discrete locations along the length of the two caps were necessary. This was not an issue in the Macon County tests since the majority of the length of the rods were inside of the bent cap. The most efficient and cost effective method for supporting these rods prior to the test was to use steel reinforcing bars bent at a 135 degree angle to catch the rods at points along the length of the bent cap. A piece of number four steel reinforcing bar was bent with one bend being 90 degrees and the other being a 135 degree bend. The 90 degree bend was then placed between the girder pedestal and bottom of the girder, and wooden shims were used to wedge the hook into place. The rods were lifted over the hook and set on the steel hooks, and were then coupled at these locations to avoid having to lift long lengths of threaded rod at once.

6.3.5 Reference Frame for Wirepots

The displacement wirepots used to measure bent lateral deflection were anchored to a wooden reference frame. The frame consisted of two A-frames with a vertical member, diagonal kicker and horizontal member at the base. A diagonal brace was used in between the two A-

144

frames in order to prevent movement of the frame in the transverse direction. A stiff frame was necessary for this test so that accurate lateral deflections were obtained from the wirepots. An image of the reference frame used to anchor the wirepots can be seen in Figure 6-8.

Figure 6-8 Wooden Reference Frame for Wirepots

6.4 Testing Procedure

This section contains the procedures followed for each of the load tests performed on the US 331 Bridge. Two tests were performed: the first was a combined lateral and gravity load test and the second was a purely lateral load test. This section also contains the means for monitoring the load during each of the tests.

6.4.1 Load Monitoring During Test

Steel threaded rods were used as tension members to apply lateral load to the system during each of the load tests. Having a means for monitoring the load at all times during the test was extremely important. A laptop which was connected to the data acquisition system was set up near the test bent. The output for the load in each of the hydraulic jacks, the total load in the

hydraulic jacks, and the average wirepot displacement were displayed on the laptop for the entire duration of the test. These outputs were displayed to know when the target load increment had been reached. Deflections were of interest during the test to ensure that the bridge remained linear elastic throughout the test and large lateral displacements did not occur.

6.4.2   Combined Gravity and Lateral Load Test

The first test performed was a combined gravity and lateral load test. An ALDOT load truck in load configuration LC-5 was used for gravity load application for this test. Since the test bridge was in service during the time of the test, traffic control was an important aspect of the test. When the load truck approached the bridge, traffic was stopped until the load truck was in its desired location so that initial data could be recorded with only the load truck on the bridge. The load truck was positioned so that its center of gravity was directly over the test bent. The truck was positioned in this location to ensure that most of the load was being transferred to the test bent and not the adjacent bents. The truck's position over the bent can be seen in Figure 6-9. In the transverse direction, the load truck was positioned so that its left wheel axle was over the left exterior girder of the test bent. This positioning was chosen so that the load truck would induce additional compression into the piles that would theoretically be in axial compression due to overturning of the bent under lateral loading. This position can be seen in a sketch in Figure 6-10.

Figure 6-9 Load Truck Positioned Over Test Bent

GIRDER
CENTERLINES

EDGE OF
ROADWAY

BENT
CENTERLINE

6' - 3"   6' - 3"   6' - 3"   6' - 3"   6' - 3"
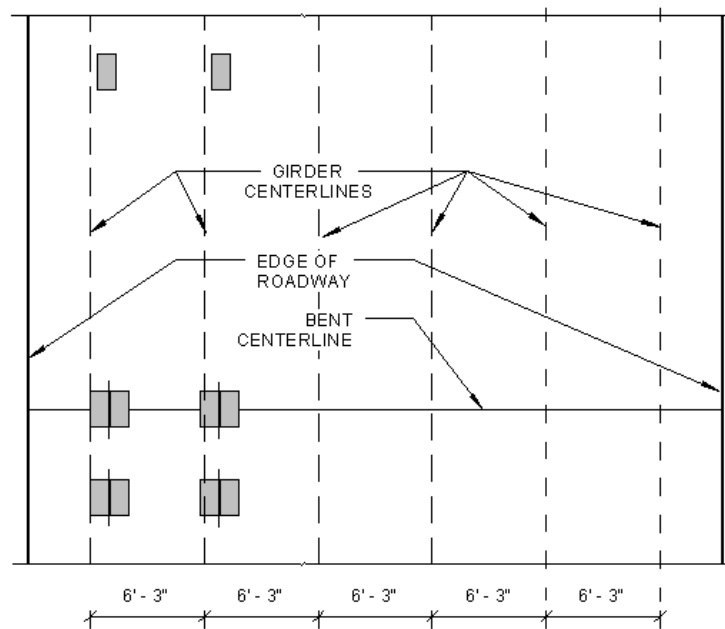
Figure 6-10 Load Truck Positioning Over Exterior Girder

Once the truck was positioned, traffic was stopped for three minutes and a data reading was taken with the truck in its intended position to simulate a gravity load only condition. Once this

reading was taken, the bent was loaded laterally in 10 kip increments to a total load of 90 kips. Due to the rods between the test bent and reaction bent sagging initially, the end anchorage on the jack end and the reaction end had to be hand tightened prior to jack load being applied. This hand tightening procedure was performed instead of applying jack load to ensure that the stroke of the cylinders was not used prematurely to remove the sag out of the rods. An initial load of 12 kips was induced into the threaded rods due to hand tightening of the end anchorages. Therefore the net load at the last increment was 80 kips. However, the loads reported are all total loads seeing that the bent was still subject to this initial 12 kip load.

The bent was loaded laterally by setting the hydraulic pump into "extend" mode and increasing the hydraulic pressure using a hand-held remote. Once the target load increment had been met, traffic was stopped for three minutes so that data could be recorded without additional noise due to traffic. Traffic was not stopped while the load was being increased. Once the 90 kip load increment had been met, the bridge was unloaded in a series of three unloading increments. The load in the jacks at each of these increments was properly recorded since there were no target loads for the unloading increments. The final unloading increment was when the load in the jacks was at the initial load of 12 kips.

6.4.3   Static Lateral Load Test

The second load test performed was a static lateral load test with no live load application. Before the load test began, traffic was stopped for three minutes so that data could be collected with no noise due to traffic. Following this initial reading, the bent was loaded in 10 kip increments up to a total lateral load of 90 kips, holding the load and stopping traffic for three minutes at each load increment. The bent was loaded using the same procedure described in section 6.4.2. Once data was recorded at the 90 kip load increment, the bridge was unloaded in a

series of unloading increments. The load in each jack and the total load was recorded at each unloading increment.

6.5 Analysis, Results and Discussion of Load Test

This section contains measured data as well as results from each of the load tests performed on the US 331 bridge. The methods and assumptions made for calculating axial forces and bending moments are also outlined in this section.

6.5.1 Strains

Strain gages were not instrumented on the steel pile sections for this series of load tests, therefore the level of composite behavior between the steel and concrete encasements was unable to be determined. Upon initial observations of strain profiles across the concrete encasement cross section, it was apparent that the tensile and compressive strains were very similar, indicating a bending condition due to lateral load effects. This was the case especially in piles 2 through 5. The tensile strains in pile 1 and the compressive strains in pile 6 were higher in absolute value than the opposite, indicating net axial compression or tension. Due to the batter of these exterior piles, this net axial load due to lateral load effects was to be expected.

6.5.2 Calculation of Axial Forces and Bending Moments

Axial forces and bending moments during the load tests were computed from the measured concrete strains on each of the six piles. A few basic assumptions needed to be made to take into account the stiffness of the steel piles since there was not instrumentation installed on the steel sections. From data analysis from the Macon County test, it was found that the concrete and steel strains at low load levels were quite similar meaning that small amounts of slipping occurred. The levels of strain at the highest instrumented locations on each of the piles were relatively small during each of the load tests performed. Therefore it was determined that linear interpolation of strain at the location of the flange tips could be used to determine the stresses,

149

forces and bending moments in the steel piles. Although the exact locations of the steel piles within the concrete encasements were unknown, it was assumed that the piles were centered within the encasements. Figure 6-11 shows the assumed location of the steel piles flanges used for linearly interpolating strains for axial force and bending moment calculation. The steel strains used were at the flange tips, three inches from the face of the concrete encasements.
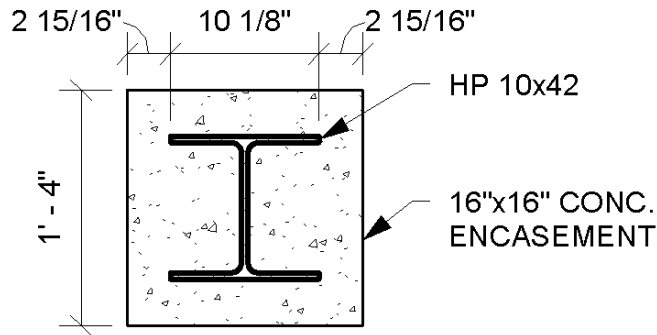
Figure 6-11 Composite Pile Cross Section

The axial force in the piles during the load tests were calculated by taking the average of the tensile and compressive interpolated steel strains and multiplying that value by the modulus of elasticity of the steel piles then multiplying that by the gross cross-sectional area of the HP10x42 pile. This axial load in the steel pile was then added to the axial load contribution of the concrete encasement. The total pile axial load was calculated using Equation 6-1. Notably, the area used in computing the concrete contribution to the axial load is the gross cross-sectional area of the composite pile minus the cross-sectional area of the steel pile.

$$P = \left(\frac{\varepsilon_{c,s}+\varepsilon_{t,s}}{2}\right)E_s A_s + \left(\frac{\varepsilon_{c,con}+\varepsilon_{t,con}}{2}\right)E_c\left(A_g - A_s\right) \qquad \text{(Equation 6-1)}$$

Where:

P = total pile axial load (kips)

$\varepsilon_{c,s}$ = interpolated steel compressive strain (in./in.)

$\varepsilon_{t,s}$ = interpolated steel tensile strain (in./in.)

150

E_s = modulus of elasticity of steel (ksi)

A_s = steel pile cross-sectional area (in^2)

$\varepsilon_{c,con.}$ = measured concrete compressive strain (in./in.)

$\varepsilon_{t,con.}$ = measured concrete tensile strain (in./in.)

E_c = modulus of elasticity of concrete (ksi)

A_g = gross cross-sectional of composite pile (in.^{2})

The bending moments at each cross section during each of the load tests was calculated by taking the curvature at the cross section and multiplying it by the stiffness at the section. A linear strain distribution over the cross section was assumed, so that the stiffness of the steel pile could be included in the moment calculation as well. The curvature for the cross section was calculated using Equation 6-2.

$$\varphi = \frac{\varepsilon_{c,con.} - \varepsilon_{t,con.}}{h} \qquad \text{(Equation 6-2)}$$

Where:

φ = curvature at cross-section (in.$^{-1}$)

h = distance between two measured strains (in.)

The bending moment at each cross section takes into consideration the stiffness of the concrete encasement as well as the steel pile. One uncertainty in these calculations is the compressive strength of the concrete. No information regarding the specifications for concrete used for this bridge during its construction was readily available, therefore an assumption had to be made regarding the strength of the concrete. A compressive strength of 5,000 psi was used to determine the modulus of elasticity to use in the bending moment calculation. Calculations performed using the data from each of these tests also assumed the concrete was uncracked. The modulus of elasticity was approximated using Equation 6-3, which was simplified from the

151

equation for the approximate concrete modulus of elasticity from ACI 318-11 (ACI 2011). A modulus of elasticity of 4,031 ksi was used for computation of bending moments and axial forces for each of the tests.

$$E_c = 57,000\sqrt{f'_c} \qquad \text{(Equation 6-3)}$$

Where:

E_c = approximate concrete modulus of elasticity (psi)

fc= specified 28 day concrete compressive strength (psi)

Equation 6-4 was then used to compute the bending moment at each instrumented cross section during each of the load tests. Note that since the steel strains were linearly interpolated from the measure concrete strains, the curvature over the cross section is constant.

$$M_b = \varphi\left(E_c\left(I_g - I_s\right) + E_s I_s\right) \qquad \text{(Equation 6-4)}$$

Where:

M_b = bending moment at specified cross-section

I_g = gross moment inertia of the composite section (in^4)

I_s = moment inertia of the steel pile (in^4)

6.5.3   Test Bent Axial Forces – Combined Gravity and Lateral

Axial forces in each of the piles in the test bent during the combined gravity and lateral load test were calculated from measured strains. The stiffness of the steel piles was taken into consideration in the calculation of these axial forces; however, due to the large stiffness of the concrete cross section relative to the steel pile, the contribution of the steel pile is small. The axial forces in each of the piles plotted against the total lateral load applied can be seen in Figure 6-12 through Figure 6-17.

Due to axial load effects, the bent will want to overturn meaning that the exterior pile on the jack end will be in axial tension and the exterior pile on the opposite end of the bent will be in axial compression. The exterior piles will tend to carry the largest amount of axial load due to overturning because of the batter and position of the piles. The interior vertical piles will tend to resist the load through flexure and carry little axial load due to overturning. The data from this test indicates this prediction, with the exterior pile on the jack end having a significant amount of axial tension and the exterior pile on the opposite end having a significant amount of axial compression due to overturning. Note that in each of the axial load figures, negative values are assumed to be tension and positive values are assumed to be compression.
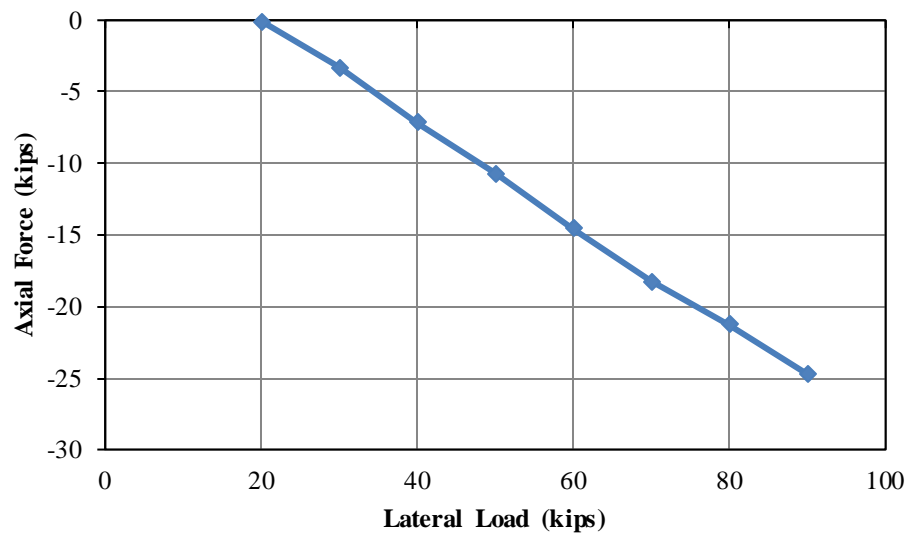
Figure 6-12 Pile 1 Axial Force vs. Lateral Load
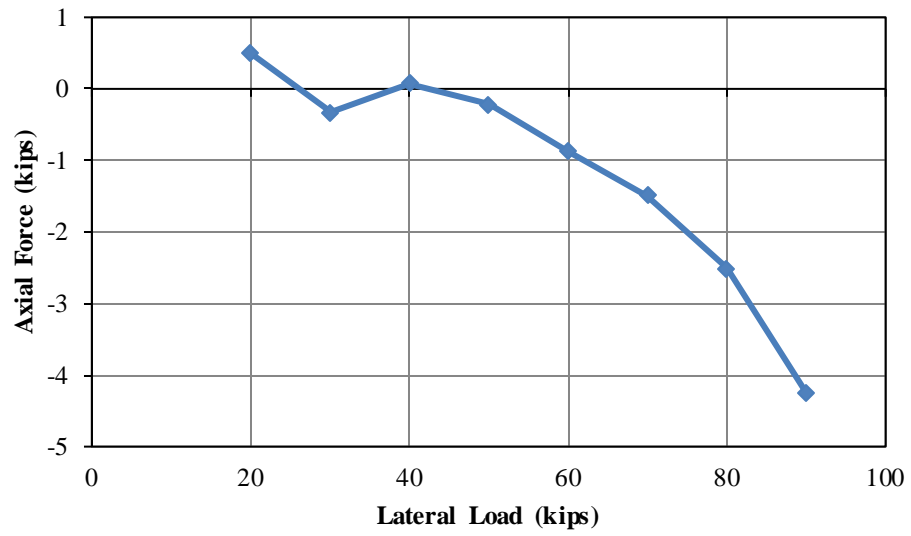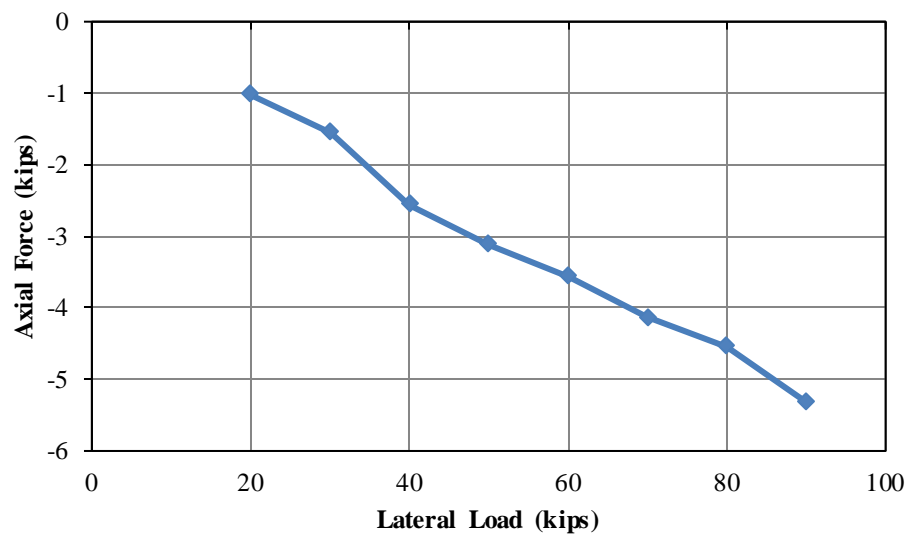
Figure 6-13 Pile 2 Axial Force vs. Lateral Load

Figure 6-14 Pile 3 Axial Force vs. Lateral Load

154

Figure 6-15 Pile 4 Axial Force vs. Lateral Load

Figure 6-16 Pile 5 Axial Force vs. Lateral Load

Figure 6-17 Pile 6 Axial Force vs. Lateral Load

The strain gage readings at the upper instrumented sections were used in order to calculate the axial forces in each of the piles. The axial load transfer from the bent cap to the pile is of most interest to designers which was why this location was chosen to calculate axial forces.

6.5.4   Test Bent Bending Moments – Combined Gravity and Lateral

Bending moment profiles in each of the piles during the combined gravity and lateral load test can be seen in Figure 6-5 through Figure 6-16. For each of the plots, zero elevation is considered to be the centerline of the bent cap. The initial bending moment profile represents the condition with only the load truck on the bridge and no lateral load applied. The shape of the moment profiles for each of the piles is relatively linear over the three instrumented sections. The bending moment appears to begin as a positive values in the piles near where the load truck was positioned. The moment decreases in magnitude as the lateral load is increased, eventually transitioning from positive to negative moment around the 30-50 kip load increment. Piles 1-3 are not as significantly affected by the load truck. The magnitude of the moment becomes more negative as the lateral load increases. Bending moment values calculated during the load test

156

were much less than expected, with the maximum moment six inches below the top of the pile around 14.5 kip-ft. Note that only the concrete encasements were instrumented during these tests; it is very difficult to gage how the steel pile is behaving relative to the concrete encasements. Data from the Macon County tests indicates that the piles do not behave purely composite, meaning that the steel pile strains a significant amount more than the concrete encasement. Due to the lack of instrumentation on the steel piles, it was decided to assume a linear strain distribution across the composite cross section, interpolating the strain values at the steel piles. For a bending moment calculation, the contribution of the steel pile relative to the concrete section is small due to the large difference in moment of inertias of the two sections. This large difference in stiffness would mean that the strain differential between the concrete surface and the steel pile would have to be very large as well to compensate.

Figure 6-4 Pile 1 Bending Moment Profile

157

Figure 6-5 Pile 1 Bending Moment Profile

Figure 6-7 Pile 2 Bending Moment Profile

Figure 6-8 Pile 2 Bending Moment Profile
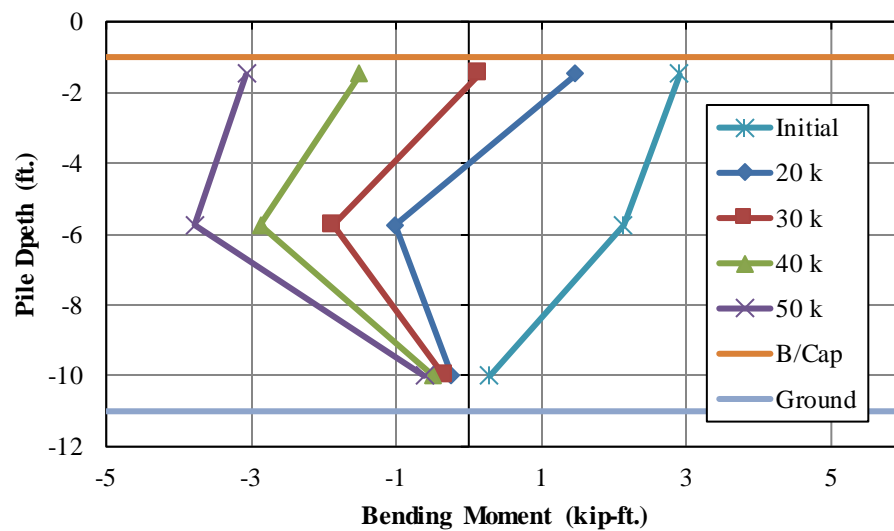
Figure 6-9 Pile 3 Bending Moment Profile

159

Figure 6-10 Pile 3 Bending Moment Profile

Figure 6-11 Pile 4 Bending Moment Profile

Figure 6-12 Pile 4 Bending Moment Profile

Figure 6-13 Pile 5 Bending Moment Profile

161

Figure 6-14 Pile 5 Bending Moment Profile

Figure 6-15 Pile 6 Bending Moment Profile

162
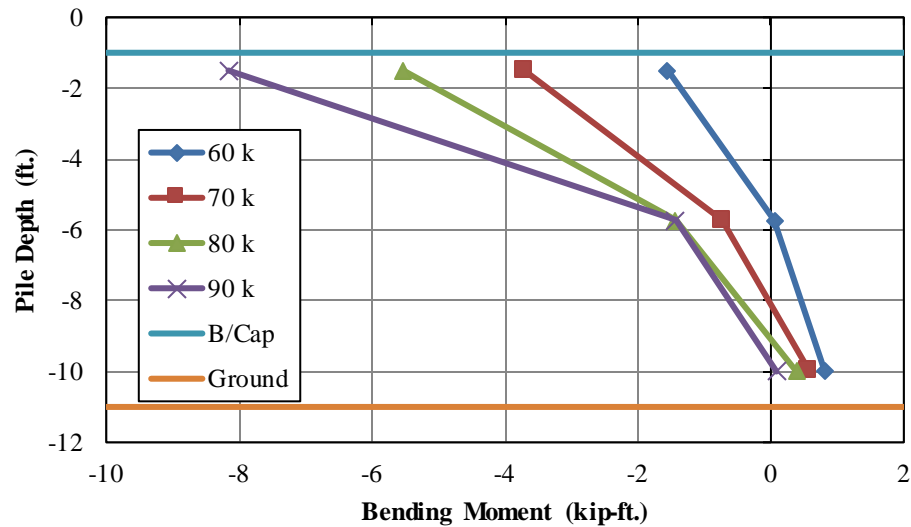
Figure 6-16 Pile 6 Bending Moment Profile

6.5.5 Reaction Bent Axial Forces – Combined Gravity and Lateral

The three exterior piles in the reaction bent looking south were instrumented in order to compare the performance of the reaction bent to the test bent during the load tests. Axial forces versus applied lateral load in each of the instrumented piles in the reaction bent can be seen in Figure 6-17 through Figure 6-19. Similar to the calculations for axial load for the test bent, the upper instrumented section in each of the piles in the reaction bent was used to calculate the axial force.

The bents were loaded by essentially pulling them together, meaning that the bents would tend to overturn towards each other. This overturning would result in the exterior piles closest to the reaction bent which were instrumented being in axial compression due to overturning from the lateral load. The results indicate that each of the three instrumented piles were in axial compression with Pile 7, the exterior battered pile, having the highest value of axial compression.

163
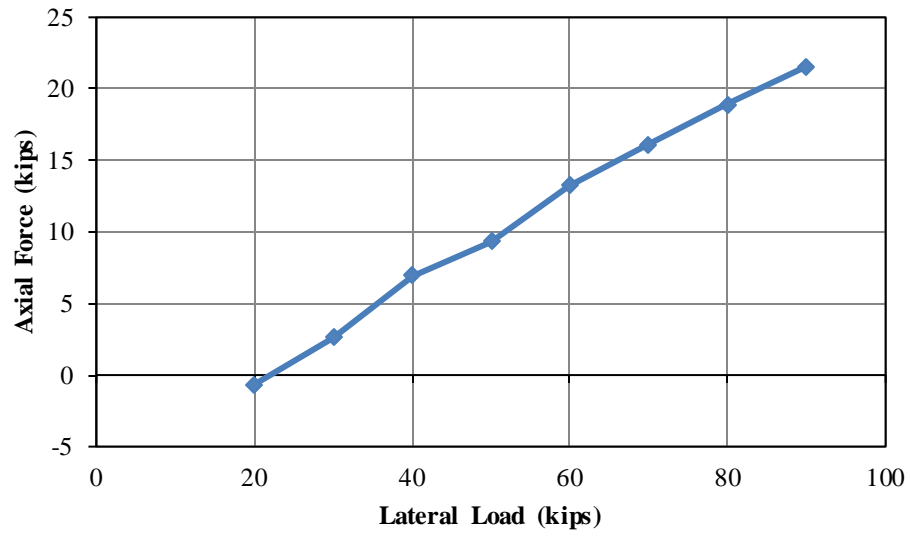
Figure 6-17 Pile 7 Axial Force vs. Lateral Load
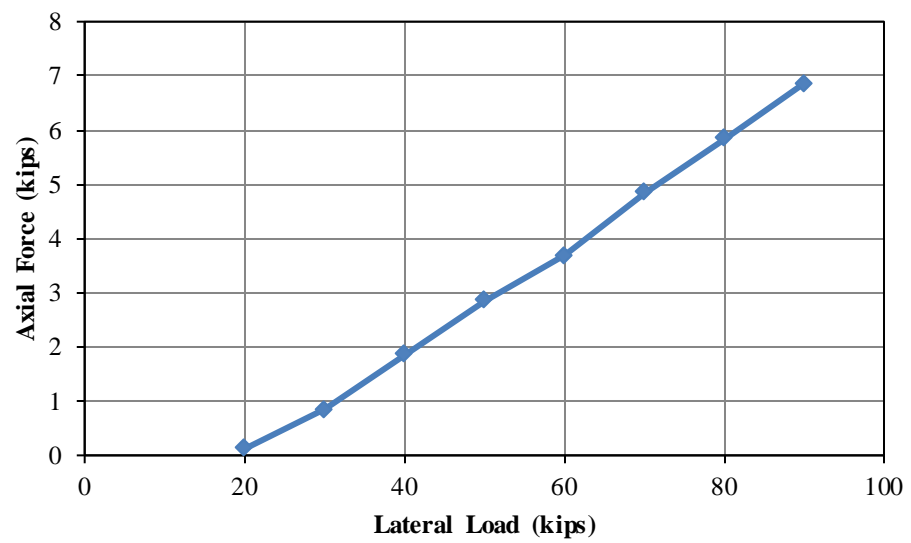
Figure 6-18 Pile 8 Axial Force vs. Lateral Load
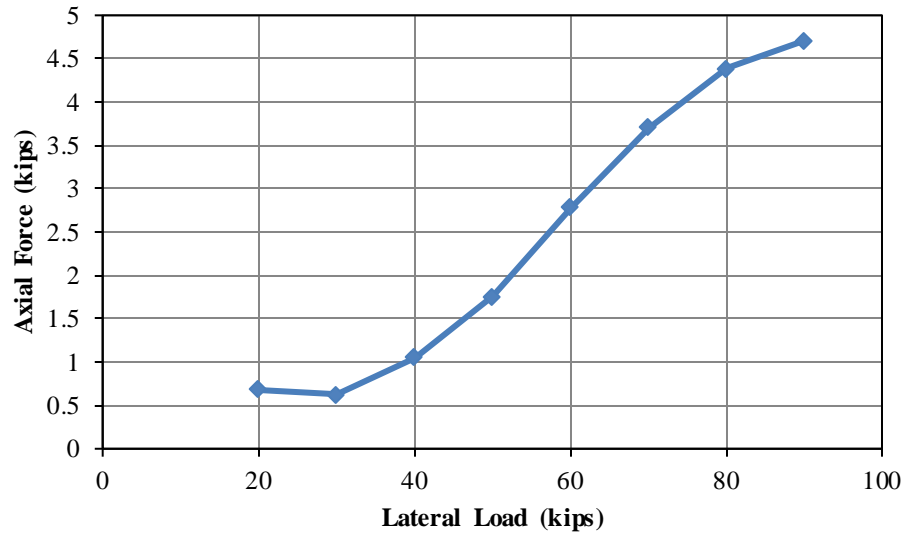
Figure 6-19 Pile 9 Axial Force vs. Lateral Load

6.5.6 Reaction Bent Bending Moments – Combined Gravity and Lateral

The bending moment profiles for each of the instrumented piles in the reaction bent can be seen in Figure 6-20 through Figure 6-25. Note that only two sections along the length of the pile were instrumented in the reaction bent. The maximum moment near the bottom face of the bent cap and the lowest instrumented section were used to compare the bending moment profiles of the instrumented piles in the reaction bent to the piles in the test bent. Similar to the test bent, the lowest instrumented sections on the reaction bent piles were found to be located near the inflection point, with the value of the bending moment close to zero. The maximum bending moments at the upper instrumented sections ranged from about 5 kip-ft. to about 10 kip-ft at a total load of 90 kips. These maximum values are less than the moment values in the test bent, most notably in Pile 7, the exterior battered pile. The compressive axial force in this pile, however, is much greater than the compressive axial force in Pile 6 in the test bent. This indicates that Pile 6 resisted the lateral load more through axial forces transfer rather than flexure.

165
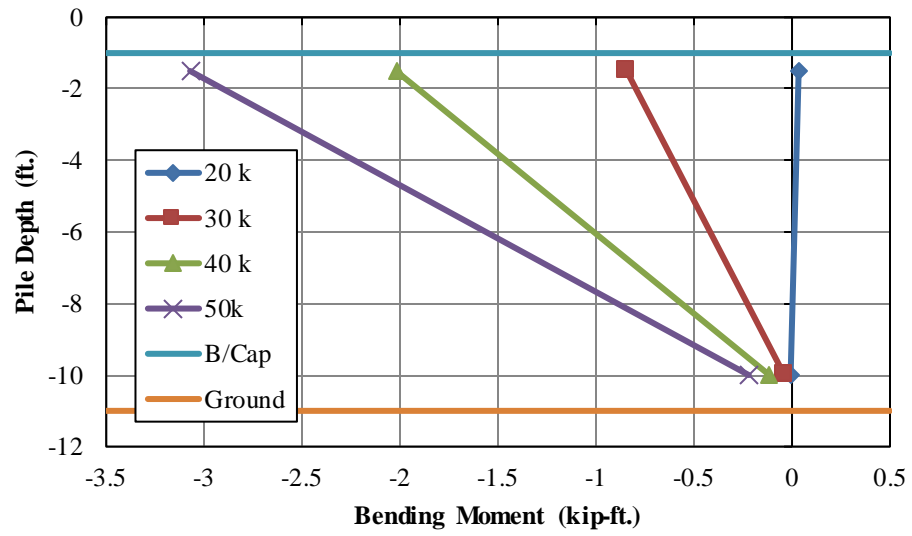
Figure 6-6 Pile 7 Bending Moment Profile
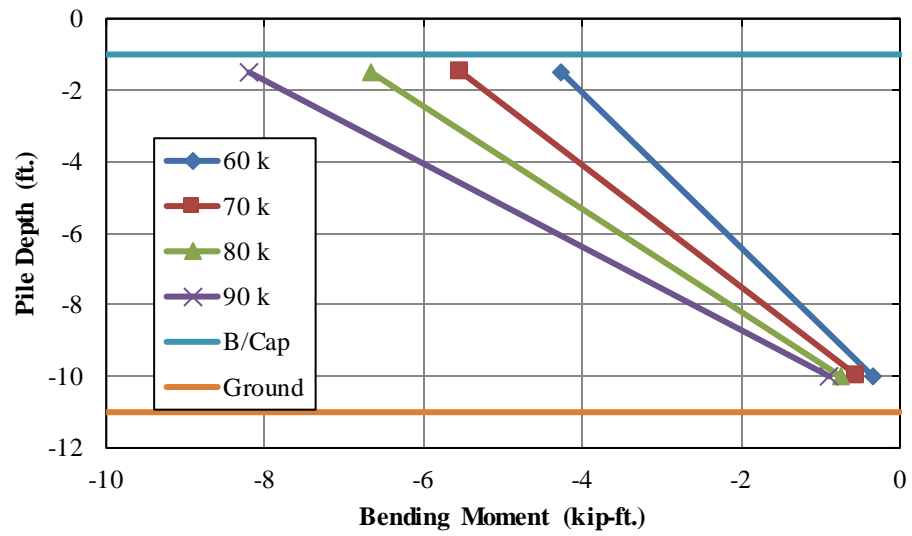
Figure 6-7 Pile 7 Bending Moment Profile

166
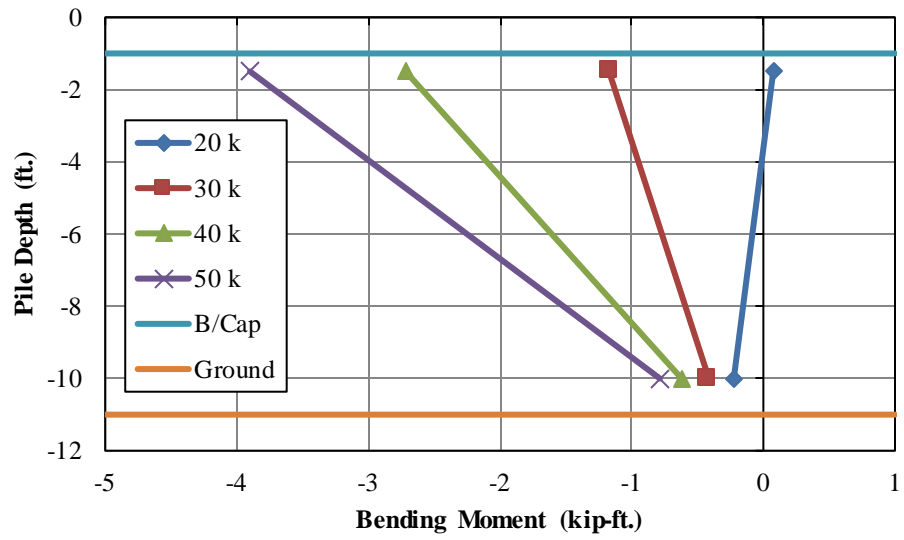
Figure 6-8 Pile 8 Bending Moment Profile
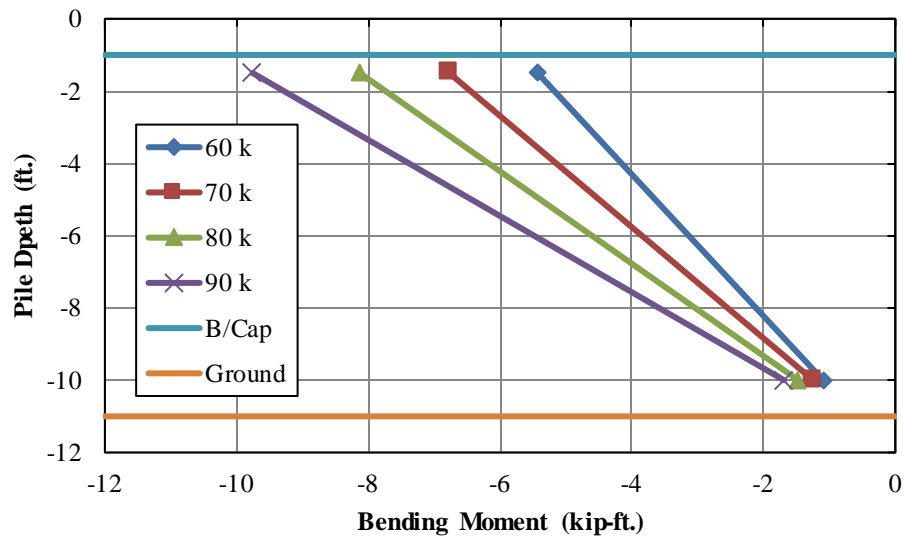
Figure 6-9 Pile 8 Bending Moment Profile

167
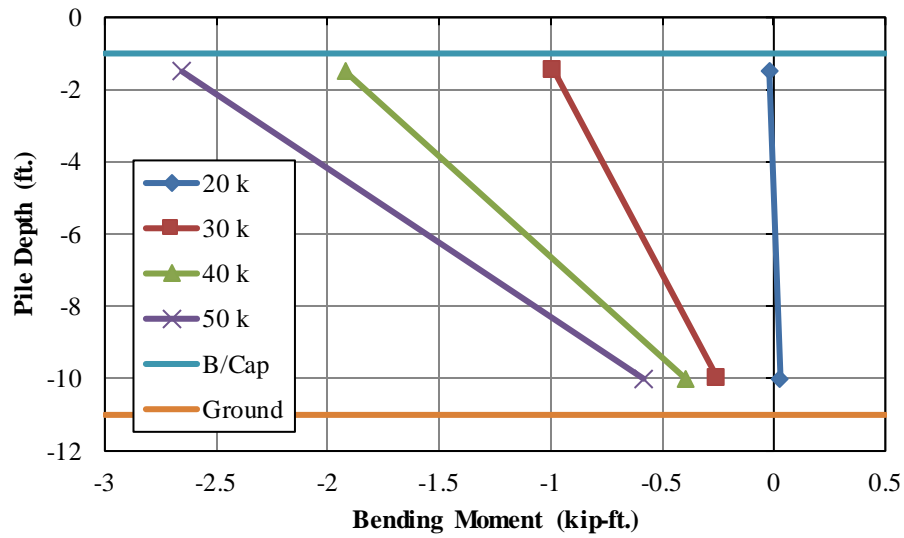
Figure 6-10 Pile 9 Bending Moment Profile
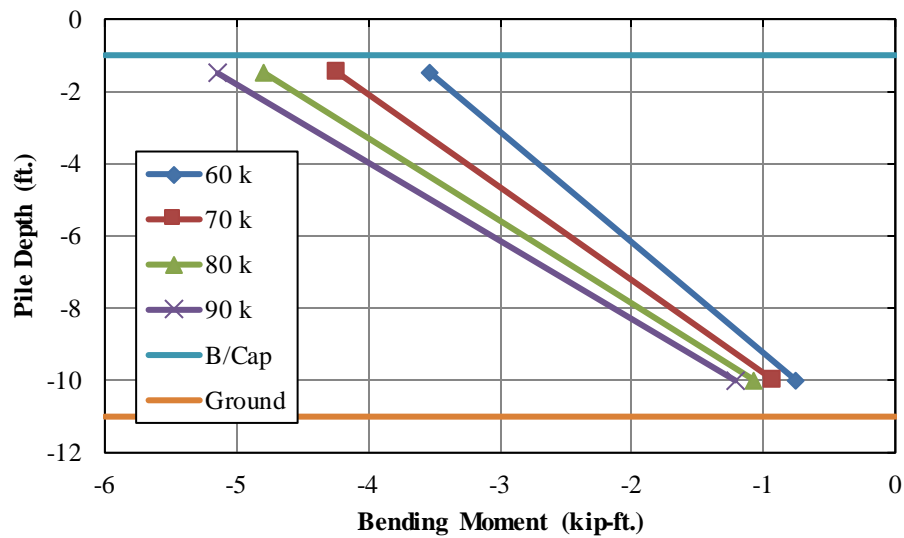
Figure 6-11 Pile 9 Bending Moment Profile

6.5.7 Test Bent Axial Forces – Lateral Load Only

Axial force versus lateral load plots for each of the six piles in the test bent during the lateral only load test can be seen in Figure 6-26 through Figure 6-31. The piles indicated similar behavior during the lateral only load test as the combined gravity and lateral test with the exterior

168

piles carrying a majority of the axial load due to their batter. Piles 1, 2, and 3 seemed to be in net axial tension while piles 4, 5 and 6 were in net axial compression due to overturning. These results were to be expected. Notably, the compressive axial force in pile 6 was considerably larger than the tensile axial force in pile 1.
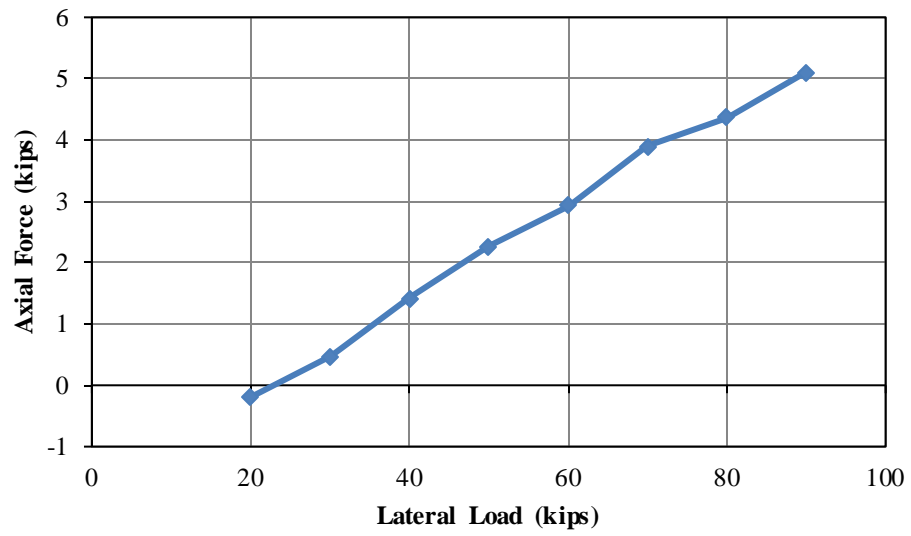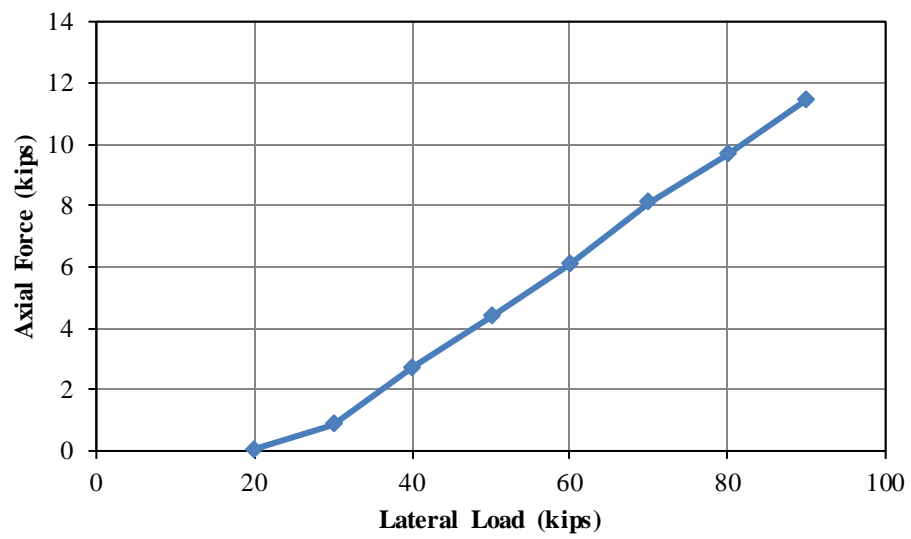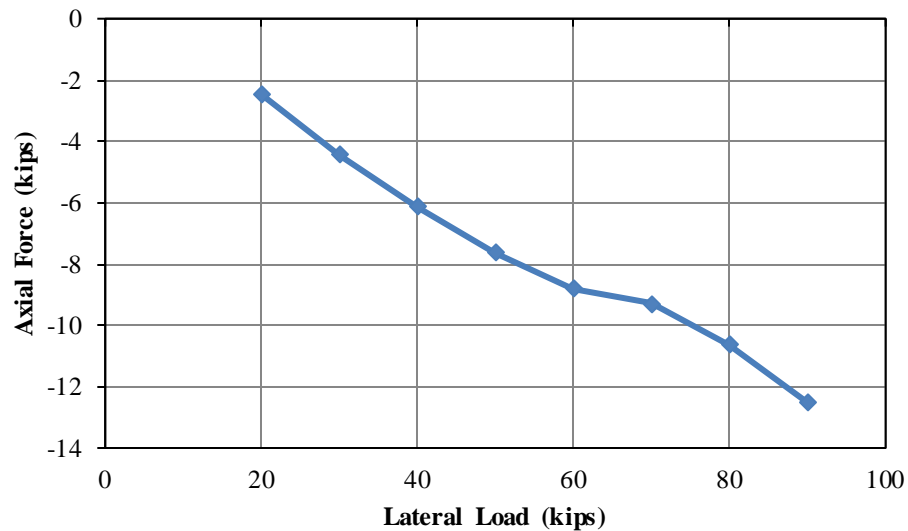

Figure 6-12 Pile 1 Axial Force vs. Lateral Load
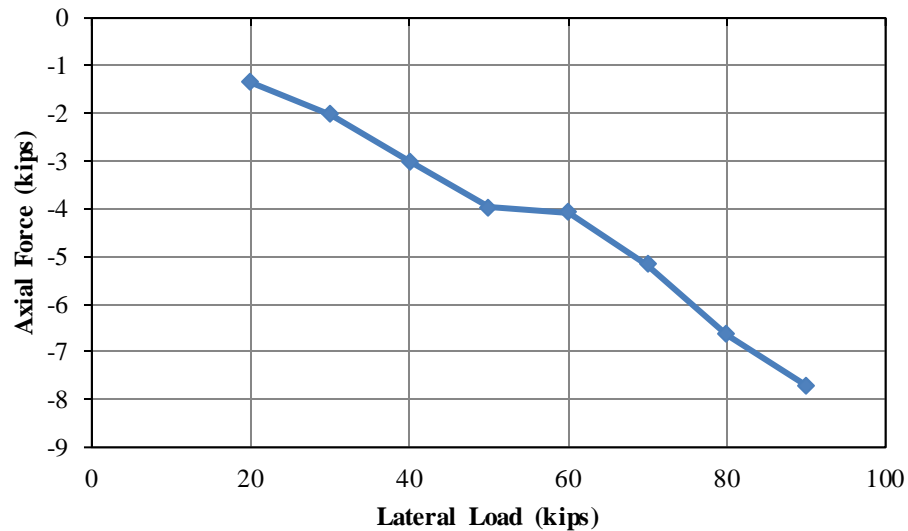
Figure 6-13 Pile 2 Axial Force vs. Lateral Load
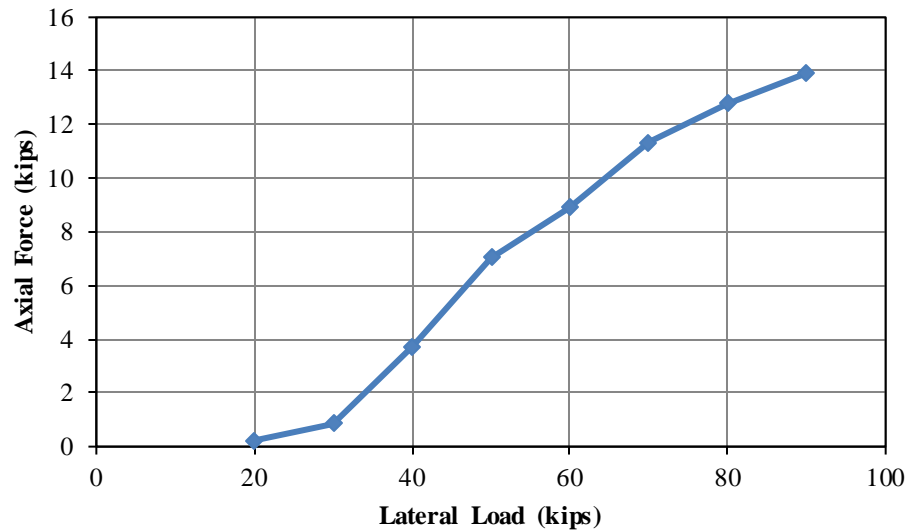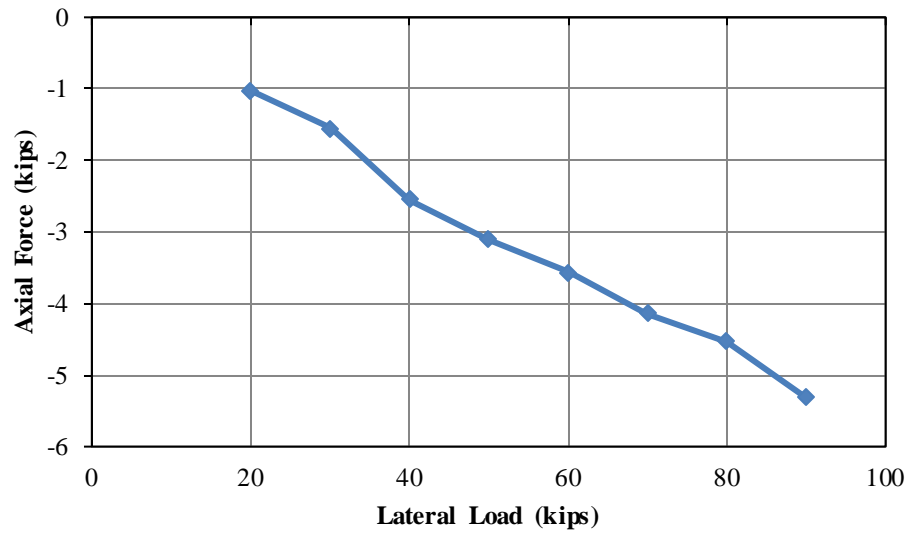
Figure 6-14 Pile 3 Axial Force vs. Lateral Load
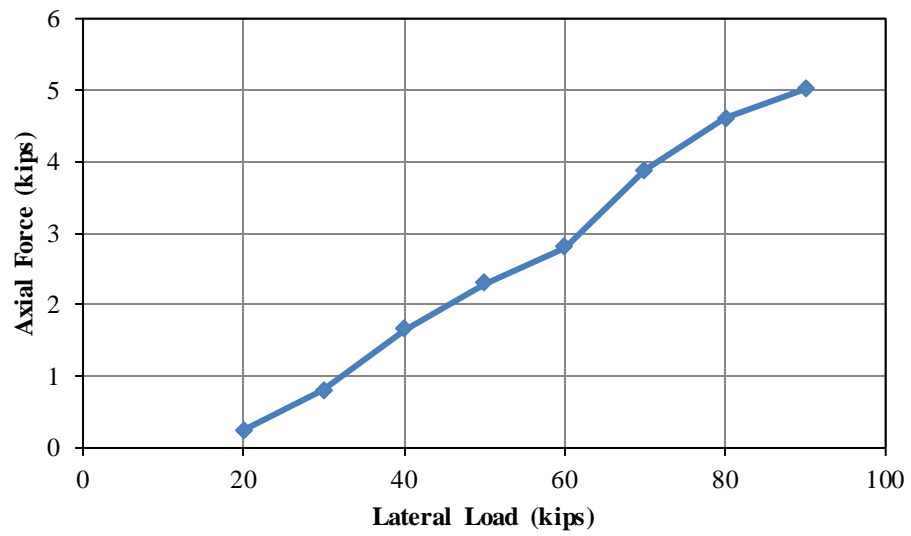
Figure 6-15 Pile 4 Axial Force vs. Lateral Load
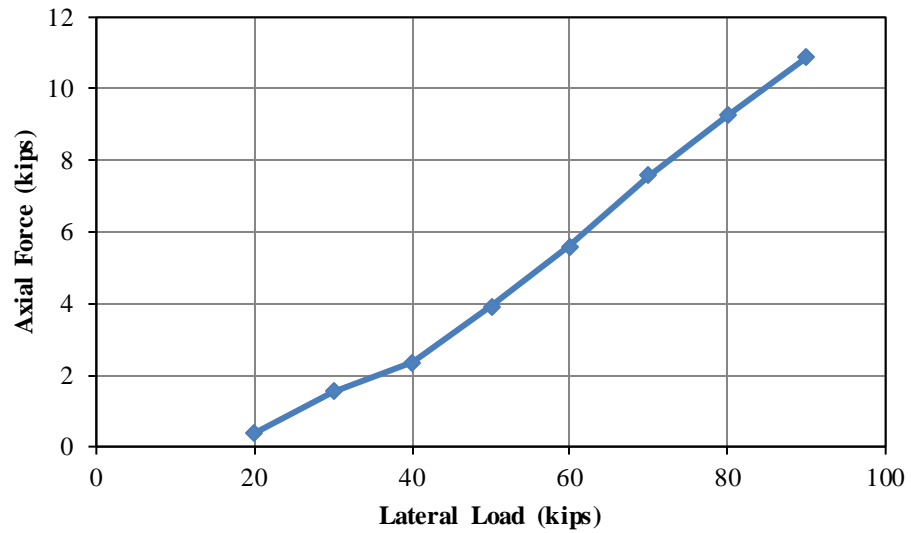
Figure 6-30 Pile 5 Axial Force vs. Lateral Load
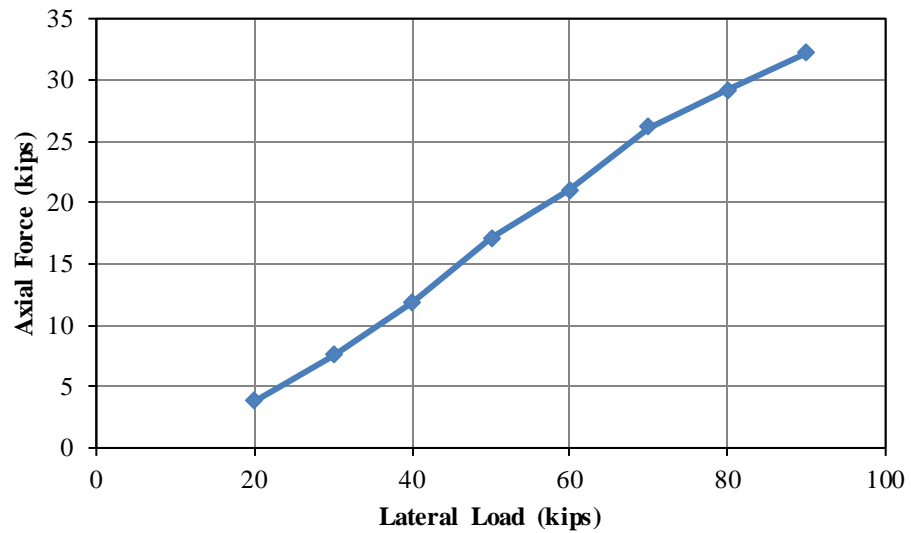
Figure 6-16 Pile 6 Axial Force vs. Lateral Load

The upper instrumented section was used in computing the axial forces in the piles. The transfer of load from the bent cap into the piles is of most importance to designers; therefore, this location was chosen. The axial force diagram over the length of the pile should remain relatively constant over the length of the pile until the pile enters the ground where the load will then be transferred into the subsurface.

6.5.8 Test Bent Bending Moments – Lateral Load Only

Bending moment profiles in each of the piles during the combined gravity and lateral load test can be seen in Figure 6-32 through Figure 6-43. The shape of the bending moment profile for each of the piles is similar to the combined gravity and lateral load test with the maximum bending moment appearing to be located near the bottom of the bent cap. The magnitude of the bending moments for the piles during the lateral load test with no additional gravity load are small, but similar to the moments calculated during the combined gravity and lateral test. The maximum calculated moments ranged from 11 kip-ft. to 20 kip-ft.
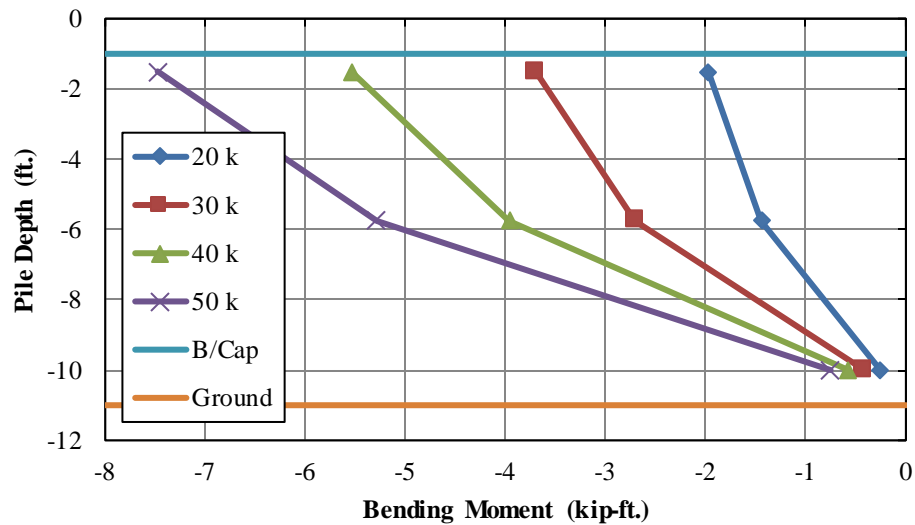
Figure 6-17 Pile 1 Bending Moment Profile
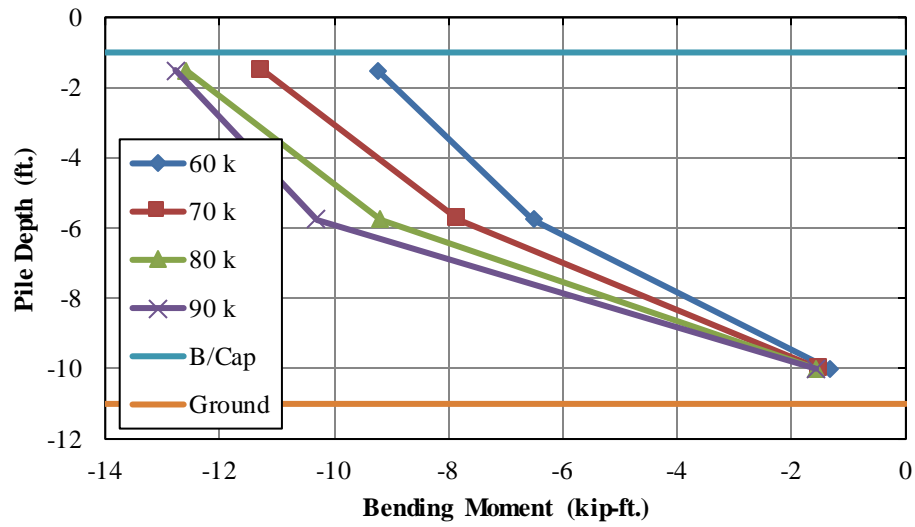
Figure 6-18 Pile 1 Bending Moment Profile
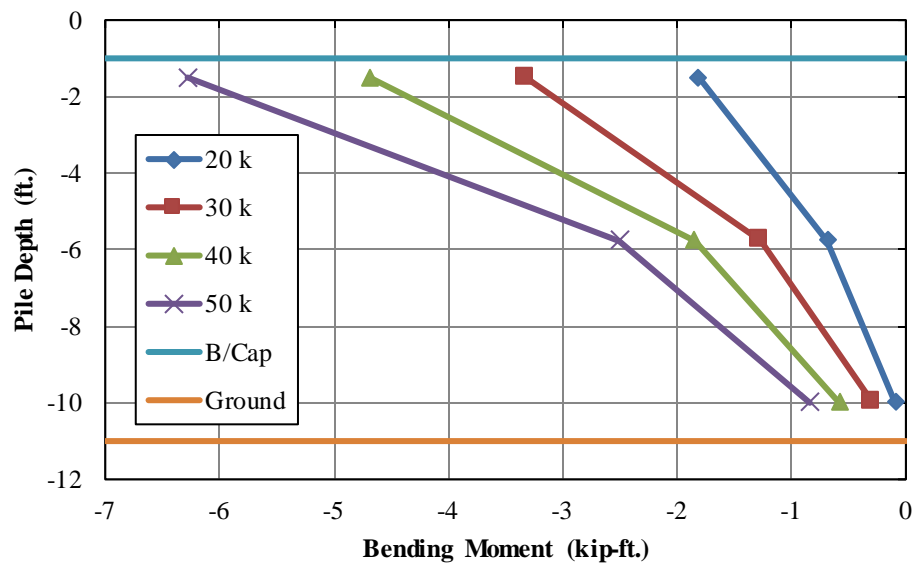
Figure 6-19 Pile 2 Bending Moment Profile

173
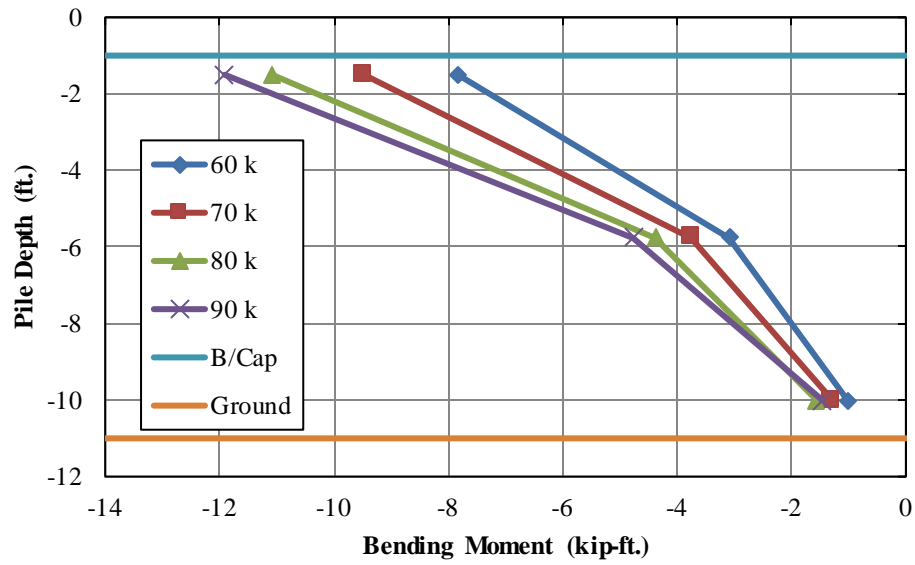
Figure 6-20 Pile 2 Bending Moment Profile
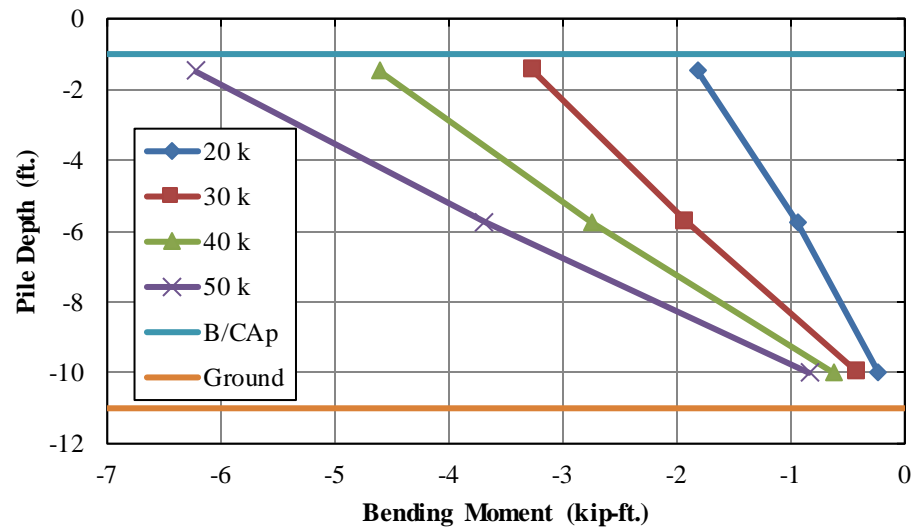
Figure 6-21 Pile 3 Bending Moment Profile

174
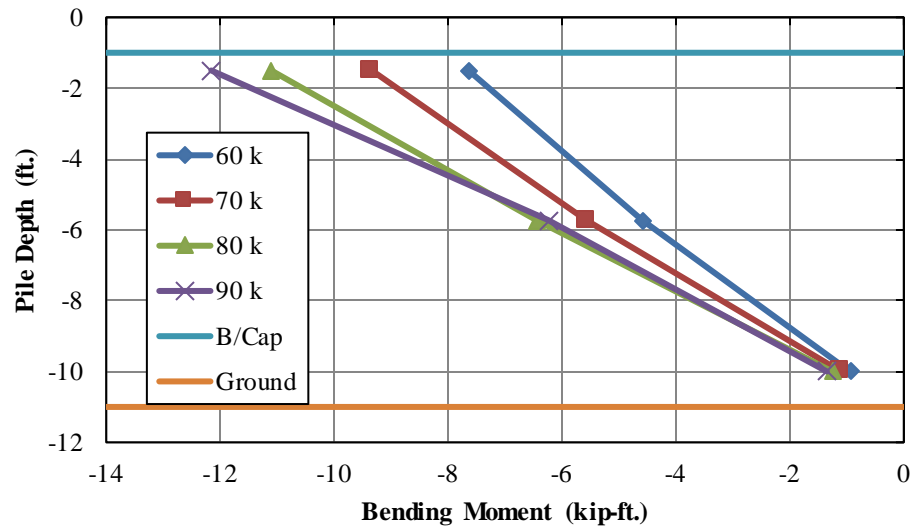
Figure 6-22 Pile 3 Bending Moment Profile
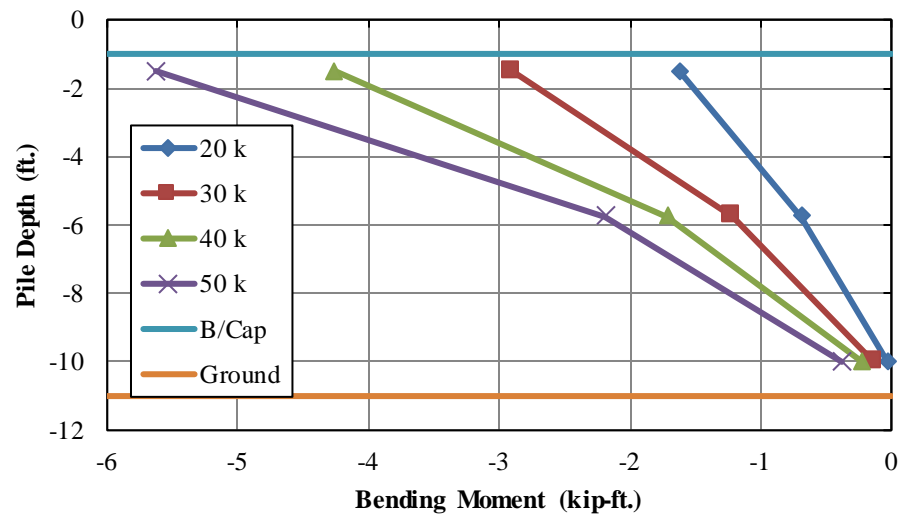
Figure 6-23 Pile 4 Bending Moment Profile

175
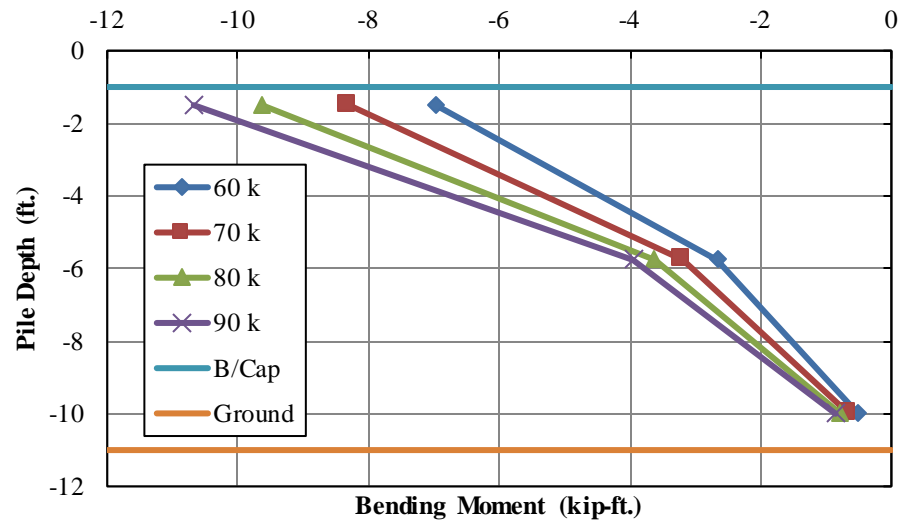
Figure 6-24 Pile 4 Bending Moment Profile
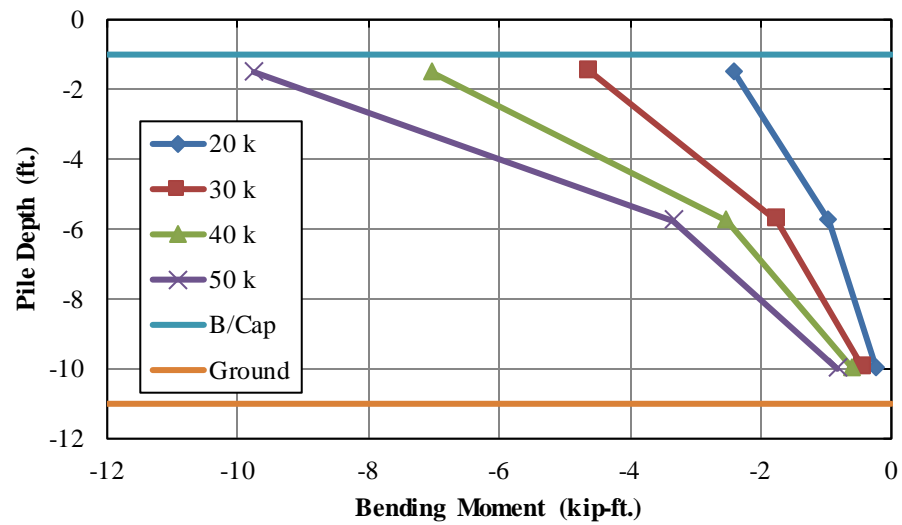
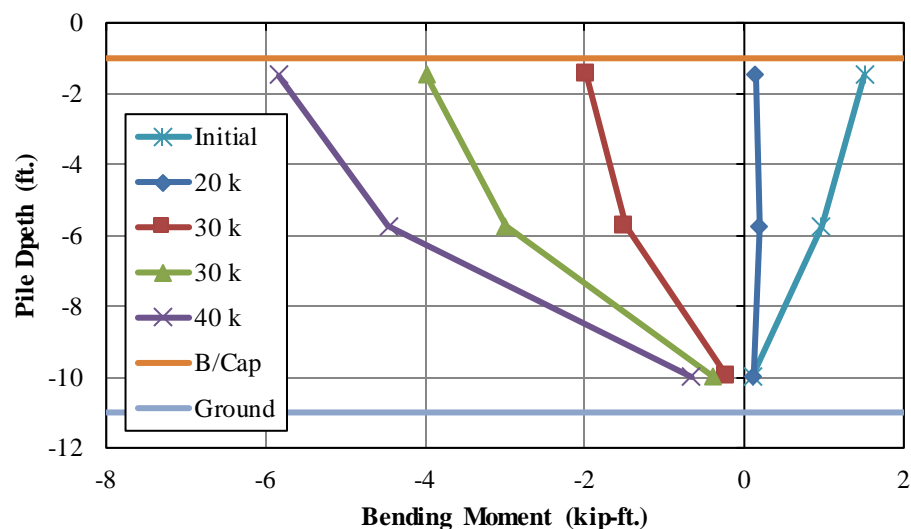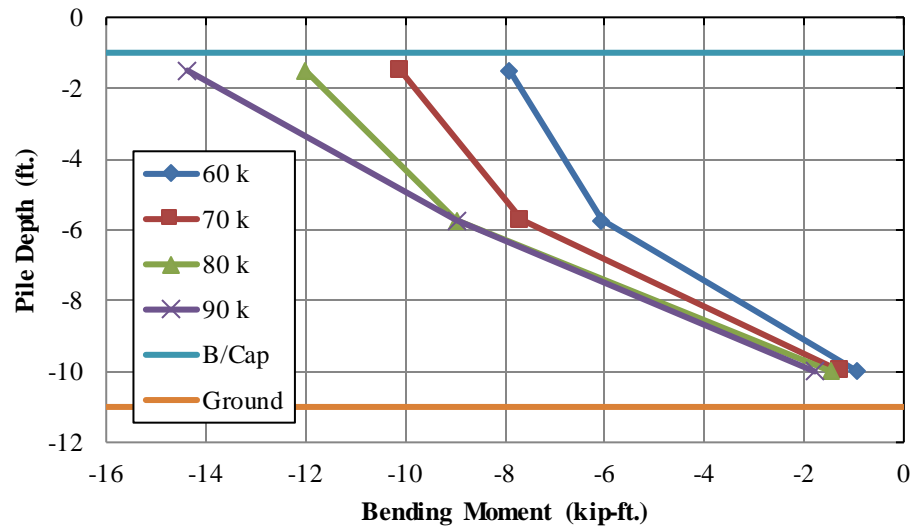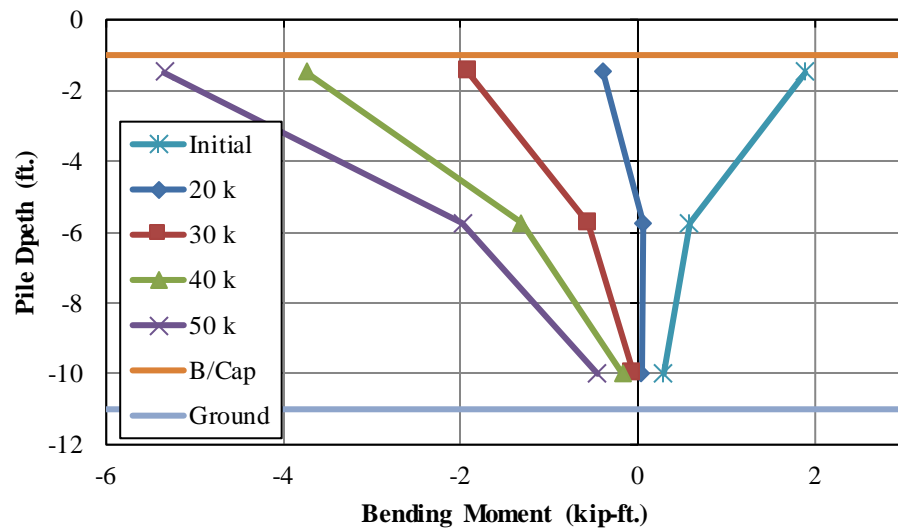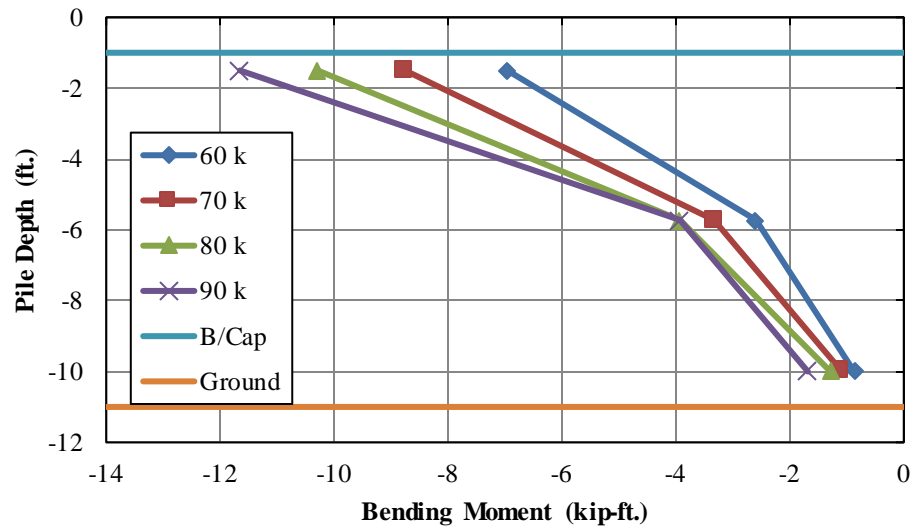**Figure 6-40 Pile 5 Bending Moment Profile**

176
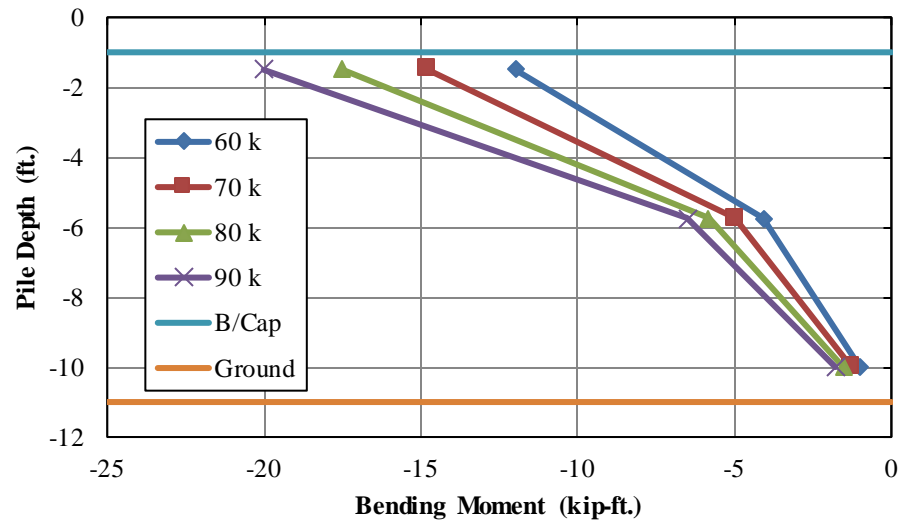
Figure 6-25 Pile 5 Bending Moment Profile
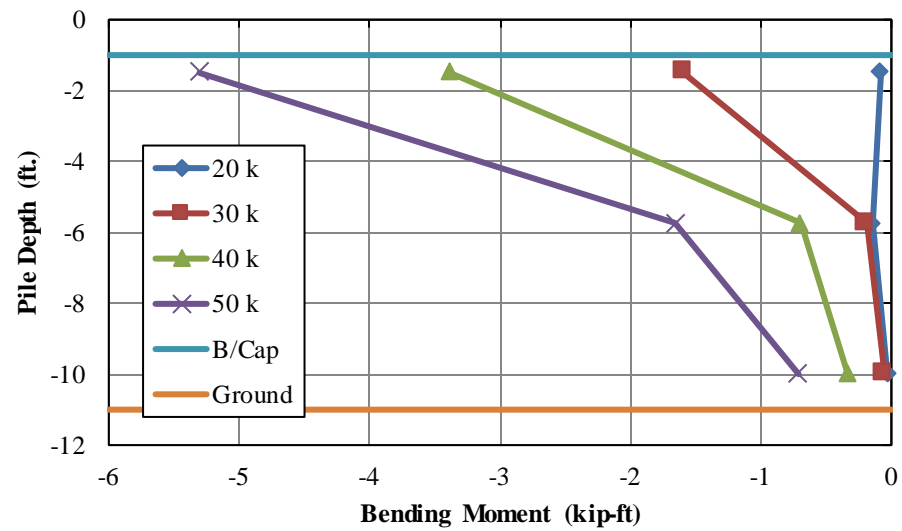
Figure 6-26 Pile 6 Bending Moment Profile
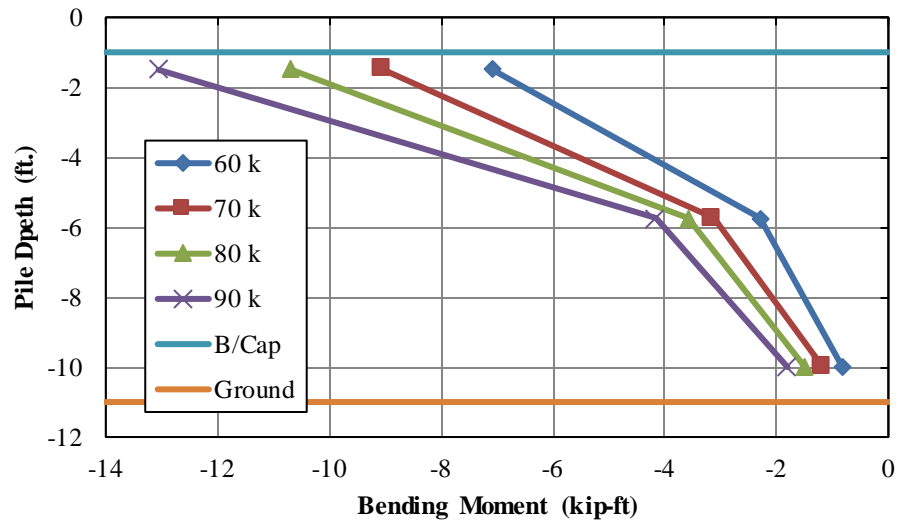
Figure 6-27 Pile 6 Bending Moment Profile

6.5.9   Reaction Bent Axial Forces – Lateral Load Only

Axial force versus applied lateral load for piles 7, 8 and 9 of the reaction bent during the lateral load test with no additional gravity load can be seen in Figure 6-44 through Figure 6-46. The instrumented section located six inches from the bottom of the cap were used to calculate axial forces. The axial load in pile 7 of the reaction bent appeared to have the highest magnitude during the load test, which was to be expected. Each of the instrumented piles in the reaction bent were in axial compression due to lateral load effects. The magnitude of the axial load in piles 8 and 9 were considerably smaller than in pile 7.
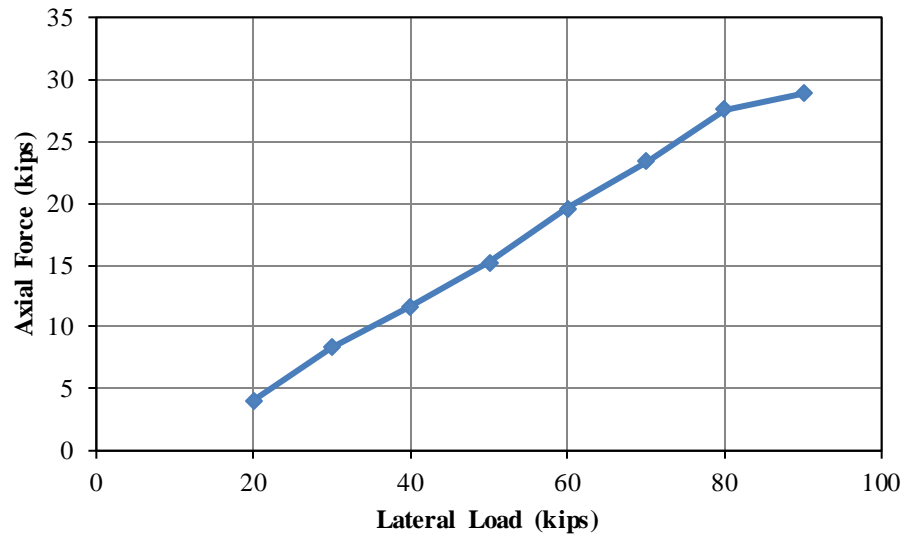
Figure 6-28 Pile 7 Axial Force vs. Lateral Load
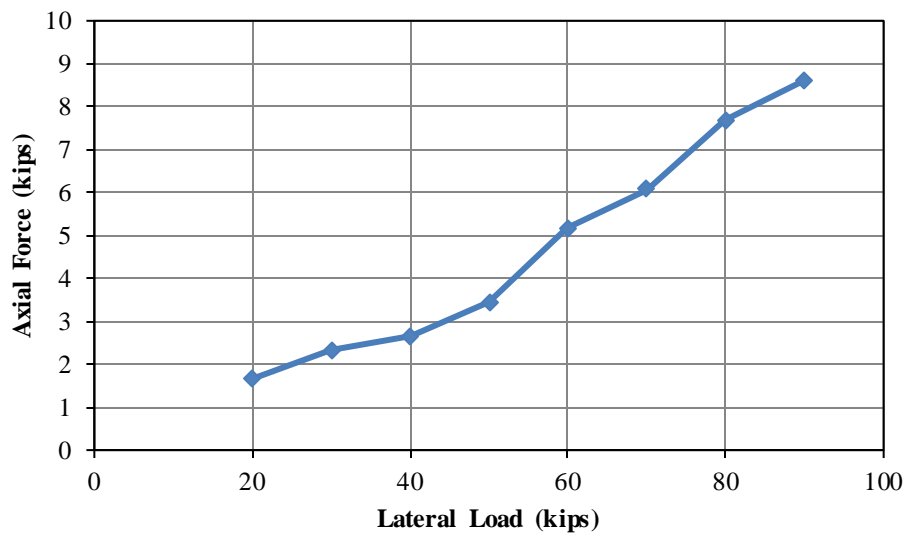
Figure 6-45 Pile 8 Axial Force vs. Lateral Load
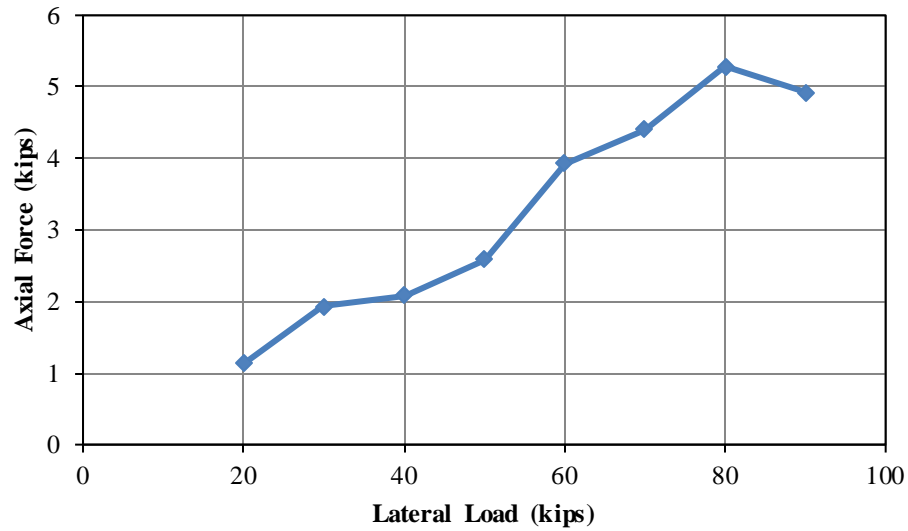
Figure 6-29 Pile 9 Axial Forces vs. Lateral Load

6.5.10 Reaction Bent Bending Moments – Lateral Load Only

The bending moment profiles for each of the instrumented piles in the reaction bent can be seen in Figure 6-47 through Figure 6-52. The maximum bending moments at the total lateral load increment ranged from 7 kip-ft. to 12 kip-ft. The magnitude of the bending moments are still relatively small, but comparable to the magnitude of the bending moments calculated in the test bent at the same load levels.
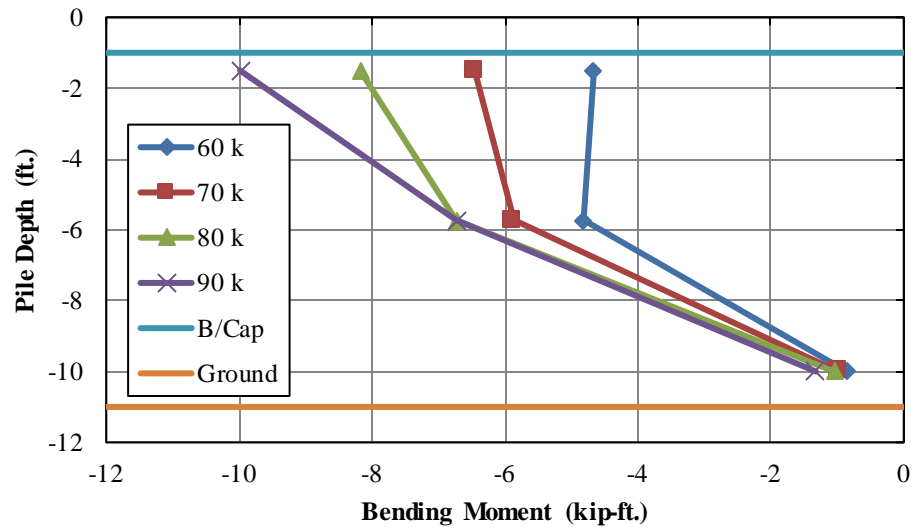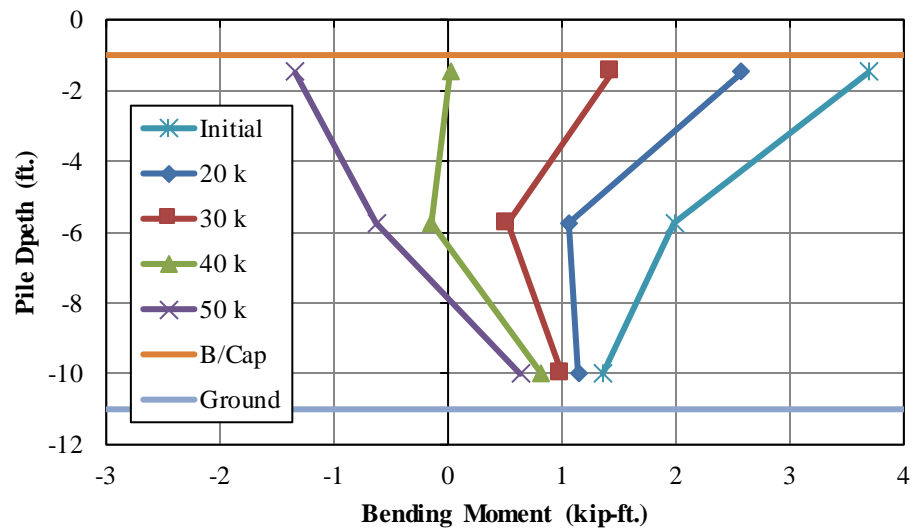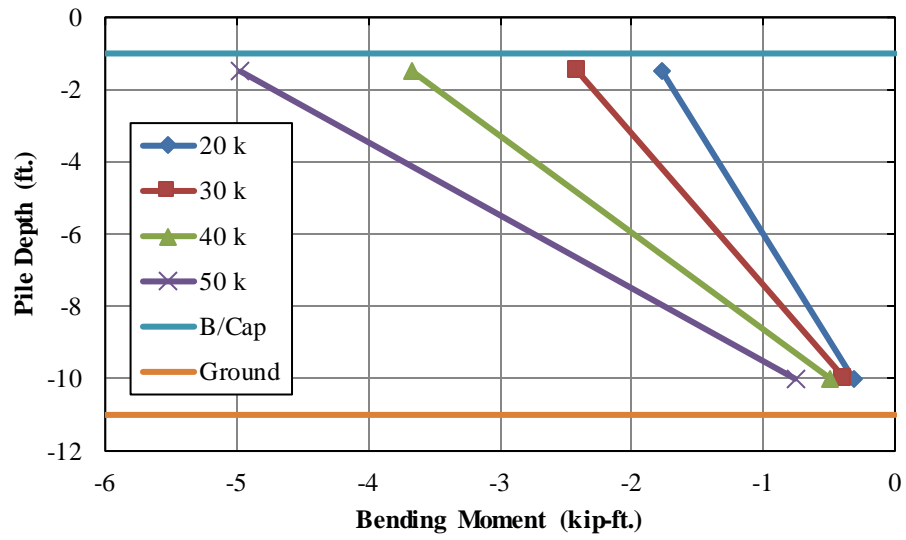
Figure 6-30 Pile 7 Bending Moment Profile
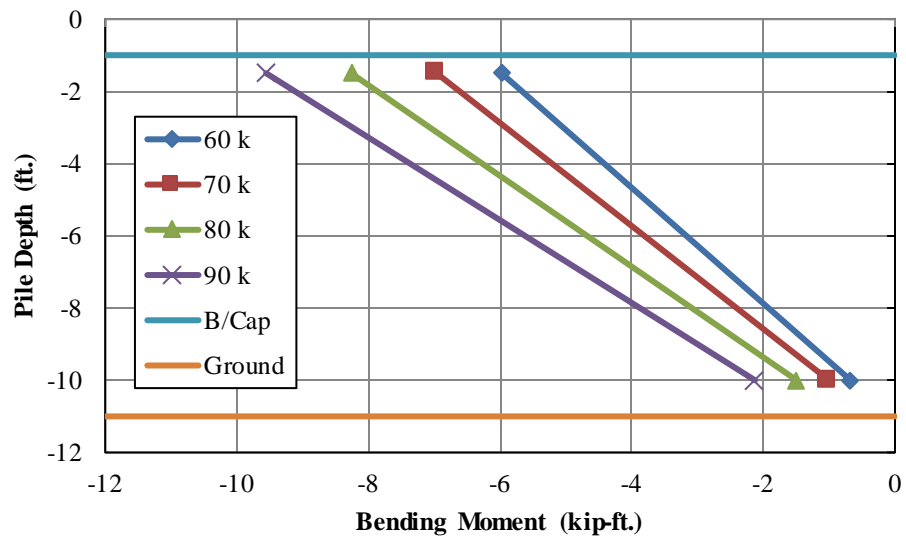
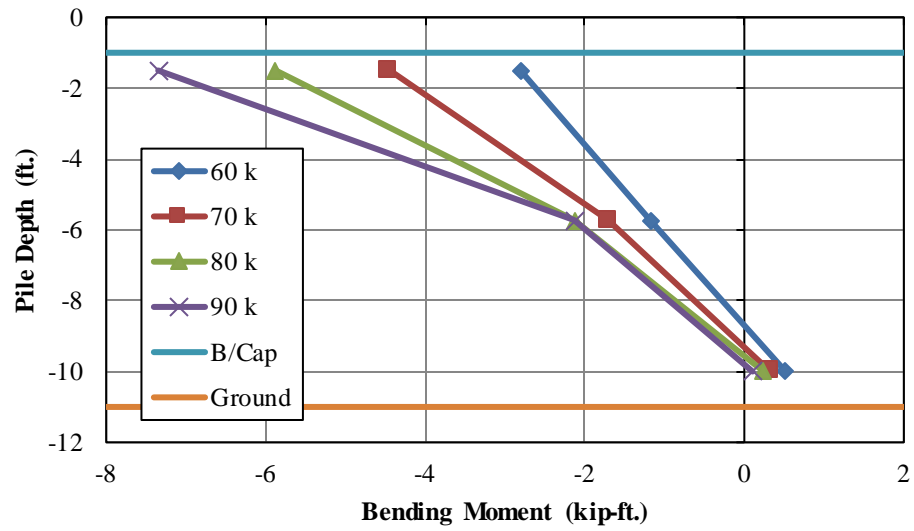**Figure 6-31 Pile 7 Bending Moment Profile**

181
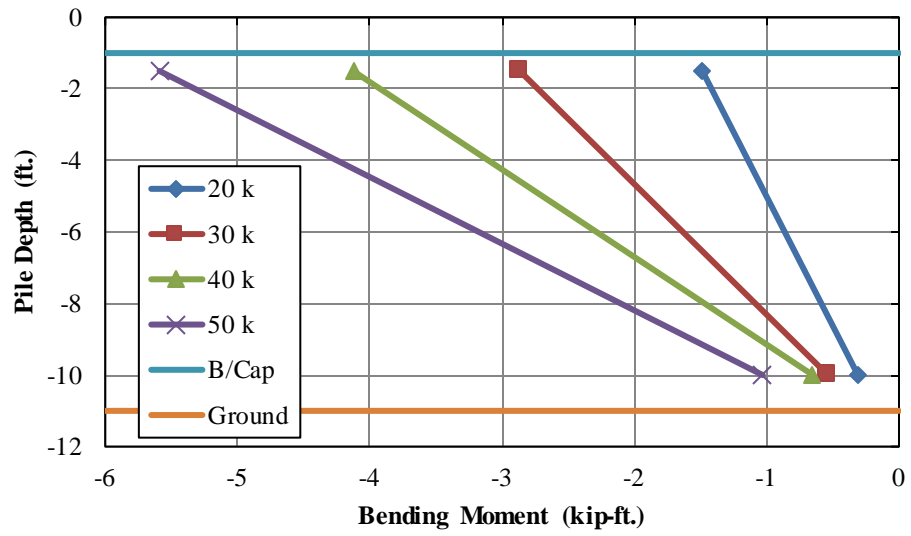
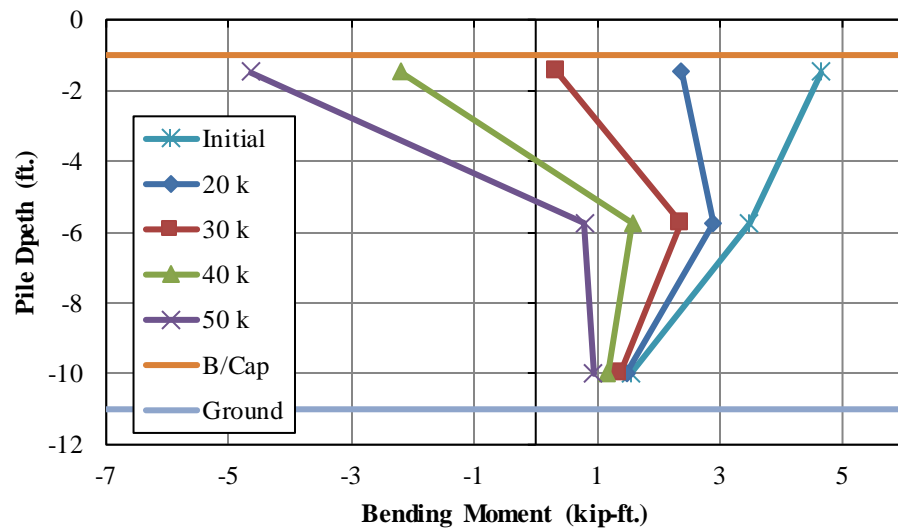**Figure 6-32 Pile 8 Bending Moment Profile**
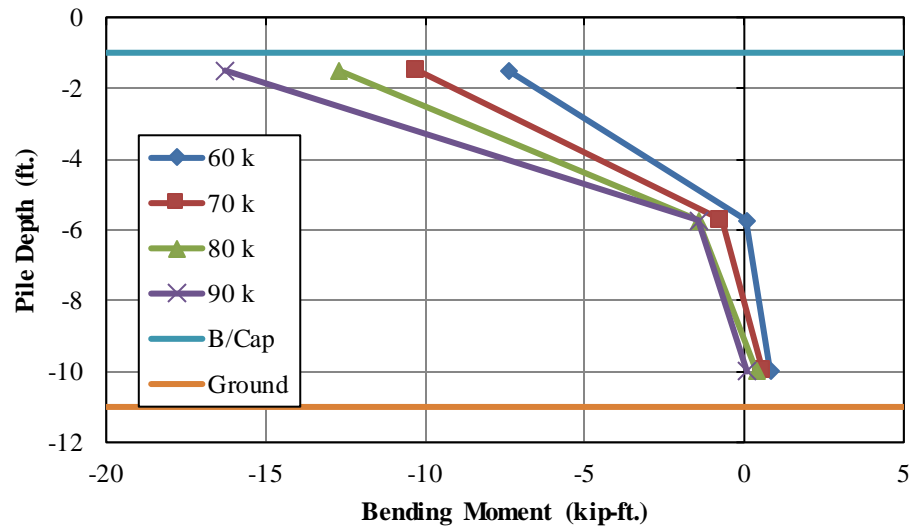

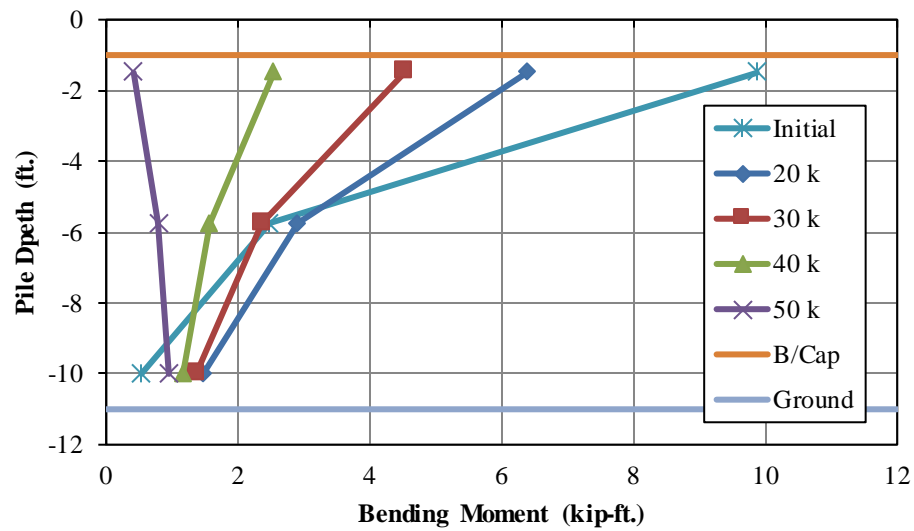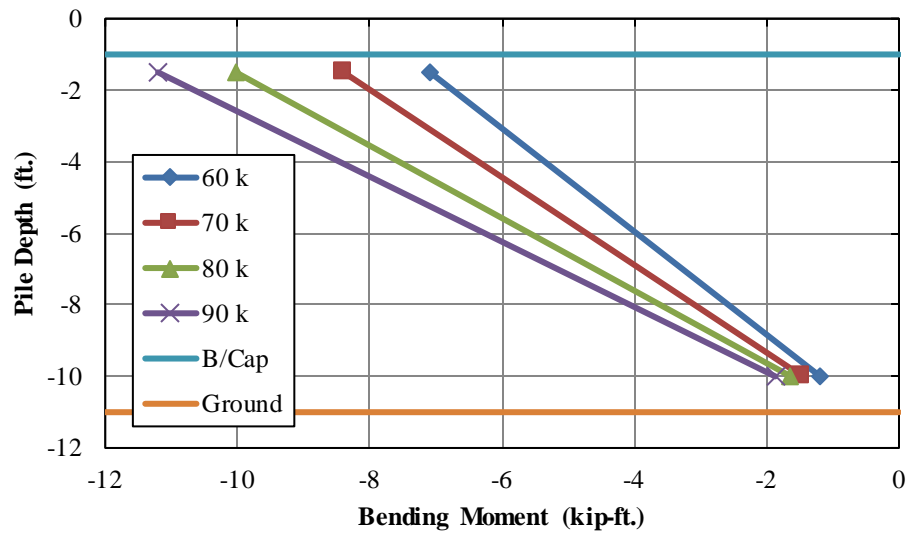**Figure 6-33 Pile 8 Bending Moment Profile**

182
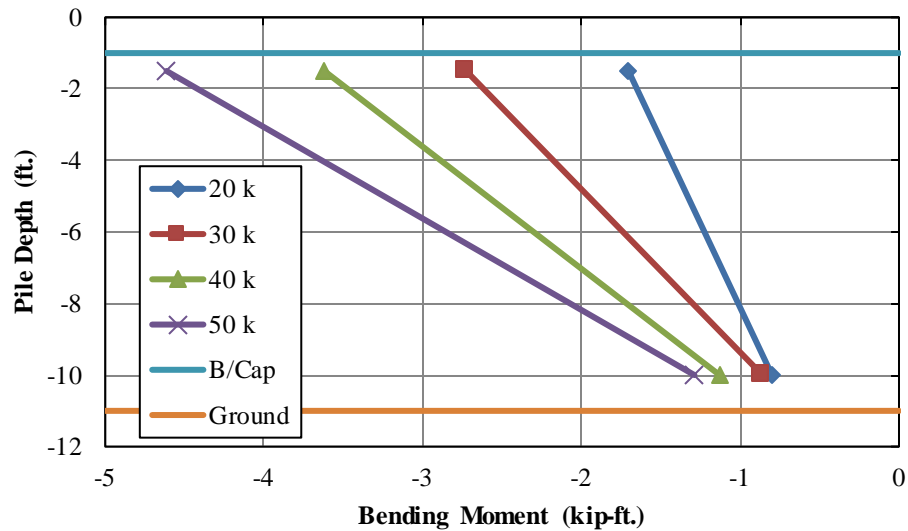
Figure 6-34 Pile 9 Bending Moment Profile
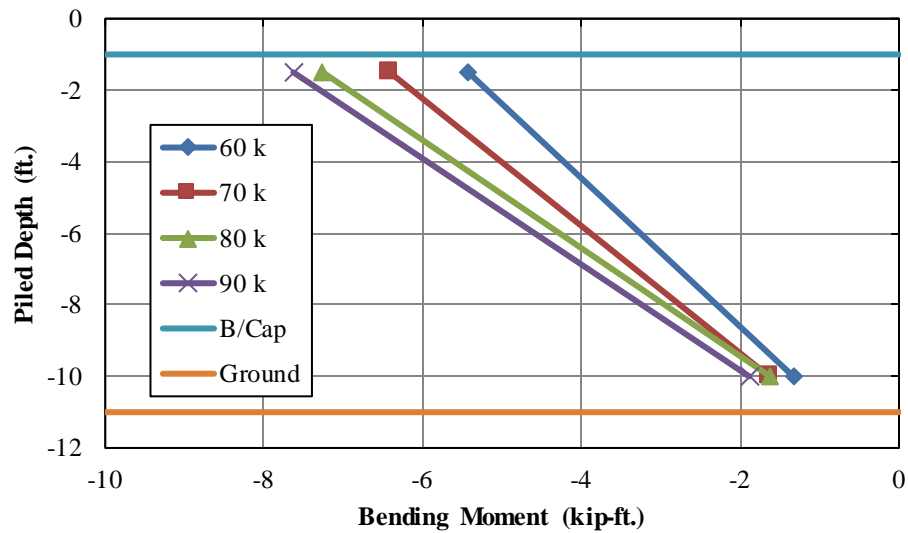
Figure 6-35 Pile 9 Bending Moment Profile

6.5.11 Displacement Wirepots

Two displacement wirepots were installed to the end face of the bent cap to measure lateral deflection of the bent during each of the load tests. One wirepot was located in the top right corner of the cap and the other was located in the bottom left corner so that an average total deflection of the cap during the tests could be obtained.

183

The load versus deflection curve for the combined gravity and lateral load test can be seen in Figure 6-53. The measured deflection in each of the two wirepots as well as the average deflection of the two is shown in the figure. The measured deflections in each of the two wirepots are very similar during this test indicating that there was little twisting of the cap during the load test. The bent was extremely stiff during the test, deflecting a maximum of less than 0.1 in. at 90 kips of total applied lateral load.
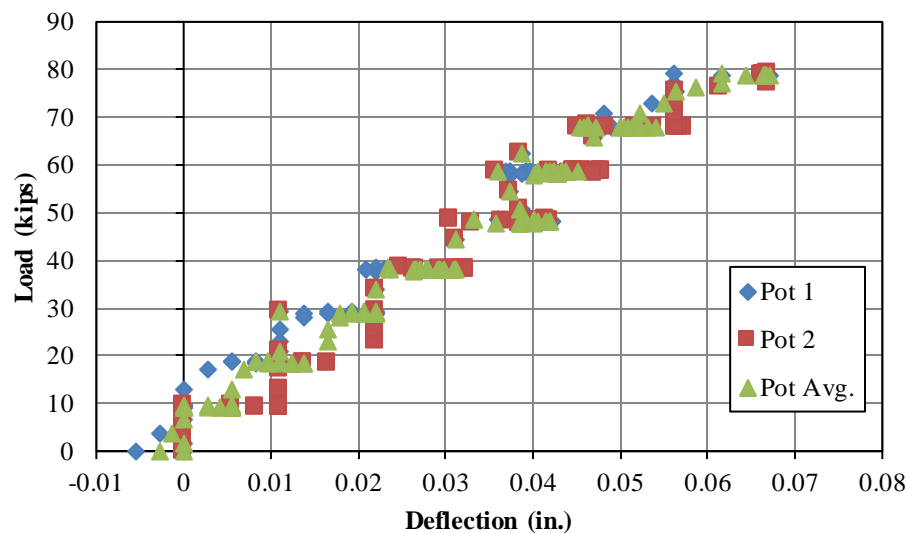
Figure 6-36 Load-Deflection with Load Truck Positioned at Road Edge

The load vs. deflection curve for the test bent during the lateral only load test can be seen in Figure 6-54. The average total deflection of the bent at a total lateral load of 90 kips was again under 0.1 in. indicating an extremely stiff response to the lateral load test.
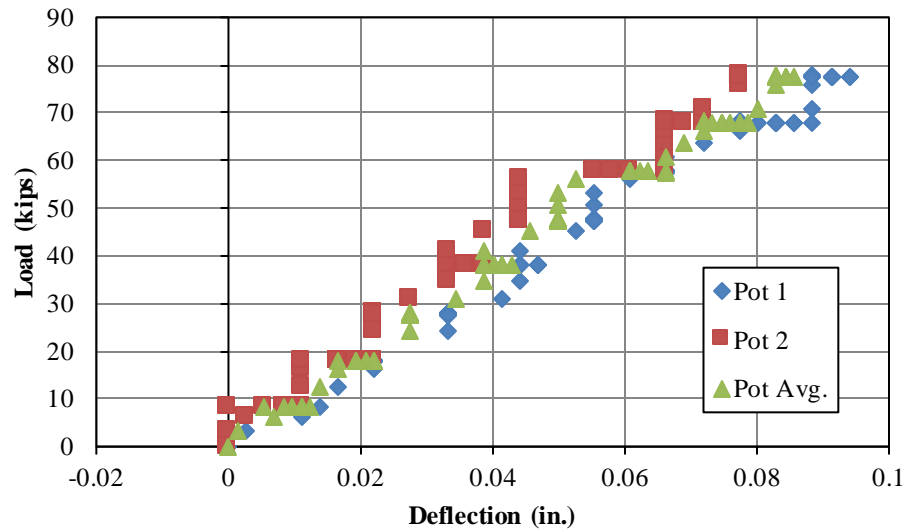
Figure 6-37 Load-Deflection with No Load Truck

A comparison of the average load vs. deflection curves for each of the two load tests performed can be seen in Figure 6-55. The average total deflection was greater with no additional truck load. However, in each load test, the bent was extremely stiff, deflecting less than 0.1 in. in each case.
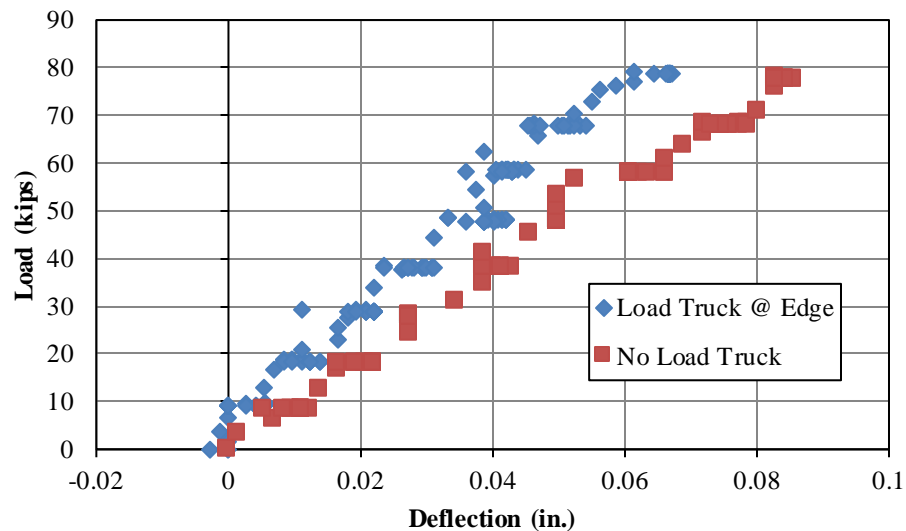
Figure 6-38 Load Deflection Comparison of Both Load Tests

The stiffness of the bents can be attributed to a number of factors. Even though the clear height of the piles is over 11 feet, the number of piles in the bent increases the lateral stiffness dramatically. The shedding of load to the adjacent bents can also attribute to the large stiffness of a single bent. The load-deflection response of the test bent appeared to be linear throughout the duration of each of the test which was to be expected at the intended load levels.

6.5.12 Bridge Bent Behavior

The test bent in the US 331 bridge was extremely stiff during each of the two load tests performed. The bent deflected less than 0.1 in. during each of the two tests. The extreme stiffness can be attributed to the number of piles in the bent and the additional stiffness from the adjacent bents. The bridge superstructure essentially ties the bents together allowing a portion of the lateral load to be transferred to each of the bents on the forward and back spans of the test bent through the intermediate diaphragms and bearing pad connection. The bent deflected approximately 20% more without the load truck on the bridge. The decrease in deflection during the test with the load truck on the bridge can be attributed to the lateral deflection in the opposite direction due to the truck load. The initial negative displacement results in a smaller net displacement at each lateral load increment. The increased flexural stiffness of the bent can also be attributed to the effects of cracking of the pile encasements. The moment of inertia of the encased piles is larger with the addition of compressive force which will result in a larger flexural stiffness.

The values of the computed bending moments were lower than expected with the maximum bending moments being between 10 and 18 kip-ft. The change in bending moment magnitude from the 80 kip to 90 kip load increment was smaller than the change in moment between the other load increments. This small change can also be seen in the load-deflection response. The change in deflection between these two load increments was also small relative to the other load

increment. The moment in the piles is related to the pile displacement meaning that a small change in displacement will result in a small change in moment.

Due to instrumentation only being installed on the concrete encasement surfaces, it was nearly impossible to monitor the behavior of the steel piles during the load tests. A linear strain distribution over the cross section was assumed to interpolate the strains at the flange tips of the steel pile and therefore consider their effects in axial force and bending moment calculation. The shape, however, of the moment diagrams was as expected with the maximum bending moment being at the bottom of the bent cap suggesting a fixed head condition for the piles. The moment diagram decreased linearly along the height of the piles which was instrumented with the lowest instrumented section being relatively close to the inflection point. The inflection point was expected to be close to the ground surface; therefore this observation is considered to be reasonable. The bending moments calculated in the piles in the reaction bent during each of the tests were significantly less than the calculated bending moments in the test bent. The axial compressive force in the leading pile of the reaction bent were higher in magnitude than the compressive force in the test bent.

6.6 Chapter Summary

The test bent performed well during each of the three load tests performed and was extremely stiff, deflecting less than 0.1 in. in each loading condition. The bending moments calculated from measured strains on the concrete encasements were very low in magnitude. The moments that were calculated included an approximated stiffness of the steel piles; however, the behavior of the steel piles during each of the load tests is uncertain. The shape of the moment diagram above the ground surface for each of piles was as to be expected with the maximum bending moments occurring near the bottom of the bent cap and the approximate inflection point being at or near

187

the ground surface. The location of the maximum bending moment clearly indicates a fixed head condition at the pile to pile cap connection.

The load-displacement response for the test bent remained fairly consistent during each of the combined gravity and lateral load tests as well as the test with no additional gravity load applied. The lateral stiffness of the bent did appear to increase by a small margin with the addition of gravity load; however, this increase in stiffness or decrease in displacement is seemingly negligible. Therefore it can be determined that addition of gravity loads in the service level range causes minimal effects on the lateral stiffness of bridge bent.

7. Analytical Modeling of Macon County Route 9 and US 331 Bridges

7.1 Introduction

Finite element structural models were created in order to determine how well the results from the field tests correlated with analytical results. The models were also used in order to determine behavior of the bent that was unable to be instrumented in field testing. Two-dimensional bridge bents were developed using SAP 2000. The bents tested in both Macon County and on US 331 remained well within the elastic range during the tests; therefore, a linear elastic static analysis was deemed to be acceptable. The models created in SAP 2000 simulated the geometry of the as-built bents. Composite cross-sectional elements and soil-structure interaction were also included in the models. The loads applied to the models simulated the actual applied loads to the bents during each of the load tests performed on the Macon County and US 331 Bent.

7.2 Geometric Properties

The structural models were created based on geometry obtained from construction documents and physical measurements taken from the as-built structure. A two-dimensional frame model was used to develop each of the bents, therefore the XZ plane remained the primary working plane.

For the Macon County test, the actual pile lengths for the as-built bent were known and were modeled accordingly. The pile lengths for the US 331 bridge were unknown; therefore an approximate pile length of 35 ft. was assumed. In most cases, the bending moment is dissipated well before the bottom of the pile making the assumed pile length reasonable. Once the piles

were drawn in, linear springs were applied at the pile tips in the z-direction. These properties of these springs were determined from models created in FB-Multipier. The axial reaction at the tip of the pile was divided by the vertical displacement of the pile tip in order to compute an axial spring at the pile tip. The bent cap was created as one continuous frame element. Due to the piles having an embedment of 12 in. into the 24 in. deep cap, a centerline model with the pile heads connected to the centerline of the bent cap was determined to be acceptable. This centerline model eliminated the need for additional connection springs or link elements to model the pile to cap connection. The results from the field test indicated that the maximum bending moment occurred at the top of the pile and decreased linearly; therefore it was deemed acceptable to fully restrain rotation at the connection between the piles and the bent cap. Results from load tests by Richards et al. (2011) and Gerber and Rollins (2009) indicated that a fully fixed head condition is difficult to achieve; however, piles embedded into a cap behave very similar to a fixed condition under working level loads when there is no apparent non-linear behavior. Once the bent geometry was drawn in, linear springs were added along the length of the piles to model the soil-pile interaction.

7.3 Material and Frame Section Properties

Once the geometry of the bents was in place, the frame sections and material properties for the bents were modified so that the elements in the bents reflected their as-built condition. The default material properties and user-generated material properties were used in the models.

For the bent elements in the Macon County bridge, the material properties were much easier to model due to the availability of information from the as-built structure. Concrete cylinder breaks performed at 7 days and 28 days from the concrete encasements and the bent cap were used in the Macon County model. Modulus of elasticity tests were not performed; therefore, the

190

modulus of elasticity of the concrete encasements and the bent cap was approximated using the empirical equation.

The bent cap was modeled using the section designer within SAP 2000. The trapezoidal cross-section of the bent cap was drawn within the section designer and was assigned the appropriate material property based on concrete strengths recorded from cylinder breaks at 28 days. Modeling the composite cross section including the steel pile and the concrete encasement proved to be fairly challenging. The piles were split into two separate elements at the location in which the encasements terminated. Below the termination of the encasements, which occurred five feet below finished grade, the piles were modeled using the HP14x89 section from the SAP 2000 AISC database. The local axes of the piles were rotated 90 degrees to ensure that they were loaded about the same axis in which they were loaded in the experimental tests. The composite cross section including the concrete encasements was modeled using the section designer within SAP 2000. A 30 in. diameter concrete cross section was drawn in and given the appropriate material properties, then a steel I-section was drawn in on top of the concrete cross-section to ensure that it was included appropriately in the calculation of areas and moments of inertia about each of its axes. The dimensions of the piles were manually entered in accordance with the AISC Manual for Steel Construction (AISC 2011) and the piles were assigned as A992 Grade 50 steel. An isometric view of the SAP 2000 model of the Macon County Bent including the overall geometry can be seen in Figure 7-1.

Figure 7-1 SAP Model Geometry for Macon County Bent

The model for the US 331 Bent was built similarly to the Macon County Bent. The overall geometry of the bent was built, and then the frame elements were designated their appropriate material and section properties. The trapezoidal cross section of the concrete bent cap was built using the section designer within SAP 2000 so that the geometry of the cap could be simulated. The depth of the encased piles was unknown, so an assumption as to how deep the piles were embedded into the ground had to be made. A typical embedment of the encasements is five feet; therefore, this embedment was used in the SAP model. The encased pile sections were also built in the section designer. A 16 in. x 16 in. square concrete section was input first. A structural steel I-shape was then placed on top of the square concrete section. The depth, flange width, flange

192

thickness and web thickness of the steel section were taken from the section properties listed for an HP10x42 in the AISC Manual for Steel Construction. For the pile depth below the encased pile section, the HP10x42 section from the AISC 14 pro database within SAP 2000 was used. After the pile sections were input, the local axes of the piles were rotated 90 degrees so that the piles would be loaded about the axis they were loaded during the load tests. An isometric view of the overall geometry of the model for the US 331 bent can be seen in Figure 7-2
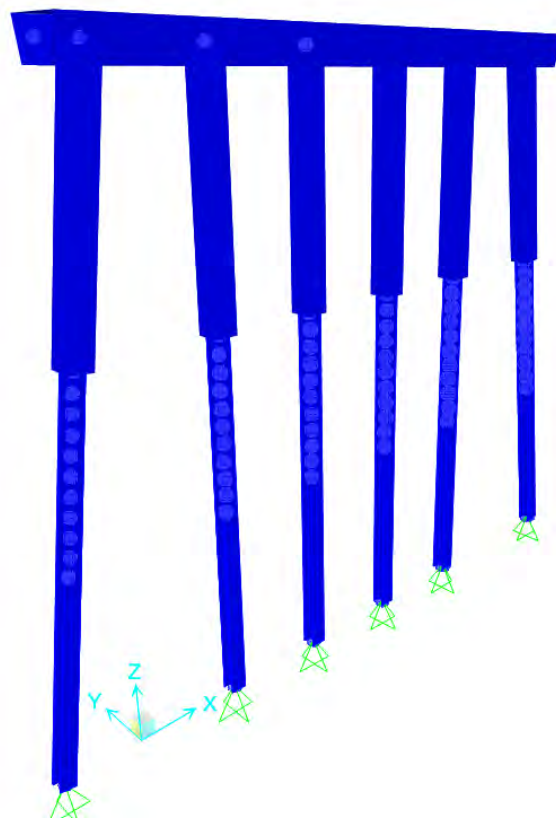
Figure 7-2 SAP Model Geometry for US 331 Bent

7.4 Modeling of Soil Interaction

To approximately model the interaction between the piles and the soil, linear springs were applied at discrete locations along the length of the piles. The properties of these springs were dependent on the soil properties at different pile depths. Prior to each of the load tests,

193

preliminary models were developed in FB Multipier in order to determine maximum loading targets that would result in an acceptable deflection that would not cause permanent damage to the steel piles, the encasements or the overall bent itself. The preliminary models created in Multipier considered soil properties, concrete encasement and embedment depth into the concrete bent cap. An image of the preliminary models for the Macon County Bent and the US 331 Bent can be seen in Figure 7-3 and Figure 7-4 respectively.
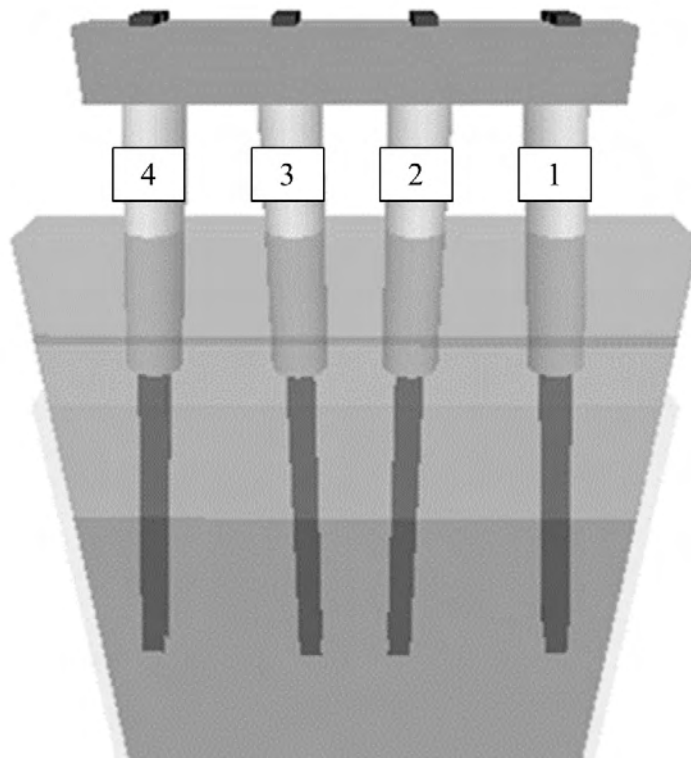
Figure 7-3 Preliminary FB Multipier Model of Macon County Bent
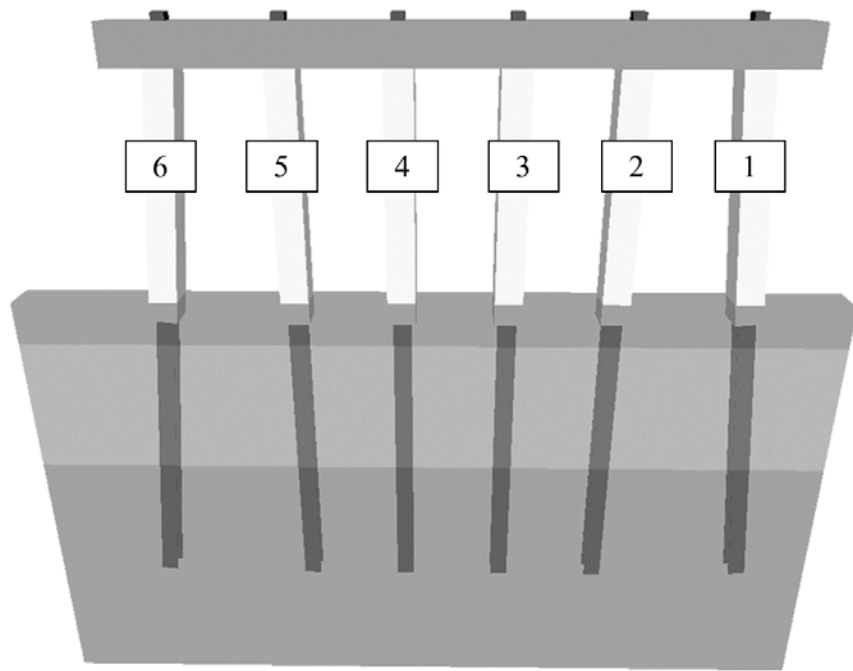
Figure 7-4 Preliminary FB Multiper Model of US 331 Bent

The FB multipier model consisted of soil data taken from boring logs from design drawings of the bridges. Soil layers were input into the model at the elevations determined from the boring logs. Each soil layer contains its appropriate properties, as seen in Figure 7-5 and Figure 7-6. These figures were previously presented in Chapter 3.
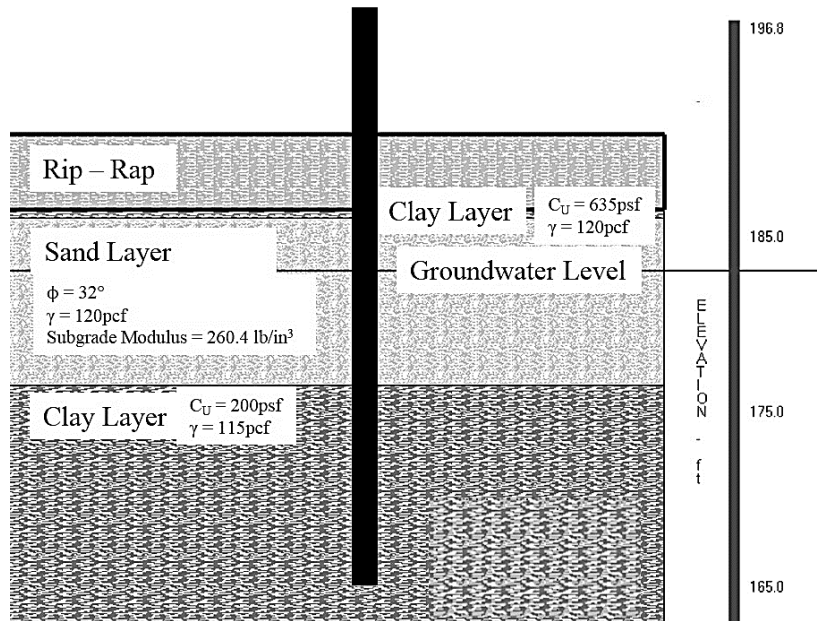
Figure 7-5 Macon County Bent Soil Profile
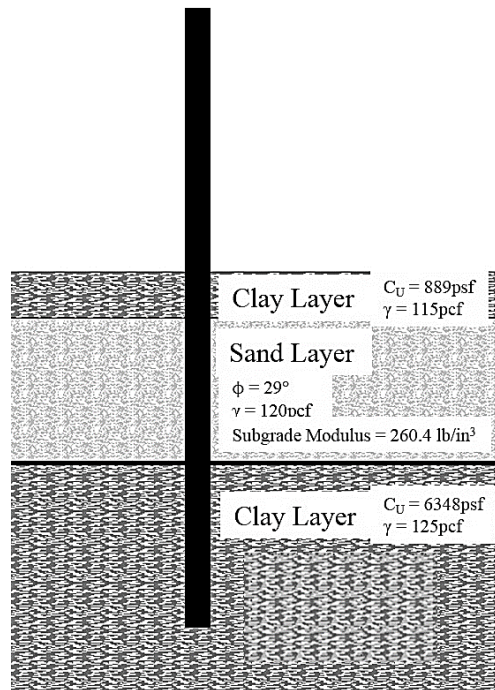
Figure 7-6 US 331 Bent Soil Profile

The springs were applied to simulate lateral resistance of the soil in the X-direction, which was the direction of loading for the bent models. The magnitudes of these springs were input

196

with units of kips/in. at locations along the lengths of each of the piles. The springs were determined by taking the shear force from the FB-Multipier model in the pile at a given depth and dividing it by the lateral displacement of the pile at that particular depth. The lateral displacement was essentially equal in each of the piles at every load increment; therefore it was deemed adequate to take an average of the spring magnitude for each pile and apply that spring magnitude to all piles at each location along the length of the pile. The first spring was placed at ground level and springs were placed at roughly one foot intervals along the remaining pile length. A summary of the average soil spring constants used for the Macon County test and the US 331 Bent can be seen in Table 7-1 and Table 7-2.

Table 7-1 Macon County Bent Spring Constants

Depth (ft.)	Average Spring Constant (k/in.)
10.78*	144.5
12.11	137.8
13.44	92.4
14.78	27.1
16.11	131.2
17.44	703.3
18.77	1742.2
20.1	3243.8
21.44	659.4
22.77	353.4
24.1	682.7
25.43	35.9
26.76	24.4
28.1	256.4
29.43	4.41
30.76	2.72

*Indicates average ground surface not including 5 feet of rip-rap

Table 7-2 US 331 Bent Spring Constants

Depth (ft.)	Average Spring Constant (kip/in.)
12*	47.5
13	53.9
14	25.7
15	256.2
16	6541.3
17	974.6
18	387.8
19	110.8
20	77.2
21	67.3
22	66.8
23	289.3
24	485.7
25	75.6
26	49.5

*Indicates average ground surface

7.5 Loads

Loads were applied to the models created for the Macon County Bent and the US 331 Bent to simulate the actual loads applied during the load tests. Static loads were applied to the Macon County Bent model to simulate the lateral load from the hydraulic cylinder. Due to the uncertainty of the lateral load transfer to other structural elements of the US 331 Bent, it was decided to perform a displacement-based analysis. Nodal displacements equal to the displacements measured during the field tests were applied to the US 331 bridge to simulate the lateral load applied by the hydraulic cylinders. In each of the models, the wheel loads from the load truck, and the self-weight dead load from the girders and bridge deck were simulated by applying static point loads applied at the girder locations. Three separate types of load pattern

were created: Dead, Truck Live, and Lateral. The dead load case consisted of the self-weight of the piles and bent cap, the girders framing into the bent, and the bridge deck. For the first load test on the Macon County Bridge, the deck weight was not included because the deck had not yet been cast. The truck live load case consisted of the wheel loads from the load truck. The truck wheel loads were applied as point loads at the girder locations. A deck strip was analyzed at each of the axle locations to determine the wheel load reaction on the each of the girders. The girders were then analyzed as a simple span beam to determine the reactions at the bent. The wheel load reactions for the center axle were not analyzed in a beam run, but applied directly to the bent since the center axle was positioned directly over the bent. Lateral load cases were developed for each lateral load increment for each of the tests. The lateral loads were applied as point loads at the centroid of the face of the bent cap.

For the test performed on the Macon County Bent prior to the deck being case, the only loads applied were the lateral load due to the hydraulic jacks and the self-weight reactions of the girders on either side of the bent. The self-weight of the girders was calculated using the cross-sectional area of a Type I AASHTO girder. A reaction of 11.52 kips was applied at each of the girder locations to simulate the girder self-weight. An image of the loading diagram of the first test performed on the Macon County bent can be seen in Figure 7-7. The soil springs along the length of the piles are graphically shown in this figure as well.
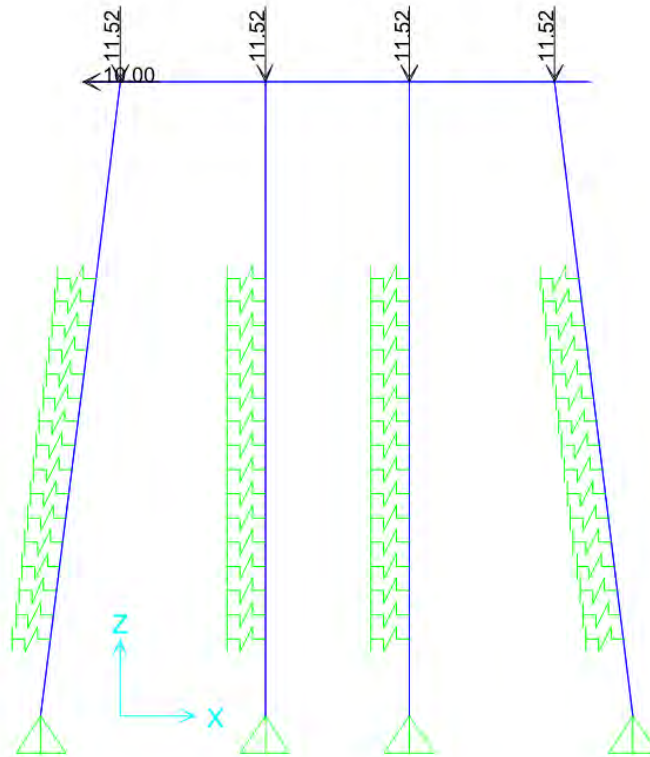
Figure 7-7 Loading Diagram for First Macon County Test

Additional loads needed to be applied for the second load test performed on the Macon County Bent. The weight of the bridge deck needed to be accounted for in this test. The deck load is transferred to the girders then the girders transfer the load to the bent at the bearing pad location. To correctly model this load transfer, point loads were applied at the girder locations. The deck loads were applied by taking the deck cross-section and converting it into an equivalent line load on each of the girders based on their tributary width. The deck cross section provided in the design drawings was used in order to determine deck thicknesses used in self-weight calculations as well as tributary widths used for the girder analyses. The equivalent line loads were then multiplied by the girder span to account for the reaction from the girders on the forward and back spans of the bent. The self-weight deck reactions applied were determined to be 20.77 kips at the exterior girders and 18.6 kips at the interior girders. The reactions are larger

200

at the exterior girders due to the deck thickening from 7 in. to 8 in. from the center of the exterior girders to the edge of the roadway at the location of the barrier.

The wheel loads from the load truck were also transferred from the deck to the girders to the bent. The centerline of the wheels of the load truck were not directly over the girders in either of the loading conditions where the load truck was on the bridge. A deck strip was first analyzed to determine the reactions on the girders in each of the truck positions. After these reactions were determined, they were applied to the girder at the location of the wheel axle. The point loaded girder was then analyzed as a simple span beam in order to determine the girder reaction on the bent.

The loads applied to the bent during each of the load test performed on the Macon County Bent with the deck in placed were assigned to different load patterns: dead, truck live, and lateral. Load combinations were built using the three different load patterns. Dead + Truck Live + Lateral was built for every lateral load increment. A summary of the girder point loads applied to the bent for each of the three tests performed on the Macon County Bent with the bridge deck in place can be seen in Table 7-3.

Table 7-3 Macon County Bent Loading Summary

Pile	P_{deck} (kips)	P_{girder} (kips)	$P_{truck\ centered}$ (kips)	$P_{truck\ at\ edge}$ (kips)
1	27.42	11.52	-1.65*	37.67
2	27.84	11.52	38.25	38.3
3	27.84	11.52	38.25	-3.53*
4	27.42	11.52	-1.65*	1.0

*Negative value indicates uplift reaction

Loads were applied to the US 331 Bent to simulate the loading conditions of the load tests performed. Similar to the Macon County test performed after the deck had been cast, self-weight loads, truck wheel loads, and static lateral loads were applied. Each of the gravity load cases

201

were applied as point loads at the girder locations. The method for calculating slab and girder self-weight was the same as the Macon County test, using tributary area of the girders to determine the girder reactions on the bent. The method for calculating girder reactions from the truck wheel loads was also the same as the Macon County test which consisted of analyzing a deck strip to determine the deck reaction on the girder then analyzing the girder to determine the girder reaction on the bent. All lateral loads were applied as static point loads applied at the centroid of the bent cap face. Load cases were created for self-weight, truck wheel loads, and lateral loads. Load combinations were created combining self-weight and truck loads with each of the lateral load increments. A summary of the girder reactions applied to the US 331 Bent can be seen in Table 7-4.

Table 7-4 US 331 Bent Loading Summary

Pile	P_{deck} (kips)	P_{girder} (kips)	$P_{truck\ at\ edge}$ (kips)
1	22.54	9.79	0
2	19.24	9.79	0.1
3	19.24	9.79	-0.50*
4	19.24	9.79	1.87
5	19.24	9.79	40.45
6	22.54	9.79	26.87

*Negative value indicates uplift reaction

7.6 Analysis Results

The structural models were built in order to determine how well the models correlated with the results from each of the field tests. This section contains a detailed comparison of the results from the structural models created in SAP 2000 and the results from the field tests. Bending moments and cap deflections were used in order to determine how well the field test results correlated with the structural models.

7.6.1 Macon County Bent Without Deck

Bending moments and deflections from the SAP model of the Macon County bent without the bridge deck are compared to the bending moments and deflections from the field test in this section. The model for this test consisted of nine different lateral load cases from 10 kips to 75 kips, simulating the same loading conditions from the field test. The bent behavior from the SAP model correlated well with the field test results. The maximum cap deflection was within 12% of the maximum deflection predicted in the model. The deflected shape of the bent model at a scale factor of 200 can be seen in Figure 7-8. The figure depicts the deflected shape at the 75 kip load increment; however, the overall deflected shape of the structure remained the same for each loading increment.
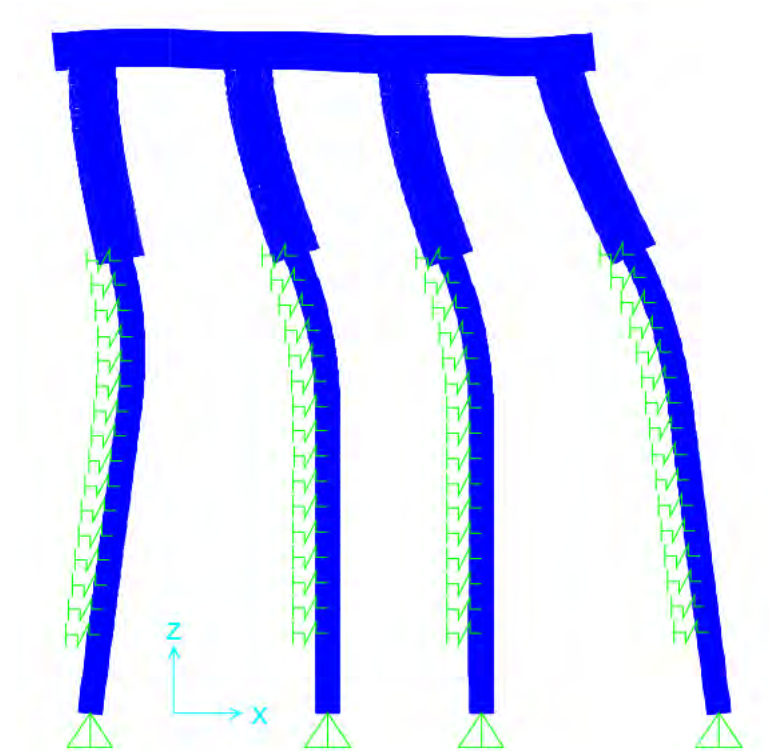
Figure 7-8 Macon County Bent with no Deck Deflected Shape at 75 kips

The bending moment diagrams from the SAP model for each of the piles at the 75 kip loading increment can be seen in Figure 7-9. Notably, the interior piles appear to take roughly 25

percent more moment than the exterior battered piles. The inflection point for each of the piles occurs at or near the location of the ground surface specified in the model by the first soil spring. The rip-rap was not included in models created in FB Multipier; therefore it was not included in the SAP model. The comparison of the results shows the location of the inflection points to slightly vary between the field test and the model. The moment appears to dissipate around a depth of 20 feet for each of the piles in the model and actually reverses curvature a second time, though the moment magnitudes are seemingly negligible at these depths.
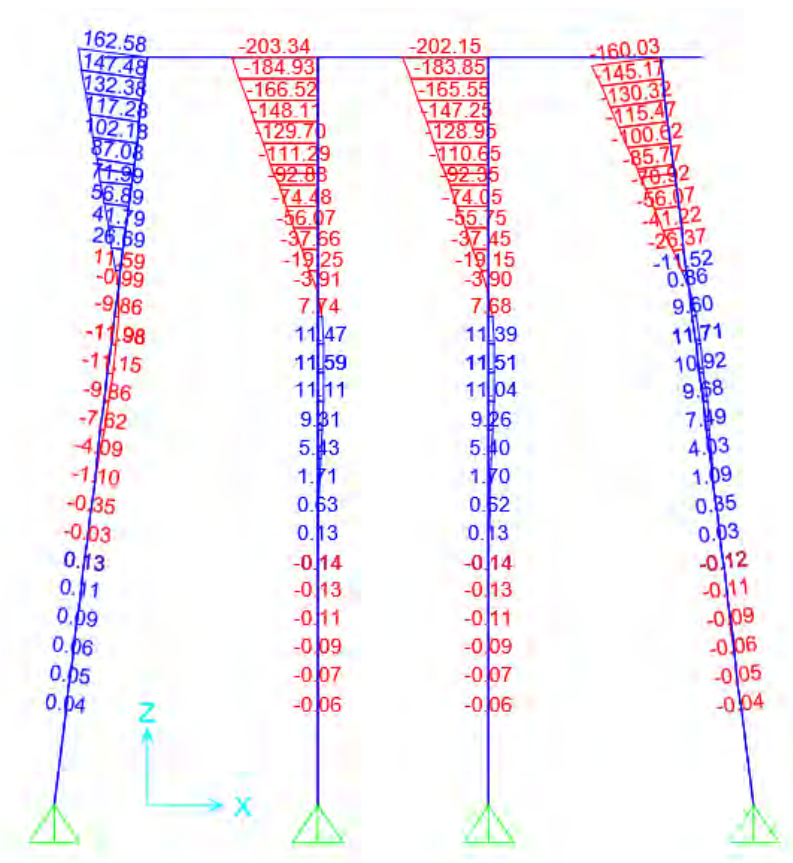
Figure 7-9 Macon County Bent with no Deck Moment Diagram at 75 kips

The moment diagrams for each of the four piles from the SAP model can be seen in Figure 7-10 through Figure 7-13. The data points from the calculated experimental results are also shown on these plots. For every pile with the exception of pile 4, the SAP model predicted

higher magnitudes of bending moment than the calculated values. The field test bending moments correlated well with the moments predicted in the SAP model aside from pile 1. The moments at the lowest instrumented section were very small relative the moments above grade due to the termination of the pile encasements. The location of the inflection point varied between the SAP model and the field test results. This variation of inflection point locations can be attributed to the exclusion of the rip-rap, which may provide a considerable amount of lateral resistance. The amount of lateral resistance provided by the rip-rap layer is highly uncertain which is why it was not accounted for in the model. Although the lowest instrumented section moment was calculated to be positive from the field test result and negative in the SAP models, it is clear that this instrumented section was near the inflection point of each of the piles.
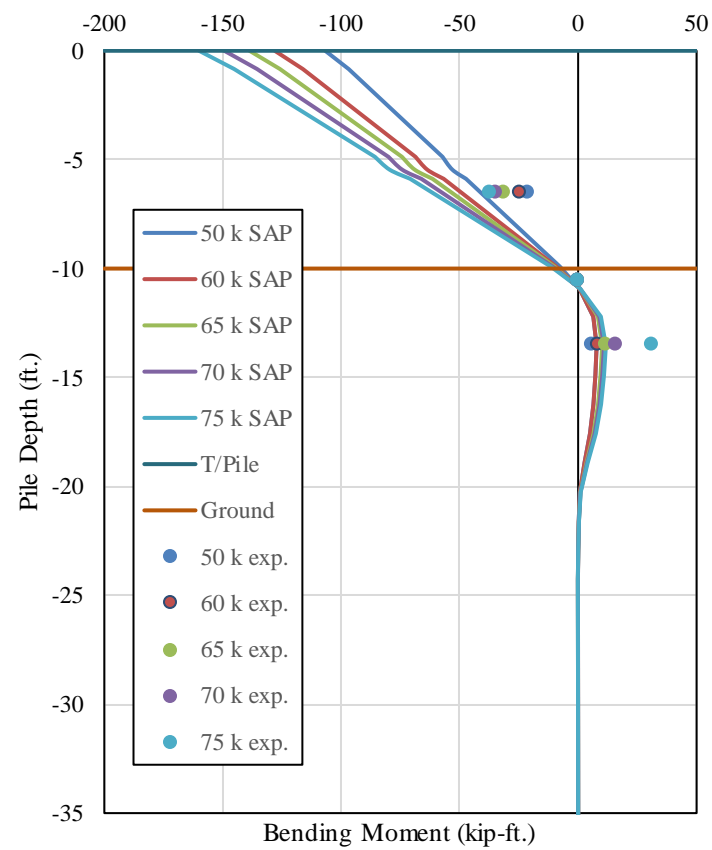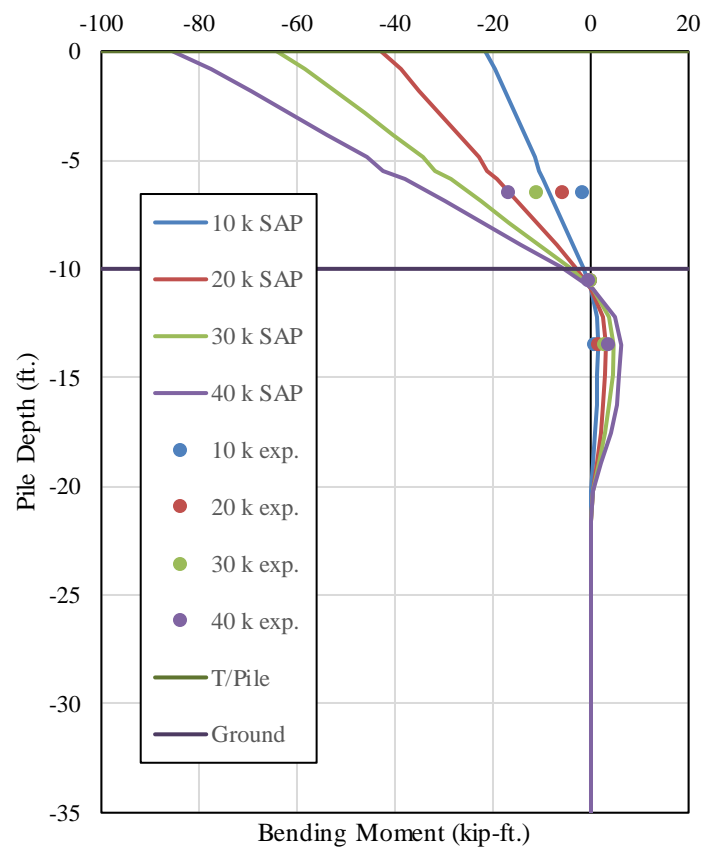
Figure 7-10 Pile 1 Bending Moment Comparisons
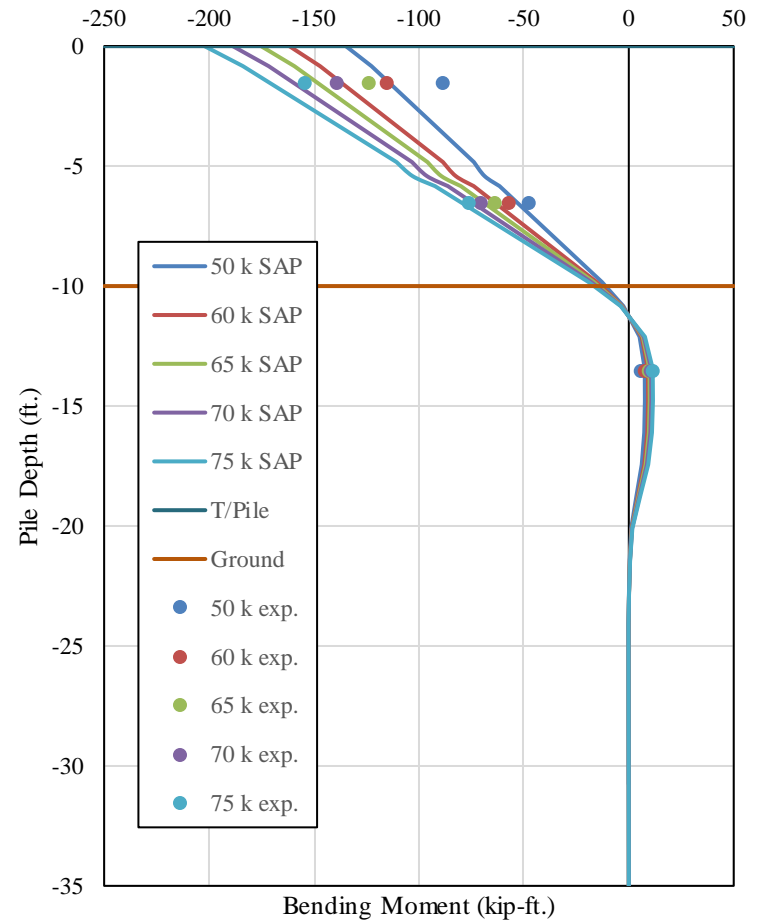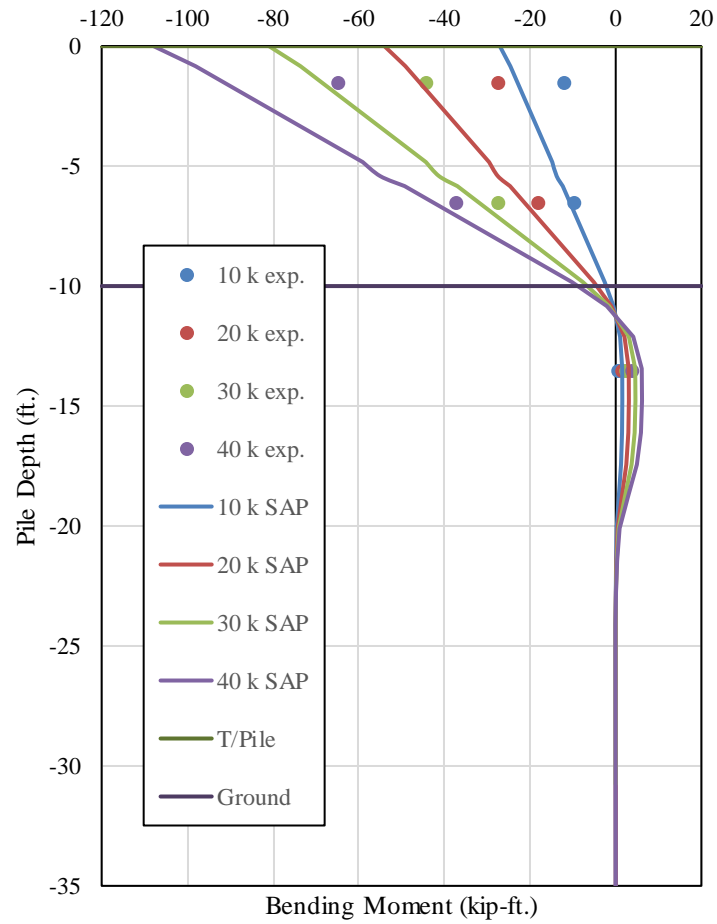
Figure 7-11 Pile 2 Bending Moment Comparison
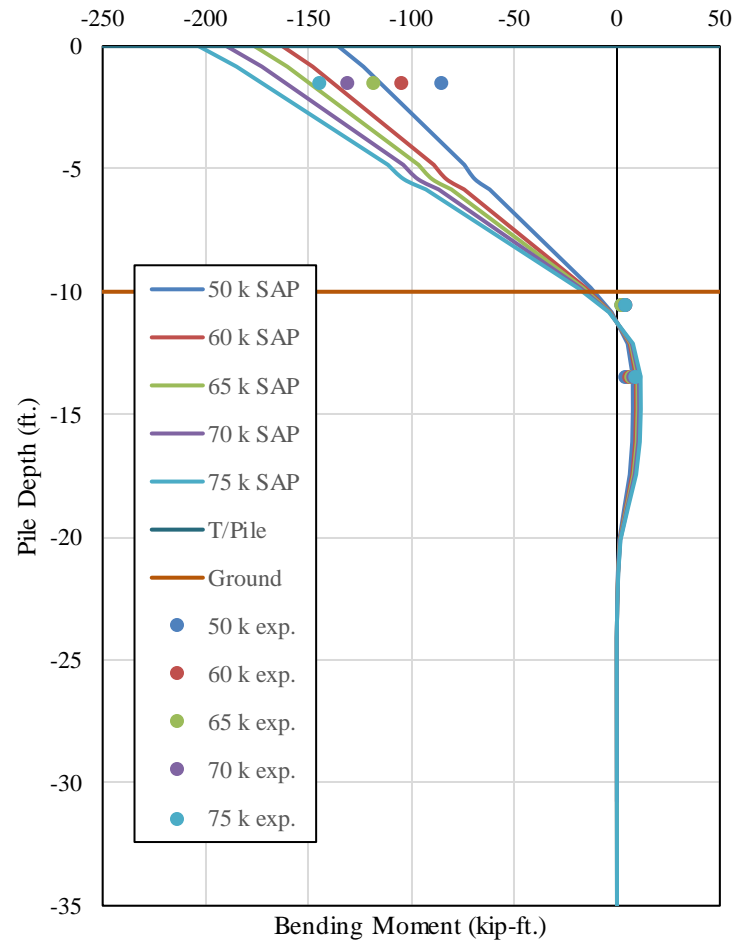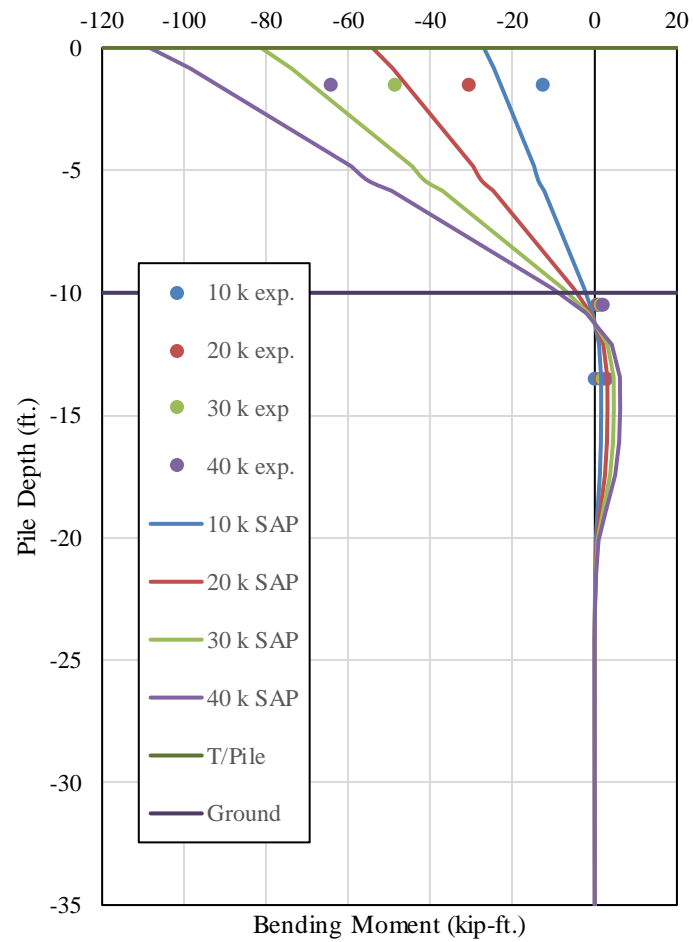
Figure 7-12 Pile 3 Bending Moment Comparison
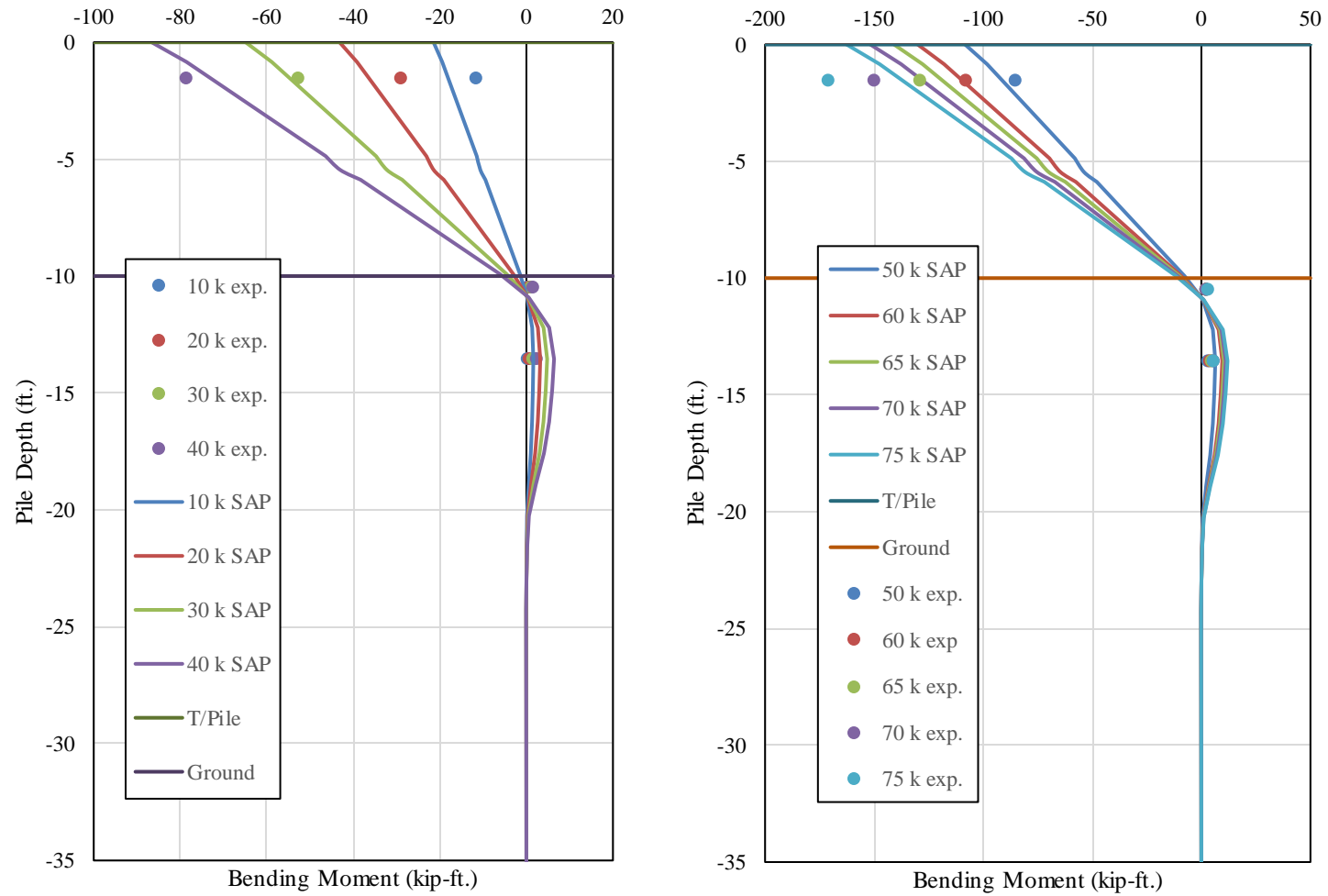
Figure 7-13 Pile 4 Bending Moment Comparisons

Axial forces versus lateral load for the lateral load cases from the SAP model are shown in Figure 7-14 through Figure 7-17. The axial forces shown in the figures below are from the lateral loads only, not including any self-weight of the structure. The axial force diagrams are constant over the length of the piles; therefore the axial forces are plotted against the applied lateral load as opposed to depth. Due to the large cross-sectional area of the encased pile sections, axial loads computed from measured strains were deemed to be unreliable and were not reported. However, the axial force in the piles under the lateral load cases is of interest to designers. Most notably, the exterior battered piles carry the largest axial forces due to their batter. The interior pile axial forces are roughly 25 percent of the axial forces in the exterior battered piles. The leading pile has a compressive axial force and the leading pile has a tensile axial force which is to be expected due to the bent wanting to overturn under lateral loading. The magnitudes of these compressive and tensile forces are equal and opposite in sign.
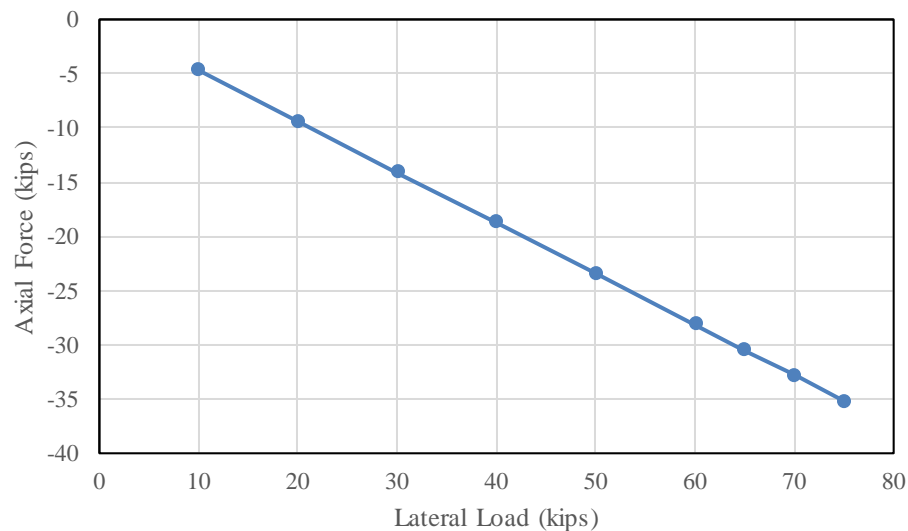
Figure 7-14 Pile 1 Axial Load versus Lateral Load

210
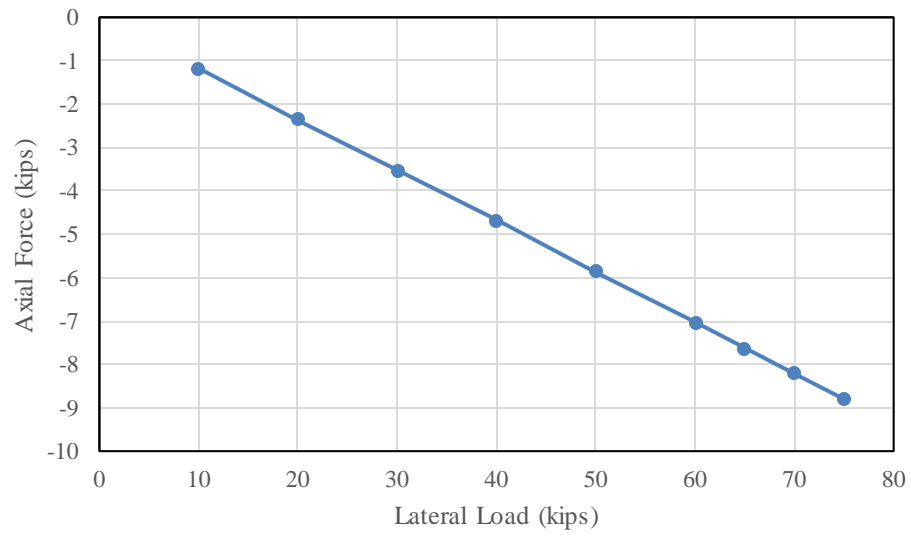
Figure 7-15 Pile 2 Axial Load versus Lateral Load
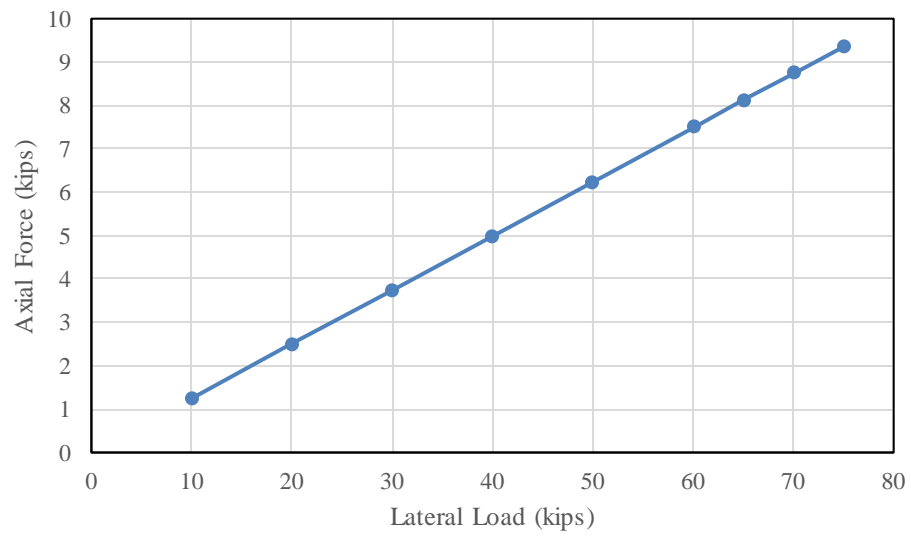
Figure 7-16 Pile 3 Axial Force versus Lateral Load

211

Figure 7-17 Pile 4 Axial Force versus Lateral Load

The load versus deflection from the Macon County test compared to the load versus deflection predicted from the SAP model can be seen in Figure 7-18. The model deflection was compared to the average deflection from the four wirepots used in the field test. The load-deflection responses from the field test and the SAP model correlated well throughout the majority of the load increments. The load-deflection from the SAP model is linear due to a linear elastic analysis being performed. The load-deflection from the field test is relatively linear with virtually no deflection at the 10 kip increment. This small amount of deflection could be due to the loading apparatus initially setting in, creating a small load effect at this increment. The deflection appears to increase linearly starting at the 10 kip increment throughout the rest of the test. The maximum deflection at 75 kips from the SAP model was within 12 percent of the average deflection from the field test. The SAP model does not account for nonlinearity in the soil which is likely the reason for the softening of the experimental force-deformation.
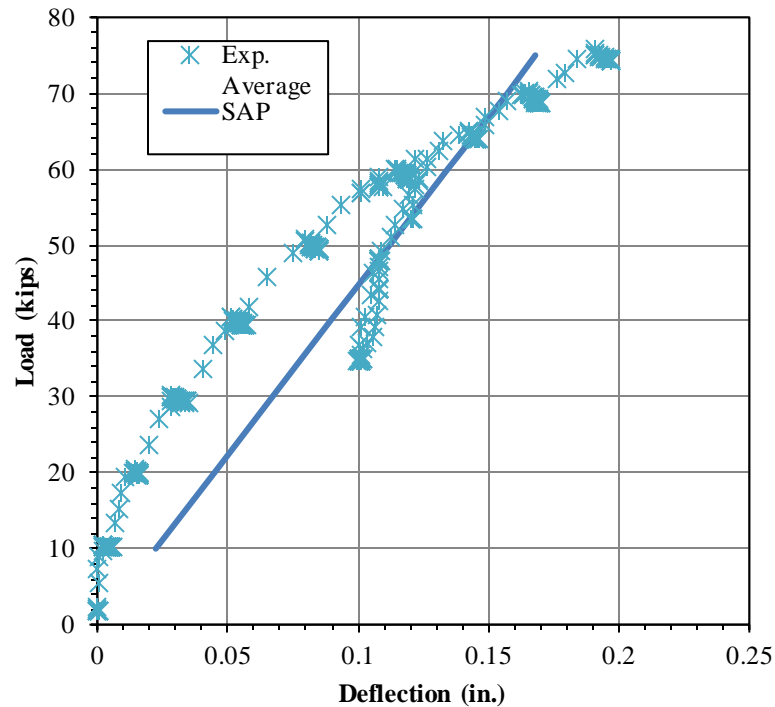
Figure 7-18 Load Deflection Comparison from Macon County Test with no Bridge Deck

7.6.2   Macon County Test with Deck

The bending moments and deflections for each of the load tests performed on the Macon County bent after the bridge deck had been cast are compared to the results from the SAP model created for the bent in this section. For this model, the same frame elements used in the model from the first load test were used. The magnitude of the springs used in the model for the first test were used again in the model with the bridge deck. For the models created for the bent in which the bridge deck was in placed, the additional stiffness provided by the bridge deck needed to be accounted for. It was apparent from the field test results that a portion of the lateral load was distributed to structural elements other than the test bent. The decrease in deflection under the same lateral load with the deck in place suggests that some of the lateral load is transferred to the adjacent bents. The load-deflection data from the field tests were used to approximate the

213

additional lateral stiffness of the bent due to the bridge deck transferring the lateral load to the adjacent bents in the bridge. The primary objective was to provide additional means of stiffness in the model so that the deflections from the field test correlated well with the model deflections. A spring was applied at the face of the bent cap in which deflections were measured in the field test in order to account for the additional stiffness provided by the bridge deck. To determine the magnitude of this spring, an average overall lateral stiffness of the bent for the load test without the bridge deck and the load test with the bridge deck without the addition of the truck load was computed. This stiffness was computed by taking the lateral load applied and dividing it by the bent deflection at each loading increment for each of the tests. The difference in these values was used as the applied spring for the bent model to account for the stiffness of the bridge deck. The overall stiffness of the bent without the bridge deck was determined to be 385 kip/in. and 588 kip/in. for the bent with the bridge deck. Therefore a spring with a magnitude of 203 kip/in. was applied to the node at the face of the bent cap on the trailing pile end (Pile 1).

A comparison of the bending moments from the SAP model and the field test results can be seen in Figure 7-19 and Figure 7-20. Due to the large variation in strains during the tests, the gages on Pile 1 were considered to be unreliable. Therefore, the field test results for Pile 1 are excluded from the figures below. Similarly to the results from the bent without the bridge deck, the SAP model predicted higher bending moments in each of the piles with the exception of pile 4. The results from the field test correlate well with the SAP model with the exception of the lowest gage on pile 3, in which the bending moments calculated from the field test results are significantly higher than the moments predicted from the SAP model.
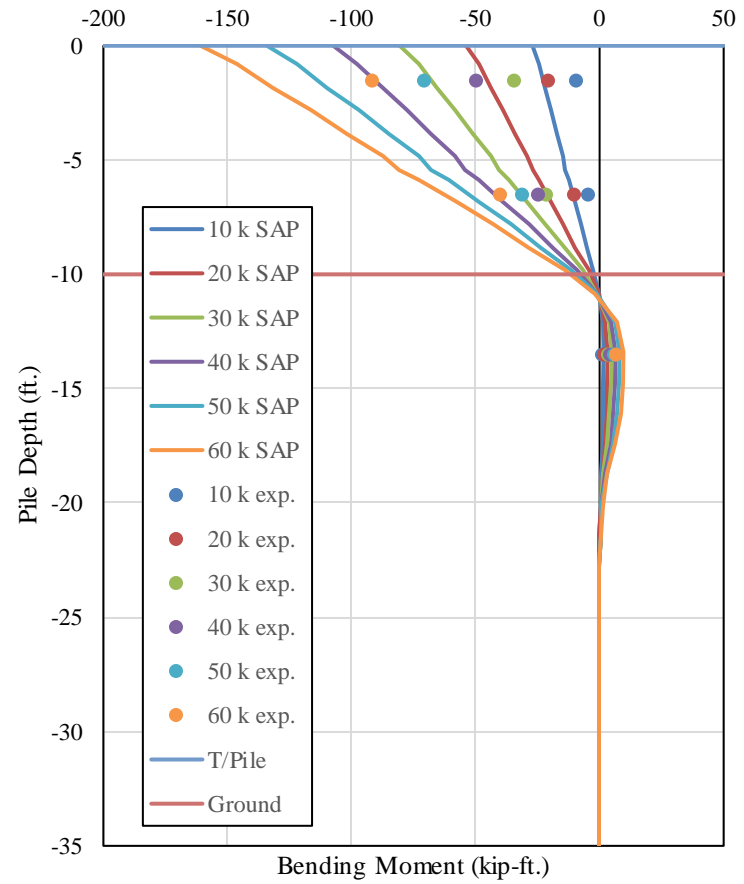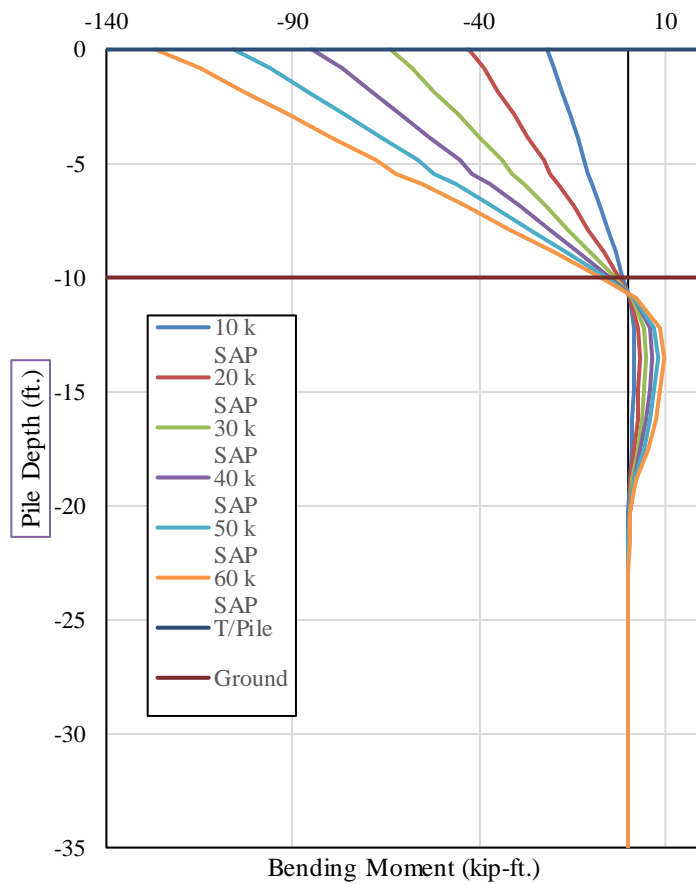
Figure 7-19 Pile 1 & 2 Bending Moment Comparisons with no Load Truck
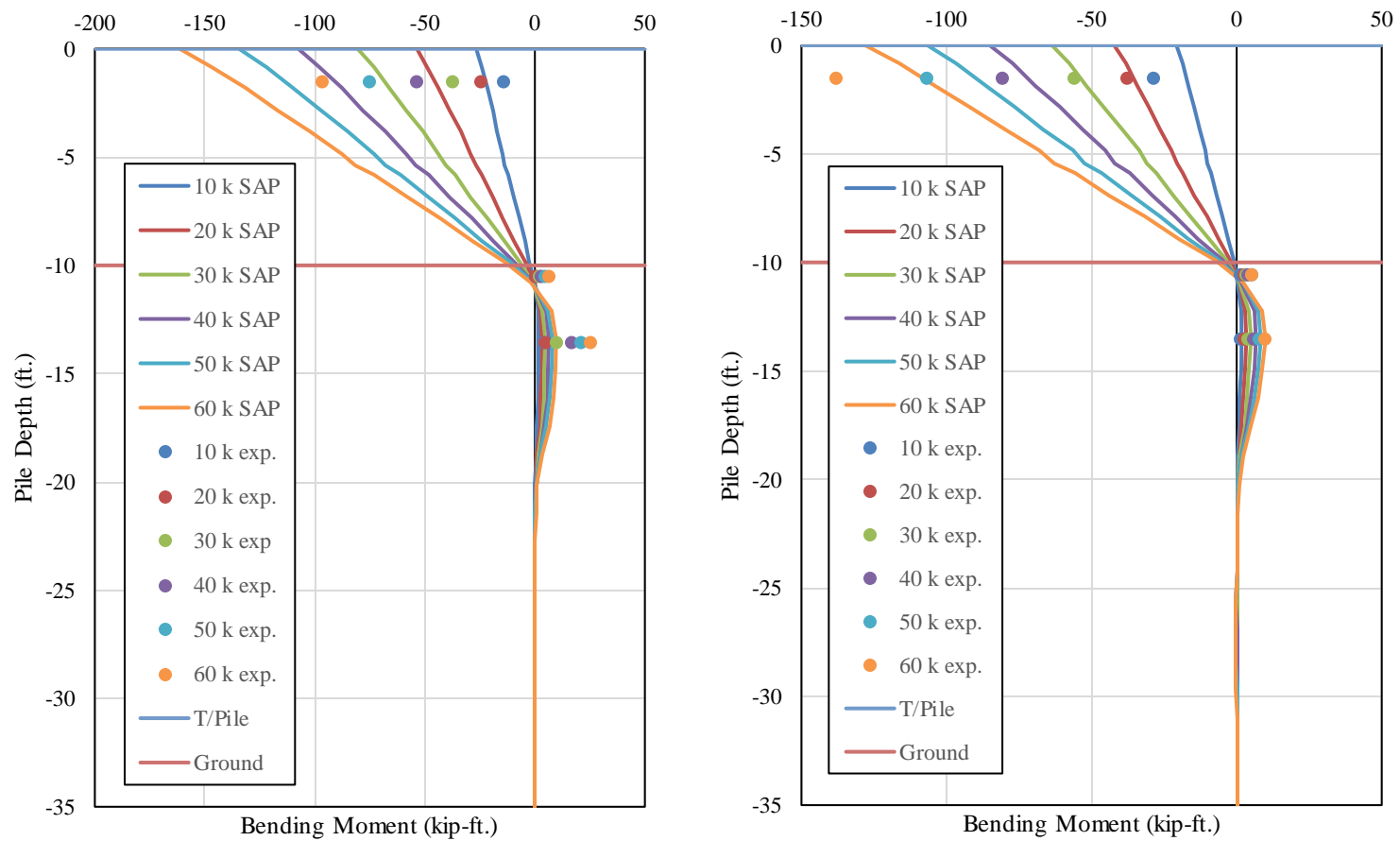
Figure 7-20 Pile 3 & 4 Bending Moment Comparisons with No Load Truck

216

The moments from the load test with the load truck centered over the roadway are compared to the moments predicted from the SAP model in Figure 7-21 through Figure 7-24. The results from the field test for Pile 1 are not included in these figures again. The SAP model predicts higher bending moments in each of the piles with the exception of Pile 4. Notably, the bending moment diagram from the SAP model for Pile 1 under the 10 kips loading increment predicted the location of the inflection point to be significantly higher than each of the other piles in the bent. Overall, the results from the field test correlated well with the results from the SAP model with the bending moment values varying from the field test by lower than 5 percent in some instrumented sections to as high as 40 percent. The lowest instrumented section in Pile 3 showed bending moment magnitudes significantly higher than the predicted values from the SAP model. However, the magnitude of these bending moments at this location is small relative to the bending moments at sections above grade.
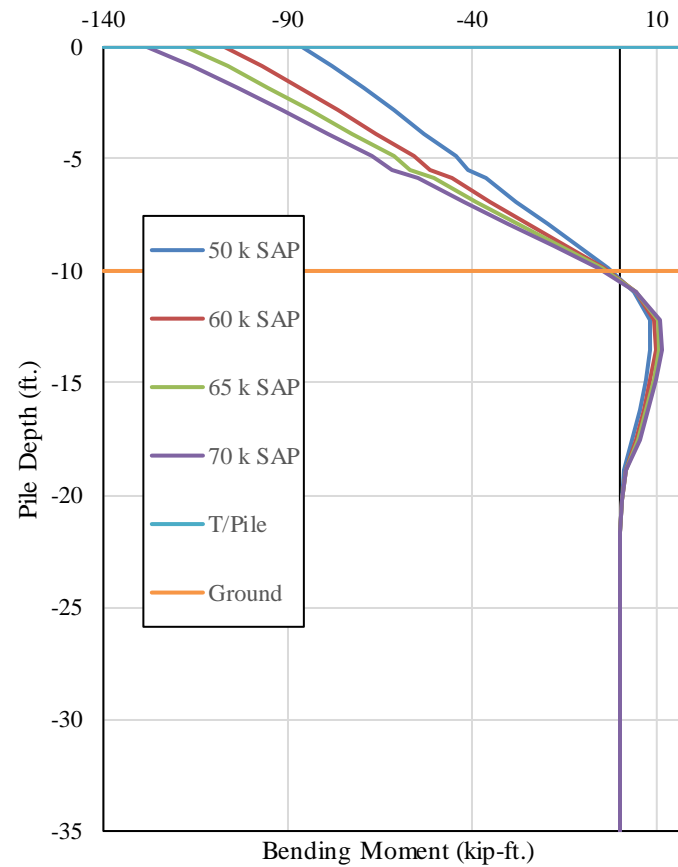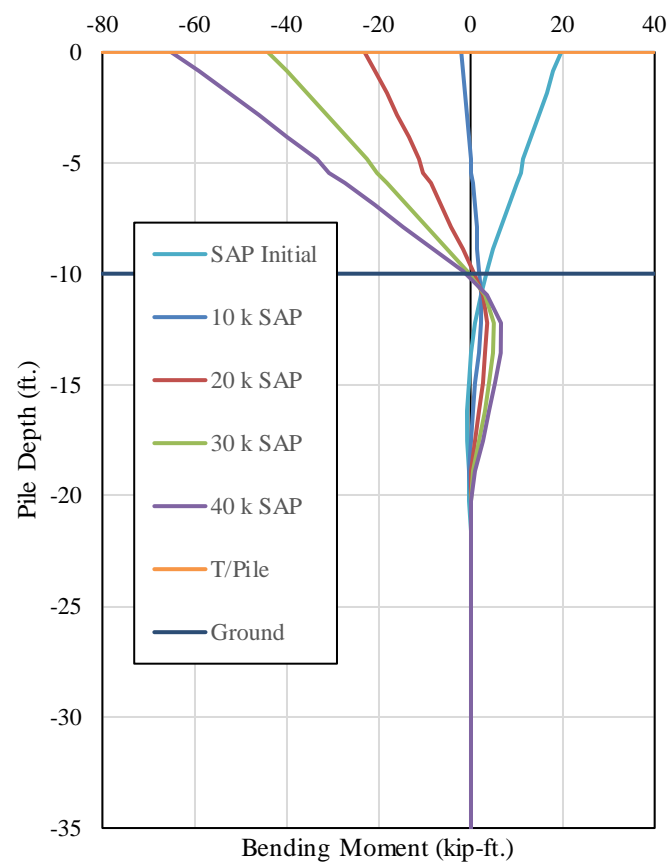
**Figure 7-21 Pile 1 SAP Bending Moment Profiles with Load Truck Centered on Roadway**

218
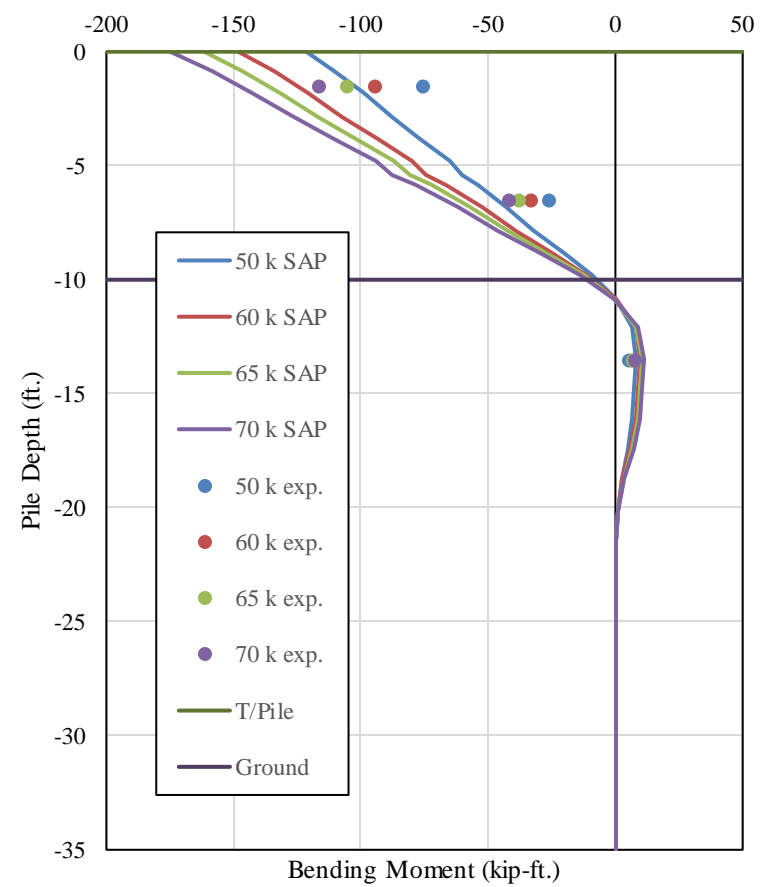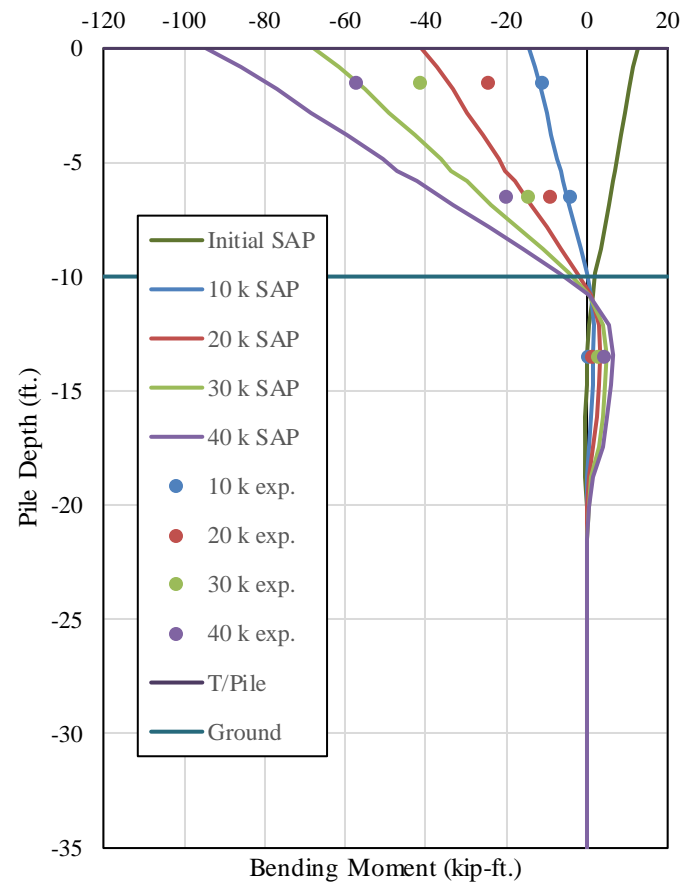
Figure 7-22 Pile 2 Bending Moment Comparisons with Load Truck Centered on Roadway

219
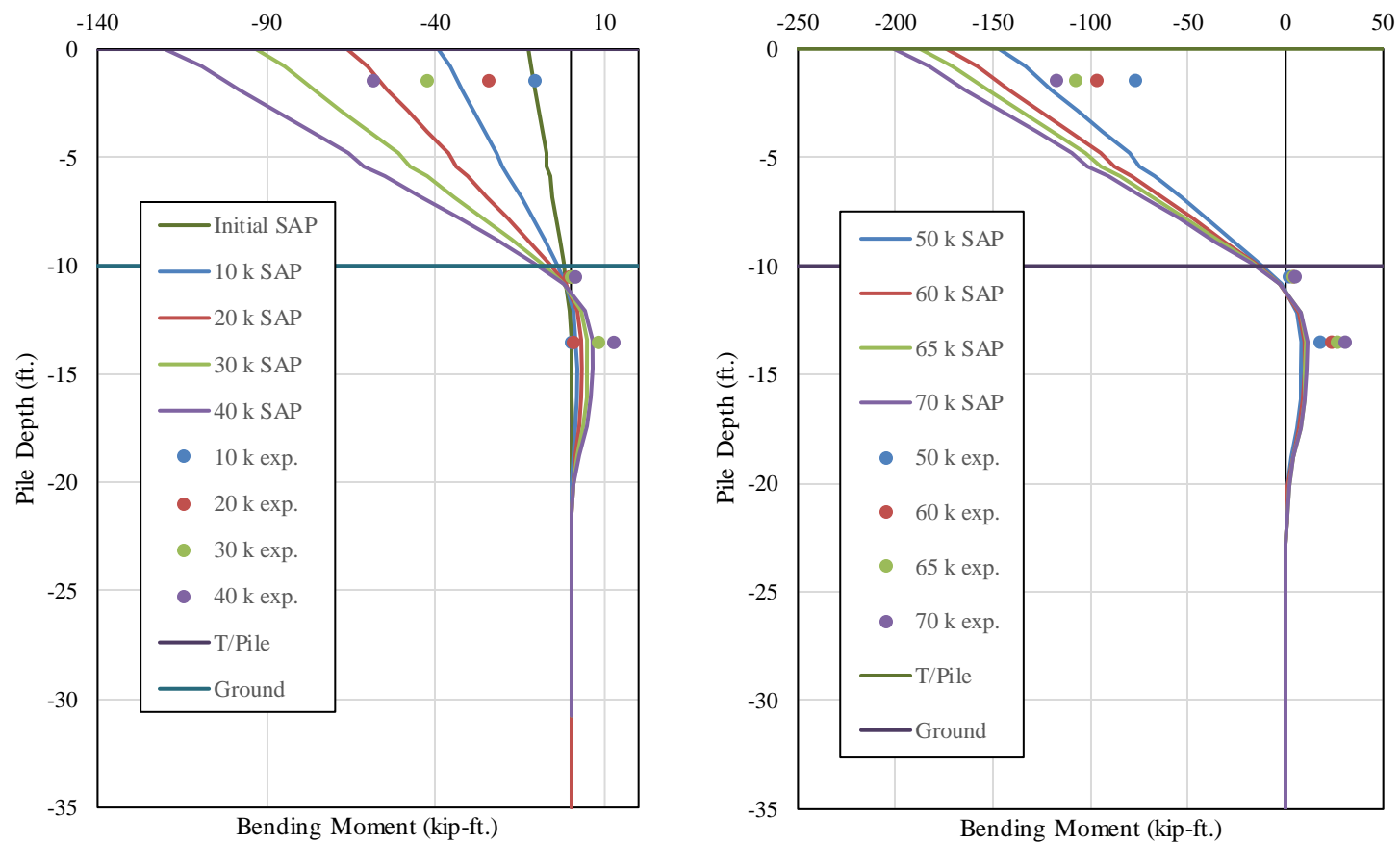
Figure 7-23 Pile 3 Bending Moment Comparisons with Load Truck Centered Over Roadway
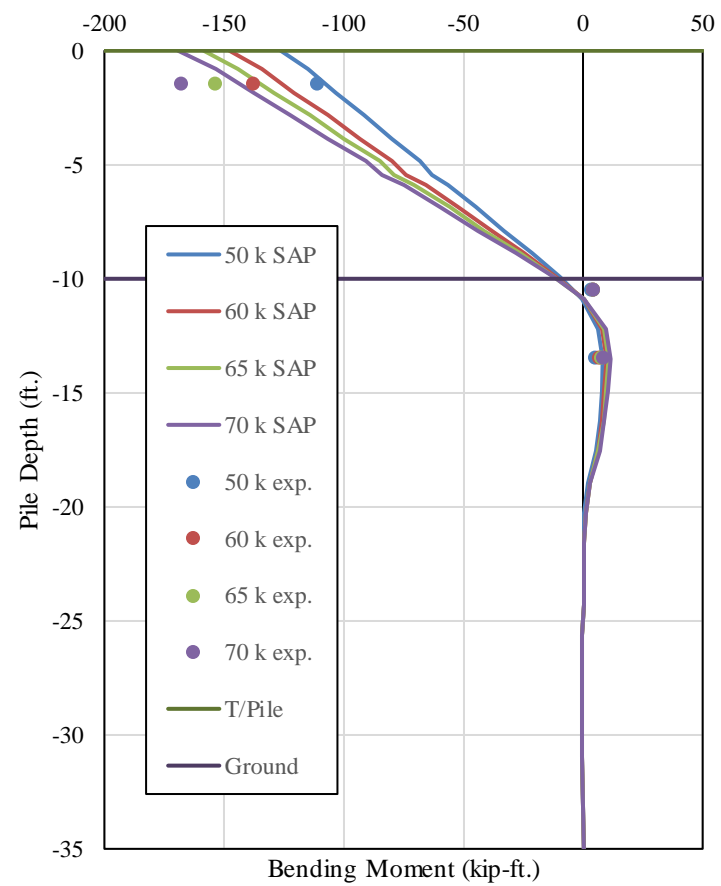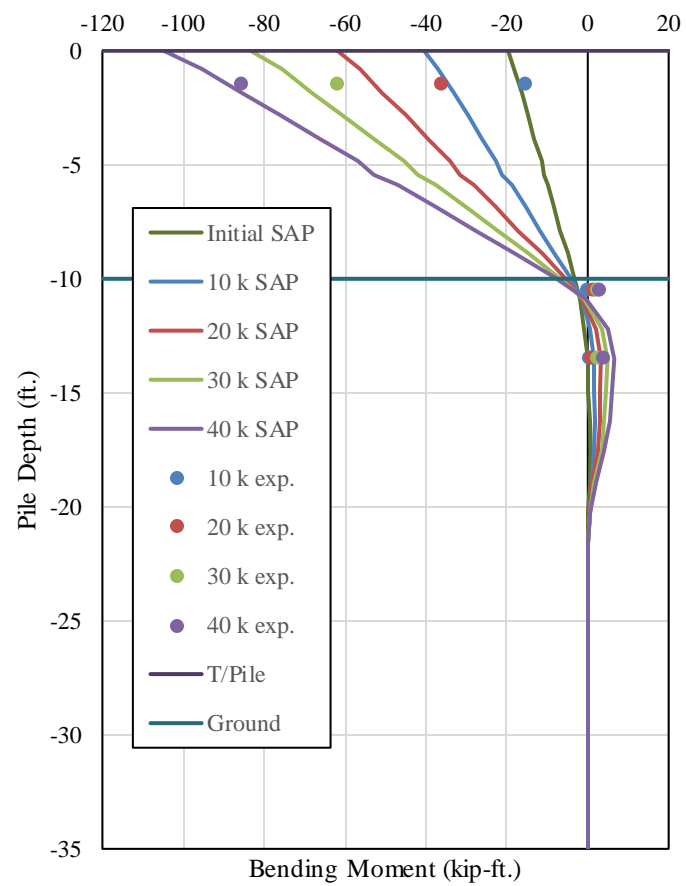
Figure 7-24 Pile 4 Bending Moment Comparisons with Load Truck Centered Over Roadway

221

The results from the load test with the load truck positioned at the edge of the roadway compared to the results from the SAP model can be seen in Figure 7-25 and Figure 7-26. The bending moments from the field tests compared to the bending moments from the SAP model shows the same trend as the previous test with higher predicted moment values from the SAP models with the exception of Pile 4 under higher loading increments. Results from the field test for Pile 1 are not included. Overall the results correlate well between the field test and the SAP model for lower load levels with the results from Pile 4 correlating significantly better at all load levels. The bending moments at instrumented sections were within 10-30 percent of the predicted values from the SAP model. The model predicted higher bending moments in the interior piles with smaller bending moments in the exterior piles. The results from the field test show bending moment values that are relatively similar for each of the piles, with the largest moment values occurring in Pile 4 which is the leading pile.

Figure 7-25 Pile 1 & 2 Bending Moment Comparisons with Load Truck Positioned at Edge of Roadway

223

Figure 7-26 Pile 3 & 4 Bending Moment Comparisons with Truck Positioned at Edge of Roadway

224

Axial forces versus lateral load for each of the piles under the lateral load cases are shown in Figure 7-27 through Figure 7-30. Similarly to the axial forces plotted for the first Macon County test, the axial forces reported below are from the cases in which the lateral load was only applied. The self-weight of the structure and the wheel loads from the truck are not included in these plots. The axial forces are similar to the results from the model from the test without the bridge deck. The magnitudes of the axial forces are roughly 80 percent of the axial forces from the test without the bridge deck. This 20 percent loss can be attributed to a portion of the lateral load being transferred to other structural elements in the bridge. The overall bent behavior is consistent with the model from the first test with the exterior battered piles carrying larger axial forces than the interior vertical piles and the leading pile carrying a compressive axial force and the trailing pile having a tensile axial force. Similar to the load deflection response for the bent, the axial force appears to increase linearly with applied lateral force. This linear trend is due to no geometric or material non-linearity being specified within the model.
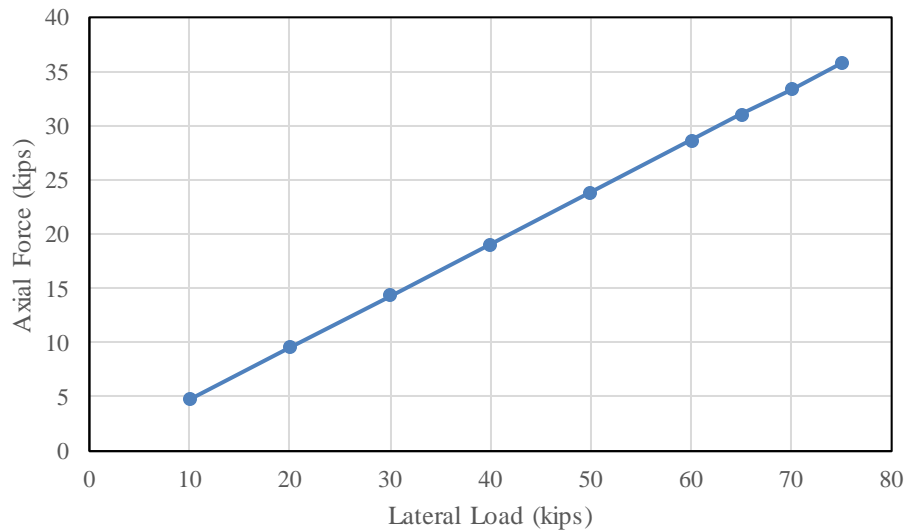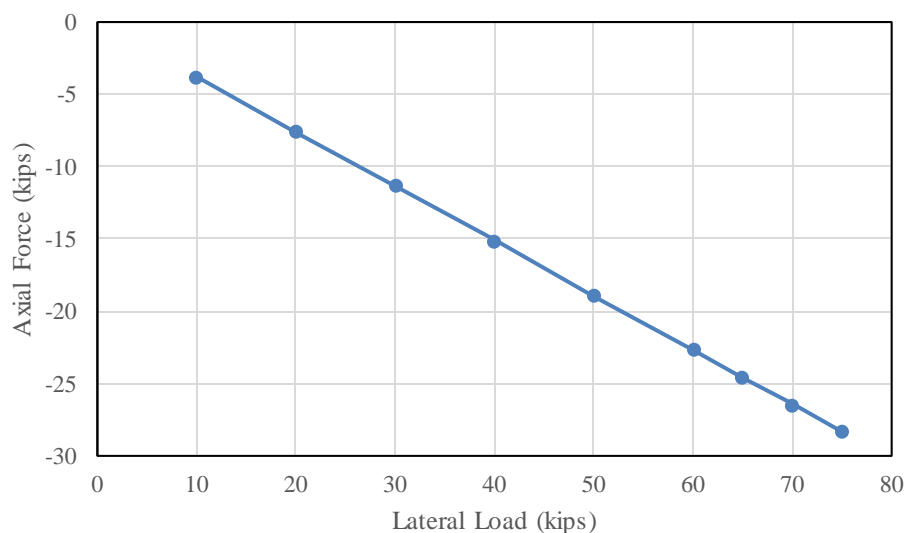

Figure 7-27 Pile 1 Axial Force versus Lateral Load
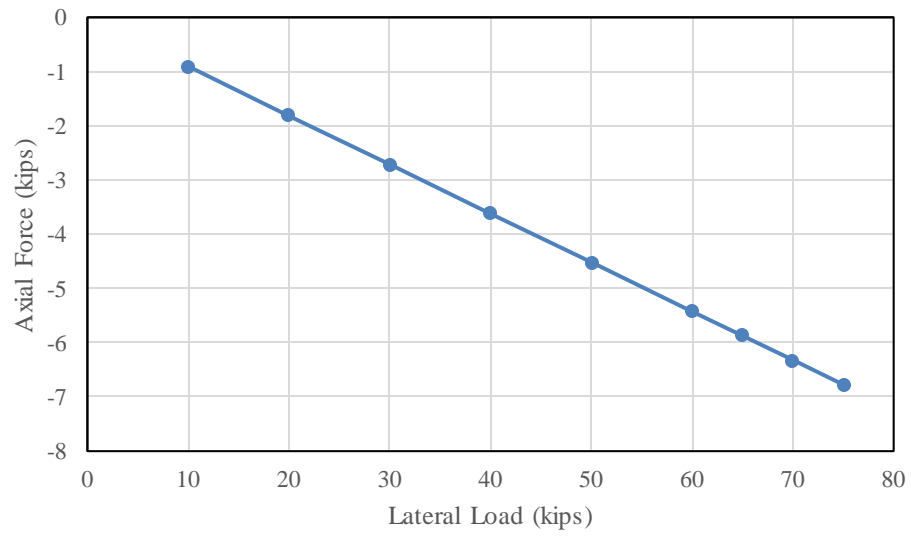
Figure 7-28 Pile 2 Axial Force versus Lateral Load
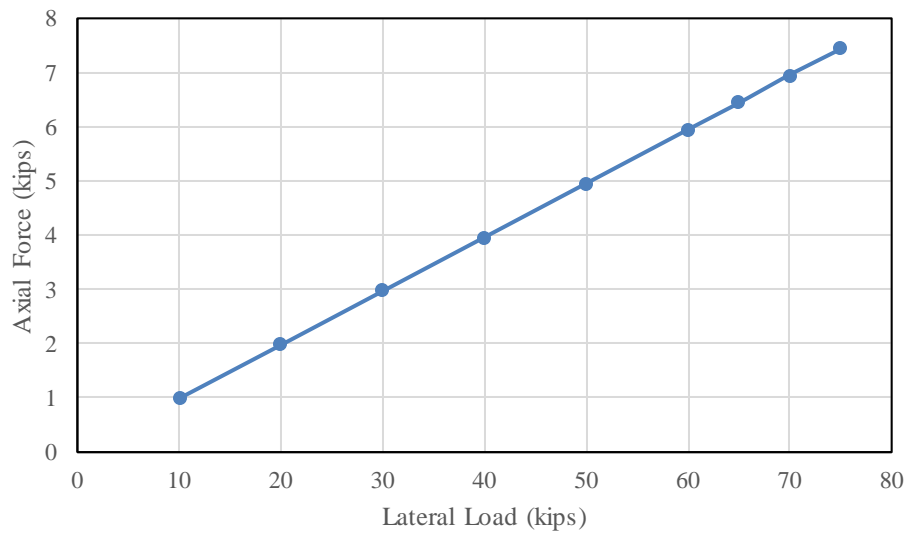

Figure 7-29 Pile 3 Axial Force versus Lateral Load
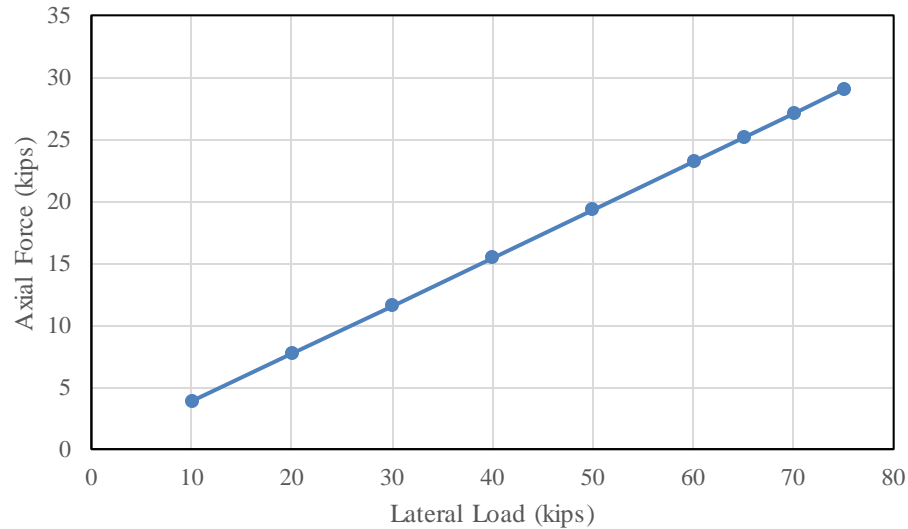
Figure 7-30 Pile 4 Axial Force versus Lateral Load

The objective of the SAP model was to provide a correlation to the field results in terms of

bent deflection. With the addition of the springs at the face of the bent cap, the deflection of the

bent in the SAP model was 0.105 in. at the 60 kip loading increment with gravity loading

simulating the condition without the load truck. The average deflection of the bent from the field

test under these same loading conditions was 0.102 in., varying 3 percent from the predicted SAP

deflection. The deflections from the field tests appear to be linear with the respect to applied load

as shown in Figure 7-31; however the increase in deflection does not seem to begin until the 20

kip loading increment. The slopes of the load-deflection diagrams shown in Figure 7-31 appear

to be very similar indicating the stiffness approximated in the model correlates well with the

actual stiffness of the bent during the load tests. The SAP model predicts a linear load-deflection

response which is to be expected. Notably, the deflections predicted by the SAP model do not

vary significantly from the loading condition without the truck and with the truck centered over

the roadway. However, the deflections are slightly smaller, roughly 5 percent, in the loading

condition with the truck positioned at the edge of the roadway compared to the other two

227

loadings. The deflections from the field test were 10-15 percent greater in the test without the

load truck compared to the both of the test with the load truck. These lateral deflections, however

are very small in terms of the overall clear height of the bent, resulting in a ratio of nearly h/1200

if the clear height of the bent excluding the rip-rap is used.
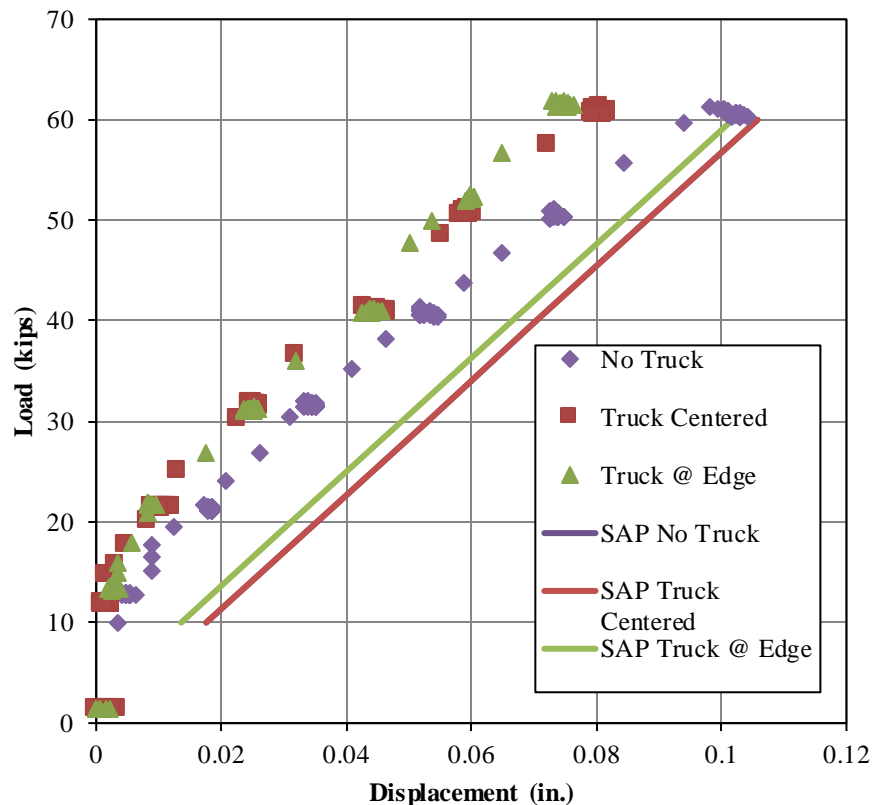
Figure 7-31 Load-Deflection Comparisons of Macon County Bent with Bridge Deck

7.6.3 US 331 Test

Bending moments and deflections from the US 331 test are compared to moments and

deflections from the SAP model in this section. A number of uncertainties existed with the US

331 bent that made modeling the bent to simulate its behavior during the field tests fairly

challenging. The most significant uncertainties were material properties of the concrete used in

the encasements and bent cap and the level of additional lateral stiffness provided by the bridge superstructure during the load tests. An assumption had to be made regarding the concrete strengths of the encasements and the bent cap in order to approximate the modulus of elasticity to use for the materials of the frame elements in the structural model. A concrete strength of 5,000 psi was determined to be acceptable for the encasements and the bent cap. The modulus of elasticity of the concrete was approximated using the empirical formula.

The additional lateral stiffness of the bridge superstructure and the simulation of load being transferred to the adjacent bents needed to be accounted for in the model. An approach similar to the one used for the Macon County bent was not used for the US 331 bent due to a lack of field test load-deflection data for the bent without the deck in place. No additional means of lateral stiffness were applied to the bent the take into the account the stiffness of the deck. However, it was decided to perform a displacement-controlled analysis in SAP to determine the correlation between the forces and moments from the model to the results obtained from the field tests. Non-linear load cases for each lateral load increment were created, and a limiting displacement was added to the node at the face of the bent cap in which deflections were measured in the field test. This non-linear load cases was used in load combinations including the self-weight and wheel loads from the truck, similar to the Macon County bent model. Arbitrary lateral loads had to be applied corresponding to each of the non-linear load cases; however, the displacement at the controlled node would be limited to the specified displacement in the load case. The average displacements at each load increment from each of the two field tests were used as the control displacements. The displacement increments are still referred to by the loading increment naming convention from Chapter 5.

Bending moment comparisons of the test with the load truck positioned over the edge of the roadway and the SAP model are shown in Figure 7-32 through Figure 7-37. The initial moment diagram from the SAP model represents the condition with just the load truck on the bridge. The shape of the moment diagram above ground varies from the exterior piles to the interior piles. The slope of the moment diagram in each of the interior piles is linear at higher lateral load levels (above 30 kips). The slope of the moment diagram for Pile 1 from the SAP model is concave up above ground and concave down for Pile 6. A kink in the moment diagram from the SAP models occurs below ground at each of the locations where springs are applied beginning at a depth of 14 feet below the top of the pile. The kink in the moment diagram appears to be dependent on the soil reactions at each of these spring locations. For every pile with the exception of Pile 5, the SAP model predicted higher moments at the location six inches below the bottom of the cap and the inflection point of the piles appears to be shifted down in the SAP model.

In each of the piles, the values of moment are positive at low load increments and begin to increase negatively as the magnitude of the applied lateral displacement increases. The transition from positive to negative bending moment is due to the gravity load applied to the bent and the location at which the load is applied. The truck is positioned over the piles expected to be in axial compression due to lateral load effect, therefore the magnitude of lateral load resulting in a transition from positive to negative bending moment is higher. The results from the field test appear to exhibit this behavior, but other than Pile 6, the initial positive moment values are significantly less than the predicted values from the SAP model. As a result, the maximum negative moments at larger applied lateral displacements are less than the moments calculated from the field tests.

230
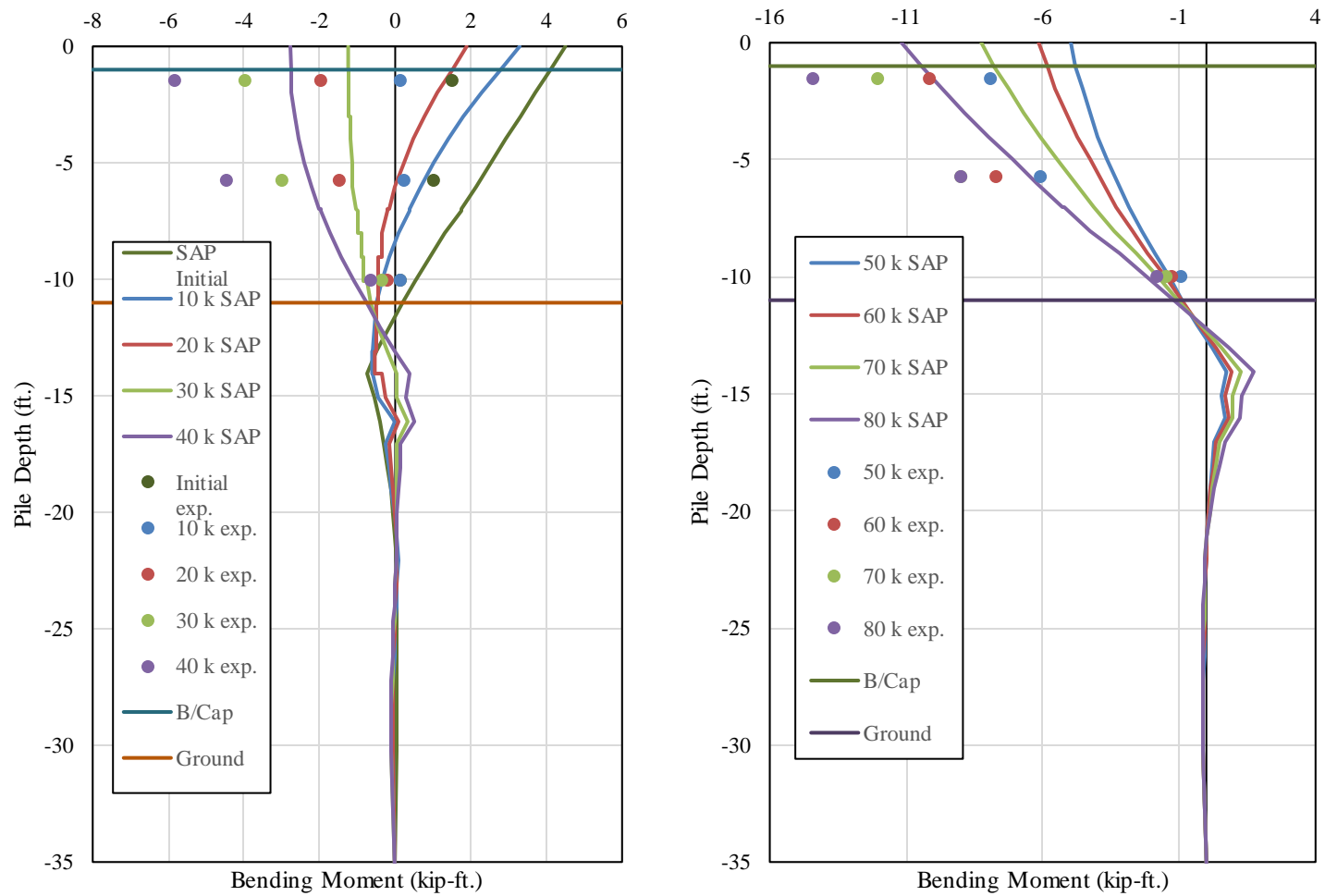
Figure 7-32 Pile 1 Bending Moment Comparisons with Truck at Edge of Roadway

231
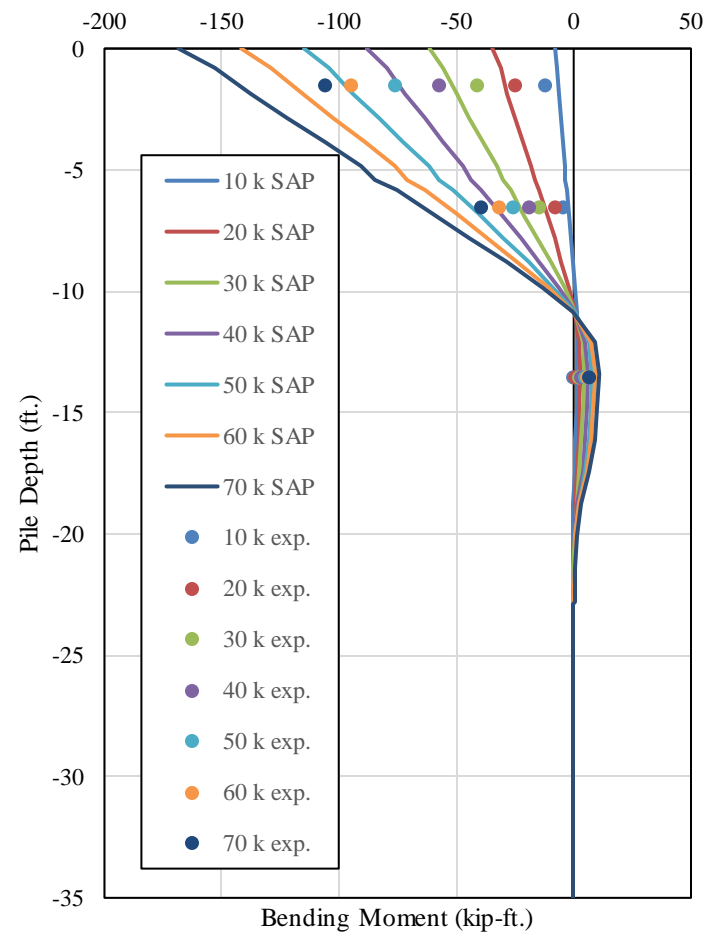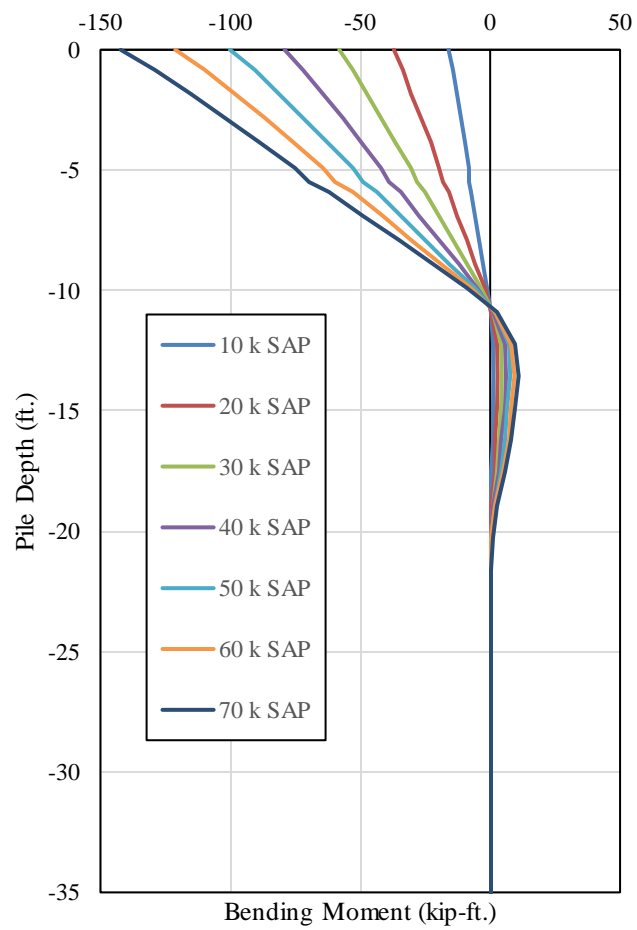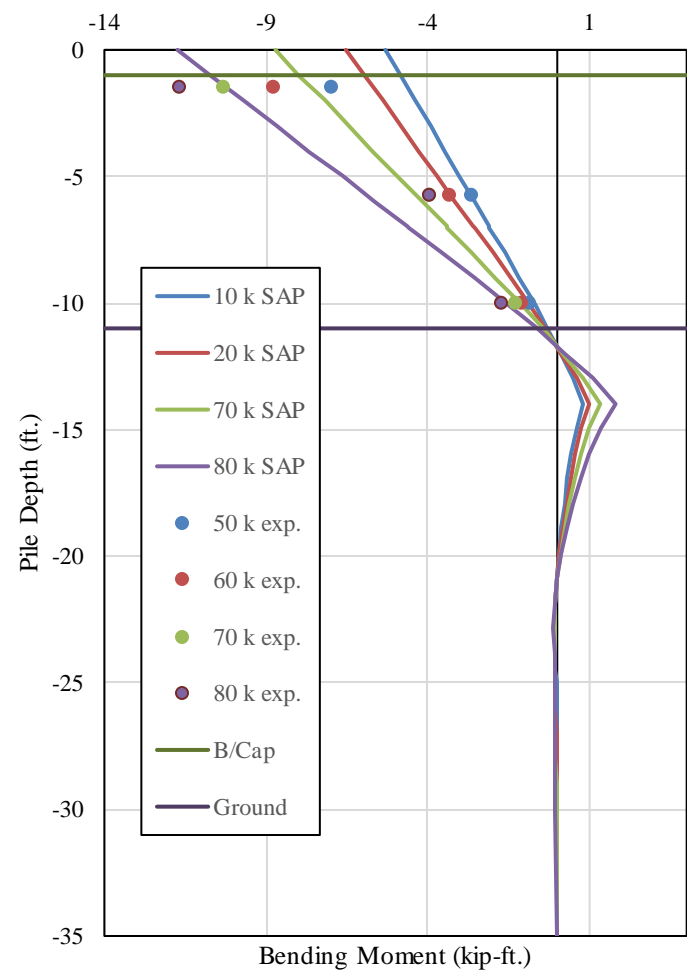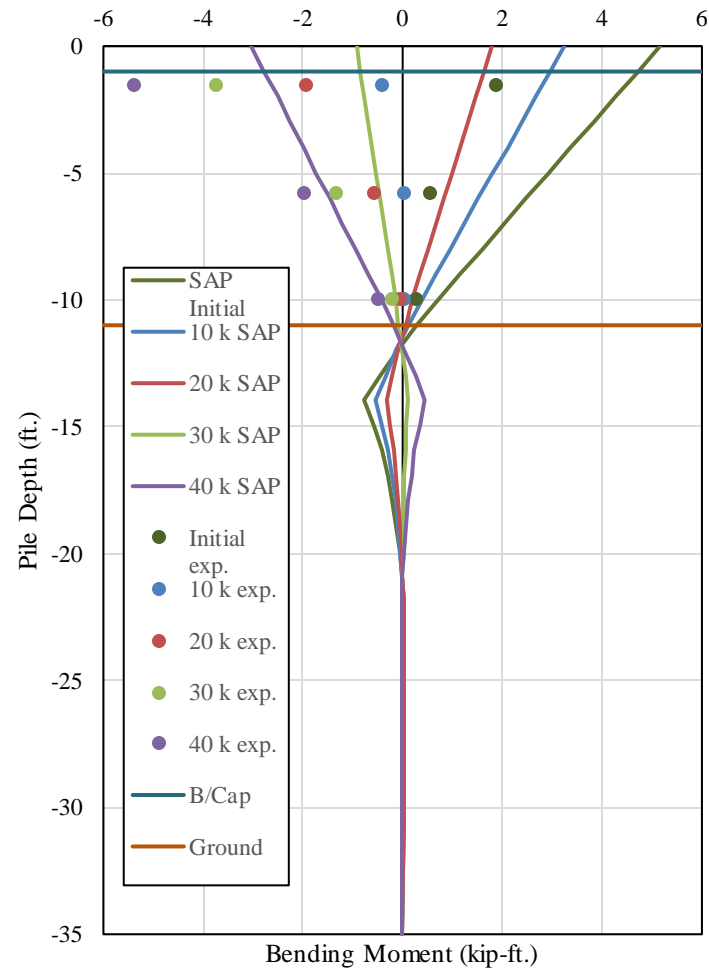
Figure 7-33 Pile 2 Bending Moment Comparisons with Truck at Edge of Roadway
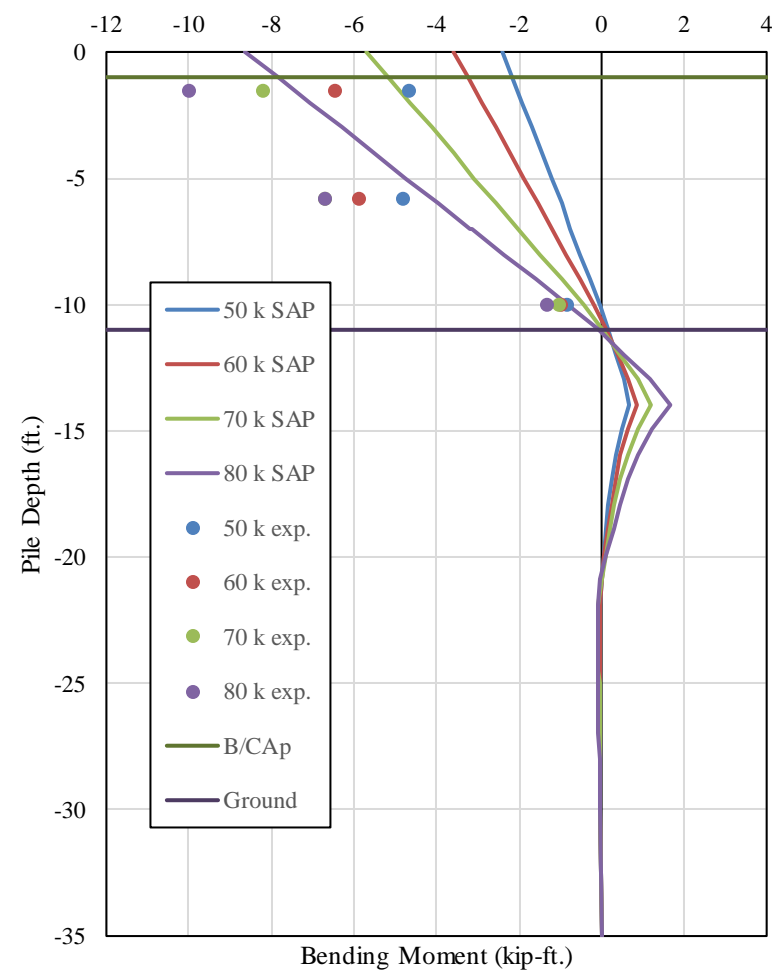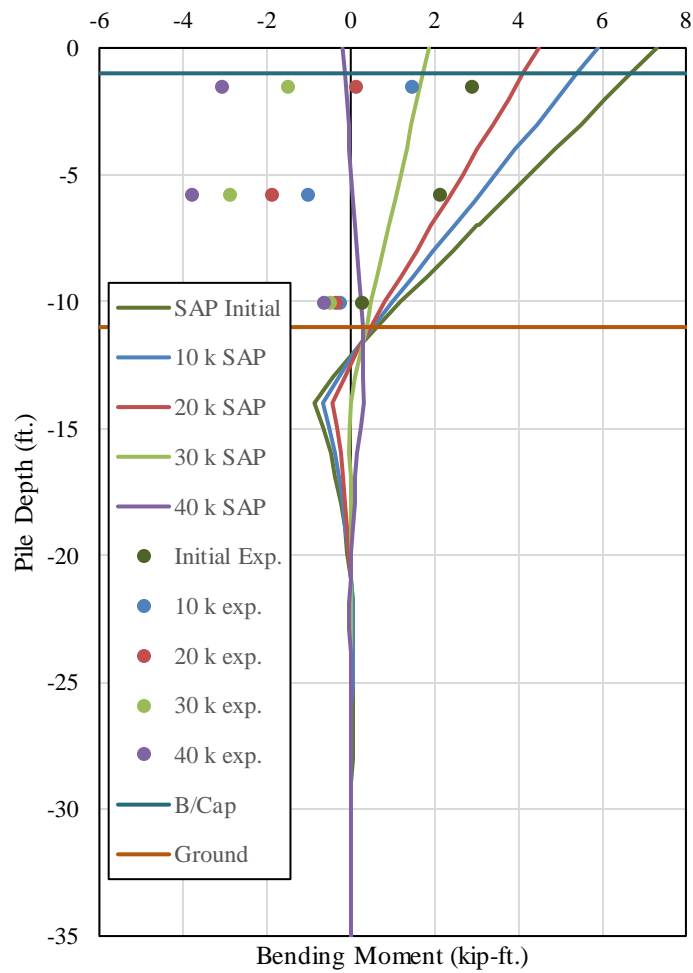
Figure 7-34 Pile 3 Bending Moment Comparisons with Truck at Edge of Roadway

233
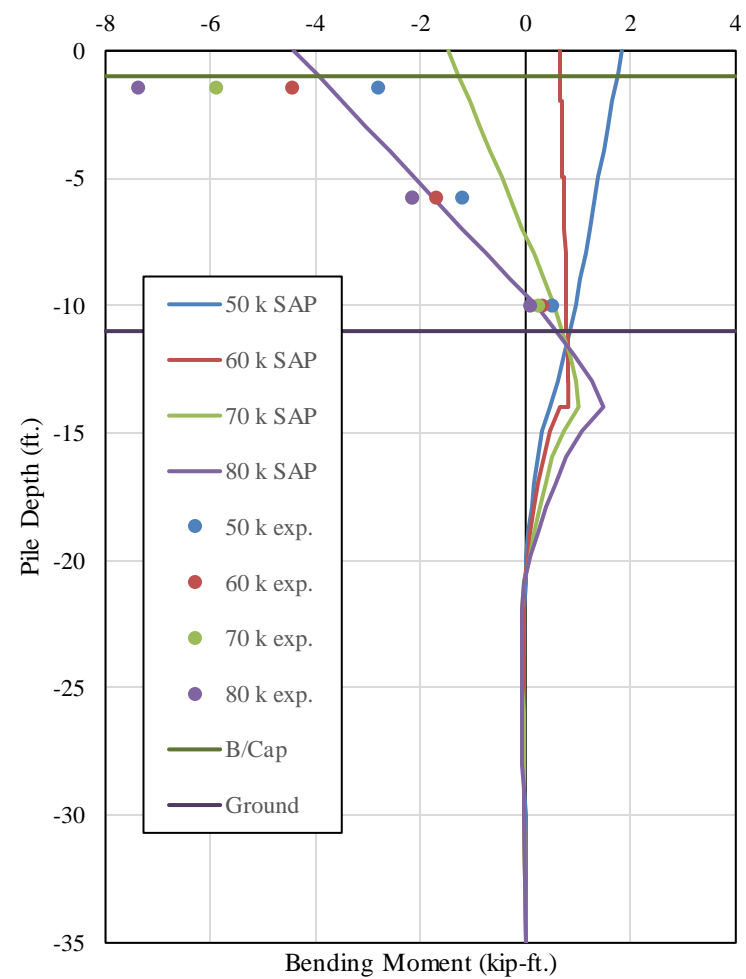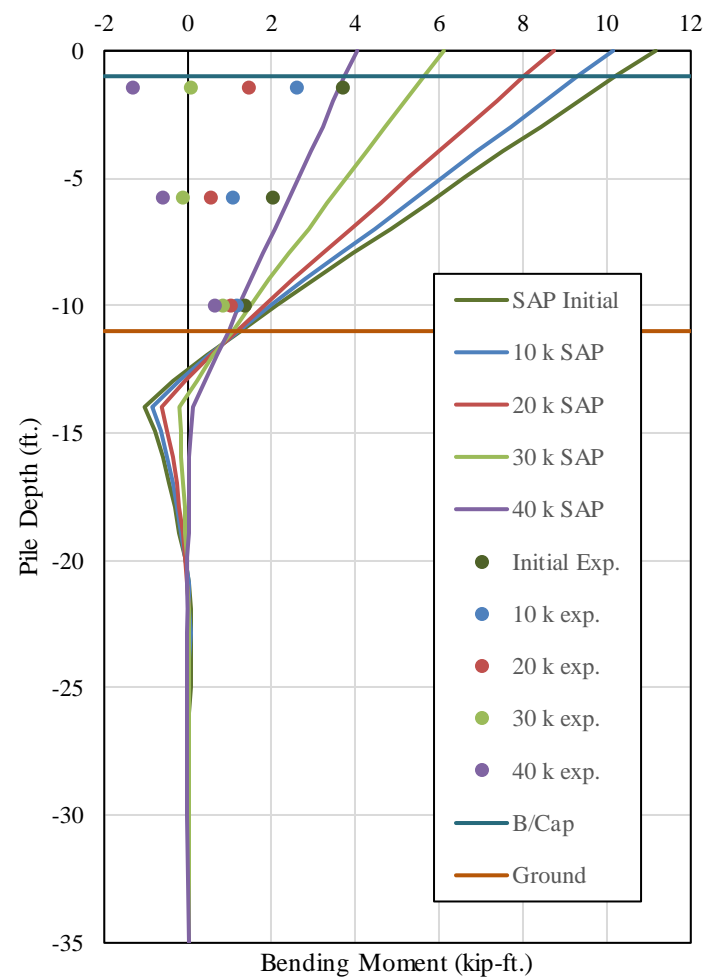
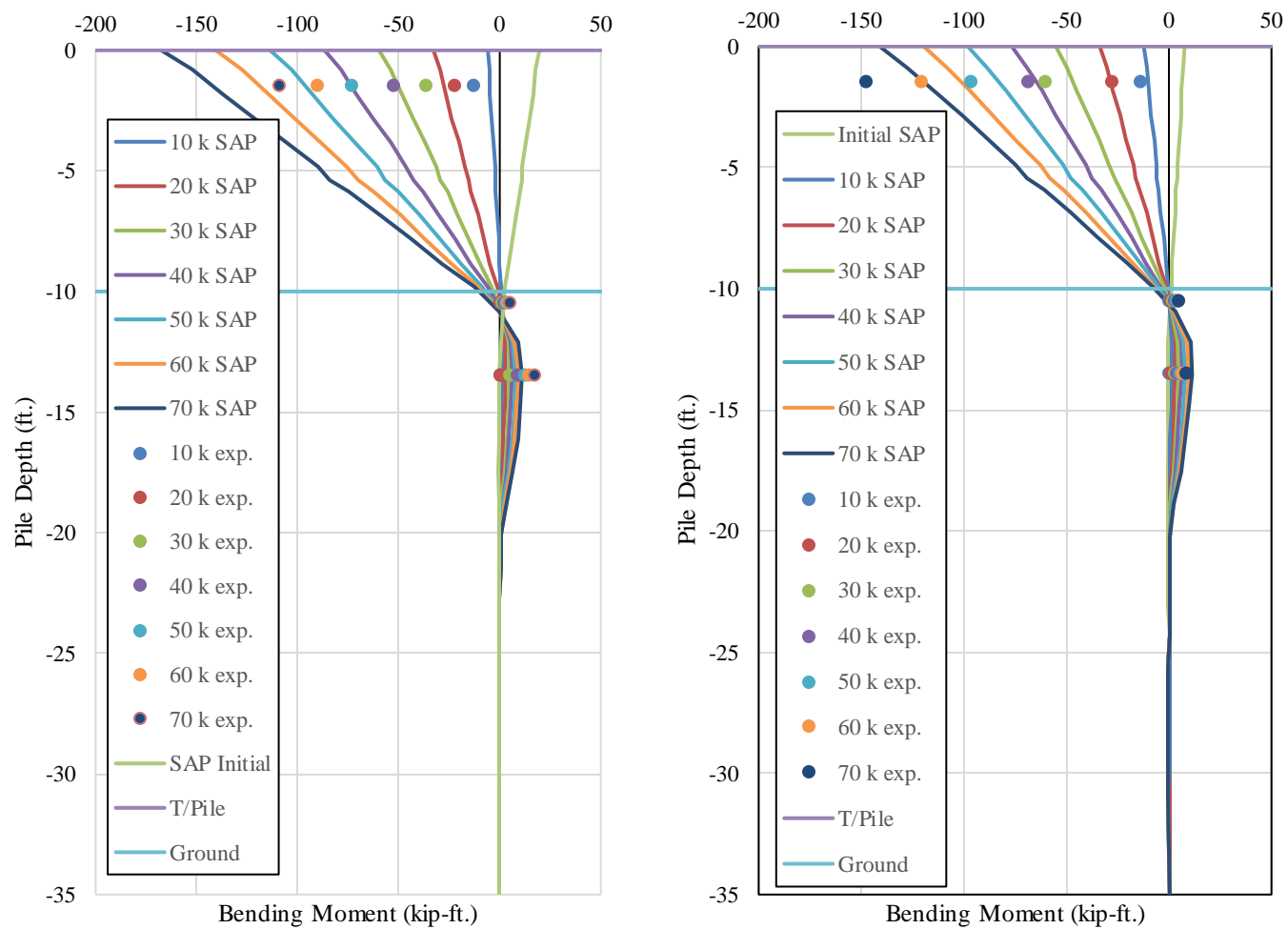**Figure 7-35 Pile 4 Bending Moment Comparisons with Truck at Edge of Roadway**

234
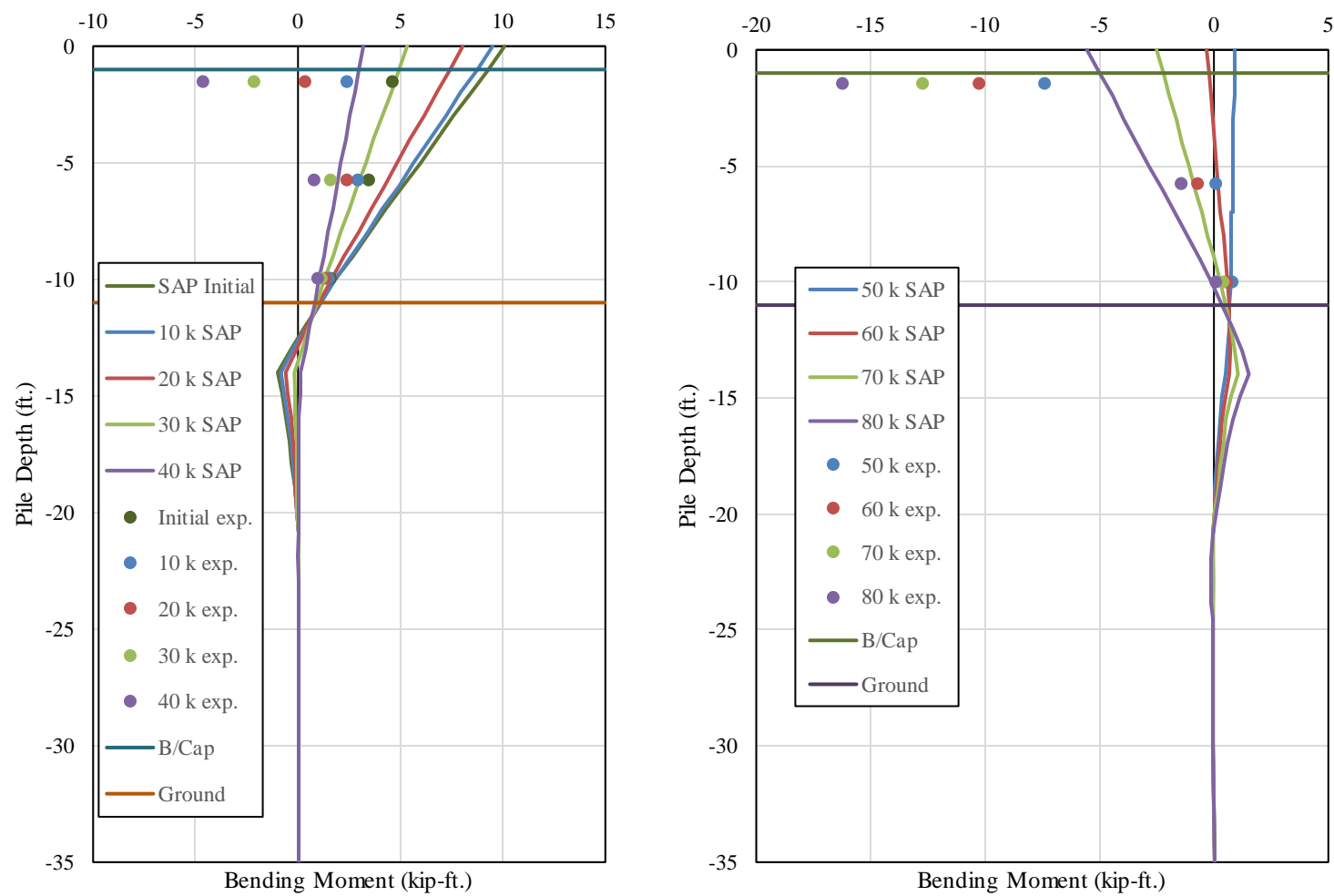
Figure 7-36 Pile 5 Bending Moment Comparisons with Truck at Edge of Roadway
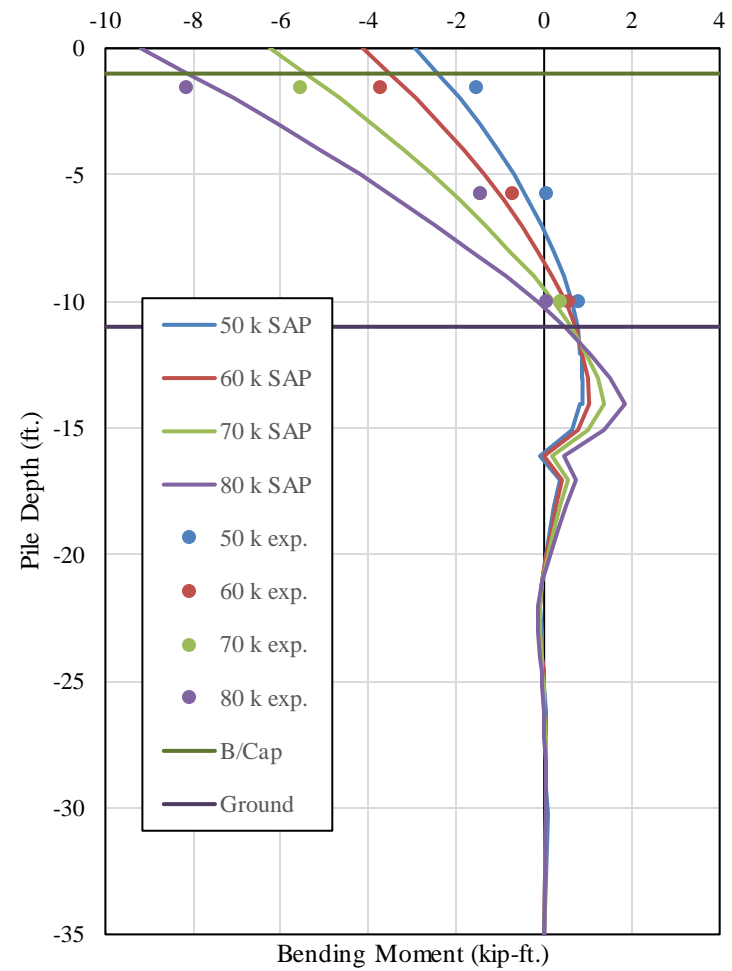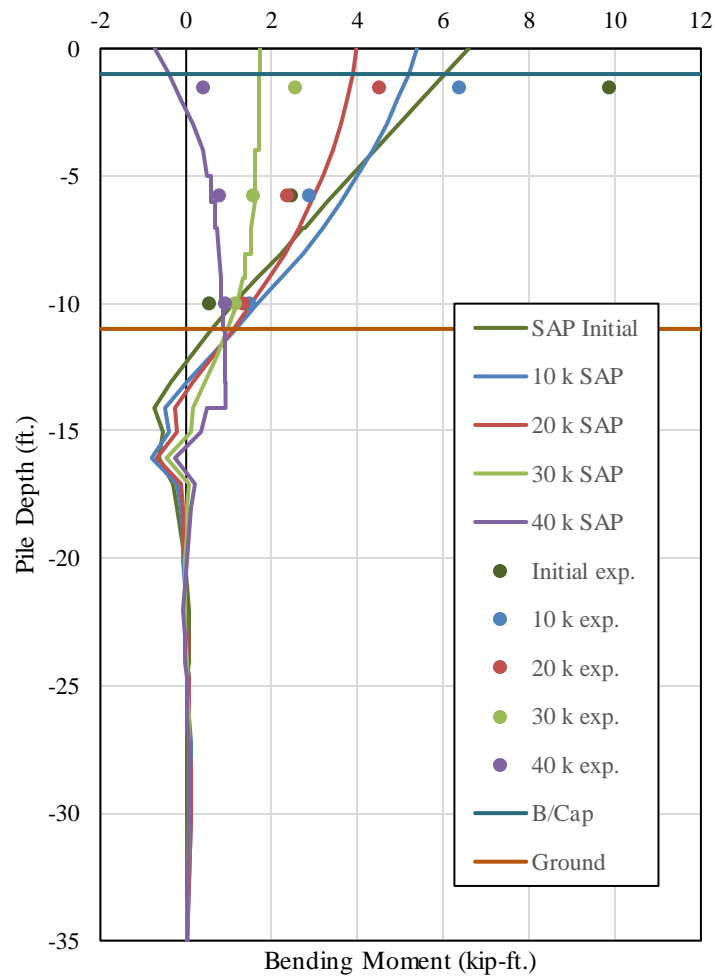
Figure 7-37 Pile 6 Bending Moment Comparisons with Truck at Edge of Roadway

236

The bending moments from the SAP model are compared to the results from the field test without the load truck in Figure 7-38 through Figure 7-43. The slope of the moment diagrams in the exterior piles in the SAP model was similar to the moment diagrams from the loading condition with the load truck at the edge of the roadway. For each of the piles, the maximum bending moment increases negatively as the magnitude of the applied lateral load increases. The kink in the moment diagrams in the SAP model at the spring locations occurs in this loading condition as well. Overall, the SAP model again predicted higher bending moments than the results from the field test at each of the instrumented locations, and the location of the inflection point appears to be higher in the field test results. The maximum bending moments predicted by the SAP model at the highest instrumented location ranged between 16-18 kip-ft. for the six piles in the bent compared to an average of 12-14 kip-ft. from the field test results.
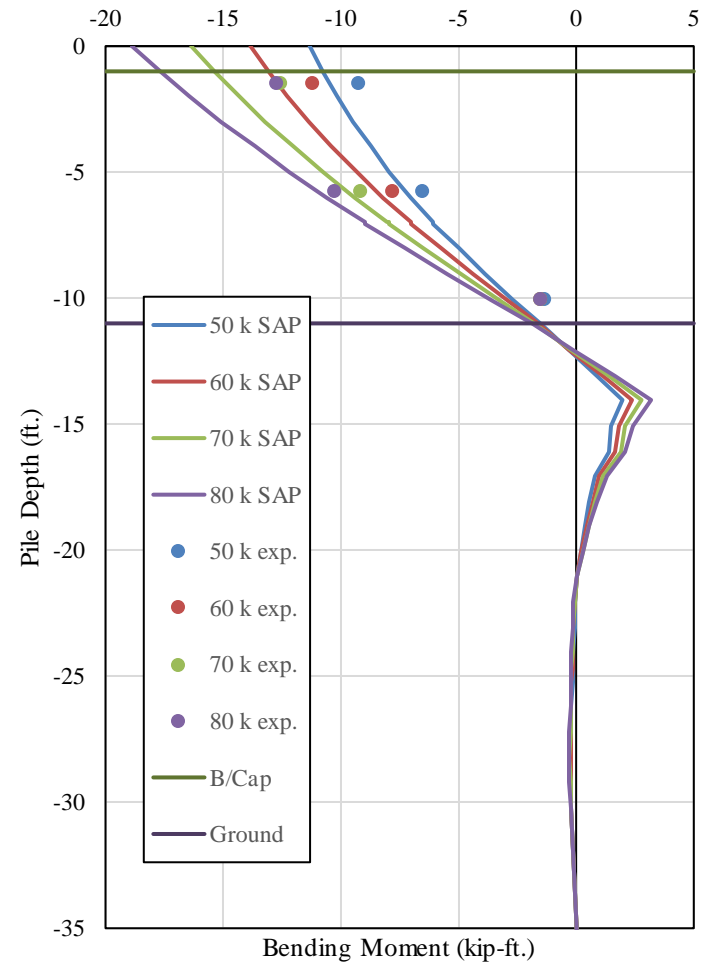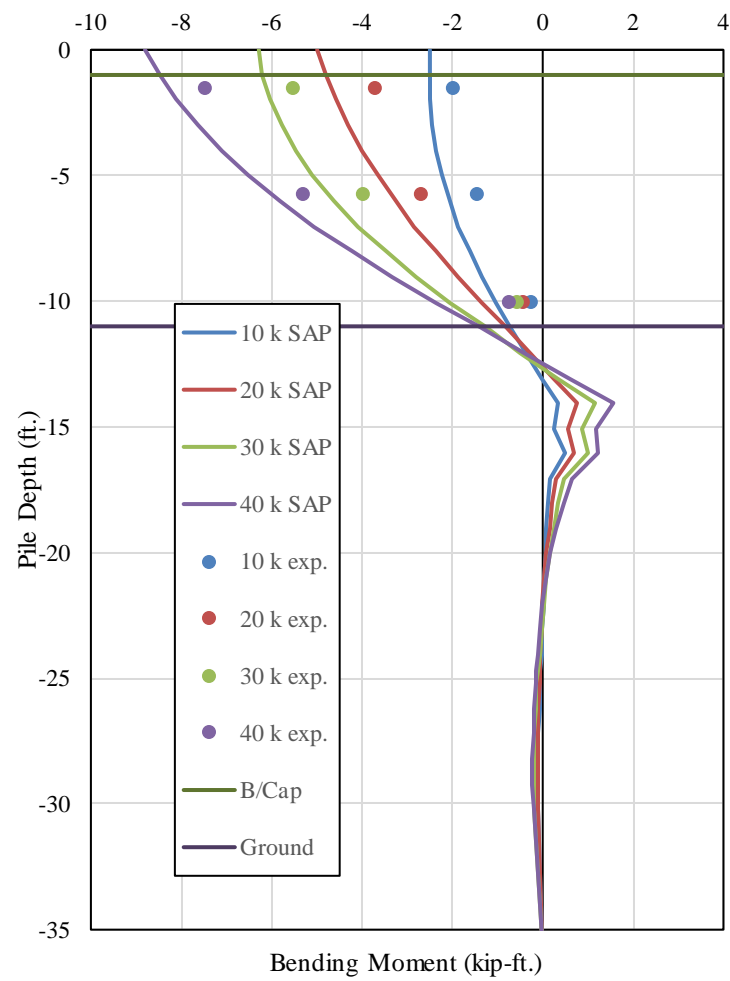
Figure 7-38 Pile 1 Bending Moment Comparisons with no Load Truck

238
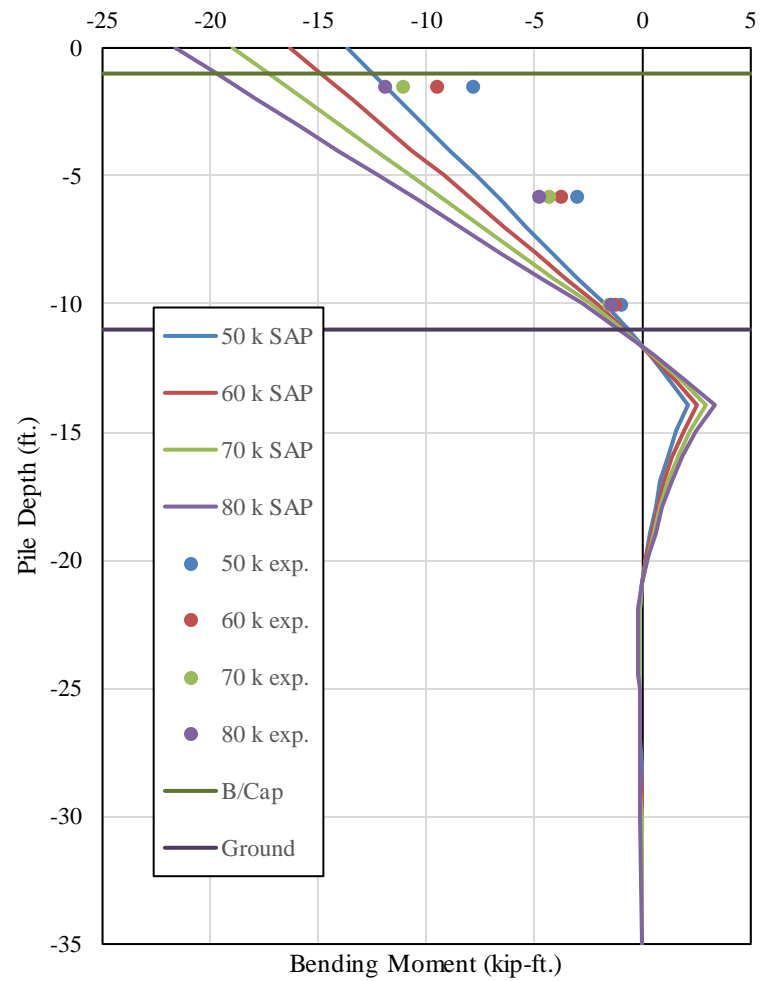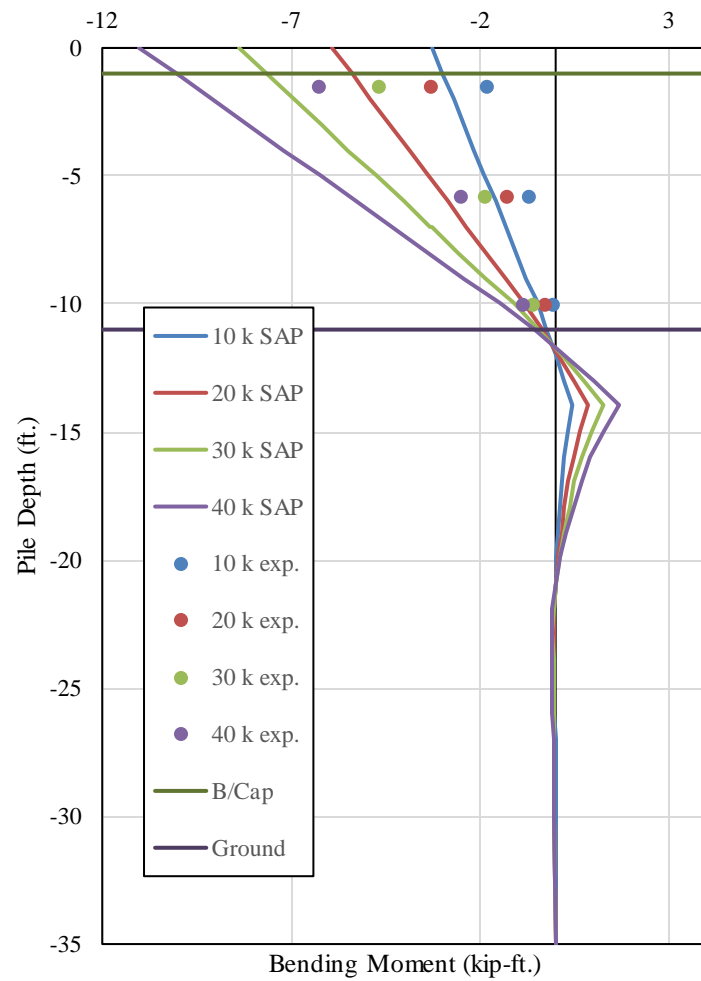
Figure 7-39 Pile 2 Bending Moment Comparisons with no Load Truck

239
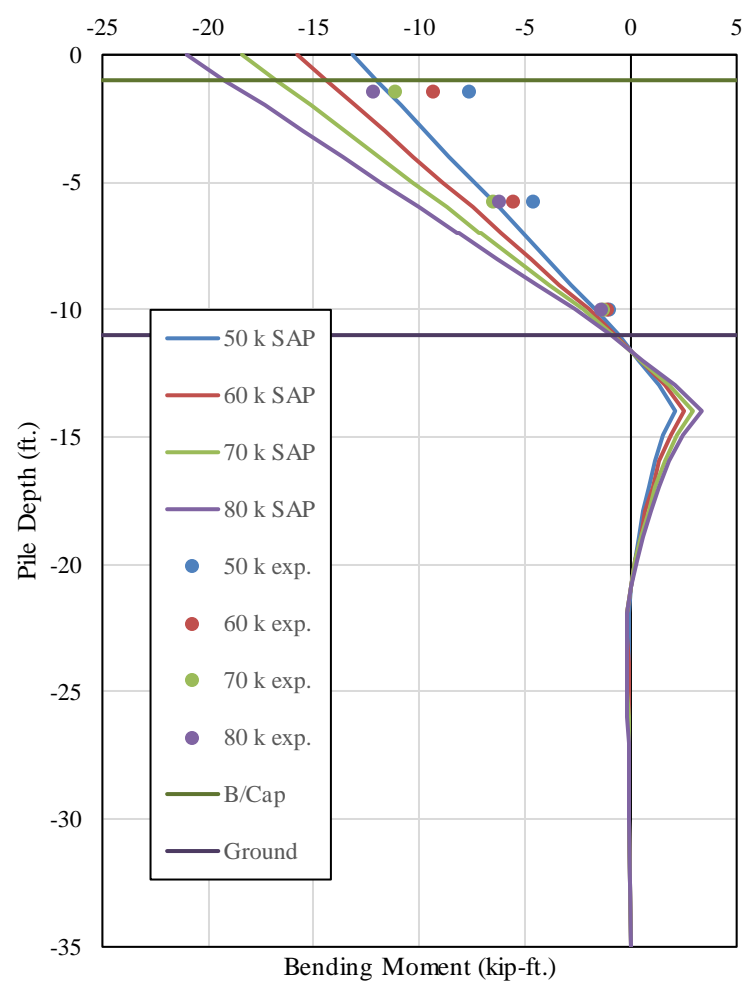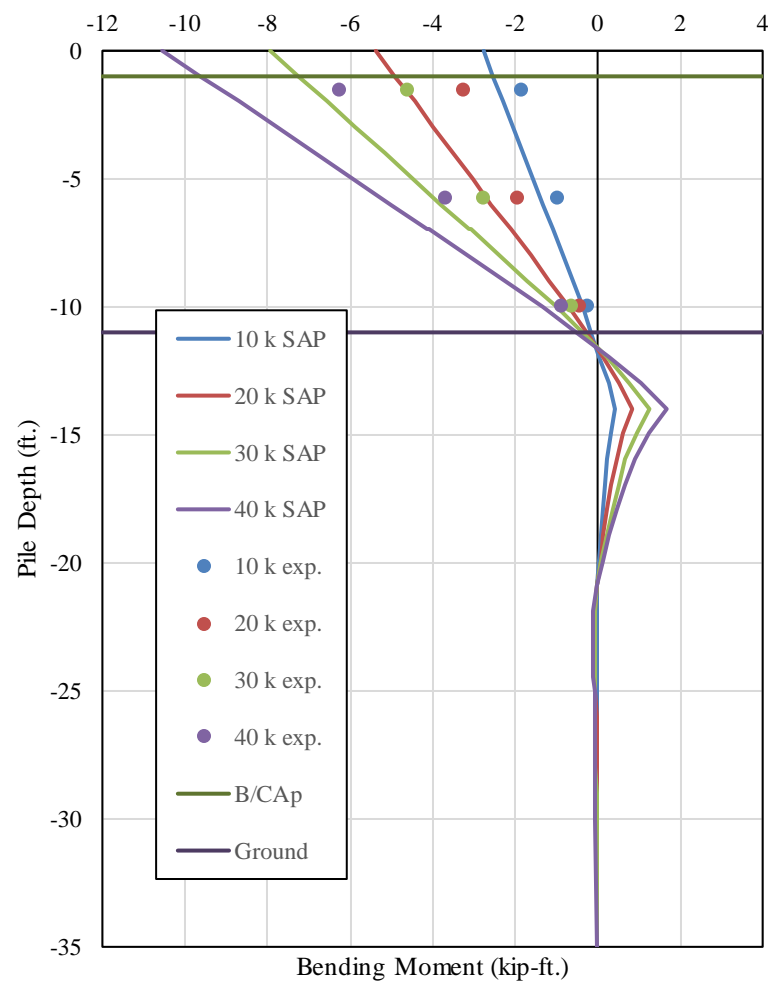
Figure 7-40 Pile 3 Bending Moment Comparisons with no Load Truck

240
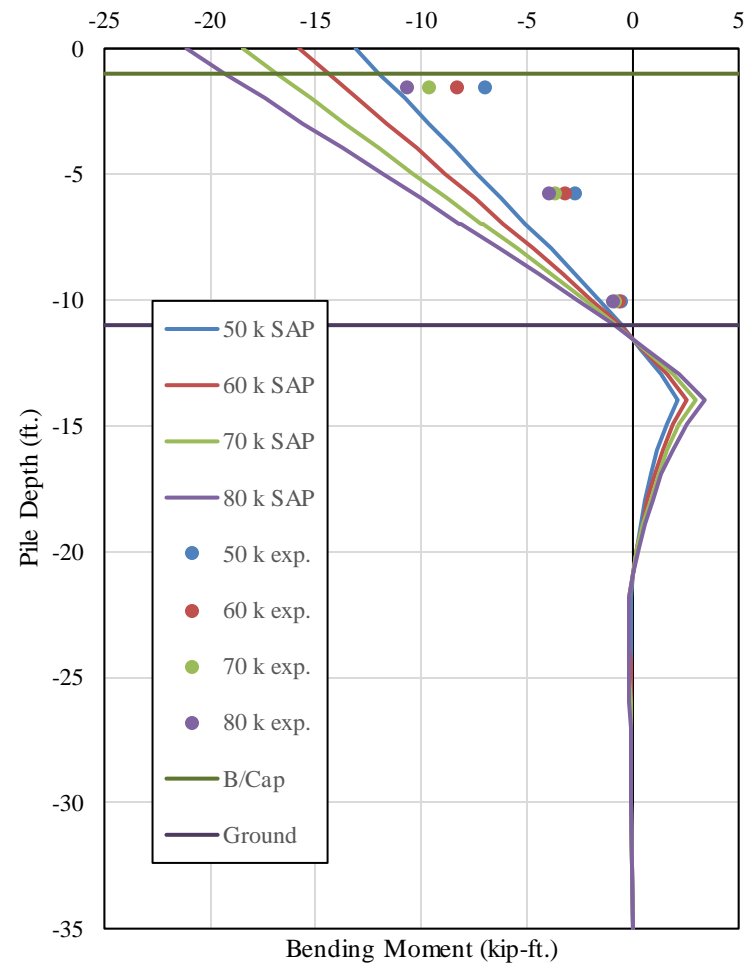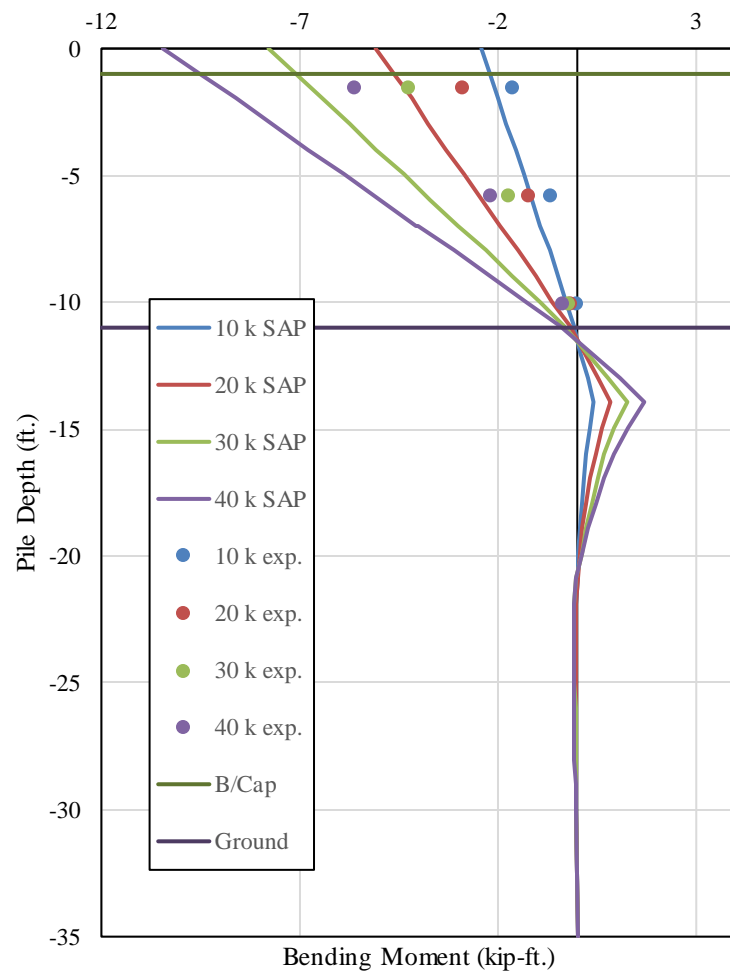
Figure 7-41 Pile 4 Bending Moment Comparisons with no Load Truck

241
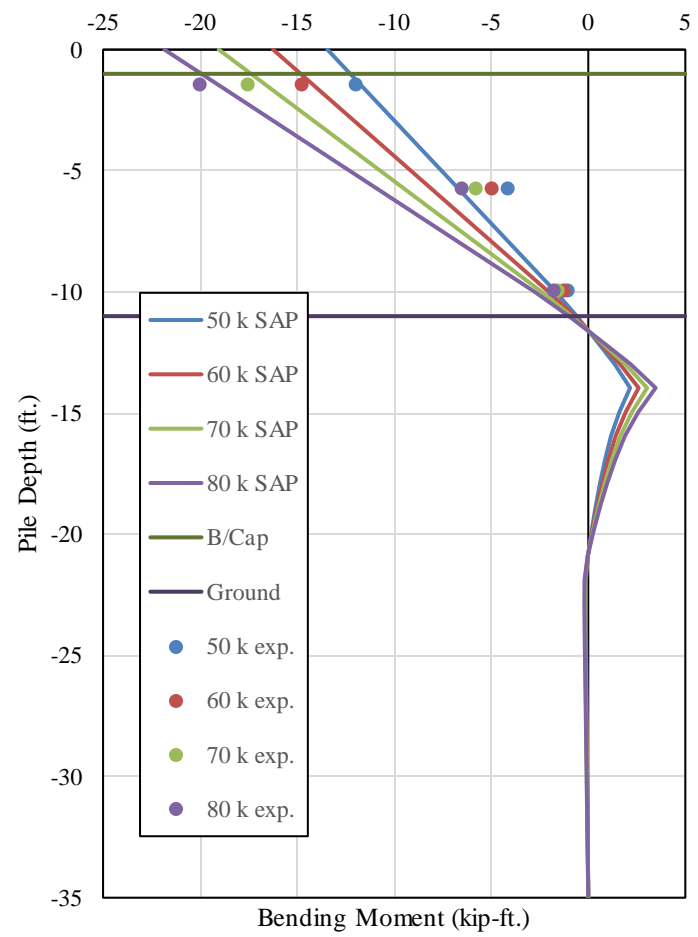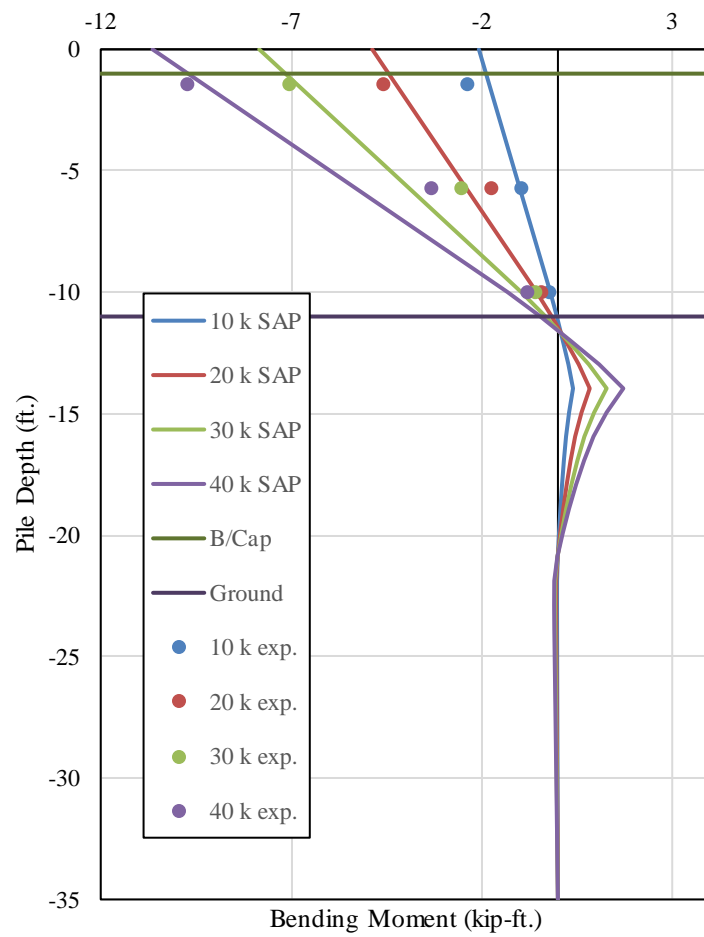
Figure 7-42 Pile 5 Bending Moment Comparisons with no Load Truck

242
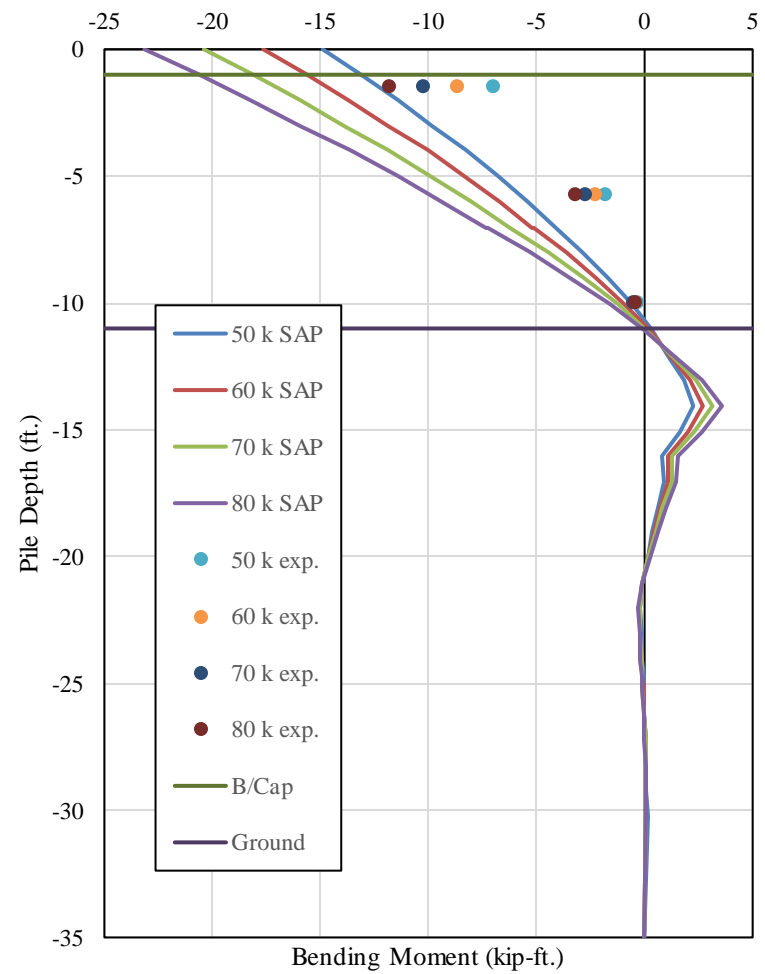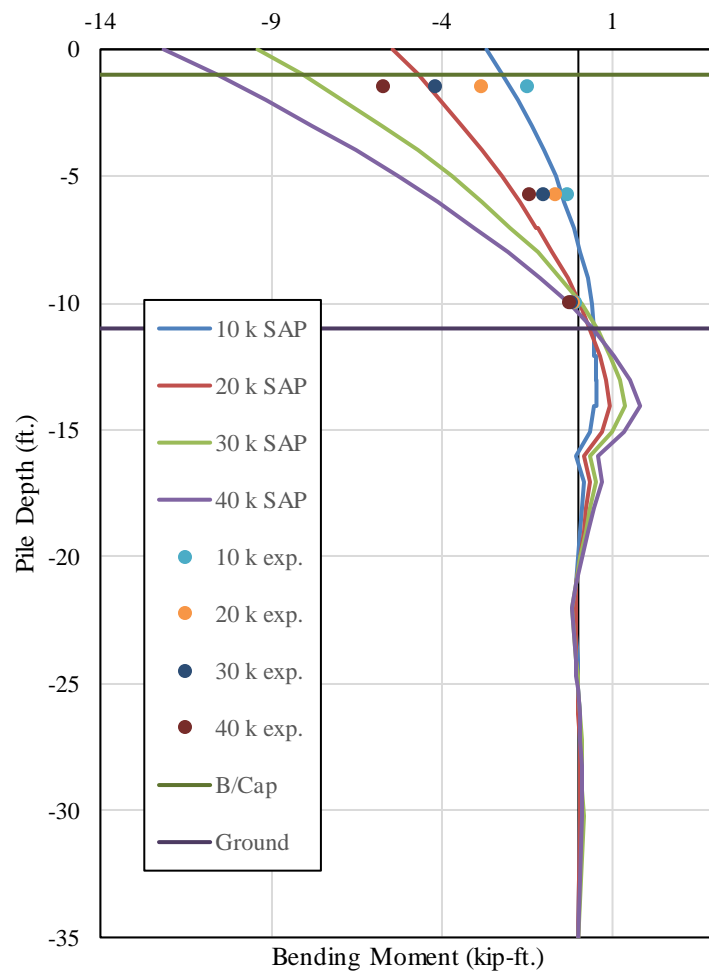
Figure 7-43 Pile 6 Bending Moment Comparisons with no Load Truck

243

Axial forces versus applied lateral load for each of the six piles are shown in Figure 7-44 through Figure 7-49. The axial forces computed from measured strains during the load test without the load truck are shown in these figures as well. The forces from the SAP model are the forces corresponding to only the lateral load being applied without the addition of the self-weight of the structure. The model and the field test results indicate that the exterior battered piles have the largest axial forces with the leading pile in axial compression and the trailing pile in axial tension. Notably, the axial force is plotted versus lateral load for the model forces, when in actuality a lateral displacement corresponding to the lateral load measured from the field tests was applied. The lateral displacements that were applied to the bent were not perfectly linear; therefore the axial force does not increase linearly with applied displacements. The model predicted much lower axial forces than were calculated from the measured strains during the field tests. The large axial forces can be attributed to the large cross sectional area of the composite pile section. With a large cross-sectional area, small changes in strains can result in large changes in the axial force computed on the cross section. In terms of the cross-sectional area of the section, the axial forces computed from the measured strains in the field test are seemingly negligible. Overall, the field test results did not correlate well with the predicted axial forces from the SAP model. The leading pile was in compression and the trailing pile was in tension for both the model and the field test results; however, the magnitudes of these forces varied significantly.
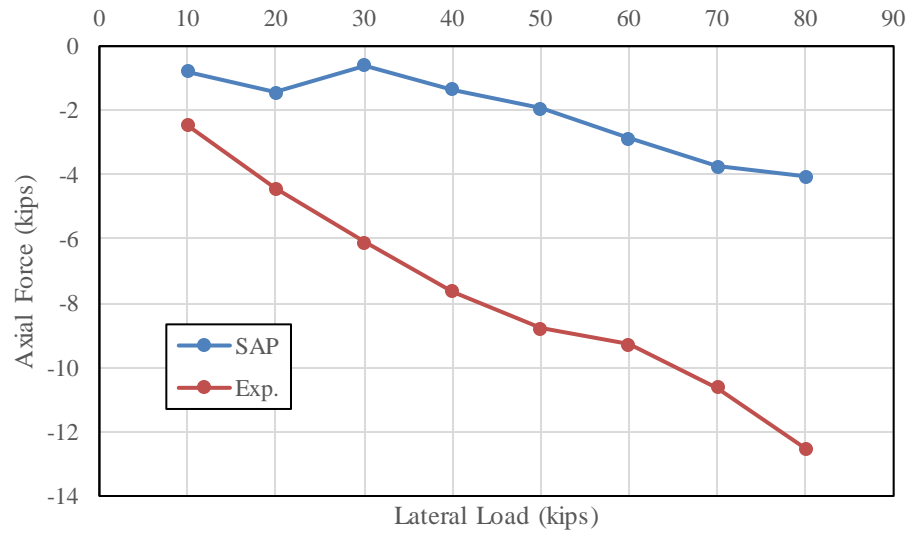
Figure 7-44 Pile 1 Axial Force versus Lateral Load Comparison
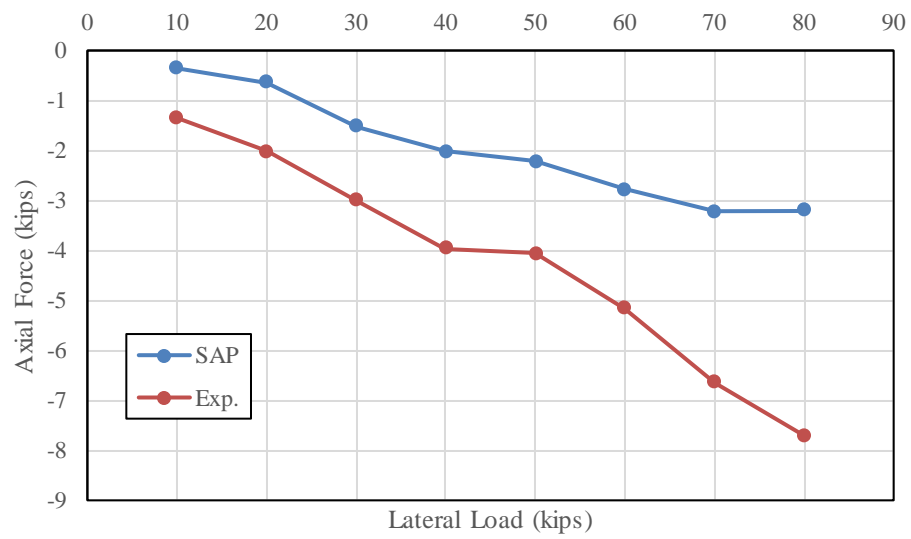
Figure 7-45 Pile 2 Axial Force versus lateral Load Comparison
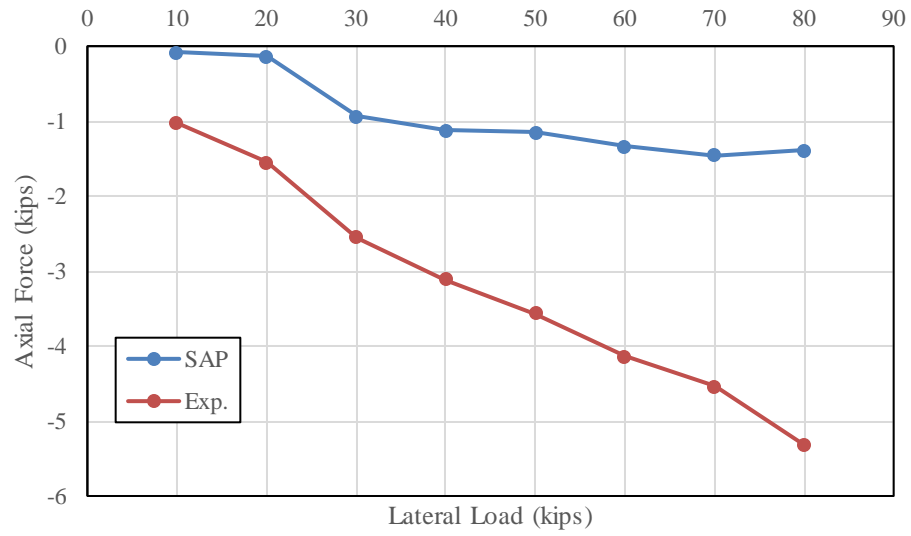
Figure 7-46 Pile 3 Axial Force versus Lateral Load Comparison
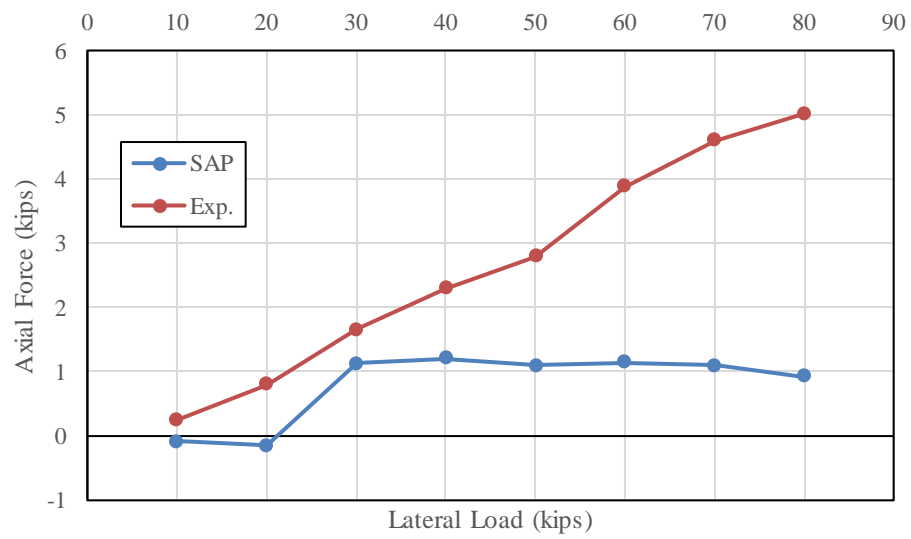
Figure 7-47 Pile 4 Axial Force versus Lateral Load Comparison
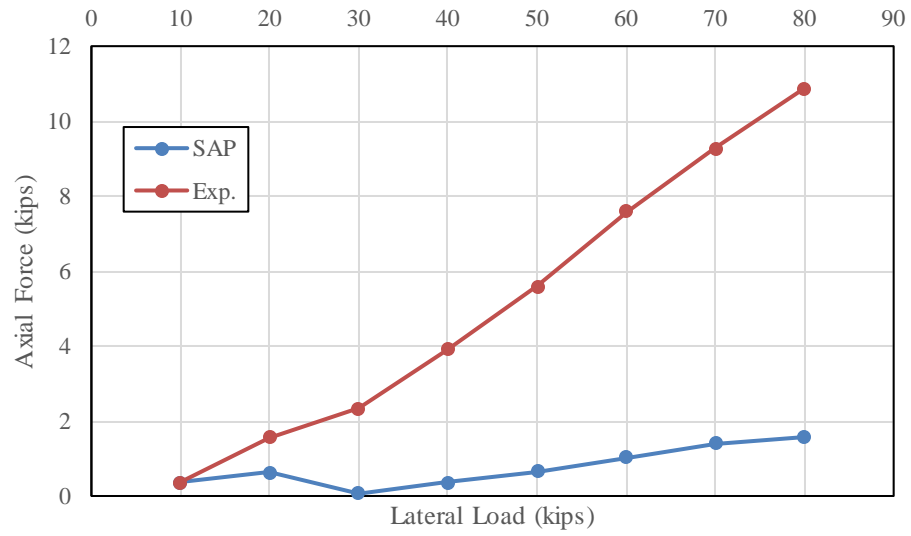
Figure 7-48 Pile 5 Axial Force versus Lateral Load Comparison
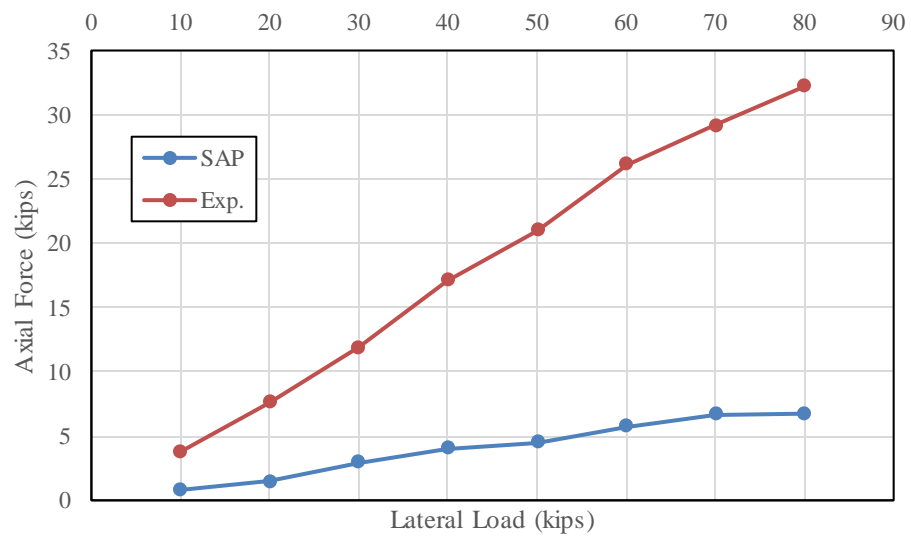
Figure 7-49 Pile 6 Axial Force versus Lateral Load Comparison

Deflections from the SAP model were applied to simulate the lateral load applied in each of the field test. Since these deflections were identical in the SAP model to the measured deflections in the field, they are not presented in this section.

7.7 Chapter Summary

The results from the SAP model created for the Macon County bridge correlated well with the results from the field test without the bridge deck. The model predicted a linear load-deflection response for the duration of the load test with the maximum deflection at the 75 kip varying from the measured deflection by 12%. The model seemed to over predict the magnitude of bending moments when compared to the results from the field test by 10-20 percent. The model clearly predicted that the bending moment dissipates significantly once the pile encasements are terminated, and the values of moment are very small at the below ground locations relative to the moments near the bottom of the cap.

The bridge deck provided an alternate load path in which the lateral loads were transferred to other structural elements in the bridge, most likely the adjacent bents. The transfer of loads into the adjacent bents was accounted for by applying a linear spring to the bent. The magnitude of this spring was determined using measured deflections from previous field tests. In the SAP model, the addition of the load truck had minimal effect on the load-deflection response of the bent, similar to the results from the field tests. The SAP model again over-predicted the values of bending moments at each of the instrumented locations. Overall the results from the field tests seemed to correlate reasonably well with the results from the SAP model.

A displacement-controlled analysis was performed to simulate the lateral load for the US 331 bent model. The measured displacements from the field tests were applied as nodal displacements at the face of the bent cap in order to determine how well the pile forces and moments correlated with the SAP model. For the test in which the load truck was positioned over the edge of the roadway, the bending moments at the top of the piles were positive at low load increments due to the effect of the load truck, and decreased in value becoming more negative as the applied lateral displacements increased. This transition from positive to negative moment

248

was especially apparent in the piles that were closer to the position of the load truck. The moments from the field tests showed the same trend, beginning positive and becoming more negative as the magnitude of the lateral load increased; however, the positive moment at lower load levels was smaller than predicted by the SAP model. As a result, the maximum negative moment at larger load levels was greater than the maximum negative moments predicted by the SAP models at applied displacements corresponding to the same lateral loads. For the load test without the load truck, the bending moments were negative moments at the top of the pile at all load levels, becoming more negative as the lateral load increased. The moments from the field test without the load truck correlated well with the SAP model under the same loadings. The SAP model over-predicted the moments in this test by 10-30% on average for each of the pile. As a result, the location of the inflection point predicted by the SAP model is lower than the apparent inflection point from the field test results.

The SAP models predicted the largest axial forces due to lateral load effects to occur in the exterior battered piles with the leading pile being in axial compression and the trailing pile being in axial tension. The interior vertical piles carried very roughly one fourth of the load that the battered piles carried. The axial forces increased linearly with applied lateral load in the SAP models created for the Macon County bent. The axial forces did not vary linearly with applied displacement for the US 331 model due to the displacements at corresponding with applied lateral loads in the test not having a linear trend. The magnitudes of the axial forces computed from measured strains from the US 331 tests were much larger than the axial forces predicted in the model which can be attributed to the large cross-sectional area of the pile sections.

8. Field Test 4 – AUNGES Test Bents

8.1 Bent Test Set-up

The last bents tested were located in Lee County, Alabama at the Auburn University National Geotechnical Experimentation Site (AUNGES) located at the National Center for Asphalt Technology Test Track Facility. Two bents were constructed by Scott Bridge, LLC for the sole purpose of testing the bents to failure. The test bents featured four HP12x53 piles 35 feet long. The piles were driven using a vibratory hammer, and each pile achieved at least 20 feet of embedment into the ground. Once the piles were driven, the tops were cut off so that there would be uniform embedment in the pile cap. The bents were designed to have 9 feet of clear pile length above the ground surface. The first bent tested was an experimental design of all vertical piles embedded 18 inches into the pile cap. The second bent was constructed according to standard ALDOT design practice with two vertical piles and two battered piles embedded 12 inches into the pile cap. The exterior piles were battered at a 1.5/12 slope. The piles in both test bents were oriented for weak axis bending in the direction of the lateral load. The pile caps were 3 feet by 3 feet by 28 feet long. The concrete in the bent caps was a 3,000 psi mix design. During construction, 6 inch by 12 inch test cylinders were made in order to gauge the strength of the concrete at the time of the load tests. The strength tests were used in order to assure that the concrete would not be a limiting factor during the tests. Cylinders were broken at 7 days, 28 days, and on the day of the load tests. Concrete strength recorded on the day of the load tests was used in model calibration to more accurately model the behavior of the bents during the load tests.

250

Two load tests were conducted on each test bent. The first test was purely a lateral test to ensure the hydraulic jacks and loading apparatus was functioning properly. The second test was a purely lateral test until an observable failure occurred, or the jacks reached full load or extension capacity. The following sections will provide in depth details of the instrumentation locations, the loading apparatus, and load schedules for the field load tests.

8.1.1   Battered Bent

Two load tests on the battered pile bent were conducted on July 17, 2015. Figure 8-1 shows the battered pile bent constructed for this research prior to the lateral load test.

Figure 8-1 – AUNGES Battered Pile Test Bent

The piles were named Pile 1, Pile 2, Pile 3, and Pile 4. Pile 1, the leading pile, and Pile 4, the trailing pile, were battered at a 1.5/12 slope. The piles were instrumented at three cross sections along the depth of the piles. The first location was 6 inches from the bottom of the bent cap, the second gage location was 42 inches from the bottom of the bent cap, and the lowest gage location was 84 inches from the bottom of the bent cap. Each instrumented location featured two

gages on the exterior of the flanges to measure strain during weak axis bending. The two center piles, Pile 2 and Pile 3, were also instrumented with a third gage at the lowest instrumented cross section so that any strong axis rotation could be observed. Figure 8-2 shows the instrumented cross-sections for the battered pile test bent and their designated names. Figure 8-3 shows the locations of the gages for a typical pile cross-section.
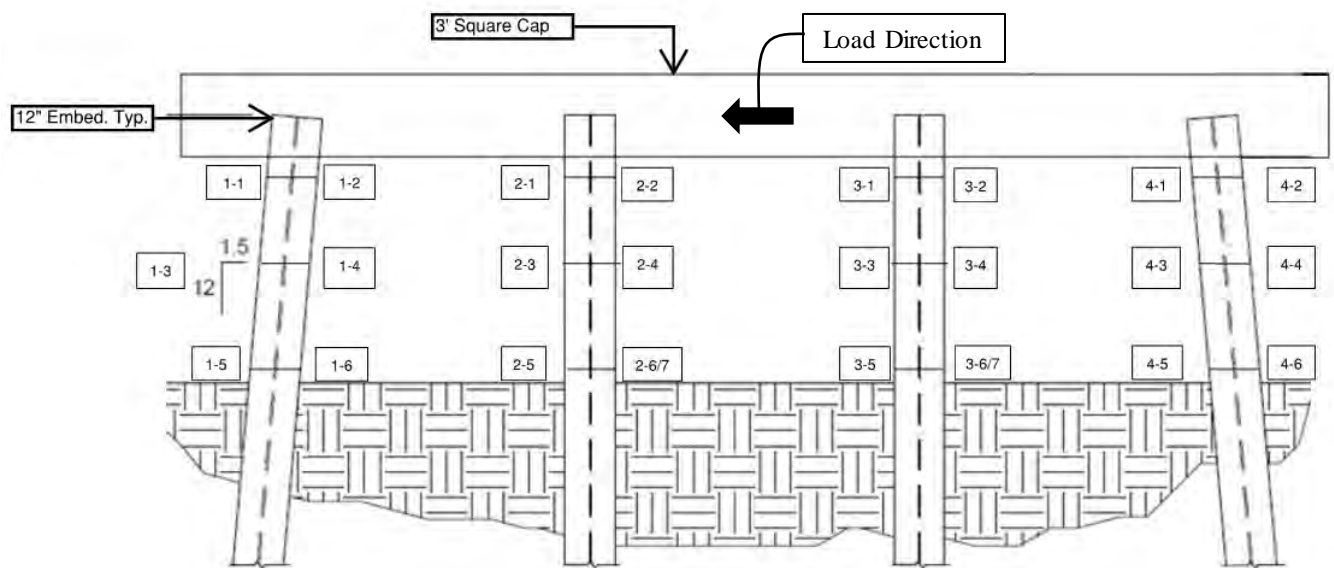
Figure 8-2 – AUNGES Battered Pile Test Bent Gage Locations
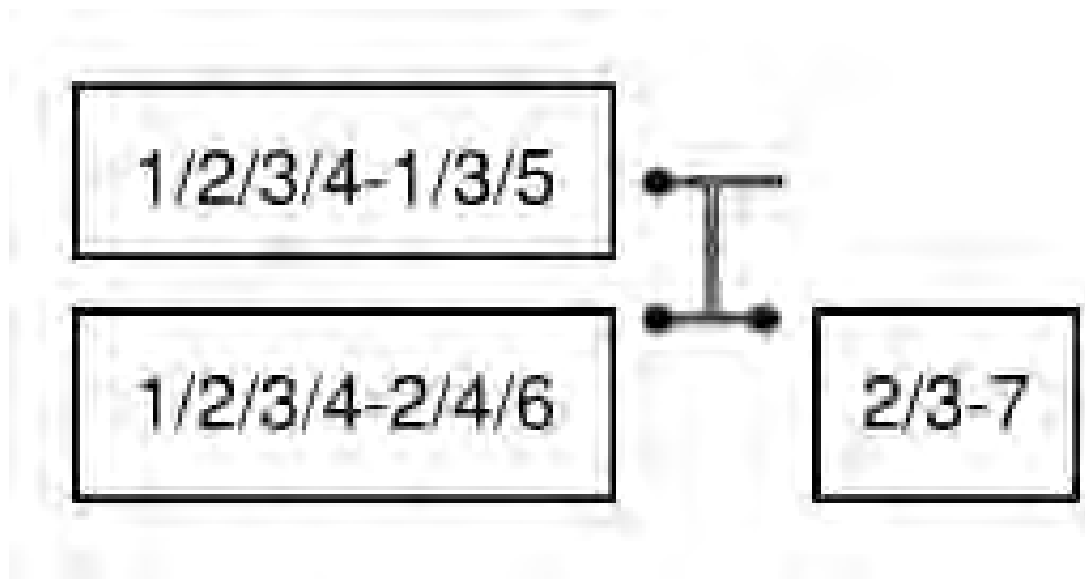
Figure 8-3 – AUNGES Battered Pile Test Bent Cross-section Gage Locations

Pile 2 and Pile 3 were also fitted with 2.5 inch hollow tube steel to serve as tracks for inclinometer testing. Figure 8-4 shows the inclinometer casing at Pile 2 with the inclinometer downhole.

Figure 8-4 – Inclinometer Downhole at Pile 2

A baseline shape was found by conducting an inclinometer test on each pile while the bent was not loaded. During the load tests, inclinometer readings were conducted at every 20 kip loading increment until 80 kips, when the inclinometer tests were conducted at every subsequent load increment. The large curvature in the piles prevented inclinometer readings from being conducted at higher load increments and on the unload portion of the test. This was due to the fact that a weld joint was present in the area of maximum bending moment. Permanent deflection in the piles caused the joint at the weld to become misaligned, which prevented the inclinometer

from traveling down the corners of the tube. The inclinometer tests for the 140 kip load increment and all of the unload increments were unable to be performed.

The lateral load in the test bent was induced by running high strength threaded rods on either side of the bent cap. A bearing tube was placed on one end of the bent cap. The threaded rods passed through predrilled holes in the tube and were used to pull the bent cap towards the reaction pile group. This is shown in Figure 8-5.

Figure 8-5 – High Strength Threaded Rod and HSS Bearing Tube

The reaction pile group was an existing 9 pipe pile group. Two W10x23 sections were used to engage the reaction pile group. The two beams were stacked on top of each other with spacers in place to allow the threaded rod to pass between the two beams. The threaded rod then passed through slotted holes in tube sections and through the hydraulic jacks. The tube steel transferred load through bearing on the two beams which engaged the pipe piles that projected out of the 9

pile cap in bearing. Figure 8-6 shows the reaction pile group and the W-sections used to spread the load from the two threaded rods to the reaction pile group.

Figure 8-6 – Reaction Pile Group with W10x23 Load Beams

The initial test was conducted to ensure the jack system and loading apparatus was functioning properly. The test bent was loaded at 10 kip increments to approximately 40kips. At each loading increment, once the target load was achieved, the load was held for 10 minutes or until the inclinometer tests were completed. Inclinometer tests were conducted at the initial, 20 kip, and 40 kip loading increments.

The full load test was conducted on July 17, 2015. The vertical pile test bent was loaded until the stroke capacity of the jacks was exceeded. The lateral load on the piles was increased by 10 kips for each load increment. Inclinometer profiles were captured at every 20 kip increment until the 80 kip increment. After reaching 80 kips an inclinometer profile was captured for each subsequent load increment. Table 8 shows the target load schedule for the load test to failure.

Table 8-1 – Target Load Schedule for the AUNGES Battered Pile Test Bent

Target Load (kip)	Hold Time (min)	Inclinometer Test
0	-----	Yes
10	10	No
20	10	Yes
30	10	No
40	10	Yes
50	10	No
60	10	Yes
70	10	No
80	10	Yes
90	10	Yes
100	10	Yes
110	10	Yes
120	10	Yes
130	10	Yes
140	10	Yes
100	10	Yes
50	10	Yes
20	10	Yes
0	-----	Yes

The first significant development during the load test occurred at 100 kips of applied lateral load. Flexure cracking began to occur in the bent cap above Pile 2 and extending toward Pile 1. As further load was applied, the bent significantly deflected and the flexure crack widened. At 110 kips, mill scale began to flake off the pile as the flanges at the bottom of the pile cap began to yield. At 130 kips, shear cracks began to open next to the flexural crack at pile 2 which opened up along the path of the flexural reinforcement at the bottom of the bent cap. The flanges at Piles 1 and 3 began to experience significant buckling in the region 5-7 inches below the

256

bottom of the bent cap. At 140 kips, the cracks became significantly larger and the drift of the bent increased drastically, shedding the energy from the jacks through deflection. At 140 kips, the stroke capacity of the jacks was maxed out and the primary loading was completed. The deflection of the bent was significant enough to prevent any further inclinometer testing due to damage to the welded connections of the inclinometer tubing. Wire pots determined the maximum deflection to be approximately 6 ¾ inches with a residual drift of 4 ½ inches. Figures 8-7 through 8-10 show pictures of the bent and piles at failure.

Figure 8-7 – Bent Cracking at Pile 2

Figure 8-8 – Flexural Cracking below the Bent Cap

Figure 8-9 – Flange Buckling at Pile 3

Figure 8-10 – Residual Drift due to Lateral Load Test

8.1.2 Vertical Bent

The two load tests on the vertical pile test bent were conducted on Thursday June 18, 2015 and Friday June 19, 2015. Figure 8-11 shows the vertical pile test bent constructed for this research prior to the lateral load test.

Figure 8-11 – AUNGES Vertical Pile Bent

The piles were named Pile 5, Pile 6, Pile 7, and Pile 8. Pile 5 was the leading pile and Pile 8 was the trailing pile. The piles were instrumented at three cross sections along the depth of the piles. The first location was 6 inches from the bottom of the bent cap, the second gage location was 44 inches from the bottom of the bent cap, and the lowest gage location was 82 inches from the bottom of the bent cap. Figure 8-12 shows the instrumented locations along each pile for the test bent. Each instrumented location featured two gages on the exterior of the flanges to measure strain during weak axis bending. The two center piles, Pile 6 and Pile 7, were also instrumented with a third gage at the lowest instrumented cross section so that any strong axis rotation could be observed. Figure 8-13 shows the gage locations for the instrumented cross sections and the strong axis gage present at the bottom gage locations of the two center piles. The bent cap was also instrumented with two sister bars at Pile 6. Each sister bar was instrumented with 4 strain gages meant to capture the strain in the bent cap in the zone around the embedded pile.
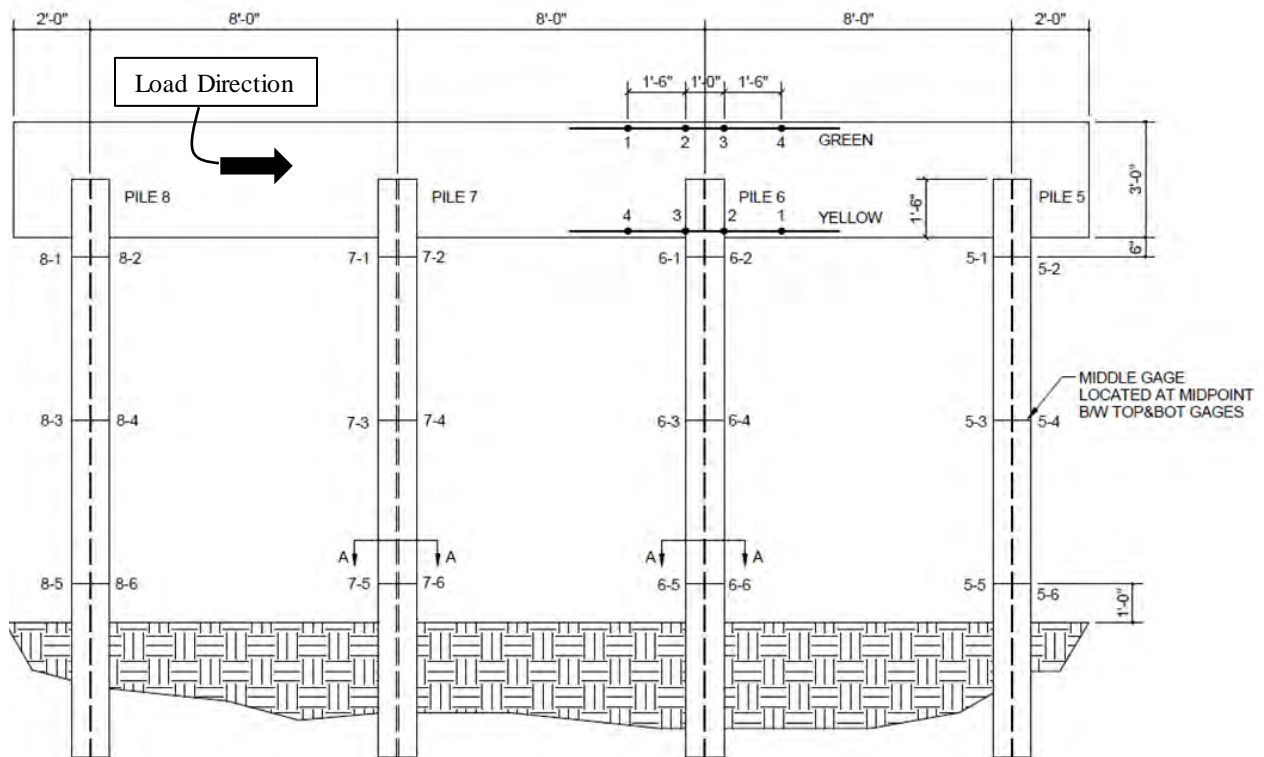
Figure 8-12 – Gage Positions for Vertical Pile Bent Load Test
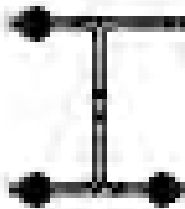
Figure 8-13 – Instrumentation Locations at Gaged Cross Section

Pile 5 and Pile 7 were also fitted with 2.5 inch hollow tube steel to serve as tracks for inclinometer testing. Figure 8-14 shows the inclinometer casing attached to Pile 5. A baseline shape was found by conducting an inclinometer test on each pile while the bent was without lateral load. During the load tests, the inclinometer readings were conducted at every 20 kip

loading increment until reaching loading increments close to the predicted failure load. Inclinometer tests were also conducted at each unload increment and in the final unloaded case to observe any residual deformations.

Figure 8-14 – Inclinometer Casing on Pile 5

The initial test was conducted to ensure the jack system and loading apparatus was functioning properly. The test bent was loaded at 10 kip increments to approximately 50% of the predicted failure load. At each loading increment, once the target load was achieved the load was held for 10 minutes or until the inclinometer tests were completed.

The second load test was conducted on June 19, 2015. The vertical pile test bent was loaded until a structural failure occurred or the capacity of the jacks was exceeded. The lateral load on the piles was increased by 10 kips for each load increment. Inclinometer profiles were captured for every 20 kip increment until the 80 kip increment. After reaching 80 kips an inclinometer profile was captured for each load increment. Table 8-2 shows the target load schedule for the load test to failure.

263

Table 8-2 – Load Schedule for the AUNGES Vertical Pile Test Bent

Target Load (kip)	Hold Time (min)	Inclinometer Test
0	-----	Yes
10	10	No
20	10	Yes
30	10	No
40	10	Yes
50	10	No
60	10	Yes
70	10	No
80	10	Yes
90	10	Yes
100	10	Yes
110	10	Yes
120	10	Yes
130	10	Yes
140	10	Yes
100	10	Yes
80	10	Yes
40	10	Yes
0	-----	Yes

The maximum load applied to the test bent was 140 kips. At this point, the piles were experiencing localized yielding in the pile flanges. The bent cap deflection began to increase nonlinearly once the yielding occurred. Yielding was observed on the flanges of each pile to a depth of 5 to 7 inches below the bent cap. Strain gages in this area experienced excessive strain and failed at the higher load increments. Pile 5, the leading pile, was the best visual example of the deflection the bent cap experienced with respect to the ground surface. Figure 8-15 shows the drift of the bent at Pile 5. Figure 8-16 and Figure 8-17 show the localized buckling in the trailing pile flanges. The lateral force induced in the pile bent was distributed into the surrounding soil structure. Evidence of large amounts of energy imparted into the soil is evident in ground cracks opening up around the test bent. Figure 8-18 shows one of the ground cracks caused by the lateral load test. The test resulted in residual drift of the pile bent. Figure 8-19 shows the residual drift in the vertical pile test bent.

Figure 8-15 – Lateral Deflection Induced in Pile 5 during Field Load Testing

Figure 8-16 – Pile 5 Flange Buckling

Figure 8-17 – Pile 7 Flange Buckling

Figure 8-18 – Ground Crack Due to Lateral Deformations

Figure 8-19 – Lateral Displacement of Test Pile

8.2 Bent Test Results

The two AUNGES test bents were loaded to failure. Strain gages captured strain data during the load tests. The data was used to calculate the moment at each cross-section that was instrumented for each loading increment. Data readings were recorded every 15 seconds during testing. Detailed notes were taken to determine the time frame in which the target load was applied at each target increment. The strain values collected in each increment on each flange

269

were adjusted to consider the strain over the entire pile cross-section. The values were then averaged together over the hold period to calculate a composite average strain due to the target lateral load at each flange. The composite strain values were then used to calculate the curvature of the section. Using the curvature and the material properties of the piles, the composite bending moment on the cross section was calculated. Coupon tests determined that the yield stress of the piles was 58 ksi. When strain values produced stresses exceeding this value, the moment was not reported as the strain gages are not reliable beyond yield of the pile. In the sections below, the composite moment values were graphed against the depth of the piles to produce moment profile for each pile in the test bents.

Inclinometer data was also recorded during these two load tests. Inclinometer tests were conducted at every other loading increment until the higher load levels were reached at which point they were conducted for each increment unless the bending of the piles prevented the probe from reaching the pile bottom. The data recorded from the inclinometer tests was used to graph the deflected shape of the piles with depth. The deflected shape profiles produced during each test are presented in the sections below.

The wire pots connected to the pile caps of the test bents recorded the deflection of the pile caps during the load tests. The deflection of the pile cap versus the applied lateral load for each test bent is presented in the sections below.

8.2.1 Battered Pile Test Bent

The battered pile test bent was conducted on July 17, 2015. The test bent was loaded until the hydraulic jacks used to load the test bent reached maximum stroke. The yield stress of the piles was determined from steel coupon tests. The yield stress was 58 ksi. During data reduction, this value was used to cap the stress in the piles. When calculating moments, if the strain differential produced a stress higher than 58 ksi, then the stress used for calculating the bending moment on

270

the section was 58 ksi. This limit only came into effect at the top gages where yielding occurred in the pile flanges. The calculated moment and axial force profiles for the battered pile bent tests are presented in Figure 8-20 and Figure 8-21, respectively. The results for the inclinometer tests on Piles 2 and 3 are presented in Figure 8-22. The load deflection behavior captured from the wire pots is presented in Figure 8-23.
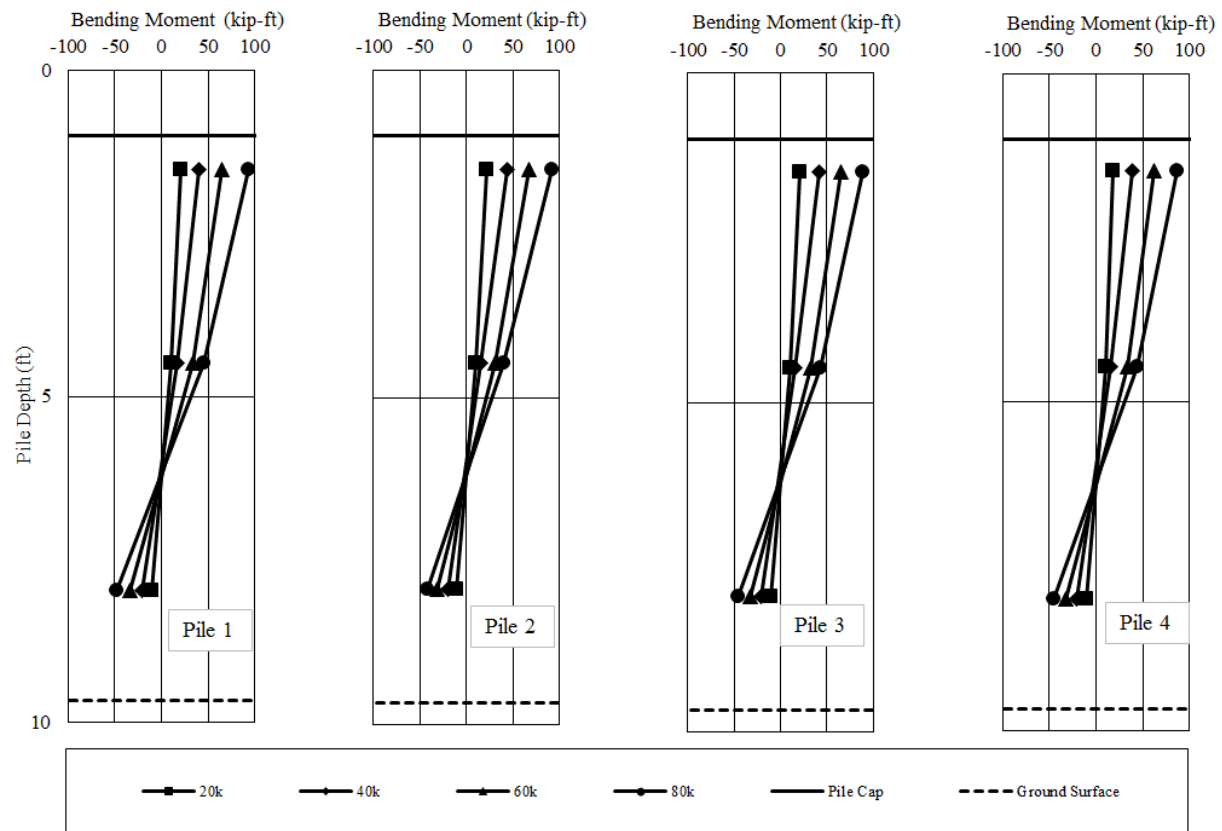
Figure 8-20 – AUNGES Battered Bent Moment Results
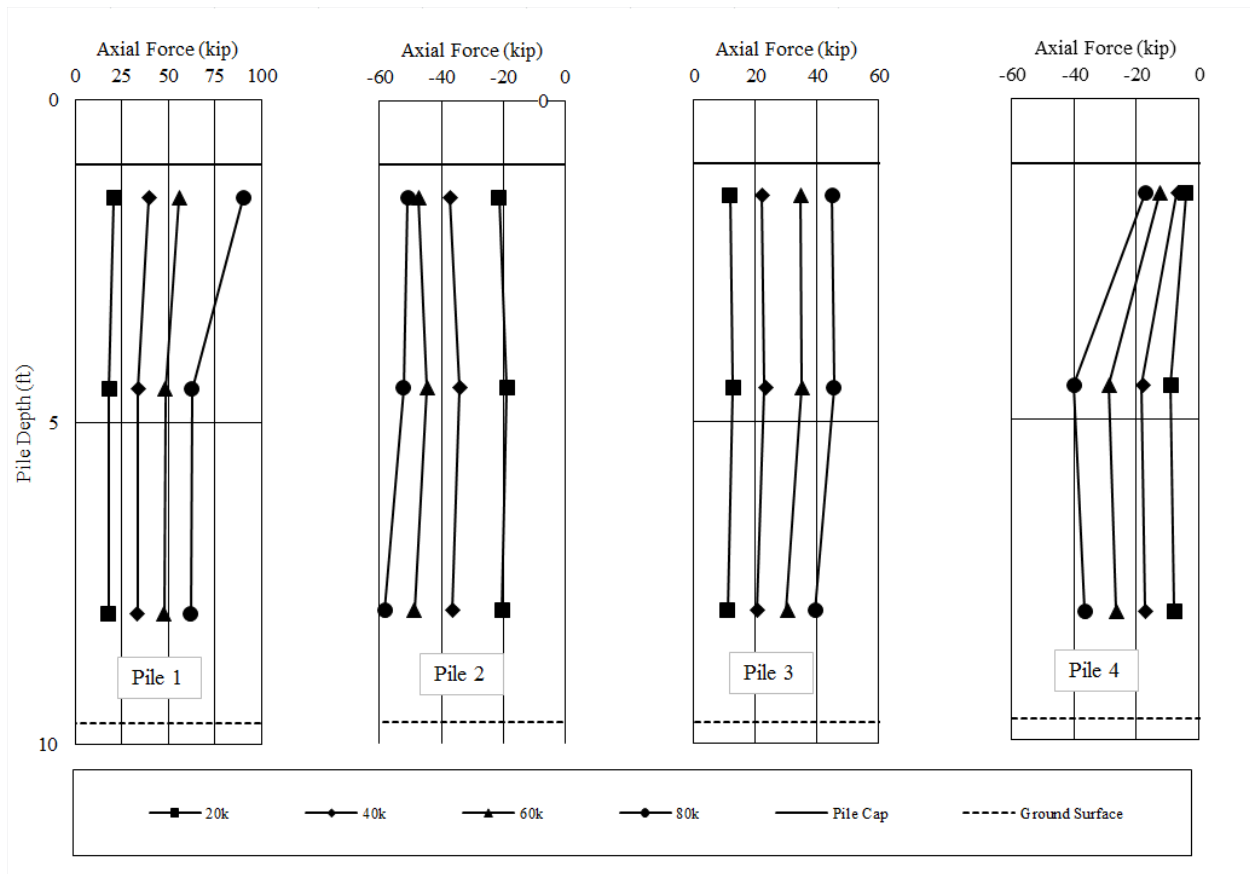
Figure 8-21 – AUNGES Battered Bent Axial Results
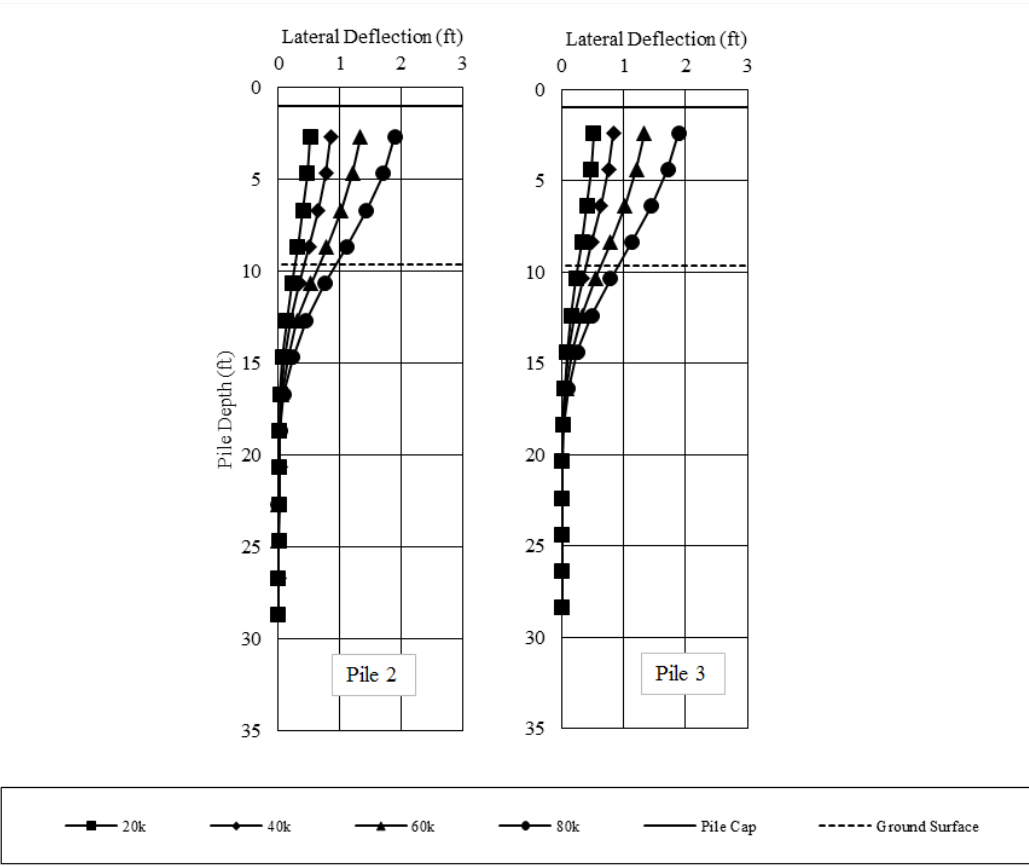
Figure 8-22 – AUNGES Battered Bent Inclinometer Test Results
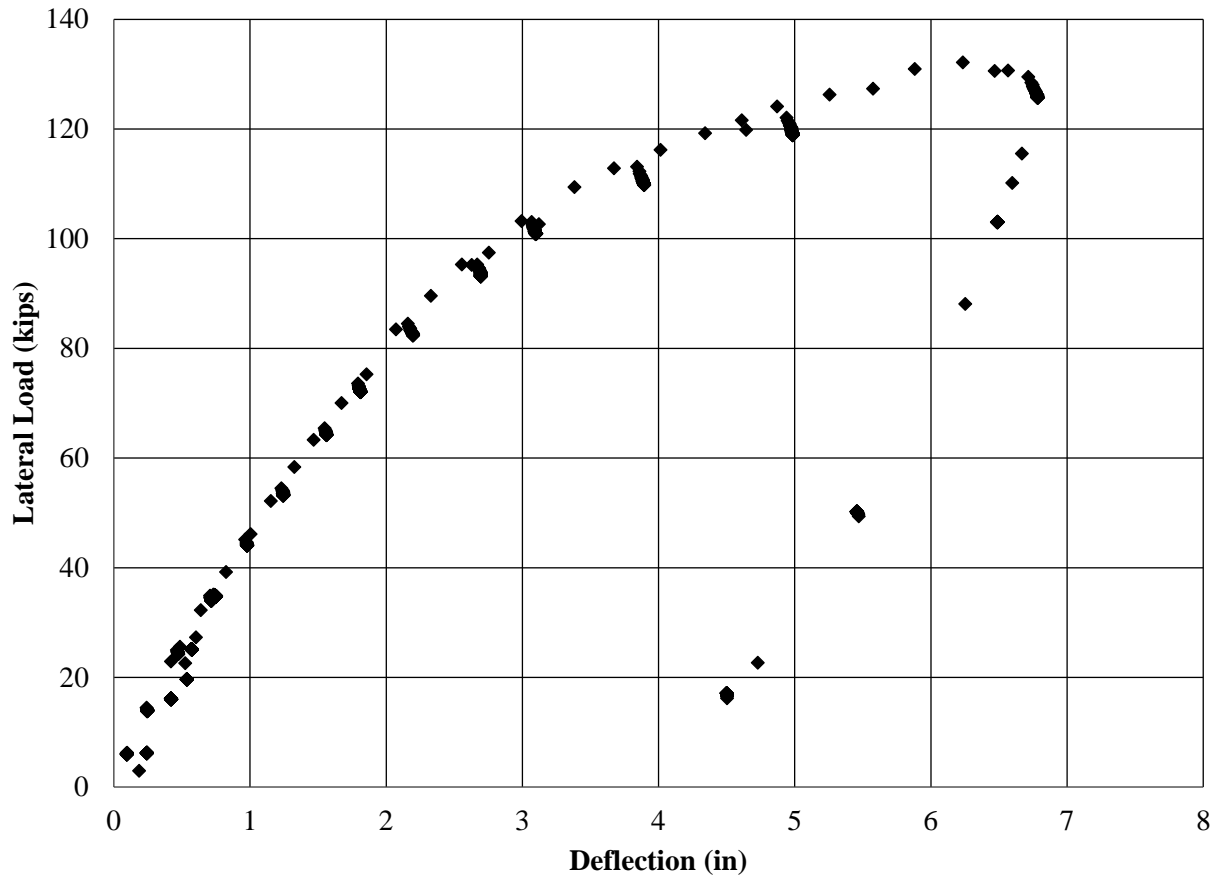
Figure 8-23 – Battered Pile Bent Wire Pot Load Deflection Behavior

8.2.2 Vertical Pile Test Bent

The battered pile test bent was conducted on June 27, 2015. The test bent was loaded until the hydraulic jacks used to load the test bent reached maximum stroke. The yield stress of the piles was determined from steel coupon tests. The yield stress was 58 ksi. During data reduction, this value was used to cap the stress in the piles. When calculating moments, if the strain differential produced a stress higher than 58 ksi, then the moment is reported as the yield moment due to the inaccuracy of the strain gages beyond yield strain. This limit only came into effect at the top gages where yielding occurred in the pile flanges. The calculated moment and

274

axial force profiles for the vertical pile bent tests are presented in Figure 8-24 and Figure 8-25, respectively. The results for the inclinometer tests on Piles 5 and 7 are presented in Figure 8-26 . The load deflection behavior captured from the wire pots is presented in Figure 8-27.
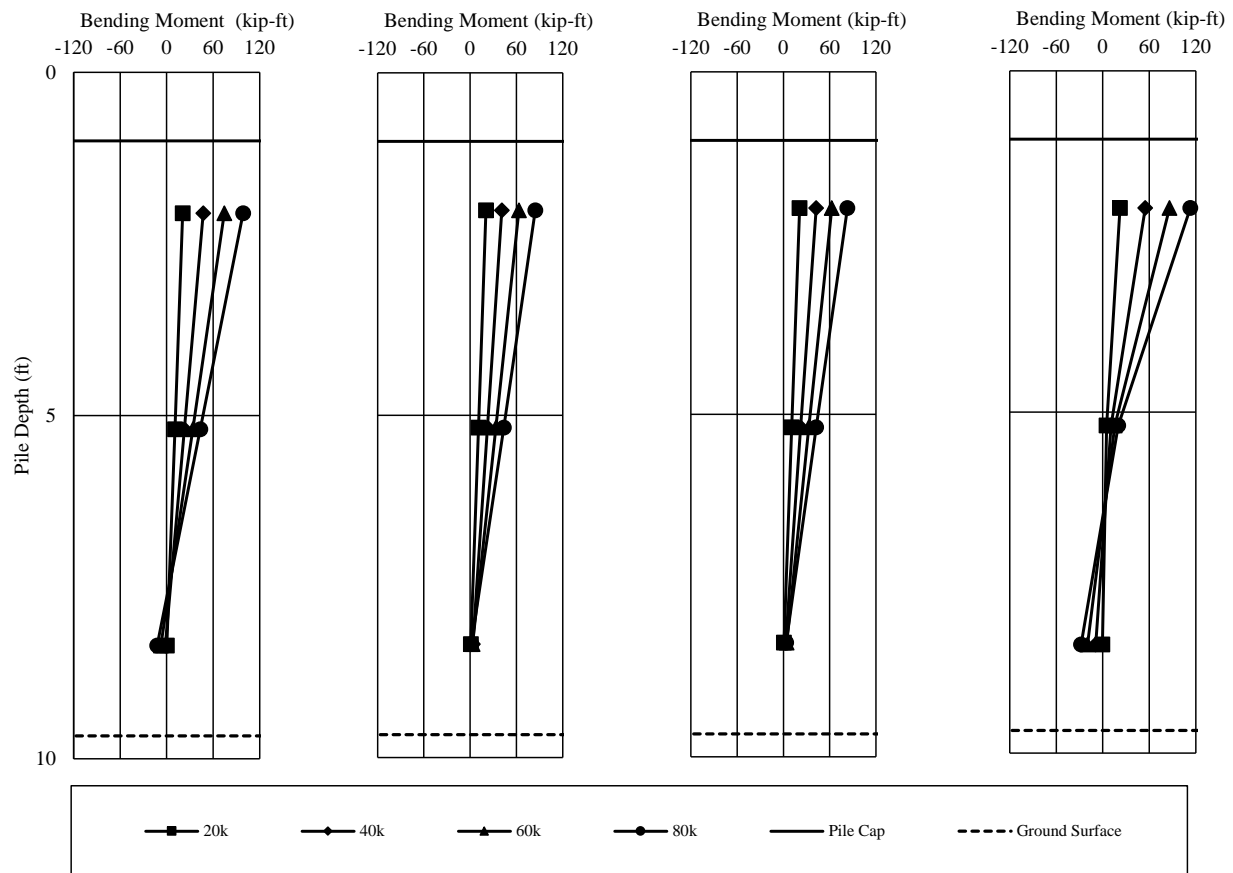
Figure 8-24 – AUNGES Vertical Bent Moment Results
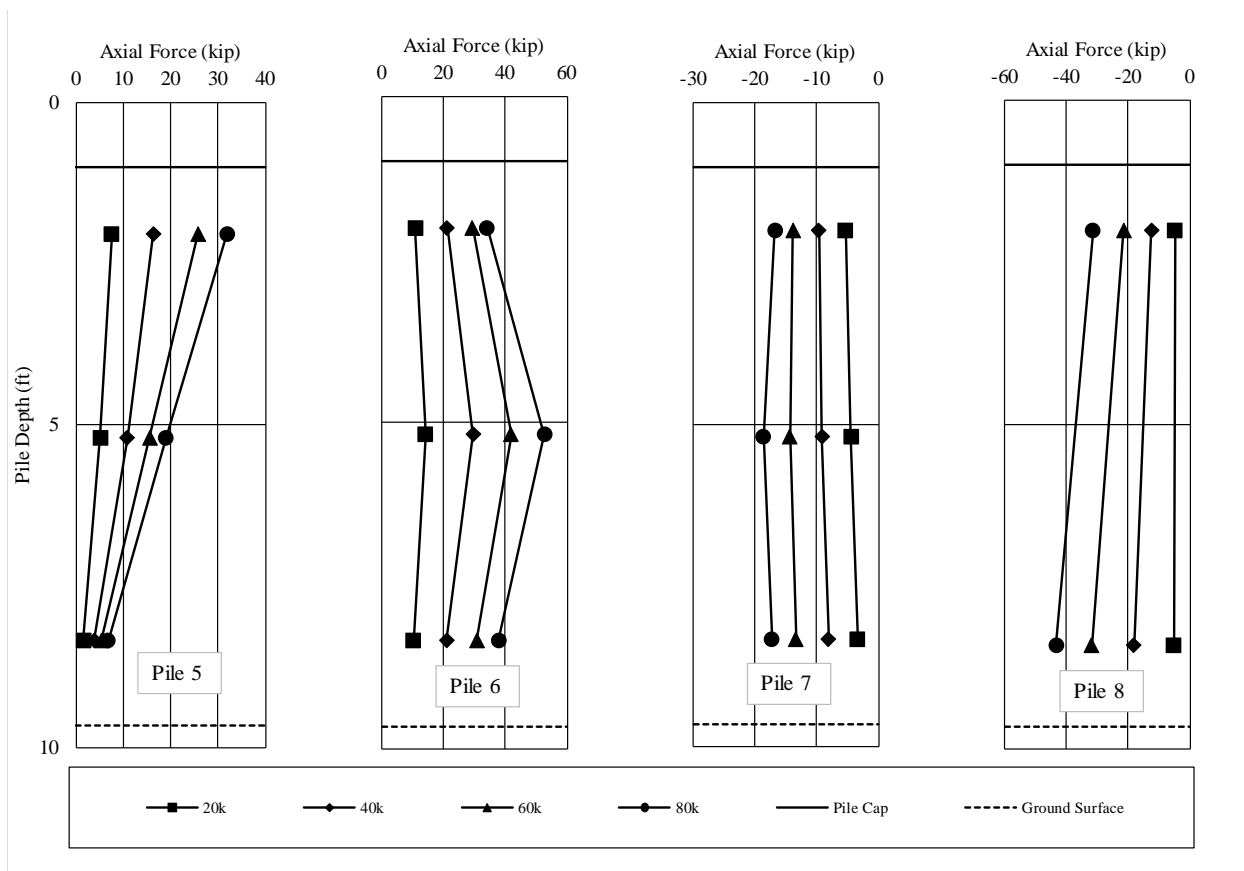
Figure 8-25 – AUNGES Vertical Bent Axial Results
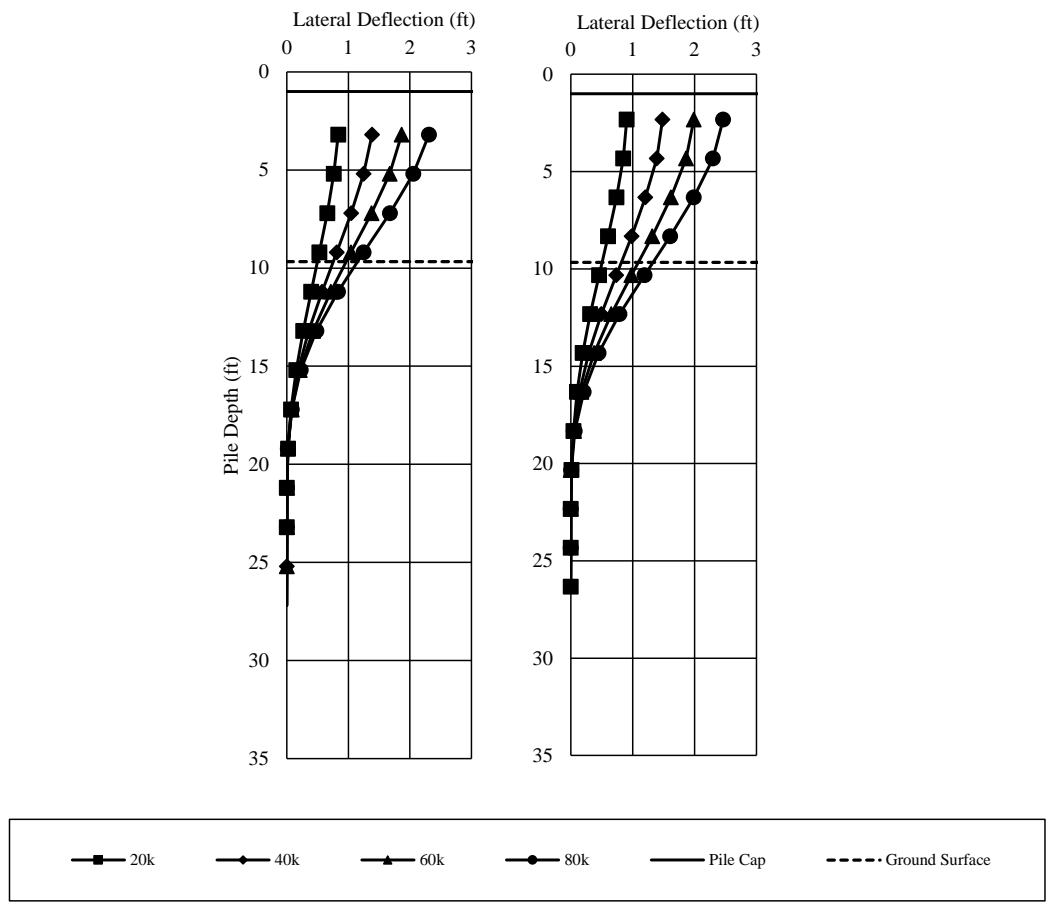
Figure 8-26 – AUNGES Vertical Bent Inclinometer Test Results
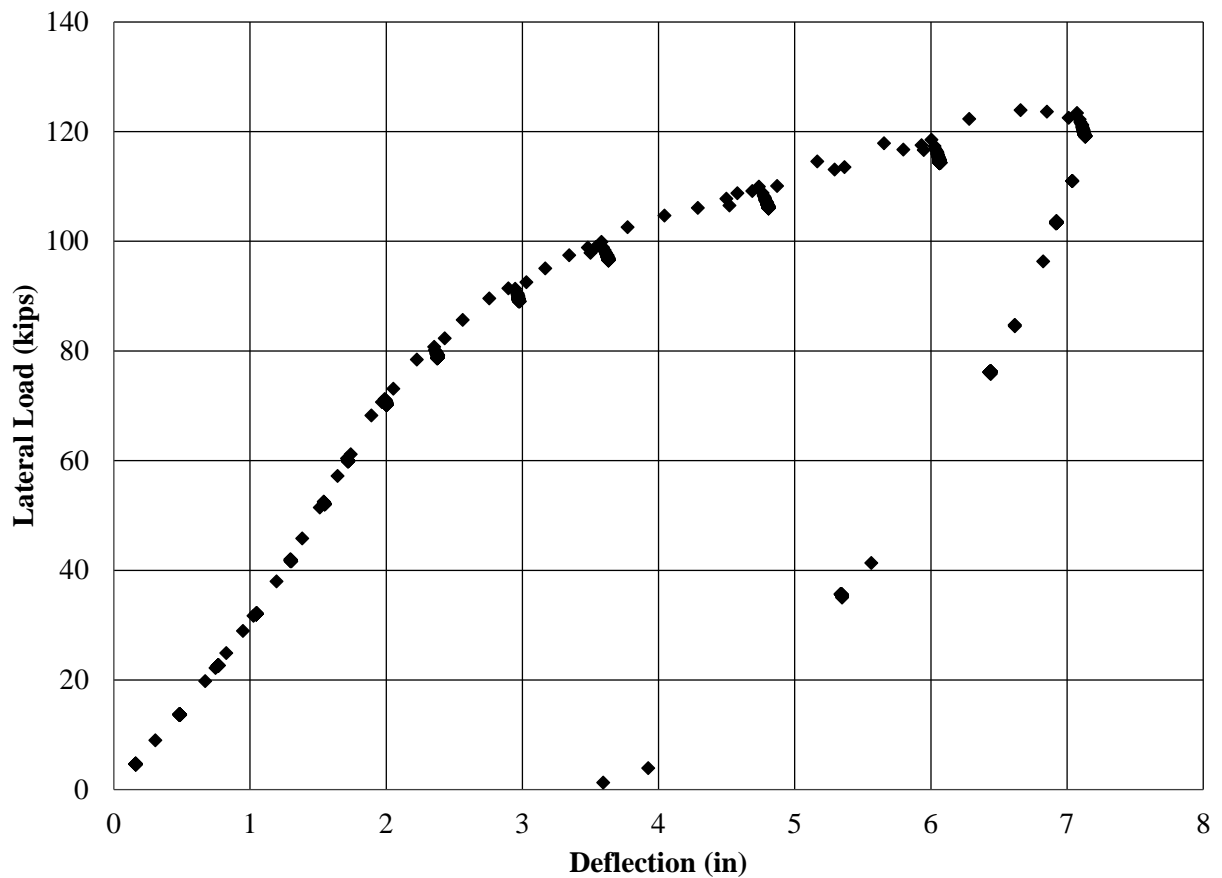
Figure 8-27 – Vertical Pile Bent Wire Pot Load Deflection Behavior

8.3 Summary

The test results showed several important conclusions about steel pile bents. One of the first results of interest is the failure mode of the battered bent. The vertical bent only experienced yielding of the piles while the battered pile experienced both pile yielding and significant cap cracking above Pile 2. This cracking is due to the tension the pile experienced due to the battered pile in compression wanting to rotate to vertical causing tension in Pile 2 and compression in Pile 3 which is opposite from what is expected and what occurred in the vertical bent. Both of the pile bents experienced significant soil deformation and cracking at the ground level. Additionally it should be noted that the magnitude of the axial forces in the piles are higher in the battered bent.

278

The last conclusion of importance is that in both cases the pile was able to develop yielding of the flanges at the bottom of the pile cap. This indicates that the 12 inch embedment is sufficient to develop the yield moment in the weak direction of the W12x53 pile.

9. Calibration of Analytical Models

9.1 Approach

Initial models for the AUNGES bents were built using data collected during the construction process. Soil properties such as unit weight, p-y behavior, and undrained shear strength, were estimated from previously conducted standard penetration tests and recent dilatometer testing. The yield stress of the steel was determined from coupon testing conducted by the steel pile supplier. Concrete compressive strength and elastic modulus were determined from cylinder testing conducted in the Auburn University structures lab. Several strategies were used to attempt to match the models to the observed data. The models were calibrated by matching the observed deflection behavior from the field load tests and comparing the axial and moment results. The comparisons between the calibrated models and the observed data are shown in the sections below.

9.2 Battered Pile Bent

Initial attempts to calibrate the bent models resulted in substantial deviation. In order to bring the models into the best alignment, the soil was simplified by reducing the number of layers to two, and converting from a custom p-y curve to standard curves based on undrained shear strength and friction angle values. The deflection profiles that were observed from the inclinometer tests suggested that the actual ground surface at the piles was lower than the true ground surface. This was likely due to the use of a vibratory hammer to install the piles, resulting in a disturbed zone near the ground surface. The inclinometer data also suggests that the piles were fixed at the tips, eliminating the possibility of pile tip movement.

After iterating on the soil properties, a best match among the deflection and moment profiles with depth was reached. Figure 9-1 through Figure 9-4 show the results of the final calibration. The moment and deflection were predicted reasonably well, while the axial forces, particularly those in the interior piles, were underpredicted.
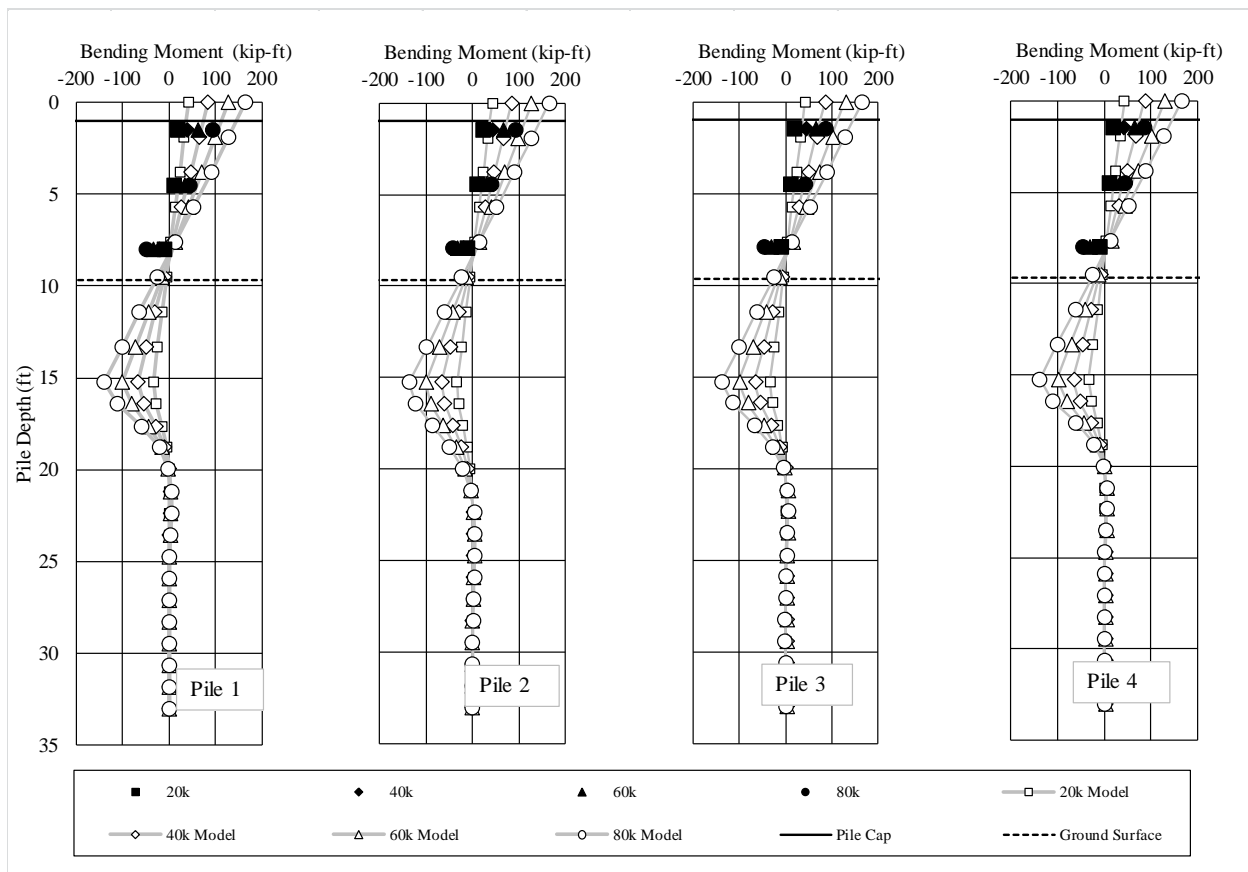
Figure 9-1 – AUNGES Battered Bent Moment Calibration
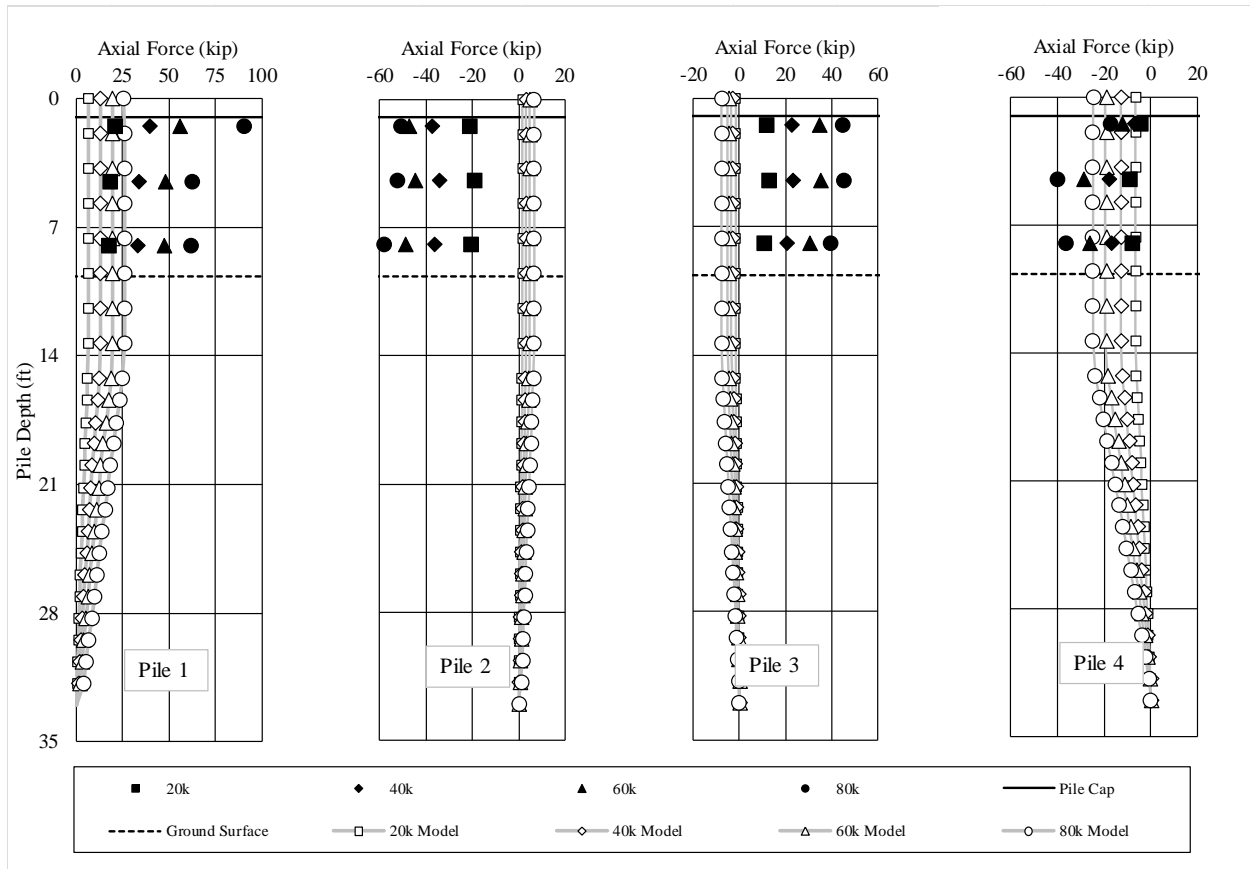
Figure 9-2 – AUNGES Battered Bent Axial Force Calibration
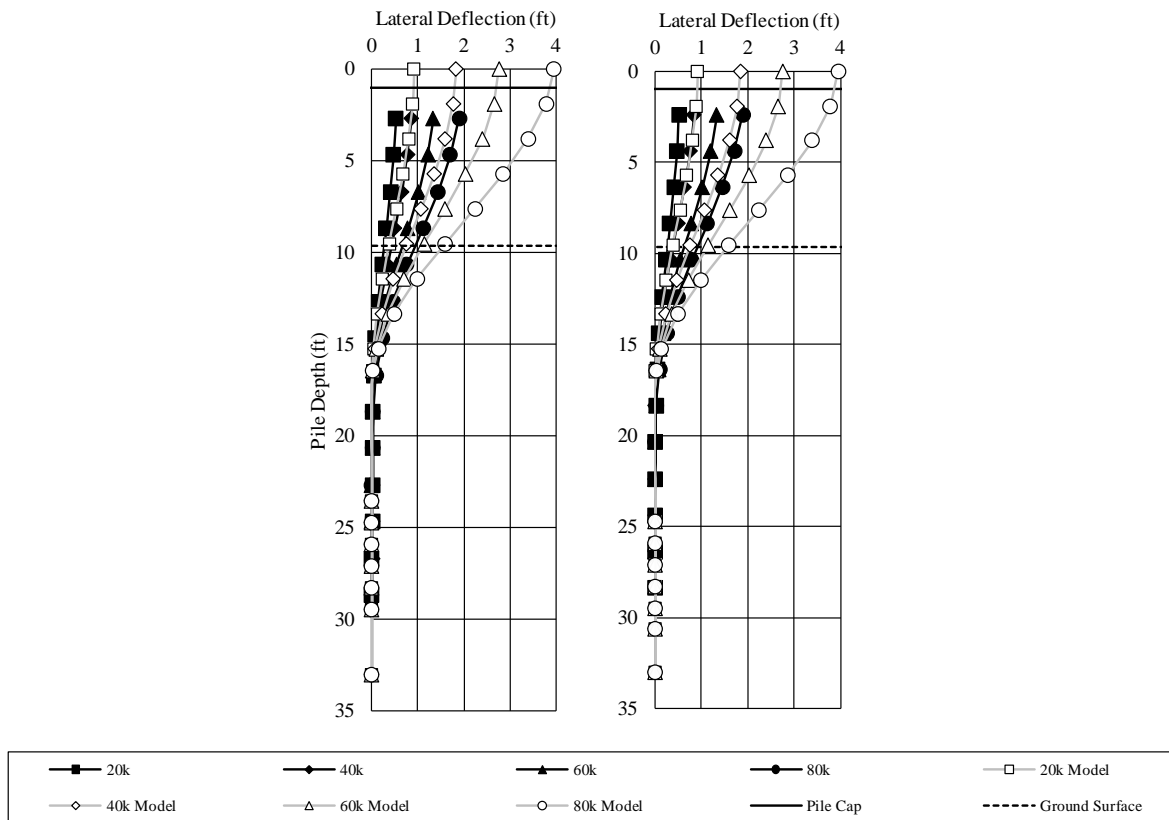
Figure 9-3 – AUNGES Battered Bent Displacement Calibration
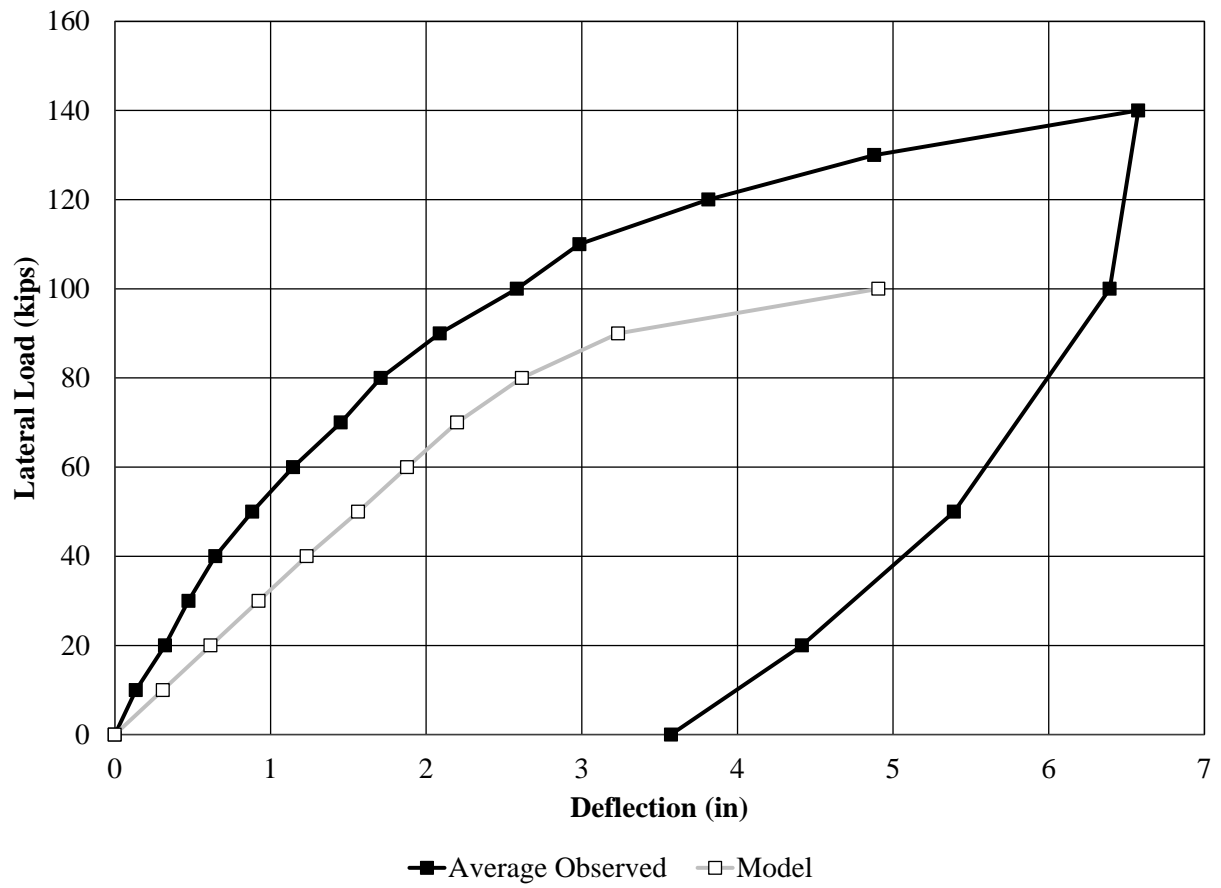
Figure 9-4 – AUNGES Battered Bent Cap Displacement Calibration

9.3 Vertical Pile Bent

A similar approach was used to calibrate the models for the vertical pile bent. Figure 9-5 through Figure 9-6 show the moment, axial force, deflected shape, and cap displacement calibration results, respectively. It's worth noting the overall behavior of this bent was better captured by the numerical models than for the battered bent.
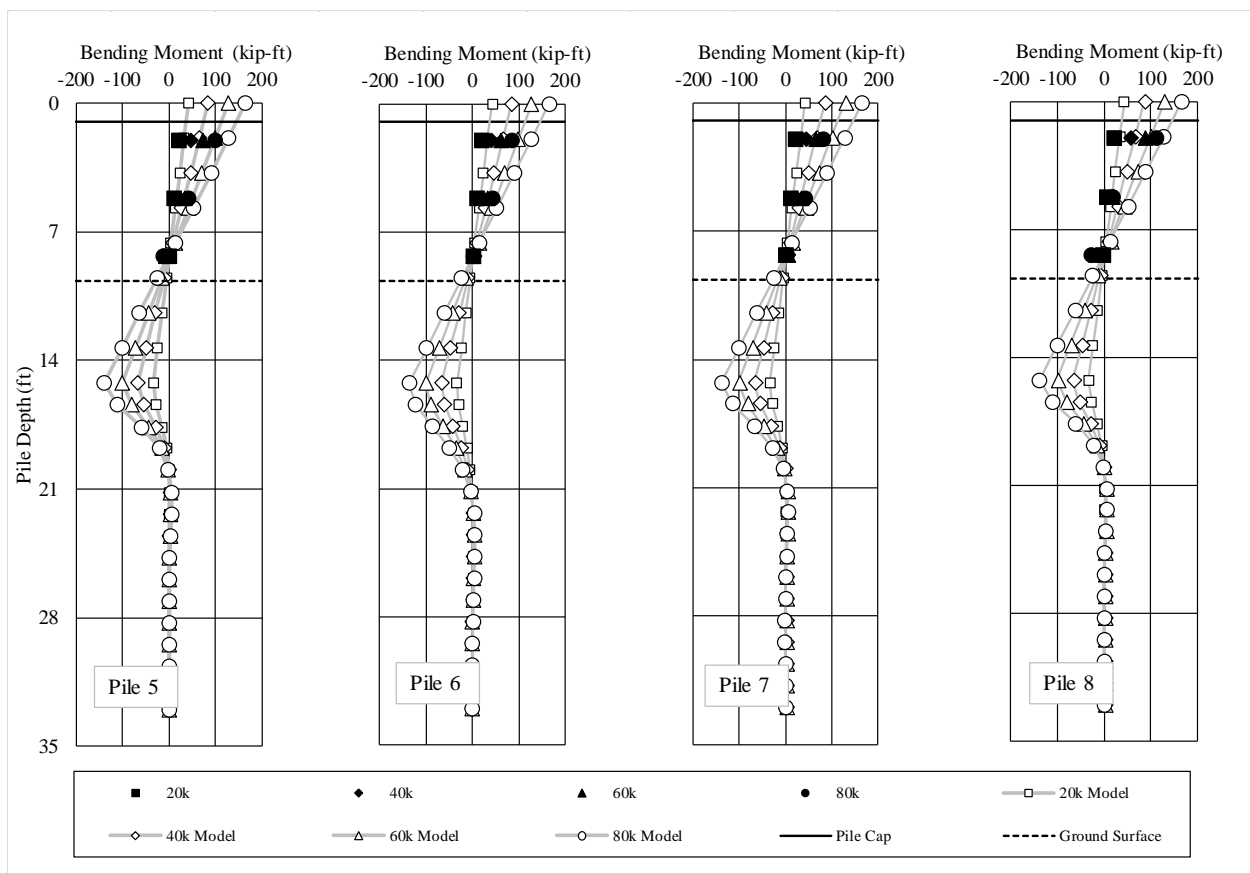
Figure 9-5 – AUNGES Vertical Bent Moment Calibration
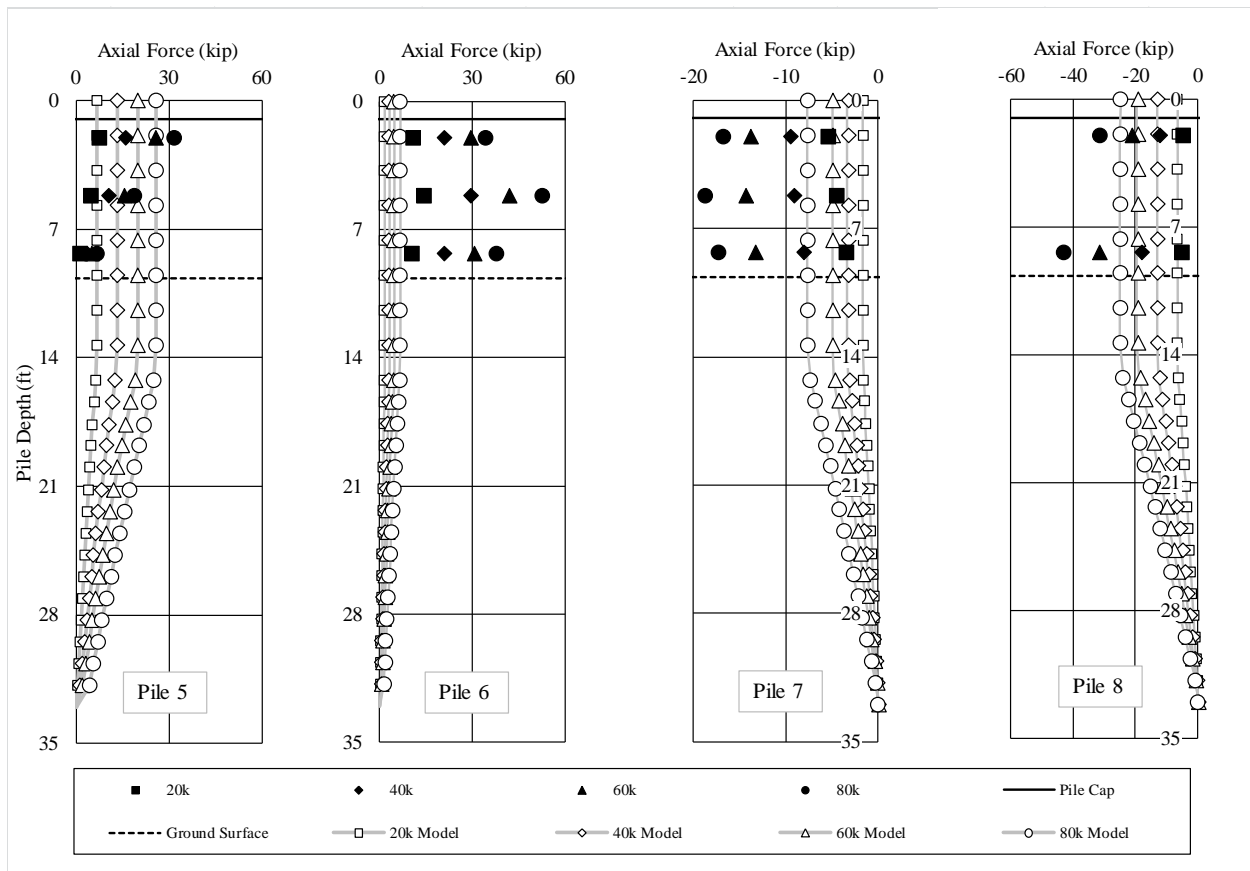
Figure 9-6 – AUNGES Vertical Bent Axial Calibration
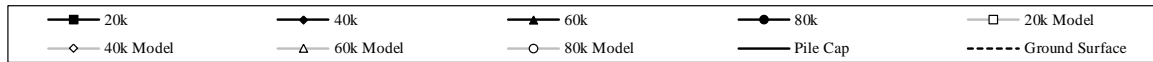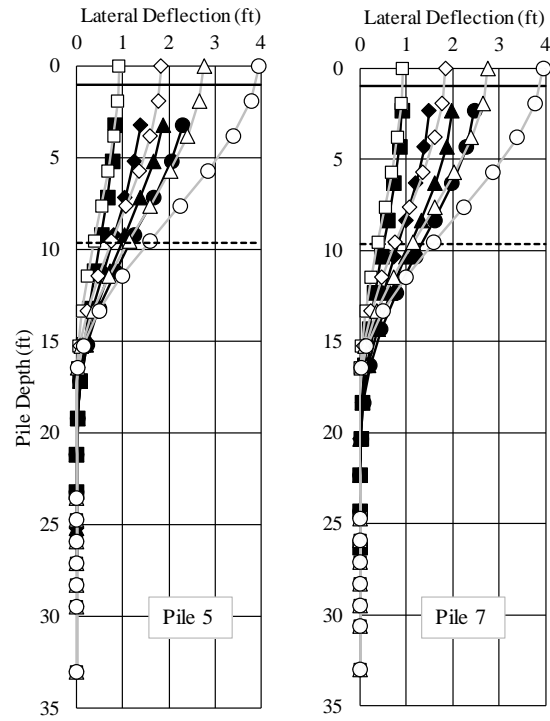
Figure 9-7 – AUNGES Vertical Bent Displacement Calibration
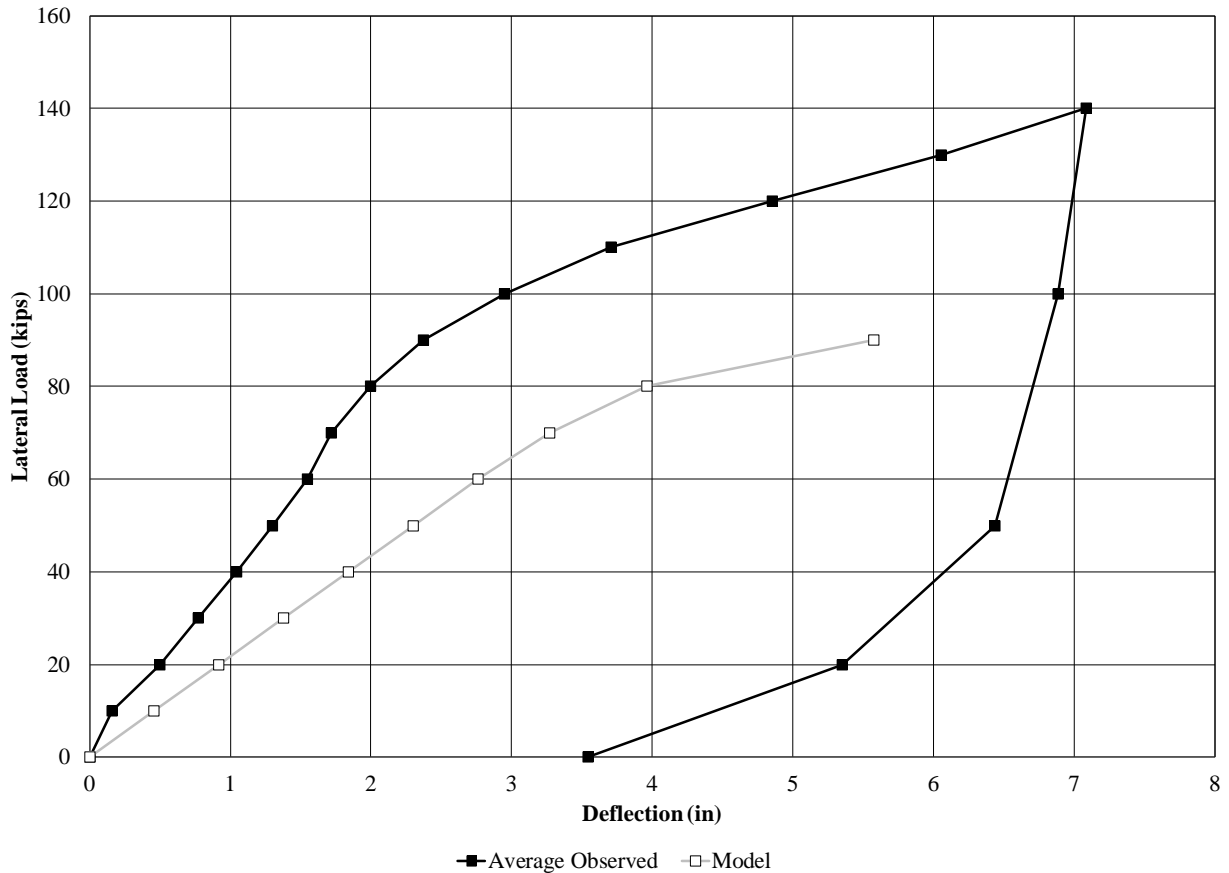
Figure 9-8 – AUNGES Vertical Bent Cap Displacement Calibration

9.4 Summary

The correlation of the experimental and analytical results was reasonable considering the uncertainty in the material properties and geometry of the specimens. One of the important conclusions from this model calibration include the fact that the axial forces in both cases from the experimental tests were higher than the model predicted. This was most significant in the interior piles. The second important conclusion was that the battered pile bent had greater discrepancy of axial force results for all the piles and the model did not capture the opposite axial force signs of the two interior piles.

10. Pile Bent Bridge Analysis and Design Process

10.1   Introduction

This chapter presents a flowchart of the analysis and design process that has been developed

from the results of the analysis and testing that has been done as part of this research project.

Start Pile Bent Design

Generate Trial Bent Geometry

In General:
- All piles should be vertical.
- The strong-axis for each pile shall exist within and be parallel to the plane of the bent so that lateral, in-plane bent displacements cause weak-axis bending in the pile section. Section axes are defined in Section 6.
- Provide one pile for each girder line.
- Locate each girder line over the centroid of its supporting pile.
- Determine the supporting soil surface elevation for Service and Strength Limit States.
- Determine the supporting soil surface elevation for Extreme Event Limit States.

Determine Boundary Conditions

- Each pile bent shall be modeled as a space frame.
- In-plane bent displacements (sidesway/drift) are assumed unrestrained, but are limited to the condition when the joint centered on the bent forms a closed wedge. See attached Figure 2 for the recommended drift limit calculation and its derivation.
- Out-of-plane bent displacements are assumed to be unrestrained, but are limited to the width of the largest of the three open deck joints on either of the two supported spans.
- Use pinned support at pile tip for piles bearing on rock. For piles not bearing on rock, replace vertical component of pinned support with an appropriate soil spring to relate pile axial load to displacement.
- Calculate lateral soil springs to model horizontal soil-structure interaction. The horizontal subgrade modulus can be used to determine linear spring values for structures exhibiting small displacements below the ground surface. The project geotechnical engineer should verify that the use of linear soil springs is appropriate for the structure considered. Linear springs should be replaced with force-displacement curves if nonlinear soil behavior is to be modeled.
- Saturated soil will often be present and should be accounted for in the model used to represent soil-structure interaction.
- Note that specialized programs such as Group or FB-MultiPier are available if a more rigorous treatment of the above considerations is deemed necessary.

1

```
                    ┌───┐
                    │ 1 │
                    └─┬─┘
                      │
                      ▼
┌─────────────────────────────────────────────────────────┐
│              Determine Individual Load Cases              │
│          and Assemble Required Load Combinations          │
│                                                           │
│  • Loads acting on pile bents shall be in accordance with │
│    Section 3.                                              │
│  • Horizontal superstructure loads acting in the plane of │
│    the bent and transferred to the bent should be         │
│    resolved into equivalent horizontal and vertical       │
│    components acting through the centroid of the bent cap.│
│    The equivalent horizontal components can be assumed to │
│    be equally distributed to each girder line. The        │
│    equivalent vertical components can be determined by     │
│    assuming a rigid superstructure and summing moments    │
│    about one of the exterior girder lines. The resulting  │
│    couple consists of two equal but opposite concentrated │
│    forces acting at the exterior girder lines and creating│
│    a moment consistent with that intended by the required │
│    AASHTO LRFD loading. See attached Figure 1 for example │
│    calculations.                                          │
│  • Horizontal superstructure loads acting perpendicular to│
│    the plane of the bent and transferred to the bent can  │
│    be applied through the centroid of the bent cap without│
│    adjustment.                                             │
│  • Individual vehicular live load (LL) cases should be    │
│    established for all reasonably possible loading         │
│    conditions.                                            │
│  • A unique load combination (as required by Article 3.4) │
│    should be created for each vehicular live load (LL)    │
│    case resulting from the application of the above text. │
│    The resulting permutation is intended to generate the  │
│    system response envelope for load combinations that    │
│    include the vehicular live load (LL).                  │
└───────────────────────────┬─────────────────────────────┘
                            │
                            ▼
                         ┌─────┐
                         │  2  │
                         └─────┘
```

(2)

Perform Structural Analysis

- The structural analysis shall be performed in accordance with Section 4.
- Second-order effects shall be investigated as required by Article 4.5.3.
- Structural members should be idealized as lines elements.
- Pile-to-cap connections should be considered fixed. No relative rotation is assumed to occur between members/elements terminating at a joint.
- Pile deformations between the line element joint and the bottom face of the cap shall be included in the analysis. The magnitude of the design forces in the pile may be taken in the pile element at the bottom face of the cap.
- The cap shall be assumed uncracked for all structural analyses.
- A unique analysis for Service and Strength Limit States shall be performed using the supporting soil surface elevation and soil properties assumed to be present during the application of these loads.
- A unique analysis for Extreme Event Limit States shall be performed using the supporting soil surface elevation and soil properties assumed to be present during the application of these loads.
- The maximum allowable in-plane bent displacement (sidesway/drift) is assumed to occur when the joint centered on the bent forms a closed wedge. See attached Figure 2 for the recommended drift limit calculation and its derivation.

Are bent displacements satisfactory?

No

Yes

Modify Trial Structure

- Modify cap, piles or lateral bracing to improve bent performance. Adjustments to pile size or tip elevation will require corresponding changes to soil spring values used in model.
- Recalculate loads affected by the modifications.
- Perform structural analyses on the modified structure.

(3)

Structural Design of Bent Components

Design of Reinforced Concrete Cap:
- The design of the cap shall be performed in accordance with Section 5.
- Verify that the cap is uncracked.

Design of Structural Steel Piles:
- The design of steel piles shall be performed in accordance with Section 6 and Section 10.
- The influence of soil-structure interaction shall be considered in determining the slenderness ratios for compression members (Article 6.9.3). The pile length used in this calculation can be measured from the bottom face of the cap.
- The design pile moment can be taken at the bottom face of the cap. Larger pile moments and other localized behavior within the embedded portion of the pile can be neglected in pile design.
- Pile embedment into cap shall be at least 12 inches in accordance with Section 10.7.1.2. The actual forces transmitted through the pile-to-cap connection should be determined by analysis and may require embedment depths larger than this minimum. The 2002 papers by Shama et al. titled "Seismic Investigation of Steel Pile Bents: 1. Evaluation of Performance" and "2. Retrofit and Vulnerability Analysis" provide an approach for evaluating the capacity of pile-to-cap connections.

Modify Trial Structure

- Modify cap, piles or lateral bracing to provide a satisfactory design. Adjustments to pile size or tip elevation will require corresponding changes to soil spring values used in model.
- Recalculate loads affected by the modifications.
- Perform structural analyses on the modified structure.

Are cap and pile section properties used in structural analysis still valid?

No

Yes

4

(4)

Tabulate Pile Loads for the Geotechnical Engineer

- Refer to the ALDOT Memorandum dated September 20, 2013 for the required formatting of design axial pile load information being sent to the geotechnical engineer in the Bureau of Materials and Tests. The structural engineer shall periodically check for updates to this Memorandum.
- In-plane and out-of-plane (with respect to the bent) horizontal pile section forces acting at the supporting soil surface elevation assumed present during the load combination under investigation should be included with the axial pile loads above to permit a thorough geotechnical evaluation of each pile.
- The supporting soil surface elevation shall be clearly noted for each load combination being evaluated.

Does the geotechnical engineer concur that the assumed pile support is adequate?

No →

Yes ↓

Modify Trial Structure

- Modify pile tip elevation or section properties to provide satisfactory soil-structure interaction. Adjustments to pile size or tip elevation will require corresponding changes to soil spring values used in model.
- Recalculate loads affected by the modifications.
- Perform structural analyses on the modified structure.

End Pile Bent Design

General Notes:
- This flowchart is only intended to provide modeling and analysis guidance for pile bents.
- All Section and Article references are to the AASHTO LRFD Bridge Design Specifications, Seventh Edition, 2014
- Competent application of the referenced Sections and Articles is the responsibility of the engineers in the ALDOT Bridge Bureau.
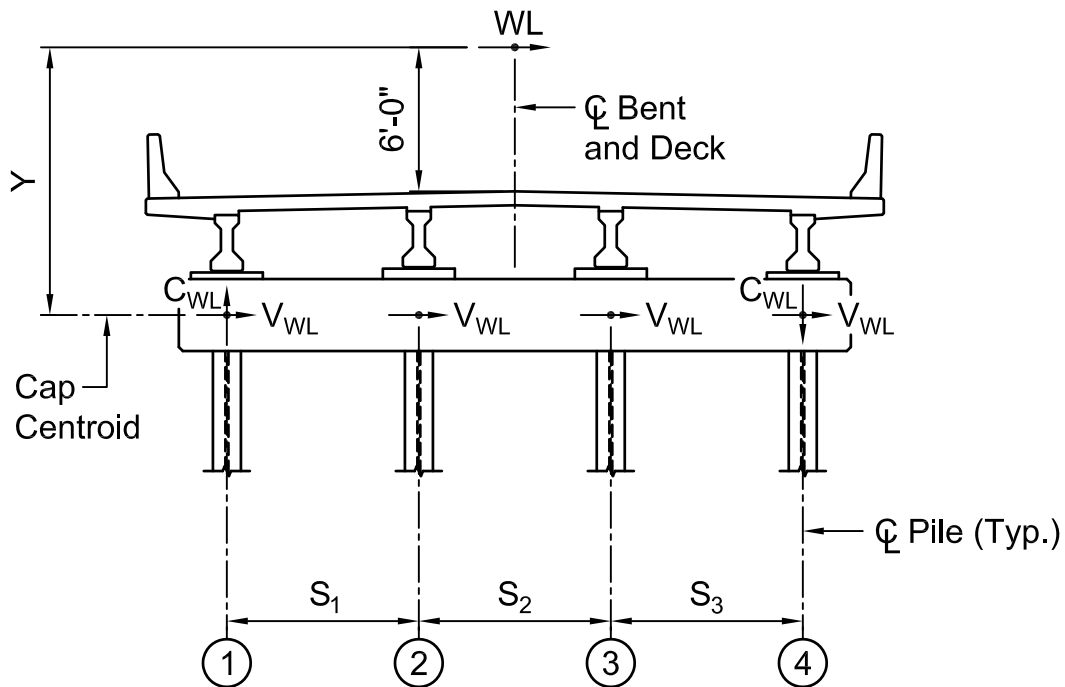
Shear from in-plane WL at each pile:

$V_{WL} = (WL)/(\text{No. of Piles})$

Couple forces from in-plane WL at exterior piles:

$\underline{\Sigma M_{Pile1} = 0:}$

$-(WL)(Y)+(C_{WL})(S_1+S_2+S_3) = 0$

$C_{WL} = (WL)(Y)/(S_1+S_2+S_3)$

EXAMPLE CALCULATIONS FOR RESOLVING HORIZONTALLY
APPLIED FORCES INTO EQUIVALENT FORCES ACTING ON BENT

FIGURE 1
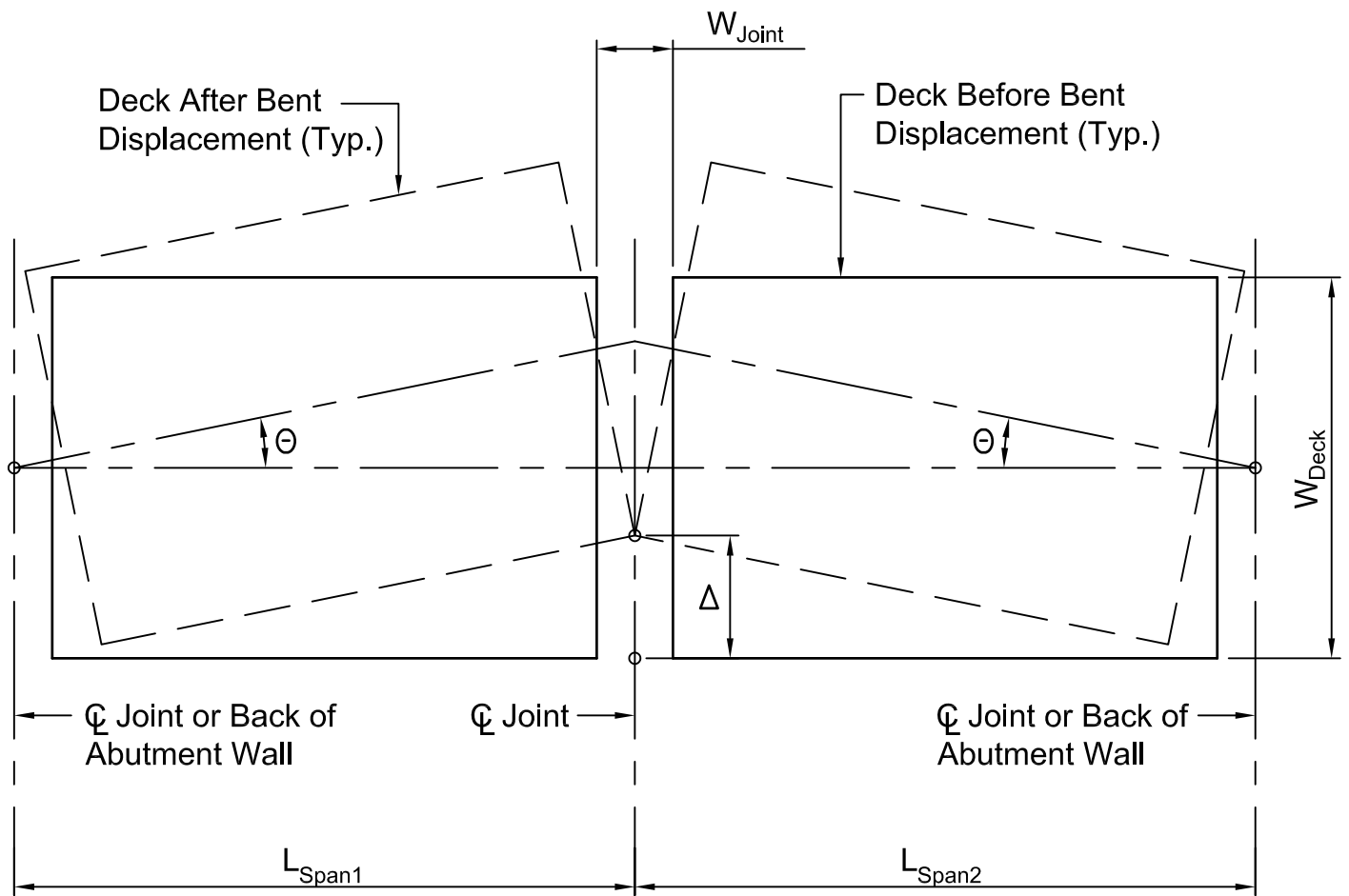
Approximate rotation required to close deck joint:

$$\Theta = S/R = (W_{Joint}/2)/(W_{Deck}/2) = W_{Joint}/W_{Deck}$$

Approximate bent drift limit corresponding to rotation:

$$\Delta = R\Theta = (L_{Min})(W_{Joint})/W_{Deck}$$

Where L_{Min} is the shorter of L_{Span1} and L_{Span2}.

Note: Adjacent bents/abutments are assumed stationary in above calculations. Any unit of length may be used, but the chosen unit must be applied consistently to all variables. Mixing units (e.g., inches and feet) is not permissible.

DERIVATION OF BENT DRIFT LIMIT EQUATION

FIGURE 2

ALABAMA DEPARTMENT OF TRANSPORTATION

Bridge Bureau, 1409 Coliseum Boulevard, Montgomery, Alabama 36110
Phone: (334) 242-6001   FAX: (334) 353-6502
Internet: http://www.dot.state.al.us
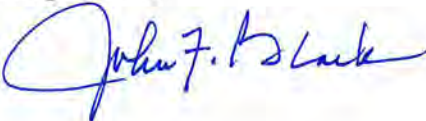
Robert Bentley
Governor

John R. Cooper
Transportation Director

MEMORANDUM

Date: September 20, 2013

To: Bridge Design Section Supervisors

From: John F. Black, P.E.
             Bridge Engineer

Re: LRFD Design Axial Loads

To insure consistency in the information the Bridge Bureau sends to the Materials and
Tests Bureau in the process of designing foundations using LRFD, please instruct
designers under your supervision to furnish design axial loads using the following format.

Location	No. of Piles/Shafts	LRFD Axial Load (tons)			Elevation @ Load 'P'	Pile/Shaft Size
		Service I	Strength I	Ext. Event II		
Abut. 1	12	30	45	N/A	533'	HP12x53
Bent 2	2	400	600	440	518'	4' diam.

Note: For the purpose of ASD design calculations, LRFD Service I shall be used.

JFB:jnw

297

11.Summary, Conclusions, and Recommendations

11.1   Summary

The multi-span bridge with intermediate bents consisting of driven steel piles and a reinforced concrete cap is commonly used in the state of Alabama. Understanding the load transfer mechanism of these pile bents under lateral loading is necessary in order to provide efficient designs. The research in this report was performed to identify the lateral load transfer mechanism of pile bents through a series of lateral load tests performed on a new construction bridge, an in-service bridge set of sister bridges and two stand-alone four-pile bents.

Results from field testing indicated that the maximum bending moments in the piles due to lateral loads were developed near the top of the pile. The Macon County and U.S. 331 bents consisted of steel piles encased in concrete. While these encasements are considered as non-structural elements, it was found through testing that these encasements provide a significant amount of lateral stiffness as well as participate in carrying axial loads. The addition of the bridge deck in the Macon County test provided an alternate load path resulting in a portion of the applied lateral load transferred to other structural elements in the bridge. The bents tested at AUNGES were unique in that the piles were not encased. These bents were also tested into the nonlinear range which provided significant data related to the bent and pile demands. Models from all the tests were created and compared to the experimental data to create calibrated models. These models included soil-pile interaction, composite section properties and applied loads which simulated the actual loads applied during the field tests. The results from the models correlated well with the results from the field tests in terms of bending moments and lateral

298

displacements. Axial forces were not as well correlated as the moments and deformations. The important conclusions from each of the tests are summarized in the following section.

11.2 Conclusions

Based on the field testing of the Macon County Bent:

- The bent exhibited minimal deformation under high lateral load levels without the addition of the bridge deck, deflecting less than 0.25" at a lateral load of 75 kips.

- The concrete encasements provide a large amount of additional lateral stiffness to the bent, even though they are not considered structural elements.

- The encased pile sections did not appear to behave in a fully composite manner during the load test, with the measured steel strains exceeding the measured concrete strains at instrumented cross-sections where steel and concrete strains were measured.

- The largest bending moments appeared to be near the top of the pile and decreased linearly along the length of the pile.

- The addition of the bridge deck provided an alternate load path for the lateral load resulting in a part of the load being transferred to other structural elements of the bridge

- The addition of gravity load in the center of the roadway and at the edge of the roadway had little effect on the lateral stiffness of the bent.

Based on the field testing of the US 331 Bent:

- The bent experienced very little deformation under large lateral loads, deflecting less than 0.1" in each of the tests with and without the load truck.

- Behavior of the steel piles during the test was unknown due to the inability to instrument the steel pile sections.

- The maximum bending moment appeared to occur near the top of the pile and decreased linearly towards zero at the ground surface.

- The calculated axial forces in the exterior piles were significantly higher than the axial forces in the interior vertical piles.

Based on analytical modeling of the Macon County and U.S. 331 bridges:

- Modeling soil-structure interaction through a series of linear springs appeared to provide a good representation of the soil behavior in the lateral load tests.

- The load-deflection from the SAP models was linear due to no geometric or material non-linearity being specified. The measured deflections correlated well with this linear assumption.

- The magnitude of bending moments was similar between the models and the field test results, varying by 5% in some cases to 40% in other cases.

- A fully-fixed connection between the pile head and the bent cap in the model produced similar results to the field tests in terms of deflections and bending moments.

- The addition of gravity loads from the load truck wheels had seemingly no effect on the lateral stiffness of the bent in the model.

- A displacement-controlled analysis for the U.S. 331 model provided a more accurate approach to determine the correlation between bending moments in the model and bending moments from the field tests.

Based on the testing and analysis of the AUNGES bents:

- The lateral stiffness and strength of the two pile bents was similar.

- Both bents developed the weak axis yield moment of the steel piles at the bottom of the cap and underwent significant inelastic deformations.

- The 12 in embedment of the steel piles allowed for development of the yield moment in the weak direction of the pile.

- The battered bent experienced ductile inelastic deformations followed by a tension pull-out failure of the first interior pile due to global rotation of the pile cap.

- Testing of the vertical bents was stopped due to the jack deformation capacity. Local buckling of the pile flanges occurred but the bent still had capacity to deform. The bent cap itself experienced minimal damage.

- The experimental moment and deformation results matched will with the validated numerical models.

- The measured vertical bent axial forces had reasonable correlation with analytical models although the model under predicted the force magnitude.

- The measured battered bent axial forces was not well correlated with the analytical models. The models did not capture the correct sign of the two interior piles which were opposite of the vertical bent.

11.3 Recommendations and Implementation

The following recommendations for design of steel pile bent bridges:

- The design process, with the recommended analysis procedure, shown in the flowchart in Chapter 10 should be used to design steel pile bents including the effects of soil-structure interaction.

- The benefit of battering the piles on lateral stiffness is minimal and the large axial forces and potential tension pull-out failure of piles provides a much larger negative impact. For these reasons, it is recommended to use vertical piles only in steel pile bents.

References

ACI, (2011). *Building Code Requirements for Structural Concrete (ACI 318-11) and Commentary (ACI 318R-11)*. Farmington Hills, MI.

(BSI), B. S. (2004). *FB-Multipier User Manual*. Gainsville: University of Florida.

AASHTO. (2002). *Standard Specifications for Highway Bridges* (17th ed.). Washington DC: American Association of State Highway and Transportation Officials.

AASHTO. (2007). AASHTO Ground Motion Parameters Calculator Version 2.1. Washington DC.

AASHTO. (2007). *LRFD Bridge Design Specifications* (4th ed.). Washington DC: American Association of State Highway and Transportation Officials.

AASHTO. (2009). *LRFD Bridge Design Specifications* (4th ed.). Washington DC: American Association of State Highway and Transportation Officials.

AASHTO. (2010). *AASHTO LRFD Bridge Design Specifications, 5th Edition*. Washington, D.C.

Abu-Farsakh, M. Y., Yu, X., Pathak, B., Alshibli, K., & Zhang, Z. (2011). Field Testing and Analyses of a Batter Pile Group Foundation Under Lateral Loading. *Transportation Research Record*, 42-55.

ACI 318. (2008). *Building Code Requirements for Structural Concrete and Commentary*. Farmington Hills, Michigan: American Concrete Institute.

ACI Committee 224. (2001). *Control of Cracking of Concrete Structures*. Farmington Hills, MI: American Concrete Institute.

AISC. (2005). *Steel Construction Manual* (13th ed.). United States: American Institute of Steel Construction.

AISC. (2011). *Steel Construction Manual*. Chicago.

Alabama Department of Transportation. (2008). *Bridge Bureau Structures Design and Detail Manual*. Montgomery, AL.

Alabama DOT. (2012, November 30). *ALDOT Standard Details*. Alabama Department of Transportation.

Alaska DOT. (2008). *Tanana River Bridge: Alaska Highway Bearings*. Alaska Department of Trasnportation and Public Facilities.

ALDOT. (1971). Hold Down and Anchorage Devices for Roadway Slabs: I-10 East Tunnel Interchange.

American Society for Testing and Materials. (1998). *ASTM D 6275 - Standard Practice for Laboratory Testing of Bridge Decks*. West Conshohocken, PA: ASTM International.

American Society of Civil Engineers. (2009). *Report Card for America's Infrastructure*. Retrieved June 2012, from Infrastructure Report Card: http://www.infrastructurereportcard.org/fact-sheet/bridges

American Welding Society. (2008). *AASHTO D1.5M Bridge Welding Code 5th Edition*. Washington, D.C.

Badie, S. S. (2008). *NCHRP Report 584 - Full-Depth Precast Concrete Bridge Deck Panel Systems*. Washington, D.C.: Transportation Research Board.

Barker, R. M., & Puckett, J. A. (2007). *Design of Highway Bridges An LRFD Approach*. Hoboken, NJ: John Wiley & Sons.

Bowles, J. (1996). *Foundation Analysis and Design*. New York: McGraw-Hill.

Bowles, J. E. (1996). *Foundation Analysis and Design, Fifth Edition*. New York: McGraw-Hill.

Broms, B. (1964a). Lateral Resistance of Piles in Cohesionless Soils, ASCE. *Journal of the Soil Mechanics and Foundations Division*, 123-156.

Broms, B. (1964b). Lateral Resistance of Piles in Cohesive Soils. *Journal of the Soil Mechanics and Foundations Division, ASCE*, 27-63.

Brown, D. A., Morrison, C., & Reese, L. C. (1988). Lateral Load Behavior of Pile Group in Sand. *Journal of Geotechnical Engineering*, 1261-1276.

Campbell, J. (2015). *Experimental Testing and Analytical Modeling of Driven Steel Pile Bridge Bents.* Auburn, Alabama.

Coduto, D. P. (1999). *Geotechnical Engineering Principles and Practices.* Upper Saddle River, New Jersey: Prentice-Hall, Inc.

Coulson, P. J., & Marshall, J. D. (2011). *Influence of the LRFD Bridge Design Specifications on Seismic Design in Alabama.* Auburn University, Auburn, AL.

Computer and Structures Inc. (2012). *CSI Bridge 15.* Berkely, CA: Computer and Structures, Inc.

Computers and Structures, I. (. (2011). *SAP User Manual.* Berkely, CA.

Corporation, P. T. (2007). *Mathcad 14.* Needham, MA: Parametric Technology Corporation.

Culmo, M. P. (2011). *Accelerated Bridge Construction - Experience in Design, Fabrication, and Erection of Prefabricated Bridge Elements and Systems.* McLean, VA: Federal Highway Administration - Office of Bridge Technology.

Ensoft. (2000). *GROUP 5.0: A program for the analysis of a gorup of piles subjected to axial and lateral loading .* Austin, TX: Ensoft Inc.

Georgia DOT. (2012, November 30). *Basic Drawings.* Retrieved January 28, 2013, from GDOT: http://www.dot.ga.gov/doingbusiness/PoliciesManuals/roads/Pages/BasicDrawings.aspx

Gerber, T. M., & Rollins, K. M. (2009). Behavior of a Nine-Pile Group With and Without a Pile Cap. *2009 International Foundation Congress and Equipment Expo*, (pp. 530-537).

Gerber, T., & Rollins, K. (2009). Behavior of a Nine-Pile Group With and Without a Pile Cap. *International Foundation Congress and Equipment Expo*, 530-537.

Hetenyi, M. (1946). *Beams on Elastic Foundation.* Michigan: University of Michigan Press.

Hsiung, Y., & Chen, Y. (1997). Simplified Method for Analyzing Laterally Loaded Single Piles in Clays. *Journal of Geotechnical and Environmental Engineering, ASCE*, 1018-1029.

International, A. (2007). D 3966-07 Standard Test Methods for Deep Foundations Under Lateral Load.

Lawton, E. C., Pantelides, C. P., & Cook, C. R. (2001). *Soil-Pile-Structure Interaction of Bridge Bents Subjected to Lateral Loads.* Salt Lake City, Utah: The University of Utah.

Lin, S.-S., & Liao, J.-C. (2006). Lateral Response Evaluation of Single Piles Using Inclinometer Data. *Journal of Geotechnical and Geoenvironmental Engineering*, 1566-1573.

McCarthy, D. F. (2007). *Essentials of Soil Mechanics and Foundations Seventh Edition.* Upper Saddle River, New Jersey: Pearson Prentice Hall.

Mokwa, R., & Duncan, J. (2003). Rotational Restrain of Pile Caps during Lateal Loading. *Journal of Geotechnical and Geoenvironmental Engineering, ASCE*, 829-837.

Oliver, R. S. (1999). *Rapid Replacement/Rehabilitation of Bridge Decks.* Auburn, AL: Auburn University.

Ooi, P. K., & Ramsey, T. L. (2003). Curvature and Bending Moments from Inclinometer Data. *International Journal of Geomechanics*, 64-74.

Poulos, H. (1971a). Behavior of Laterally Loaded Piles: Part I-Single Piles. *Journal of the Soil Mechanics and Foundations Division*, 711-731.

Poulos, H., & Davis, E. (1980). *Pile Foundation Analysis and Design.* New York: John Wiley and Sons.

PTC. (2007). Mathcad. Needham, Massachusetts, USA.

Reese, L. C., & Wang, S.-T. (2006). *Verification of Computer Program LPile as a Valid Tool for Design of a Single Pile under Lateral Loading.*

Reese, L., Isenhower, W., & Wang, S. (2006). *Analysis and Design of Shallow and Deep Foundations.* New York: John Wiley and Sons.

Richards, P. W., Rollins, K. M., & Stenlund, T. E. (2011). Experimental Testing of Pile-to-Cap Connections for Embedded Pipe Piles. *Journal of Bridge Engineering*, 286-294.

Richards, P., Rollins, K., & Stenlund, T. (2011). Experimental Testing of PIle-to-Cap Connections for Embedded Pipe Piles. *Journal of Bridge Engineering, ASCE*, 286-294.

Robertson, P. K., Davies, M. P., & Campanella, R. G. (1989). Design of Laterally Loaded Driven Piles Using the Flat Dilatometer. *Geotechnical Testing Journal*, 30-38.

Rodriguez-Marek, A. (2007). *DYNAMIC RESPONSE OF BRIDGES TO NEAR-FAULT, FORWARD DIRECTIVITY GROUND MOTIONS.* Pullman: Washington State Transportation Center.

Rollins, K. M., Olsen, K. G., Jensen, D. H., Garrett, B. H., Olsen, R. J., & Egbert, J. J. (2006). Pile Spacing Effects on Lateral Pile Group Behavior: Analysis. *Journal of Geotechnical and Geoenvironmental Engineering*, 1272-1283.

Rollins, K. M., Peterson, K. T., & Weaver, T. J. (1998). Lateral Load Behavior of Full-Scale Pile Group in Clay. *Journal of Geotechnical and Geoenvironmental Engineering*, 468-478.

Rollins, K. M., Sparks, A. E., & Peterson, K. T. (n.d.). Lateral Load Capacity and Passive Resistance of Full-Scale Pile Group and Cap. *Transportation Research Record*, 24-32.

Salgado, R. (2008). *The Engineering of Foundations*. New York: McGraw Hill.

Skinner, Z. (2015). *Theoretical Modeling and Lateral Load Testing of Driven Steel Pile Bridge Bents.* Auburn, AL: Auburn University.

StructurePoint. (2012). *spColumn.* StructurePoint, LLC.

.

Tonias, D. E., & Zhao, J. J. (2007). *Bridge Engineering: Design, Rehabilitation, and Maintenance of Modern Highway Bridges.* New York: McGaw Hill.

USGS. (2013, May 17). *2008 Interactive Deaggregations.* Retrieved September 17, 2013, from USGS: https://geohazards.usgs.gov/deaggint/2008/

Utah Department of Transportation. (2010). *Full Depth Precast Concrete Deck Panel Manual.* UDOT.

Wight, J. K., & MacGregor, J. G. (2009). *Reinforced Concrete Mechanics and Design.* Saddle Bridge: Prentice Hall.

Wight, J. K., & MacGregor, J. G. (2009). *Reinforced Concrete: Mechanics and Design.* Upper Saddle River, NJ: Pearson Prentice Hall.